



Departament d'Enginyeria Química
Escola Tècnica Superior d'Enginyeria Química
Universitat Rovira i Virgili

**OLIGONUCLEOTIDE BASED-BIOSENSORS FOR LABEL-FREE
ELECTROCHEMICAL PROTEIN AND DNA DETECTION**

Mònica Mir Llorente

Tarragona, 2006

UNIVERSITAT ROVIRA I VIRGILI
OLIGONUCLEOTIDE BASED-BIOSENSORS FOR LABEL-FREE ELECTROCHEMICAL PROTEIN AND DNA DETECTION.
Mònica Mir Llorente
ISBN: 978-84-690-7601-9 / DL: T.1389-2007

UNIVERSITAT ROVIRA I VIRGILI
OLIGONUCLEOTIDE BASED-BIOSENSORS FOR LABEL-FREE ELECTROCHEMICAL PROTEIN AND DNA DETECTION.
Mònica Mir Llorente
ISBN: 978-84-690-7601-9 / DL: T.1389-2007

UNIVERSITAT ROVIRA I VIRGILI
OLIGONUCLEOTIDE BASED-BIOSENSORS FOR LABEL-FREE ELECTROCHEMICAL PROTEIN AND DNA DETECTION.
Mònica Mir Llorente
ISBN: 978-84-690-7601-9 / DL: T.1389-2007

IOANNIS KATAKIS, Professor titular del Departament d'Enginyeria Química de la
Universitat Rovira I Virgili

FAIG CONSTAR

que el present treball que porta el títol

OLIGONUCLEOTIDE BASED-BIOSENSORS FOR LABEL-FREE
ELECTROCHEMICAL PROTEIN AND DNA DETECTION

Que presenta na MÒNICA MIR LLORENTE per optar al grau de Doctora en
Enginyeria Química, ha estat realitzat sota la seva direcció en els laboratoris del
Departament d'Enginyeria Química de la Universitat Rovira i Virgili, i que tots els
resultats presentats i la seva anàlisi són fruit de la investigació realitzada per
l'esmentada doctoranda.

I per a que se'n prengui coneixement i tingui els efectes que corpongui signo aquesta
certificació.

Tarragona, 26 de Setembre de 2006

Dr. Ioannis Katakis
Professor Titular d'Universitat

UNIVERSITAT ROVIRA I VIRGILI
OLIGONUCLEOTIDE BASED-BIOSENSORS FOR LABEL-FREE ELECTROCHEMICAL PROTEIN AND DNA DETECTION.
Mònica Mir Llorente
ISBN: 978-84-690-7601-9 / DL: T.1389-2007

Agraïments

En aquestes pàgines voldria agrair l'ajuda rebuda de totes les persones que han fet possible que aquesta tesis sortís a la llum.

En primer lloc voldria agrair al meu director de tesis, Dr. Ioanis Katakis, per donar-me l'oportunitat d'entrar al fascinant món de la ciència, i per ser tant exigent amb la meua feina, fent-la hagi millor cada dia. Encara que això no era tant d'agrair fa un temps enrera.

Agraeixo als membres del tribunal de tesis que tant pacientment han llegit aquesta tesis.

Gràcies a la Comissió Europea per contribuir econòmicament mitjançant els projectes DISSARM "Development of Integratable Sensors for Screening of Antibiotic Resistance in Mycobacterium" (Quality of life and Management of resources Program, QLK2-CT-2000-00765), MICROPROTEIN "Micrometer Scale Patterning of Protein and DNA Chips" (Competitive and Sustainable Growth programme (1998-2002)) i SAFER "Isolation of foetal cells from maternal blood" (NEST-ADVENTURE 04977), la recerca assolida en aquesta tesis.

Gràcies a tots els membres del BBG amb els que he compartit la recerca al laboratori, i les preocupacions i rialles del dia a dia. Inicialment al antic colomar reconvertit en laboratori de la Imperial on vaig començar a descobrir que era un biosensor amb l'ajuda de Mònica i el surrealisme de Valeri, juntament amb Ciara i Christophe. Després al laboratori de la Laboral amb la simpatia de les Gemmes, les lliçons d'anglès d'en Philip i Paul i la marxa dels yankees, Kristin i Alex. I més endavant als laboratoris del campus de Sescelades amb les síntesis de l'Antonio i el Josep Maria, la gran ajuda administrativa de Sandra, Joaquim, Barbara i Ivonne, el suport a distància de la Teresa, Diego i Mark, les xerrades que mantenen el meu anglès amb Rasa, Guray i Srujan, les "baralles" i llargues estades davant dels potenciostats amb Paula, Vivi i Kelly, i els divertits dinars amb Marta, Mireia i Pablo.

Gràcies als amics de Bath, Lorena, Sonia, Killian, Margarida, Anye, John, Walter, Jorge, Cristina, Diego, Laura i Luisa pels bons moments que em vam fer passar durant la meva estància, en especial als meus *homemates*, Yolanda i Frank.

Gràcies a Sergi, Alex, Paula, el germanet Leon i Maria pels inoblidables sopars i farras que em passat junts.

Gràcies a Coco i Gustavo per les lliçons apreses.

Gràcies als meus pares que no haver-me regalat mai el Quimicefa, la qual cosa va fer que acabés estudiant química i dedicant-me a la ciència.

I un especial agraïment a Sergi, què és la persona que ha tingut que suportar més els meus canvis d'humor quan els resultats no sortien i en definitiva la persona més important per portat a fi aquesta tesis i la meva vida.

Table of contents

- Resumen.....	xv
- List of figures.....	xix
- List of tables.....	xxvii
- List of schemes.....	xxix
- List of equations.....	xxxii
- Abbreviations.....	xxxiii
- Chapter 1. Introduction.....	1
1.1 Biosensors.....	1
1.1.1 Definition of biosensor.....	1
1.2 DNA sensors.....	3
1.2.1 Genomic biosensors.....	3
1.2.2 Steps involved in DNA sensors.....	4
1.2.2.1 Probe immobilisation.....	5
1.2.2.2 Sample preparation.....	11
1.2.2.3 Hybridisation.....	13
1.2.2.4 Detection.....	15
1.2.2.5 Data analysis.....	21
1.1.3 Electrochemical label-free DNA sensors.....	22
1.3 Aptasensors.....	26
1.3.1 Proteomic biosensors.....	26
1.3.2 Aptamers.....	27
1.3.3 Types of aptamers.....	29
1.3.4 SELEX.....	34

1.3.5	Interaction between aptamer-target.....	36
1.3.6	Aptamer versus Antibodies.....	37
1.3.7	α -Thrombin.....	38
1.3.8	Aptasensors.....	39
1.3.9	Applications.....	41
1.4	Presentation of the thesis.....	44
1.5	References.....	46
-	Chapter 2. Detection of direct DNA hybridisation.....	61
2.1	Introduction.....	61
2.2	Materials and methods.....	62
2.2.1	Materials.....	62
2.2.2	Instrumentation.....	64
2.2.3	Real DNA sample amplification by PCR.....	64
2.2.4	Bioconjugation: synthetic 19-mer DNA labelling with HRP.....	65
2.2.5	Optimisation of hybridisation conditions by optical ELONA.....	66
2.2.6	Colourimetric detection of hybridisation of PCR products.....	66
2.2.7	Electrodes preparation.....	67
2.2.8	Electrochemical detection of direct hybridisation with diffusional mediator.....	68
2.2.9	Electrochemical detection of direct hybridisation with non- diffusional mediator.....	69
2.2.10	Electrochemical detection of direct hybridisation of PCR products with non-diffusional mediator.....	69
2.2.11	Interdigitated electrodes as demostartion of electrochemical microarrays.....	70
2.3	Results and Discussion.....	74
2.3.1	Optimisation of hybridisation conditions by optical ELONA.....	74

2.3.2	Optimisation of hybridisation conditions specific for breast cancer by ELONA.....	75
2.3.3	Optimisation of hybridisation conditions of PCR products by ELONA.....	76
2.3.4	Electrodes preparation.....	78
2.3.5	Electrochemical detection of direct hybridisation with diffusional mediator.....	81
2.3.6	Electrochemical detection of direct hybridisation with non-diffusional mediator.....	85
2.3.7	Electrochemical detection of direct hybridisation of PCR products with non-diffusional mediator.....	88
2.3.8	Interdigitated electrodes as demostartion of electrochemical microarrays.....	91
2.4	Conclusions.....	94
2.5	References.....	95
-	Chapter 3. Detection of DNA hybridisation by displacement.....	97
3.1	Introduction.....	97
3.2	Materials and methods.....	99
3.2.1	Materials.....	99
3.2.2	Instrumentation.....	101
3.2.3	Procedures involved in HRP-displacement detection.....	102
3.2.3.1	Bioconjugation of 19-mer DNA labelling with HRP.....	102
3.2.3.2	Optimisation of displacement conditions by ELONA.....	102
3.2.3.3	Electrochemical monitoring of displacement of HRP-labelled sequences.....	103
3.2.4	Procedures involved in ferrocene-displacement detection.....	104
3.2.4.1	Bioconjugation of DNA labelling with ferrocene.....	104

3.2.4.2	Electrochemical monitoring of displacement of ferrocene labelled sequences.....	106
3.2.4.3	Amplification of ferricyanide signal by ferrocene.....	107
3.3	Results and Discussion.....	108
3.3.4	Displacement of HRP-labelled suboptimum sequence.....	108
3.3.4.1	Optimisation of sub-optimum probes and displacement conditions by ELONA.....	108
3.3.4.2	Electrochemical monitoring of displacement of HRP-labelled DNA.....	122
3.3.5	Displacement of ferrocene-labelled suboptimum sequence for cystic fibrosis detection.....	123
3.3.5.1	Electrochemical monitoring of displacement of ferrocene-labelled DNA.....	125
3.3.5.2	Amplification of ferricyanide signal by ferrocene.....	144
3.4	Conclusions.....	146
3.5	References.....	147
-	Chapter 4. Electrochemical aptasensors.....	151
4.1	Introduction.....	151
4.2	Materials and methods.....	155
4.2.1	Materials.....	155
4.2.2	Instrumentation.....	156
4.2.3	Aptamer bioconjugation with ferrocene.....	157
4.2.4	Thrombin-aptamer binding assay using a sandwich format.....	158
4.2.5	Electrochemical detection of chromogenic thrombin substrate.....	159
4.2.6	Electrochemical detection of thrombin immobilised on electrode surface.....	160
4.2.7	Electrochemical aptabeacon.....	160

4.2.8 Chronoamperometric aptabeacon.....	161
4.3 Results and Discussion.....	163
4.3.1 Aptamer bioconjugation with ferrocene.....	163
4.3.2 Thrombin-aptamer binding assay using a sandwich format.....	166
4.3.3 Electrochemical detection of chromogenic thrombin substrate.....	171
4.3.4 Electrochemical detection of thrombin adsorption on electrode surface.....	175
4.3.5 Electrochemical aptabeacon.....	178
4.3.6 Chronoamperometric aptabeacon.....	183
4.4 Conclusions.....	193
4.5 References.....	194
- Chapter 5. Conclusions and future work.....	197
5.1 References.....	201

Resumen

En los últimos años, los chips de ADN han atraído una atención creciente diferentes campos, debido a su portabilidad, sensibilidad, especificidad y rápida respuesta. Los chips de ADN son aplicados en diagnóstico de enfermedades genéticas, detección de agentes infecciosos, estudios de predisposición genética, desarrollo de medicina personalizada, detección de expresión genética diferencial, medicina forense, exploración de medicamentos, columnas de separación, seguridad alimentaria, defensa militar y monitorización medioambiental.

Aunque los sensores geonómicos han avanzado de forma muy rápida llegando a sitios privilegiados en diferentes plataformas comerciales, los sensores proteómicos están cortando muy rápidamente las distancias con los sensores de ADN. Ya que los sensores proteómicos detectan directamente la proteína generada a partir de la secuencia de ADN, aportando así más información. Por lo tanto estos tipos de sensores pueden contribuir en mejor medida al descubrimiento de nuevos fármacos o en la diagnosis de medicina molecular.

Desde hace unos años los chips basados en anticuerpos han sido desarrollados para el análisis de un gran número de proteínas, no obstante los chips basados en aptámeros son mejores candidatos para la detección de proteínas, ya que no necesitan el uso de animales para su producción y por tanto son mas fáciles de producir de una manera automatizada y sin necesidad de condiciones fisiológicas. Los chips de aptámeros pueden ser reutilizados y son mas fáciles de marcar e inmovilizar sobre soportes sólidos con una densidad definida.

Aunque los chips basados en oligonucleótidos para la detección de ADN y proteínas tienen un gran futuro en diagnosis e investigación biológica, esta tecnología está aun muy lejos de su uso diario en el campo clínico y aun mas lejos de poder ser comercializado para uso doméstico como lo han sido los biosensores de glucosa.

Sus principales problemas son su alto coste y su dificultad de uso. Para su utilización es necesario, previo a la inyección del analito en el biosensor, costosos instrumentos de laboratorio y técnicos especializados en bioquímica para el marcaje y amplificación de

las muestras de ADN. La mayoría de chips de ADN que se comercializan utilizan detectores de fluorescencia, lo que hace que se encarezca mucho el precio del chip. En cambio la utilización de transductores electroquímicos aporta muchas ventajas, como la alta sensibilidad, facilidad para miniaturización del chip, coste de producción mas bajo, alta velocidad de respuesta y mayor facilidad para el tratamiento de los datos. Así pues el desarrollo de biosensores electroquímicos utilizando oligonucleótidos como molécula de reconocimiento para la detección de ADN y proteínas, los cuales no necesiten un marcaje previo del analito, son de gran relevancia.

El trabajo hecho en esta tesis describe el desarrollo de nuevos conceptos de biosensores electroquímicos basados en oligonucleótidos para la detección de ADN y proteínas no marcadas previamente.

Experimentos preliminares para la detección directa de la hibridación de ADN marcado se llevó a cabo para establecer protocolos para la inmovilización, hibridación y detección de ADN colorimétricamente y electroquímicamente.

Se utilizó un mediador diffusional para detectar electroquímicamente la señal catalítica obtenida del oligonucleótido marcado con peroxidasa Horseradish (HRP), el cual se hibridó en una cadena de oligonucleótido inmovilizado sobre la superficie del biosensor que contenía la secuencia de nucleótidos complementarios a la secuencia del analito que se quiere detectar.

Un polímero redox inmovilizado sobre la superficie del electrodo fue utilizado con el mismo fin que el mediador diffusional, pero en este caso el mediador no diffusional mejora el sistema ofreciendo una respuesta mas rápida, el uso de menos volumen de muestra y un sistema que no requiere la adición del mediador en la detección del analito, ya que este esta incorporado al electrodo. Se detectó selectivamente una región del gen específico para la detección de *Micobacterium tuberculosis* que contiene mutaciones que confieren resistencia a la rifampicina. El analito se amplificó y marcó previamente mediante la técnica de reacción en cadena de polimerasa (PCR). La hibridación del analito fue detectada electroquímicamente con mediador no diffusional.

Se utilizó también fotolitografía biocompatible para la inmovilización selectiva de moléculas de ADN en un microchip. En esta plataforma y mediante mediador no diffusional fue detectado electroquímicamente el oligonucleótido marcado específico para la detección de cáncer de pecho.

Para no necesitar un marcaje previo de la muestra de ADN y así simplificar y reducir el coste del futuro biosensor se desarrolló un sistema electroquímico de desplazamiento. El método libre de marcaje se basa en el desplazamiento de moléculas de oligonucleótido mutado y marcado, el cual aunque contenga ciertas mutaciones es capaz de hibridar con la sonda de oligonucleótido inmovilizado, pero cuando estas se encuentran en presencia del analito desplaza la molécula mutada, disminuyendo así la señal de manera proporcional a la concentración del analito. El sistema de desplazamiento ha sido demostrado colorimétricamente y electroquímicamente utilizando marcaje de HRP sobre el mutado. También se demostró este sistema utilizando un marcaje de ferroceno en el oligonucleótido mutado, con el fin de no necesitar añadir ningún reactivo para la detección del analito.

También se llevaron a cabo diferentes estrategias para desarrollar un biosensor electroquímico basado en oligonucleótidos (aptámeros) para la detección de trombina sin el previo marcaje de este analito.

En la configuración más directa, el aptámero marcado con un grupo tiol se inmovilizó en la superficie del electrodo de oro para interactuar e inmovilizar la trombina. El enlace entre el aptámero y el analito se detectó mediante la cuantificación de la reacción de hidrólisis de β -Ala-Gly-Arg-p-nitroaniline catalizado por la trombina produciendo p-nitroaniline. Este producto de la catálisis fue detectado colorimétricamente y electroquímicamente, no obstante la detección electroquímica demostró ser más rápida y sensible.

En la segunda configuración de aptasensor se utilizó formato de sándwich. El aptámero tiolado fue inmovilizado en el electrodo e incubado con trombina de la misma manera. En el siguiente paso, el electrodo se incubó con aptámero marcado con biotina para que se enlazase con la trombina ya interaccionada con el primer aptámero. El aptámero marcado con biotina fue previamente incubado con estreptavidina-HRP, lo que permitió la detección de la interacción. La actividad del HRP se relacionó con la cantidad de trombina mediante una recta de calibrage.

En la tercera estrategia la trombina fue inmovilizada en la superficie del electrodo. Posteriormente el sensor fue incubado primero con aptámero marcado con biotina y posteriormente con estreptavidina-HRP. La detección electroquímica del HRP fue,

como en la estrategia anterior, detectada mediante peróxido de hidrogeno y mediador difusional.

En la cuarta estrategia se utilizó la interacción de trombina con el aptámero para demostrar un modelo muy simple de sensor electroquímico mediante un sistema de *beacon*, que no requiere el marcaje del analito ni de la utilización de reactivos una vez se ha inyectado la muestra. Los *beacons* utilizan cambio tridimensional detectable de la conformación del elemento de bioconocimiento debido a la interacción con el analito. Para esta detección el aptámero se marcó por un lado con un grupo tiol para su inmovilización sobre oro y en el otro lado con una molécula de ferroceno para su detección. Cuando el aptámero interacciona con el analito adquiere una conformación de silla que hace que la molécula de ferroceno se encuentre muy cerca de la superficie del electrodo, la cual cosa hace que cambie su respuesta voltamperométrica. Se demostró que el sistema era específico dando respuestas muy bajas para moléculas similares al analito.

La última estrategia es una modificación del sistema anterior. En este caso en la superficie del electrodo se coinmovilizó el aptámero modificado con tiol y ferroceno con una monocapa de microperoxidasa-11. Así pues, el centro redox de la enzima coinmovilizada reconoce la molécula de ferroceno que se acerca cuando el aptámero interacciona con la trombina. Así pues cuando el analito interacciona, en presencia del sustrato de la enzima y del mediador difusional, la enzima media la transferencia electrónica. Esta reacción catalítica ha de servir para amplificar la señal del biosensor.

Esta tesis ha sido estructurada en seis capítulos. En el primer capítulo se hace una descripción del estado del arte en el mundo de los biosensores, de los chips de ADN y de los sensores basados en aptámeros. El segundo capítulo refleja los resultados obtenidos en diferentes biosensores electroquímicos para la detección directa de ADN marcado. En el capítulo tercero se demuestra un sistema electroquímico de desplazamiento para detectar moléculas de ADN libres de marcaje. En el cuarto capítulo se describen diferentes estrategias para desarrollar biosensores electroquímicos basados en aptámeros para la detección de trombina no marcada. Finalmente el capítulo cinco y seis resumen las conclusiones y los posibles trabajos futuros.

List of figures

Figure 1. 1. Structures of deoxyribonucleic acid (DNA), locked nucleic acid (LNA), and peptide nucleic acid (PNA).....	5
Figure 1. 2. NMR image of ATP binding RNA aptamer.....	28
Figure 1. 3. Mechanism of signalling by fluorescent thrombin aptamer beacon.....	30
Figure 1. 4. Captamers for detection of human thrombin by proximity extension.....	30
Figure 1. 5. Self-cleaving aptazyme.....	31
Figure 1. 6. Chemical structure of TNA and DNA.....	32
Figure 1. 7. Chemical structure of thio-RNA and RNA.....	33
Figure 1. 8. SELEX process.....	35
Figure 2. 1. Gold IDE array picture.....	71
Figure 2. 2. Colourimetric detection of $18 \mu\text{g mL}^{-1}$ 19-mer HRP labelled oligonucleotide hybridised for 1 hour at 55°C	74
Figure 2. 3. Breast cancer oligonucleotide hybridisation detected by ELONA.....	75
Figure. 2. 4. Colourimetric detection of 255-mer oligonucleotide amplified by PCR.....	76
Figure 2. 5. Detection limit of 255-mer oligonucleotide hybridisation by colourimetric detection.....	77
Figure 2. 6. Chronoamperometric plots from the detection of 19-mer DNA hybridisation by diffusional mediator.....	82
Figure 2. 7. Amperometric detection of 19-mer complementary-HRP hybridisation by diffusional mediator was plotted with control.....	83
Figure 2. 8. Detection limit of 19-mer DNA hybridisation by diffusional mediator.....	83
Figure 2. 9. Redox polymer structure used in the DNA detection.....	85

Figure 2. 10. Amperometric detection of 19-mer complementary-HRP hybridisation by redox polymer immobilised on the electrode. Optimisation of redox polymer concentration.....	87
Figure 2. 11. Amperometric detection of 19-mer complementary-HRP hybridisation by redox polymer immobilised on the electrode. Optimisation of PEG-DE concentration.....	87
Figure 2. 12. Amperometric detection of 19-mer complementary-HRP hybridisation by redox polymer immobilised on the electrode. Sample response was plotted with different controls	88
Figure 2. 13. Chronoamperometric plots from the detection of 255-mer amplified oligonucleotide by PCR with redox polymer immobilised on the surface.....	89
Figure 2. 14. Sample and control response from the amperometric detection of amplified 255-mer oligonucleotide hybridisation with redox polymer immobilised on electrode.....	90
Figure 2. 15. Cyclic voltamperometry of films contained the 19-mer oligonucleotide and 255-mer oligonucleotide, after hybridisation.....	91
Figure 2. 16. Amperometric response of IDE on photolithographic array with two electrodes immobilized. On the first set of electrodes oligonucleotide-HRP was immobilized and a potential of -0.1 V was applied and oligonucleotide-ALP was immobilized on the second set of electrodes where 0.3 V potential was used.....	93
Figure 2. 17. Breast cancer oligonucleotide amperometric detection on IDE using biocompatible photolithography. Complementary capture probe was immobilized on the electrode to detect the target, control with complementary capture probe but without target, control with mutated capture probe immobilized.....	94
Figure 3. 1. Tubes eluted from a size exclusion chromatography to separate ferrocene labelled oligonucleotide from ferroceneacetic acid.....	105
Figure 3. 2. MALDI-TOF graph of amino-oligonucleotide.....	106
Figure 3. 3. MALDI-TOF graph of ferrocene-oligonucleotide.....	106

Figure 3. 4. Colourimetric detection of mutated-HRP and complementary-HRP hybridisation with immobilised capture probe. Effect of blocking and controls without capture probe were tested.....	111
Figure 3. 5. Colourimetric detection of 30 $\mu\text{g mL}^{-1}$ mutated-HRP and 30 $\mu\text{g mL}^{-1}$ complementary-HRP hybridisation with immobilised capture probe for 60 minutes at various temperatures of incubation.....	112
Figure 3. 6. Colourimetric detection of 30 $\mu\text{g mL}^{-1}$ mutated-HRP and 30 $\mu\text{g mL}^{-1}$ complementary-HRP hybridisation with immobilised capture probe at 50 °C and various times of incubation	115
Figure 3. 7. Colourimetric detection of 30 $\mu\text{g mL}^{-1}$ mutated-HRP and 30 $\mu\text{g mL}^{-1}$ complementary-HRP hybridisation with immobilised capture probe at 60 °C and various times of incubation.....	115
Figure 3. 8. Colourimetric detection of different concentrations of mutated-HRP and complementary-HRP hybridisation with immobilised capture probe for 60 minutes at 50 °C of incubation.....	117
Figure 3. 9. Colourimetric detection displacement of pre-hybridised mutated-HRP with complementary or buffer (control) was carried out. Conditions of pre-hybridisation; 10 $\mu\text{g mL}^{-1}$ of mutated-HRP for 1 hour at 50 °C. Conditions of displacement; 30 $\mu\text{g mL}^{-1}$ of complementary at 55 °C for various time of incubation.....	119
Figure 3. 10. Colourimetric detection displacement of pre-hybridised mutated-HRP with complementary or buffer (control) was carried out. Conditions of pre-hybridisation; 10 $\mu\text{g mL}^{-1}$ of mutated-HRP for 1 hour at 50 °C. Conditions of displacement; 30 $\mu\text{g mL}^{-1}$ of complementary for 5 minutes at various temperatures of incubation.....	120
Figure 3. 11. Colourimetric detection displacement of pre-hybridised mutated-HRP with complementary or buffer (control) was carried out. Conditions of pre-hybridisation; 10 $\mu\text{g mL}^{-1}$ of mutated-HRP for 1 hour at 50 °C. Conditions of displacement; Incubation at 60 °C for 5 minutes at various concentrations of complementary.....	121

Figure 3. 12. Electrochemical displacement detection of pre-hybridised mutated- HRP with an immobilised capture probe.....	122
Figure 3. 13. e-SPR-ogram of pre-hybridisation of ferrocene-mutated oligonucleotide at 5' and in 3' end.....	127
Figure 3.14.CV before and after displacement of ferrocene-CF mutated oligonucleotide in the presence of 10 mM PBS, 150 mM NaCl, pH 7.5.....	128
Figure 3. 15. DPV before and after displacement of ferrocene-CF mutated oligonucleotide in the presence of 10 mM PBS, 150 mM NaCl, pH 7.5.....	129
Figure 3. 16. Nyquist plot of ferrocene-CF mutated displacement by complementary oligonucleotide in the presence of 10 mM PBS, 150 mM NaCl, pH 7.5.....	130
Figure 3. 17. Equivalent circuit for displacement of ferrocene-CF mutated oligonucleotide system in buffer.....	131
Figure 3. 18. CV before and after displacement of ferrocene-CF mutated oligonucleotide in the presence of 1 mM of ferrocyanide/ferricyanide in 10 mM PBS, 150 mM NaCl, pH 7.5.....	132
Figure 3. 19. DPV before and after displacement of ferrocene-CF mutated oligonucleotide in the presence of 1 mM of ferrocyanide/ferricyanide in 10 mM PBS, 150 mM NaCl, pH 7.5.....	133
Figure 3.20. Nyquist plot of ferrocene-CF mutated displacement by complementary oligonucleotide in the presence of 1 mM of ferrocyanide/ferricyanide in 10 mM PBS, 150 mM NaCl, pH 7.5.....	134
Figure 3. 21. Equivalent circuit for displacement of ferrocene-CF mutated oligonucleotide system in ferrocyanide/ferricyanide.....	134
Figure 3. 22. Results obtained by SPR from the pre-hybridisation of ferrocene- mutated oligonucleotide and the subsequent displacement with complementary oligonucleotide at different concentrations of capture probe	135

Figure 3. 23. Results obtained by SPR from the pre-hybridisation of ferrocene-mutated oligonucleotide and the subsequent displacement with complementary oligonucleotide at different concentrations of ferrocene-CF mutated.....	137
Figure 3. 24. Results obtained by SPR from the pre-hybridisation of ferrocene-mutated oligonucleotide and the subsequent displacement with complementary oligonucleotide at different concentrations of NaCl in hybridisation buffer during the pre-hybridisation of ferrocene-mutated oligonucleotide.....	139
Figure 3. 25. Percentage of electrochemical displacement detection of pre-hybridised ferrocene-CF mutated by complementary oligonucleotide target. The controls were carried out displacing with buffer or with a non-complementary oligonucleotide instead of complementary. These results were obtained with DPV in ferrocyanide/ferricyanide.....	142
Figure 3. 26. Electrochemical detection displacement of pre-hybridised ferrocene-CF mutated with different concentrations of complementary oligonucleotide.....	143
Figure 3. 27. Chronoamperometry of ferrocene-CF mutated oligonucleotide hybridised with immobilised capture probe and complementary oligonucleotide hybridised with immobilised capture probe with 1 mM ferrocyanide in solution. Ferrocene-CF mutated hybridised electrodes were also detected in buffer as control.....	146
Figure 4. 1. Tubes eluted from a size exclusion chromatography to separate ferrocene labelled aptamer from ferroceneacetic acid, measured spectrophotometrically at 260 nm.....	164
Figure 4. 2. Cyclic voltammetry of aptamer-ferrocene at 0.025 V s^{-1} scanned between -0.1 and 0.5 V in 10 mM Tris HCl buffer, 150 mM NaCl, pH 7.5.....	165
Figure 4. 3. MALDI-TOF graph of aptamer-ferrocene molecule.....	165
Figure 4. 4. Colorimetric detection of thrombin bound with biotin-aptamer through a chromogenic thrombin substrate. Thrombin substrate was	

incubated at different times and controls without biotin-aptamer and without thrombin were carried out.....	166
Figure 4. 5. DPV of different concentrations of thrombin substrate (β -Ala-Gly-Arg-p-nitroaniline) in solution (peak at 0.5 V) and different concentrations of p-nitroaniline (not produced by catalytic reaction) (peak at 0.7 V) was detected.....	167
Figure 4. 6. Thiol-aptamer-thrombin modified gold electrode detected by DPV using chromogenic thrombin substrate. After 5 minutes of thrombin substrate injection and control with BSA instead of thrombin.....	168
Figure 4. 7. DPV detection of thrombin substrate and p-nitroaniline produced from the thrombin catalysis after 5minutes of substrate incubation in the aptamer-based sensor.....	169
Figure 4. 8. Variation of the substrate height peak current versus time during the hydrolysis of the substrate by thrombin detected in the aptamer-based sensor and measured by differential pulse voltammetry.....	170
Figure 4. 9. Picture of interaction between aptamer and thrombin.....	172
Figure 4.10. Amperometric detection of thrombin through a sandwich format.....	174
Figure 4.11.Chronoamperometric responses of different concentration of thrombin in a sandwich format.....	175
Figure 4. 12. Chronoamperometric response of aptamer-HRP interacted with thrombin immobilised on modified gold. Test of different blocking agent to reduce the non-specific adsorption of aptamer-HRP.....	176
Figure 4. 13. Test of different incubation time of aptamer-HRP with thrombin immobilised on the modified gold surface.....	177
Figure 4. 14. Amperometric detection of aptamer-HRP interacted with an immobilised thrombin on the gold modified surface.....	177
Figure 4. 15. Chronoamperometric response of different concentration of thrombin immobilised on electrode surface and detected with specific aptamer.....	178

Figure 4. 16. Conformational change of anti-thrombin aptamers in presence of thrombin.....	179
Figure 4. 17. e-SPR-ogram of the aptabeacon demonstration. In the insets in situ cyclic voltammetry of e-SPR disc at points indicated by the arrows.....	181
Figure 4. 18. Thrombin-aptabeacon interaction regeneration. The peak height of the CV was plotted.....	183
Figure 4. 19. Chronoamperometry results from the aptabeacon with MP-11 system in the optimisation of aptamer-ferrocene and enzyme concentrations.....	184
Figure 4. 20. Surface plasmon resonance response from the aptabeacon with MP-11 sensor. Response to thrombin, control with BSA, control with buffer and control without Fc-aptamer.....	185
Figure 4. 21. SPR response of different concentration of thrombin and BSA in an aptabeacon with MP-11 format.....	186
Figure 4. 22. Nyquist plots obtained from a ferrocene labelled aptamer and MP-11 modified electrode to detect thrombin. a) Detection of 270 nM Thrombin, b) Control with 270 nM BSA in stead of thrombin, c) Control without thrombin or BSA, d) Control without ferrocene labelled aptamer. On the top of the figure representation of the equivalent circuit used to fit the frequency scans.....	188
Figure 4. 23. Impedance response of different concentration of thrombin and BSA in an aptabeacon with MP-11 format.....	189
Figure 4. 24. Amperometric aptasensor signal to thrombin and controls. In the inset the amperometry is shown.....	190
Figure 4. 25. Amperometric aptabeacon based sensor. Response to different concentrations of thrombin and BSA.....	191
Figure 4. 26. CV of MP-11 and thiol-aptamer-ferrocene mixed monolayer modified electrodes for thrombin detection in real time. (a) Thrombin interaction with aptabeacon-ferrocene, (b) control with BSA and (c) initial CV after thiolated redox-aptamer immobilisation and before exposure to thrombin or BSA.....	192

Figure 4. 27. Amperometric aptasensor in real time. Response obtained from different concentrations of thrombin and BSA (control). In the inset the amperometry is shown.....192

List of tables

Table 1.1	Summary of electrochemical label-free methods for DNA detection.....	25
Table 1.2	Advantages of aptamers over antibodies.....	38
Table 1.3	Ultrasensitive aptasensors transducers.....	41
Table 3. 1.	Electrochemical results of capture probe concentration optimisation in ferrocene-CF mutated pre-hybridised displacement system.....	136
Table 3. 2.	Electrochemical results of ferrocene-CF mutated concentration optimisation in ferrocene-CF mutated pre-hybridised displacement system.....	138
Table 3. 3.	Electrochemical results of NaCl concentration in hybridisation buffer optimisation in ferrocene-CF mutated pre-hybridised displacement system.....	140

List of schemes

Scheme 2. 1. Lithographic scheme of biomolecules patterning on array.....	72
Scheme 2. 2. Electrocatalysis of HRP through a mediator.....	81
Scheme 2. 3. Chronoamperometric detection of hybridisation by way of a diffusional mediator.....	82
Scheme 2. 4. Chronoamperometric detection of hybridisation by way of a redox polymer.....	86
Scheme 2. 5. Scheme of catalytic current production for HRP and ALP enzymes oligonucleotide labelled in an array.....	92
Scheme 3. 1. Schematic diagram of sub-optimum HRP labelled mutated oligonucleotide displacement detection.....	98
Scheme 3. 2. Schematic diagram of sub-optimum ferrocene labelled mutated oligonucleotide displacement detection.....	98
Scheme 3.3. Representation of capture probe sequence and mutated oligonucleotide HRP labelled. The four mutations that contain the sub-optimum oligonucleotide are inside the rectangle.....	98
Scheme 3. 4. Representations of capture probe sequence and mutated oligonucleotide ferrocene labelled. The three mutations that contain the sub-optimum oligonucleotide are inside the rectangle.....	110
Scheme 3. 5. Schematic diagram of sub-optimum ferrocene labelled mutated oligonucleotide displacement detection.....	123
Scheme 3. 6. Redox reaction produced between ferrocene label and ferricyanide.....	124
Scheme 4.1. Schematic representation of thrombin-aptamer interaction detection through a specific thrombin substrate.....	152
Scheme 4. 2. Aptamer base sensor in a sandwich manner.....	152
Scheme 4. 3. Scheme of thrombin detection before its surface immobilisation.....	153
Scheme 4. 4. Schematic presentation of aptabeacon strategy.....	154

Scheme 4. 5. This scheme shows an approximation of aptabeacon with MP-11
system.....154

List of equations

Equation 1. 1. Equation for dsDNA T _m calculation.....	14
Equation 1. 2. Equation for dsDNA T _m calculation by nearest-neighbour method.....	14
Equation 2. 1. Randles-Sevcik equation.....	79
Equation 2. 2. Differential equation of capacitance respect to time.....	80
Equation 3.1. Equation for dsDNA T _m calculation.....	113
Equation 3.2. Electron transfer rate constant equation.....	130
Equation 4.1 Relation of current and concentration for differential pulse voltammetry measurements.....	170
Equation 4.2 Relation of current and surface coverage.....	180
Equation 4.3 Relation of current and enzymatic activity.....	193

Abbreviations

α -Dig-HRP: Anti-digoxigenin horseradish peroxidase

α -Dig-ALP: Anti-digoxigenin-Alkaline phosphatase

Ac: Acetic

AC: Alternate current

Ag: Silver

AgCl: Silver chloride

AFM: Atomic force microscope

Ala: Alanine

ALP: Alkaline phosphatase

Aptabeacon: 20-mer disulfide amine labelled oligonucleotide, for its modification with ferrocene in the 3' end.

Arg: Arginine

Biotin-aptamer: 20-mer biotin labelled aptamer

Biotin-BC target: 22-mer biotin-labelled breast cancer target oligonucleotide

Biotin-capture probe: 19-mer biotin-labelled capture probe oligonucleotide

Biotin-mutated BC capture probe: 18-mer thiol-labelled mutated capture probe oligonucleotide for breast cancer detection

Biotin-wild BC capture probe: 18-mer thiol-labelled complementary capture probe oligonucleotide for breast cancer detection

BSA: Bovine serum albumin

C: Cytosine

C: Carbon

C_{ads} : Capacitance of the immobilised layer

CF: Cystic fibrosis

CF complementary target: 15-mer complementary oligonucleotide

Complementary target: 19-mer complementary oligonucleotide

Complementary-HRP: 19-mer HRP-labelled complementary oligonucleotide

CV: Cyclic voltamperometry

Cys: Cysteine

dATP: deoxyadenosine triphosphates

dCTP: deoxycytidine triphosphates

dGTP: deoxyguanosine triphosphates

Diffusional mediator: ([Os(bpy)₂(pyr-CH₂-NH₂)]Cl)

DNA: Deoxyribonucleic acid

dNTPs: deoxynucleoside triphosphates

DPV: Differential pulse voltammetry

dsDNA: Double stranded deoxyribonucleic acids

DTT: Dithiothreitol

dTTP: deoxythymidine triphosphates A: Adenine

E.Coli: Escherichia Coli

EDC: 1-(3-dimethylaminopropyl)-3-ethyl-carbodiimide

EDTA: Ethylenedinitril tetraacetic acid

ELISA: Enzyme-linked immuno assay

ELONA: Enzyme-linked oligonucleotide assay

e-SPR: Electrochemical surface plasmon resonance

Fc: Ferrocene

Fe(CN)₆³⁻: Hexacyanoferricyanide

Fe(CN)₆⁴⁻: Hexacyanoferrocyanide

Ferrocene-CF mutated: 15-mer ferrocene labelled mutated oligonucleotide

G: Guanine

Gly: Glycine

GPES: General purpose electrochemical system

HCl: Hydrochloric acid

HCV: Hepatitis C virus

HIV: Human Immunodeficiency Virus

HNE: Human neutrophil elastase

HPA: 3-hydroxipicolinic acid

HPLC: High performance liquid chromatography

H₂O₂: Hydrogen peroxide

HRP: Horseradish peroxidase

HRP-complementary: 19-mer HRP-labelled complementary oligonucleotide Melimide-

HRP: Maleimide horseradish peroxidase activated

H₂SO₄: Sulfuric acid

Hybridisation buffer: 10 mM Tris-HCl, 1 mM EDTA, 0.3 x SSC and 2 x Denhardt's solution at pH 7.5

IDE: Interdigitated electrodes

Ig E: Immunoglobulin E

ITO: Indium tin oxide

IUPAC: International Union of Pure and Applied Chemistry

k_f: Heterogeneous electron transfer rate constant

KH₂PO₄: Potassium phosphate monobasic

KOH: Potassium hydroxide

LiRPAs: Ligand regulated peptide aptamers

LNA: Locked nucleic acid

Lys: Lysine

MALDITOF: Matrix assisted laser desorption ionization-time-of-flight mass spectrometry

Maleimide-HRP: Horseradish peroxidase maleimide activated

MgCl₂: Magnesium chloride

M.Tuberculosis: Mycobacterium tuberculosis

Mutated-HRP: 19-mer HRP-labelled mutated oligonucleotide NaCl: Sodium chloride

MW: Molecular weight

NaCl: Sodium chloride

NaH₂PO₄: Sodium hydrogen phosphate

NECEEM: Non-equilibrium capillary electrophoresis of equilibrium mixtures

NHS: N-hydroxysulfosuccinimide

NTPs: Deoxynucleotides triphosphate

p: para

PBS: Phosphate buffer salt

PCR: Polymerase chain reaction

PEG-DE : Polyethylenglycol diglycidyl ether

Phe: Phenilalanine

PNA: Peptide nucleic acid

Pro: Prolamine

QCM: Quartz crystal microbalance

Redox polymer: Poly-vinylpyridine-Os(bipyridine)₂Cl

R_{et} : Electron transfer resistance

RNA: Ribonucleic acid

RT-PCR: Real time- polimerase chain reaction

SA: Streptavidin

SA-HRP: Streptavidin peroxidase labelled

SAM: Self-assembled monolayer

SAW: Surface acoustic wave

SELEX: Systematic evolution of ligands by exponential enrichment

Ser: Serine

SPE: Screen-printed electrode

SPR: Surface plasmon resonance

SSC: Saline sodium citrate buffer

ssDNA: single stranded deoxyribonucleic acids

T: Thymine

Thiol-aptamer: 20-mer thiol labelled aptamer

Thiol-CF capture probe: 15-mer thiol labeled capture probe oligonucleotide

Thiol-capture probe: 19-mer thiol-labelled capture probe oligonucleotide

Thiol-capture probe-Dig: 19-mer thiol digoxigenin-labelled capture probe oligonucleotide

T_m: Melting temperature

TMAH: Tetramethyl ammonium hydroxide

TMB: 3,3',5,5'-Tetramethylbenzidine Liquid Substrate

TNA: (3',2')- α -L-threose nucleic acid

Tris: Tris(hydroxymethyl)aminomethane

Tris-Ac: Tris(hydroxymethyl)aminomethane-acetic

Tris-HCl: Trizma hydrochloride

Tween 20: Polyethylene glycol sorbitan monolaurate

UV: Ultraviolet

VEGF: Vascular endothelial growth factor

vs: Versus

Wash solution: 100 mM Tris-HCl pH 7,5, 150 mM NaCl and 1% Tween

Chapter 1. Introduction

1.1 Biosensors

1.1.1 Definition of biosensor

According to the IUPAC definition (Thevenot et al., 1999); “A chemical sensor is a device that transforms chemical information, ranging from the concentration of a specific sample component to total composition analysis, into an analytically useful signal. Chemical sensors usually contain two basic components connected in series: a chemical (molecular) recognition system (receptor) and a physicochemical transducer. Biosensors are chemical sensors in which the recognition system utilises a biochemical mechanism.”

Thus biosensors can be classified according to the type of their transducer and the recognition element.

The transducers commonly used in biosensors are optical detection, surface plasmon resonance (SPR) (Attridge et al., 1991), fluorescence (Vo-Dinh et al., 1987), colourimetric (Samuleson et al., 1994), or chemiluminiscence (Chiu and Christopoulos, 1996). Electrochemical transducers are based on amperometry (Vincke et al., 1985), potentiometry (Vincke et al., 1985), conductometry (Watson et al., 1987) and impedance spectroscopy (Keese and Giaever et al., 1990)). Moreover piezoelectric transducers are used in biosensors such as the quartz crystal microbalance (QCM) (Tessier et al., 1993), mechanical such as cantilevers (Florin et al., 1995)) and temperature (Danielsson et al., 1992), or magnetic (Kindavater et al., 1990).

The bioreceptor or biorecognition element can be either based on bio-affinity interaction or on bio-metabolic reaction. However, both of these processes involve the specific recognition of the analyte by the biorecognition element. In bio-affinity interaction the transducer detects the binding between the analyte and the receptor pair.

Some examples include antibodies (Jensson et al., 1985), cell receptors (Kingdon, 1985), nucleic acids (Palecek, 1960) or aptamers Potyrailo (et al., 1998). In biometabolic reactions the analyte-receptor interaction results in the production of a product that is converted to a signal by the transducer. In this kind of biosensor, enzymes (De Young and Garrett, 1983), microorganisms (Wang, 1984) or tissue samples (Schubert et al., 1984) are used as the biorecognition element.

Almost any kind of target can be recognised by biosensors including antigens (Jensson et al., 1985), drugs (Kingdon, 1985), xenobiotics (Valdes et al., 1988), low molecular weight molecules (Famulok, 1999), proteins (Lowe et al., 1985) cells (Kingdon, 1985), DNA (Palecek, 1960), among others. This variability permits the use of the device to a wide range of applications. The areas of diagnostics (Pace, 1985), environmental monitoring (Karube et al., 1984), food safety (Watarbe et al., 1984), chemical industry (Datta, 1990), and biosecurity (Bart, 1997) benefit particularly from the analytical advantages of these devices.

1.2 DNA sensors and arrays

1.2.1 Genomic biosensors

A deoxyribonucleic acid (DNA) sensor is a device that incorporates as the biorecognition element a short single strand of oligonucleotide.

DNA sensor technology evolved from Southern blotting, where fragmented DNA is attached to a substrate and then probed with a known gene or fragment complementary to the DNA target. In the case of DNA sensors the attached or immobilised sequence is a known bases sequence of single stranded DNA complementary to the target called probe. In today's practice the oligonucleotide target is isolated and afterwards amplified and labelled by the polymerase chain reaction (PCR) for a subsequent hybridisation and recognition by the immobilised receptor.

More general is the use of DNA microarrays, which is a collection of DNA sensors on the same device, offering the possibility of screening for a large number of DNA sequences at the same time, on the same device and with a short response time.

Identifying DNA sequences of genes and their mutations using microarrays is relevant for the diagnosis of genetic diseases, detection of infectious agents, study of genetic predisposition, development of personalised medicine, detection of differential genetic expression, forensic science, drug screening, food safety and environmental monitoring

In health care, microarray data could be used to find the treatment best suited for a particular patient. Patients with identical histology have a completely different response to therapy, however this is less likely to occur in patients with similar gene expression profile. Probing the gene expression profile can give information about the prognosis of a patient with great precision. Furthermore, microarrays could be used to develop personalised medicine, measuring patient response to drugs, preventing adverse side effects of a drug and predicting the most effective drug for a specific patient. The Roche CYP750 DNA array is already on the market for this purpose.

Drug discovery is another favoured area for the use of DNA microarrays. Pharmaceutical laboratories are working on the study of pathways associated with complex diseases to target new drugs for their treatment, using the data obtained from DNA arrays. In addition, with these techniques, the costly and time-consuming clinical trial, could be come more focused and therefore shorter.

In basic research, microarrays are being used to better the understanding of tissue deterioration, protein functionality or to identify markers of disease.

DNA microarrays are now a mature technology with applications in health care and in medical and biological research. However, the technology is still far from point of care applications and even further from its implementation in home-diagnosis. In such cases, reduced numbers of arrays are necessary but still the high cost and difficulty of use are stopping penetration of DNA sensors in this market.

1.2.2 Steps involved in DNA sensors

The steps implicated in the preparation and analysis of DNA sensors can summarise as follows;

- Probe immobilisation
- Sample preparation
- Hybridisation
- Detection
- Data analysis

A further examination of each stage is detailed next.

1.2.2.1 Probe immobilisation

The first step in the manufacture of a DNA biosensor is the immobilisation of the probe. The most commonly used probes are single stranded deoxyribonucleic acids (ssDNA), although other probes have also been reported in the literature including peptide nucleic acid (PNA) and locked nucleic acid (LNA) (Figure 1.1). In general these modifications are done to improve the stability of the hybridised pair and the nuclease enzymatic degradation resistance of the probes.

PNA incorporate in the backbone repeating N-(2-aminoethyl)-glycine units linked by peptide bonds. Since the backbone of PNA contains no charged phosphate groups, the binding between PNA-DNA strands is stronger than between DNA-DNA strands due to the lack of electrostatic repulsion.

LNA is a nucleic acid analogue containing one or more LNA nucleotide monomers with a bicyclic furanose unit locked in an RNA mimicking sugar conformation. LNA oligonucleotides display unprecedented hybridization affinity toward complementary ss ribonucleic acid (RNA) and complementary ss or double stranded DNA (dsDNA).

Both modified nucleic acid probes show great hybridisation stability and are not easily degraded by either nucleases or proteases. They are also stable over a wide pH range and ionic strength.

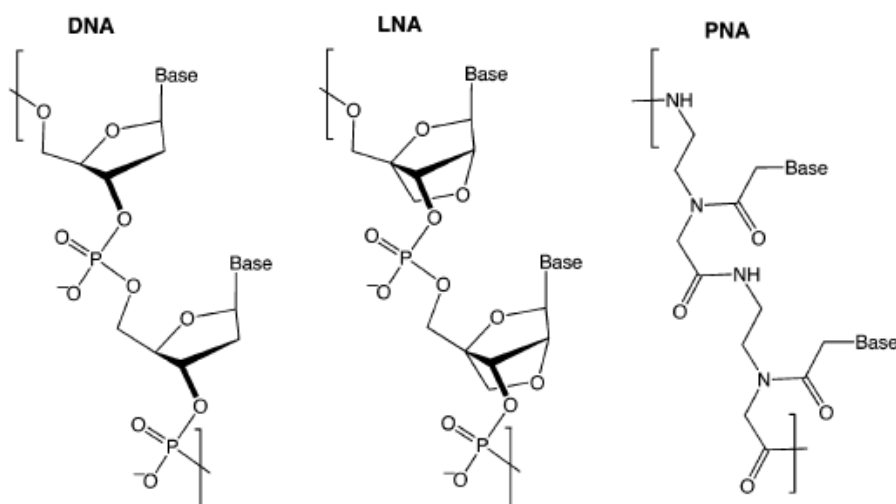


Figure 1.1. Structures of deoxyribonucleic acid (DNA), locked nucleic acid (LNA), and peptide nucleic acid (PNA).

Another way to enhance nuclease resistance of oligonucleotides is to introduce sulfur into the molecule by using phosphorothioate oligonucleotides (Crookes, 1999; Geary et al., 2001). These have been used extensively in antisense therapeutics to generate serum-stable oligonucleotides with increased plasma protein binding and pharmacokinetic profile (Kurreck, 2003).

Fabrication of microarrays begins with the selection of the capture probe sequence. In most cases, these sequences can be found directly from databases such as GeneBank (Benson et al., 1997) and UniGene (Schuler et al., 1996).

Nowadays there exist two different methods for creating microarrays: Synthesising in situ the oligonucleotide or immobilising pre-synthesised oligonucleotides.

- In situ synthesised oligonucleotide

A number of different approaches use in-situ synthesis of oligonucleotide for arraying. The most well known is the Affymetrix photolithography method. The photolithographic process begins by coating a silica wafer with a light-sensitive chemical compound for the linking of the first nucleotide on a solid support. Lithographic masks are used to either block or transmit light onto specific locations of the wafer surface, with the aim of deprotecting the surface that will subsequently be coupled with nucleotides. The coupled nucleotide also bears a light-sensitive protecting group, so the cycle can be repeated until the probes reach their full length, usually 25 nucleotides.

NimbleGen Inc. developed a Maskless Array Synthesizer technology. A similar photosensible compound is used for deprotection but a Digital Micromirror Device controls the pattern of ultraviolet (UV) light projected on the microscope slide instead of a mask, drastically reducing the production cost.

Agilent Technologies and Rosetta Inpharmatics have also developed one more maskless manufacturing process for in situ synthesized DNA microarrays. This synthesis is based on spotting four different phosphoramidite nucleosides directly on the surface and the order of added phosphoramidite nucleoside determines the probe sequence. The spot density of this technology is much lower than light directed synthesis. The standard phosphoramidite chemistry (Hunkapiller et al., 1984; Horvath et al., 1987) is very efficient and allows longer probes to be synthesized (60–100 b). A similar inkjet based in situ DNA synthesis was described by Lausted et al., 2004. The Invitrogen technology

is also based on phosphoramidite chemistry. In this case a photogenerated acid is used to deprotect the nucleosides. Combimatrix uses another variant of synthesising DNA. In this technology electrode arrays electrochemically generate acids to initiate DNA synthesis. The technology provides probes up to 40 bases long. FEBIT biotech's Genome One developed a system that contains everything needed for making a microarray experiment, in-situ DNA synthesis, hybridisation and detection units all within one instrument. Microarrays are synthesised automatically using a maskless technology similar to that described by Singh-Gasson et al., (1999).

- **Pre-synthesised oligonucleotide and cDNA immobilisation**

Pre-synthesised probes present the advantage of possibility of quality control before immobilisation. The following methods have been used for immobilisation:

i. Self assembled monolayer

A self-assembled monolayer (SAM) is formed by spontaneous adsorption or chemical binding of molecules from a homogeneous solution onto a substrate. Different kinds of SAMs are reported, depending on the nature of the adsorbed molecules. For example, alkylsilanes could be used to form very stable monolayers on hydroxylated surfaces such as glass, aluminium oxide, silicon oxide, indium tin oxide (ITO), quartz and mica (Sagiv, 1980). Alkanoic acids form stable SAMs by the production of a surface salt between the carboxylate anion and a surface metal cation such as aluminium oxide, silver, silver oxide or copper oxide (Ulman, 1996). However the most widely applied SAM in DNA immobilisation is made by the adsorption of sulphur- based compounds such as thiols, disulphides or sulphide on gold (Levivky et al., 1998), silver (Bryant and Pemberton, 1991), copper, platinum (Mebrahatu et al., 1988), palladium (Riepl et al., 2002), mercury (Rampi et al., 1998) and glass. A dative bond results from the interaction of thiol with gold surface, resulting in that are robust and stable structures. The strength of the metal- sulphur bond is on the order of 40- 50 kcal mol⁻¹ (Dubois and Nuzzo, 1992). However in electrochemical applications the stability of the film at the potential of the underlying electrode should be taken into account. SAMs are stable at potentials between -0.8 V and 1.4 V (vs. Ag/AgCl), whereas outside this range thiols are desorbed (Yang et al., 1996).

Different methods of creating DNA SAMs are reported: A monolayer of thiol-DNA on solid support (Levicky et al., 1998), a mixed monolayer of thiol-DNA with a thiol-compound (Boozer et al., 2006) or through an indirect immobilisation of DNA, which is covalently bound with a previous SAM (Wrobel et al., 2003). Direct thiol-DNA SAM can produce densely packed monolayers, which could reduce the amount of DNA hybridised. This problem can be overcome with mixed SAMs. Indirect SAM increases the number of steps and reduces the immobilisation efficiency.

In microarray platforms, mixed SAMs of thiol labelled ssDNA on gold surface is the most common method for capture probe immobilisation, due to its simplicity, low cost and robustness.

ii. Chemical binding

Immobilisation of ssDNA is usually carried out by means of covalent bonds or crosslinking, between a molecule already attached to the surface and a reactive group of the DNA. The process should not affect the hybridisation capability.

An example reported in the literature is the electrochemical copolymerization of pyrrole and oligonucleotides bearing a pyrrole group. The resulting polymer consists of pyrrole chains linked covalently to ssDNA. The pyrrole-DNA is incorporated in a polypyrrole film to a platinum surface (Livache et al., 1994). However the most commonly used technique is the activation of a carboxylic acid with carbodiimide 1-(3-dimethylaminopropyl)-3-ethyl-carbodiimide (EDC) and *N*-hydroxysulfosuccinimide (NHS) for reaction with an amine group. Following this method, carbon paste electrodes modified by stearic acid were used as a solid phase to which ssDNA was covalently bound (Mikkelsen, 1996). Like wise a synthesised ssDNA was immobilised covalently to a graphite electrode modified chemically with primary amino groups (Liu et al., 1996).

iii. Affinity

Streptavidin or avidin with biotin is the most applied affinity interaction in ssDNA immobilisation. Surface immobilised streptavidin can be used to subsequent immobilisation to a biotin labelled oligonucleotide.

Tetramer binding was formed between streptavidin and biotin, resulting in a very high affinity bond ($K_a = 1 \times 10^{15} \text{ M}^{-1}$) (Ebersole et al., 1990). This value results to stability nearly equal to that of a covalent bond. The bond can only be broken under the extreme conditions. Because of this strong interaction, the complex formation is nearly unaffected by extreme values of pH or temperature, organic solvents, and denaturing agents. However, the presence of the large protein layer may results to non-specific binding sites and compromise the sensitivity and selectivity of certain types of sensors.

A mixture of redox polymer, polyethylene glycol and streptavidin was used for biotin-DNA immobilisation on carbon electrodes (Mir and Katakis, 2005)

iv. Adsorption

This immobilisation procedure is based on the direct adsorption of DNA on the substrate. Materials reported for this type of immobilisation include nitrocellulose (Wang et al., 1996), nylon membranes (Wang et al. 1997), polystyrene, metal surfaces (Pang and Abruña, 1998) and carbon (Marrazza et al., 1999).

Two different adsorption methods are described; physical and electrochemical adsorption.

Physical adsorption is carried out by soaking the surface with the solution that needs to be immobilised and leaving the surface to dry. Brett et al., (1998), followed this procedure for DNA immobilisation on glassy carbon electrodes.

Electrochemical adsorption uses the fact that the DNA backbone is negatively charged, so that a positive potential applied to an electrode attracts these biomolecules (Palacek et al, 1998)

Adsorption is the simplest method to immobilise DNA because it does not require other reagents or any special nucleic acid modifications. However the main disadvantage of this method is the poor hybridisation efficiency and instability of the nucleic acid layer.

v. Electronic addressing

This technique uses the difference in charge between the biomolecule and the electrode to attract it to the electrode surface to immobilise the capture biomolecule on the surface.

Negatively charged colloidal gold nanoparticles conjugated with capture probe oligonucleotides were electrochemically addressed to the electrode surface, when a positive potential was applied (Campàs and Katakis, 2004).

Furthermore, the patented NanoChip[®] Electronic Microarray by Nanogen uses this technology for DNA immobilisation on microarrays. Nanogen's technology involves electronically addressing biotinylated oligonucleotides towards a streptavidin-coated surface.

vi. Entrapped in a matrix

ssDNA can be retained in a mesh that has been previously immobilised on a solid support. Meshes are characterised by their large area of adsorption, which increases the amount of oligonucleotide strands attached, increasing the sensitivity of the resulting system. The main disadvantage is the lack of oligonucleotide orientation, which decreases the accessibility to the captured molecule.

The principal matrices used for this purpose are polymers, membranes and dendrimers.

A conducting polythionine modified electrode as matrix to DNA immobilisation has been used for DNA hybridisation and electrochemical detection (Xu et al., 2005). A polylactic acid nanofiber membrane has been used as a substrate for oligonucleotide assemblies (Li et al., 2006). As well, DNA immobilisation was achieved by its adsorption onto a nylon membrane by Pirividori et al., (2001)

Additionally, dendrimers, highly branched structures with a controlled exponential growth, were used as matrix for ssDNA entrapment (Wang and Jiang, 1998)

vii. Entrapped in a composite

In this technique, the biomolecule is mixed uniformly with graphite powder and mineral oil and this mixture is used for the fabrication of electrodes. This composite then acts as

a reservoir of oligonucleotide capture probes. This method does not require the modification of the oligonucleotide, however there is a limited accessibility to the capture probe for the hybridisation of the oligonucleotide target (Millan et al., 1994)

1.2.2.2 Sample preparation

- DNA extraction and purification

Prior to analysis the DNA in the sample must be extracted and purified. Whole blood is first fractionated to isolate DNA-containing cells. The cells are then lysed with detergents and proteins are digested with proteinase K. DNA is purified from the lysate by organic extraction with phenol and chloroform and concentrated by precipitation with alcohol. The entire procedure is laborious and time consuming. However, there exists a wide variety of commercially available kits for DNA extraction and purification that greatly simplify and reduce the time for the process.

- DNA labelling and amplification.

Purified DNA needs to be amplified and labelled for its hybridisation detection into the microarray. For this purpose a PCR is carried out.

PCR is a molecular biology technique used for in vitro replication of DNA. PCR is used to amplify a short and well defined part of DNA strand and for the labelling of this DNA strand.

For DNA amplification and labelling several components are required. The DNA template, which contains the sequence regions to be amplified, two primers one of them labelled, which are short ssDNA sequences that determine the beginning and the end of the region to be amplified and also label the DNA target, the enzyme that helps in the polymerisation of the DNA, Taq DNA polymerase, and deoxynucleotides triphosphate (NTPs) that are the monomers that build the new DNA are also needed. All these reagents have to be dissolved in a buffer that provides a suitable environment for DNA amplification.

A thermal cycler is the device that makes DNA amplification possible. The tubes containing the components for the amplification are placed into the thermal cycler, and the equipment is programmed to carry out cycles of heating and cooling at the precise temperature required for the amplification.

The PCR process consists of a series of twenty to thirty cycles and each cycle has three steps. During the first step, called denaturing, the dsDNA template is heated at 94-96 °C for 1-2 minutes in order to separate the strands. After separating the DNA strands, the temperature is lowered for the hybridisation of the primers on the ssDNA target, called annealing. An accurate selection of the temperature for annealing stage is extremely important for amplification success. The temperature of this step depends on the primers and is usually 5°C below their melting temperature (45-60°C). Finally, the elongation step is carried out to polymerise the DNA target, binding the NTP blocks. The elongation temperature depends on the Taq DNA polymerase and the time for this step depends on the length of the DNA fragment to be amplified. It is assumed that this takes 1 minute per thousand base pairs. A final elongation step is frequently used after the last cycle to ensure that any remaining single stranded DNA is completely copied. This step uses the same temperature as elongation step but it takes longer, around 10-15 minutes.

These three steps are repeated to obtain an exponential growth of the amplified DNA.

Different modification of the original PCR has been developed:

- Reverse Transcription PCR: Conventional PCR requires a previous transcription of the RNA that is isolated from the cell to DNA. Reverse transcription PCR (RT-PCR) is the method used to directly amplify, isolate or identify a known sequence of RNA.
- Inverse PCR: One limitation of conventional PCR is that it requires primers complementary to the end of the target DNA. However, inverse PCR allows amplification of unknown double strand sequences. This technique involves a series of digestions and self-ligations before cutting by an endonuclease, resulting in known sequences at either end of the unknown sequence.

- **Nested PCR:** Nested PCR was developed to reduce contamination in products due to the amplification of unexpected primer binding sites. This involves two sets of primers, used in two successive runs of the PCR, the second set intended to amplify a secondary target within the first run product.
- **Asymmetric PCR:** Asymmetric PCR is used to predominantly amplify one strand of the original DNA. PCR is carried out as usual, but with a great excess of the primers for the chosen strand and due to the not completely exponential amplification later in the reaction after the limiting primer has been used up, extra cycles of PCR are required.
- **Touchdown PCR:** Touchdown PCR is a variant of PCR that reduces nonspecific primer annealing by lowering the annealing temperature between cycles more gradually.
- **Quantitative real-time PCR:** Quantitative real-time PCR uses fluorescent dyes and probes to measure the amount of amplified product in real time. It combines amplification and detection and is therefore a strong alternative method to DNA microarray.
- **Multiplex-PCR:** The use of multiple primer sets within a single PCR reaction to produce amplicons of varying sizes specific to different DNA sequences permits targeting multiple genes at once.

1.2.2.3 Hybridisation

The recognition event in DNA sensors is based on the affinity between complementary DNA sequences and the immobilised capture probe. Therefore the optimisation of

parameters for hybridisation is critical. The variables that affect the hybridisation efficiency and stringency are the salt concentration, temperature, G+C content, length of probe and type of nucleic acid duplex.

The commonly used salt in the hybridisation buffer is sodium chloride. The cations of this salt stabilise the two negatively charged backbone strands of oligonucleotide neutralising these negative charges reducing the repulsion and stabilising the hybridised duplex. Hybridisation typically is carried out in 0.45-1 M NaCl.

Temperature is an important variable to optimise in the hybridisation. The melting temperature (T_m) of the pair is the habitual factor. T_m is defined as the temperature at which 50 % of the DNA molecules form a stable double helix and the other 50 % have been separated to single stranded molecules. Typically hybridisation is performed at 5-10 °C below the T_m of the duplex. This value is dependent upon the length of the sequence, the shorter the probe sequence, the lower the melting temperature. The number of mismatches of the pair also determines the effective melting temperature of a hybrid, T_m decreasing by about 1 °C for every 1 % of mismatched base pairs (Maniatis et al., 1982). Furthermore a higher percentage of G + C bases or higher concentration of salt increases T_m . The T_m for DNA-DNA hybridisation can be approximated by the following equation (Howley et al., 1979) (equation I.1);

$$T_m = 81.5 C + 16.6 (\log_{10} [Na^+]) + 0.41 (\% G+C) - (600 / \textit{strand length})$$

The nearest-neighbour method is another option to calculate the T_m value (equation I.2);

$$T_m = (1000 \Delta H) / A + \Delta S + R \ln (C/4) - 273.15 + 16.6 \log [Na^+]$$

ΔH (Kcal mol⁻¹) is the sum of the nearest-neighbour enthalpy changes for the hybrids. A is a constant containing corrections for helix initiation, ΔS (Kcal mol⁻¹) is the sum of the nearest-neighbour entropy changes, R is the gas constant (1.99 cal K⁻¹mol⁻¹), and C is the concentration of the oligonucleotide (Breslauer et al., 1986).

The influence on T_m of G + C proportion in the sequence is due to the fact that C-G being linked through three hydrogen bonds while the A-T pair has only two hydrogen bonds. Therefore a higher percentage of C-G confers more stability to the complex.

The increase of the sequence length increases the complexity of the molecule. The complexity inherent in the sequence of the molecules renders the association extremely specific for any molecule longer than sixteen nucleotides. Thus, lengthy and complex sequences results in more difficult hybridisation.

1.2.2.4 Detection

- Optical transducers

Most commercial available DNA microarrays use fluorescence transduction. Oligonucleotides are labelled with red and green fluorophores to distinguish between sample and controls. Thus, four colours can be detected in a fluorescence DNA microarray: green is commonly used for control detection, red indicates target hybridisation, yellow fluorescence represents a combination of control and sample DNA, where both hybridized equally to the capture probe and black represents areas where neither the control nor sample DNA hybridized to the capture probe. Each spot on an array is associated with a particular sequence. Depending on the type of array used, the location and intensity of a colour will show whether the gene, or mutation, is present in either the control and/or sample DNA and the intensity will provide an estimate of the expression level of the genes in the sample and control DNA.

Indirect fluorescence labels are also used whereby the DNA target is biotinylated after the PCR. Once it is hybridised a subsequent incubation with streptavidin-phycoerythrin, links the fluorescence marker to the hybridised target.

A wide range of different optical transducers for DNA biosensors and DNA arrays are reported in the research literature.

Planar waveguide fluorescent sensors (Herron et al., 2006), and a fiber optic-based biosensor assay performed by flowing a solution containing the fluorescently tagged ligand molecules over the DNA already immobilised have been reported (Anderson et

al., 1992). A frequency-doubled diode-pumped ultrashort pulse Yb:KGW laser produces served as excitation source for an optical DNA sensor based on fluorescence lifetime measurements (Major et al., 2005). Oligonucleotides immobilised onto the waveguide surface were used to detect fluorescein-labelled complementary sequences at the nanomolar level (Graham et al., 1992). All these fluorescence sensors described require the previous label of the sample. In contrast, fluorescent molecular beacons provide a label-free platform and real time detection of the hybridisation. Molecular beacons are single-stranded oligonucleotide probes that possess a stem-and-loop structure. The loop portion is complementary to a target ssDNA, while the stem is formed by 5 to 7 bp from two complementary arm sequences that are in the two ends of the loop. A fluorophore is attached to the end of one arm, while a quencher is attached to the end of the other arm. The stem maintains a close proximity of the two moieties, causing fluorescence to be quenched by energy transfer. When the complementary target hybridises with the beacon probe, the stem is opened leading to restoration of fluorescence. Fluorescent molecular beacons have been used in single biosensor to monitor the reaction dynamics of the DNA hybridization process (Yao et al., 2003), as well as in arrays for detection of multiple analytes (Yao and Tan, 2004).

In addition to fluorescence, other kinds of optical methods are used as transducers in DNA biosensors, including colourimetry, chemiluminescence, surface plasmon resonance (SPR) and atomic force microscope (AFM).

In colourimetric transduction methods an enzyme is used for direct labelling of the oligonucleotide target or indirectly through an affinity interaction between an enzyme-antibody and the antigen labelled oligonucleotide. Enzyme labels require the addition of its substrate to produce a coloured product. This procedure was coined Enzyme-linked oligonucleotide assay (ELONA) and it is widely applied in clinical diagnostics (Schaal, 1991; Matz, 1987).

Olofsson et al., 2006 used the absorbance changes induced by hybridisation events in the interfacial region of the particles immobilised on the walls of a quartz cuvette. Interaction of streptavidin capture probe with avidin-coated colloidal gold particles and immobilisation on a biotin-modified planar lipid bilayer allows following the hybridisation kinetics of 15-mer complementary DNA strands without the introduction of labels.

Li and Rothberg, (2004), developed a label free and easy to use colourimetric method for hybridisation detection, exploiting the different effects of ssDNA and dsDNA on gold colloid nanoparticles. ssDNA stabilise colloidal suspensions and addition of salt does not produce an aggregation of the colloid. However, dsDNA adsorbed on colloidal gold is not stable. When salt is added a change of colour from red to blue is observed indicating the aggregation of colloids. The hybridisation of the DNA target ssDNA to dsDNA can thus be detected. This assay detected 100 femtomoles of DNA target in 5 minutes.

Chemiluminescence is the emission of light resulting from a chemical reaction. For example, luminol and hydrogen peroxide in the presence of a suitable catalyst produced 3-aminophthalate in an excited state. The decay of the excited state is accompanied by the emission of light. Chemiluminescence reagents include luminol, cyalume, Ru(bipyridine)₃²⁺ and pyrogallol.

Enzymatic chemiluminescence is a common technique for a variety of detection assays. An HRP molecule is tethered to the molecule of interest. This then locally catalyses the conversion of the enzymatic chemiluminescence reagent into a sensitised reagent, which on further oxidation by hydrogen peroxide, produces a triplet excited carbonyl which emits light when it decays. DNA probes covalently immobilised onto the end of the optical fibre was hybridised with a HRP labelled complementary target and the hybridisation was detected by chemiluminescence (Zhang et al., 1999).

The electrochemiluminescence combines optics and electrochemistry obtaining high sensitivity. Luminol generated by a carbon electrode and a polypyrrole-coated carbon electrode was used for the electrochemiluminescence detection of the hybridisation between a complementary ssDNA probe covalently linked to a polypyrrole support (Calvo-Nuñez et al., 2005).

Surface plasmon resonance (SPR) is a widely used optical technique for the examination of the interaction between label-free biomolecules. BIAcore from Pharmacia is the most commercialised SPR device. Surface plasmon resonance occurs under certain conditions when a thin film of metal (gold or silver) is placed inside the laser beam. When the photons of the incoming light find a dielectric medium placed on top of the gold and this dielectric medium has a different dielectric constant than gold, the free electrons in the gold fluctuate. This electron fluctuation gives charge fluctuations in the metal. The metal layer is very thin and therefore the charge

fluctuations are only taking place at the surface and cause an electromagnetic surface wave, called surface plasma oscillations. SPR is detected by measurement of the intensity of the reflected light. At the SPR angle, a dip in intensity is measured. The refractive index of the sensor surface changes upon binding of macromolecules to the surface. As a result, the SPR wave will change and therefore the angle will change accordingly. There is a linear relationship between the amount of bound material and shift in SPR angle.

SPR use for DNA detection is very commonly applied (Bianchi et al., 1997; Oyama et al., 2000; Sawata et al., 1997).

The atomic force microscope (AFM) is an optomechanical sensor typically used in the study of surfaces but has also found application in the study of biomolecule interactions. AFM consists of a microscale cantilever with a sharp tip at its end that is used to scan the surface. The cantilever is typically silicon or silicon nitride with a tip dimension in the order of nanometers. When the tip is brought into the proximity of a sample surface, forces between the tip and the sample lead to a deflection of the cantilever, which is measured using a laser spot reflected from the top of the cantilever into a photodiode array. Electrochemical DNA sensor surface and the hybridisation was characterised by AFM (Chiorcea and Brett, 2004), and ssDNA was covalently attached onto AFM tips as specific ligand. These tips were interacted with the buffer solutions with or without free complementary ssDNA target to be detected. Immobilisation and hybridisation onto the cantilever surfaces were observed by optical and fluorescence microscope (Kocum et al., 2006).

- Piezoelectric transducers

Piezoelectric transducers have been incorporated in DNA biosensors. This kind of transducer has the advantage of high sensitivity without requiring any labelling of the interacting components. The most used piezoelectric readout is the quartz crystal microbalance (QCM). This device measures mass by detecting the change in frequency of a piezoelectric quartz crystal when it is disturbed by the addition of a small mass such as oligonucleotide strand. It can work in vacuum or liquid environment thus making it useful to determine the properties of polymers and adhesion of proteins. Since frequency measurements can be made to high precision, it is easy to measure small

masses. The correlation between mass and frequency is defined by the Sauerbrey equation. A QCM DNA sensor was developed immobilising a thiolated ssDNA probe onto the QCM sensor surface through a self-assembly process. Hybridisation was induced by exposing the ssDNA probe to the biotin labelled complementary target DNA and detected by the frequency change. Streptavidin conjugated Fe_3O_4 nanoparticles were used as mass enhancers to amplify the frequency change (Mao et al., 2005). Detection of DNA hybridisation was also performed by QCM on a platinum quartz crystal modified with ssDNA probe immobilised on gold nanoparticles (Liu et al., 2005). Lee et al., (2005), developed a micro piezoelectric sensor for incorporation in Lab-on-a-chip applications. This micro sensor used the mass micro balancing technique, which is the foundation of QCM. Instead of using circular quartz crystal plate, a micro cantilever was used in the micro sensor.

Surface acoustic wave (SAW) is an alternative piezoelectric transducer that was used for detection of the immobilisation and hybridisation of DNA on gold coated SAW devices. The relative change in the frequency of the two oscillators was monitored to detect the immobilisation of probes and the subsequent hybridisation (Kwon and Roh, 2004).

- **Electrochemical transducers**

Whereas optical detection methods with fluorescent dyes have dominated the DNA sensor industry and piezoelectric techniques can achieve low limits of detection, the application of electrochemical methods can provide significant advantages including high sensitivity, small dimensions, low cost, speed, easy signal integration, and compatibility with microfabrication technology (Palacek, 2002; Popovich and Thorp, 2002).

Electrochemical techniques broadly used for sensor transduction are voltammetry, amperometry and impedance spectroscopy. Fewer of examples using potentiometry and conductimetry have been reported.

Potentiometric sensors measure the potential of the working electrode with respect to a reference electrode. DNA hybridisation on carbon paste electrodes was detected by stripping potentiometric measurement of electroactive metal complexes associated with surface hybrids (Wang et al., 1996 (b)).

Conductimetric sensors measure the change in the conductance between a pair of metal electrodes as a consequence of the immobilisation and interaction of biomolecules. A method for the introduction of polyamine-modified cytidine units into predetermined positions of the DNA chain during automated synthesis was developed. The functionality of synthesised oligonucleotide modified by thiol group for the detection of DNA hybridisation was used in conductometric experiments (Oretskaya et al., 2002).

When the current is recorded in a fixed potential as a function of time, the technique is called chronoamperometry and when the potential may vary with time in a predetermined manner and the current is measured as a function of potential that is called voltammetry or voltamperometry.

Chronoamperometry generally involves the use of an enzyme as biomarker molecule. As has been explain before in this section some colourimetric detection also involves the use of enzyme labels and are usually the same enzymes used in electrochemical detection. However, due to the higher sensitivity of electrochemistry technique, lower limits of detection are achieved with these techniques compared to ELONA. Campbell et al., (2002), reported an enzyme DNA sensing technique involving the electropolymerisation of a redox polymer, where amino labelled oligonucleotides were electrodeposited. Oligonucleotide probe was captured at the electrode surface and hybridised to a reporter strand modified with HRP. Zhang et al., (2003), reported a low limit of detection using enzyme labelling. 0.5 fM of HRP modified oligonucleotide was detected in a microelectrode.

A variety of labelling enzymes have been used such as glucose oxidase (Patolsky et al., 2002), and avidin-alkaline phosphatase, which resulted to the biocatalysed precipitation of an insoluble product on the surface, allowing lower limit of detection no PCR pre-amplification (Patolsky et al., 2001).

Various voltammetric techniques have been reported in DNA biosensors. Cyclic voltamperometry was used to detect methylene blue intercalated in the dsDNA. This detection was carried out on a multi-electrode array that was able to distinguish perfectly matched dsDNAs from both ssDNAs and ds mismatched DNA (Cho et al., 2002). Differential pulse voltamperometry was used to detect the interaction of DNA with redox-active 1,10-phenantroline-5,6-dione osmium complex (Del Pozo et al., 2005). Several other ingeniouou methods have been used to monitor directly or indirectly hybridisation: Square wave voltammetry using methylene blue as

electroactive label (Pournaghi et al., 2006), sinusoidal voltammetric detection at copper microelectrodes based on the electrocatalytic oxidation of sugars and amines at copper surfaces (Singhal and Kuhr, 1997), or ion transfer voltammetry monitoring the concentration of cations in solution, which to decrease in the presence of DNA (Horrocks and Mirkin, 1998). Anodic stripping voltammetry was used to detect the release of the gold metal atoms anchored on the hybrids (Authier et al., 2001), and alternating current voltammetry to detect DNA hybridisation events by the site-specific incorporation of ferrocene derivatives into DNA oligonucleotides (Yu et al., 2001).

Impedance is a highly sensitive electrochemical technique used in DNA biosensors.

Electrochemical impedance is measured by applying an alternating current (AC) at a fixed potential to an electrochemical cell and measuring the current through the cell. The response is an AC current signal, containing the excitation frequency and its harmonics. Electrochemical Impedance is normally measured using a small excitation signal and the circuit ability to resist the flow of electrical current is measured. An impedance spectrum is a representation of the impedance of a circuit element as a function of frequency. A DNA sensor based on double layer capacitance variations due to DNA hybridisation was developed (Brett et al., 1999; Ma et al., 2006). Peng et al, (2006), described an impedance sensor based on the detection of oligonucleotide hybridised by incorporating CdS nanoparticles on the dsDNA. However the most widely applied methodology for impedance detection of biomolecules interaction is the use of ferrocyanide/ferricyanide solution. The change on the electrode surface due to hybridisation event reveals an increase in the electron-transfer resistance at the electrode surface upon the construction of the double-stranded assembly. This is attributed to the electrostatic repulsion of $\text{Fe}(\text{CN})_6^{3-}$ upon formation of the negatively charged double-stranded superstructure (Patolsky et al., 1999; Park et al., 2005).

1.2.2.5 Data analysis

Users of DNA microarray technology are often initially overwhelmed by the amount of data generated by microarrays. To aid users in managing and mining this wealth of data,

a set of analysis tools has been developed that help transform raw hybridisation signal measurements into biologically meaningful results.

The data analysis evaluates the abundance of each transcript represented on the array and labels it as either present, absent, or marginal. The algorithm identifies and removes the contributions of stray hybridisation signals, and combines the results from probes that interrogate different fragments of a transcript. The statistical significance of each detection call is indicated by an associated value.

The algorithm also provides indicators of sample integrity, assay execution, and hybridisation performance through the assessment of control hybridisation. Therefore, users can determine the quality of the raw data and tailor subsequent analyses accordingly. Additionally this software can group together samples or genes with similar expression patterns. These algorithms can be used to address a variety of research questions, such as searching for new disease classes or novel relationships between genes.

1.2.3 Electrochemical label-free DNA sensors

In the previous sections different kinds of transducers were described. Electrochemical transduction offers some advantages that make it competitive for transduction of DNA arrays. However the majority of the examples described require the previous labelling of the target for its detection. The necessity to modify the target DNA with labels is costly, laborious and requires skilled personnel. However, labelling is an effortless part of sample preparation when PCR amplification is used. For this reason when labelless electrochemical detection is discussed, it only has sense when it also provides a low detection limit. In this section different strategies for electrochemical label free DNA detection are described.

Some examples have already been commercialised. The first example was the eSensorTM fabricated by Motorola Life Science Inc (Farkas, 2001). This electrochemical DNA sensor proceeds via a sandwich hybridisation assay, in which three DNA strands are involved. Thiol capture probe is self-assembled on gold electrode, where it is

hybridised to the DNA target. The ferrocene labelled signalling oligonucleotide serves to detect the target upon hybridisation. Other examples of electrochemical sandwich DNA sensors using dimethylcarbanyl ferrocene (Yu et al., 2001) or colloidal gold nanoparticles as labels (Ozsoz et al., 2003) were reported.

Friz biochem commercialised the EDDATM (Electrically Detected Displacement Assay) for single nucleotide polymorphism (SNP) detection. The sensor was based on displacement of the target hybridised with the capture probe that contains the SNP with a labelled complementary oligonucleotide (Liepold et al., 2005).

Toshiba Company developed the GenelyzerTM. This DNA sensor is based on the electrochemical detection of the Hoechst 33258 molecule's intercalation into the dsDNA (Hashimoto et al., 1994). When an intercalator such as Hoechst33258 or daunomycin (Wang et al., 1998) was inserted between the double-helix structure of the dsDNA with the help of its planar aromatic ring, an enhancement in the redox signal was observed. In contrast, some intercalators such as methylene blue have affinity towards ssDNA, so a decrease of electrochemical signal was observed after hybridisation (Meric et al., 2002). Several metal complexes such as cobalt phenanthroline (Erdem et al., 1999), cobalt bipyridine (Millan et al.(b), 1993) ruthenium bipyridine (Yang et al., 2002), and anticancer agents such as echinomycin (Jelen et al., 2002) and epirubicin (Erdem and Ozsoz, 2001), were used as labels for the detection of hybridisation.

GeneOhm Science Inc used the flow of the electrical charge through DNA to develop their DNA sensor, the ePlexTM, which can detect single nucleotide polymorphisms. Palecek, (1960), studied on mercury electrode the relationship between the signals of DNA reduced or oxidised to discriminate ssDNA and dsDNA, afterwards oxidation of DNA was detected by adsorption stripping voltammetry for hybridisation quantification (Palecek, 1988). However, this strategy was complicated by a significant background current. This problem was overcome by removing the sources of background interference. Wang and Kawde, (2002), used magnetic beads modified with DNA probes that after hybridisation were magnetically separated from the solution, and free from interfering adenine or guanine nucleosides. 40 femtomoles in 50 μ L was detected by this assay. A method to detect DNA oxidation indirectly through mediators has been reported. Armistead and Thorp, (2000), used a polypyridyl complex of osmium and ruthenium to mediate the electrochemical oxidation of guanine to detect DNA target

amplified by RT-PCR. This method achieved a detection limit of 550 attomoles in 50 μL .

Fan et al., (2003) reported the realisation of an electrochemical sensor involving a molecular beacon strategy. The molecular beacon was a ferrocene labelled DNA stem-loop structure that self-assembles onto gold. Hybridisation induced the opening of the stem-loop, which in turn significantly altered the electron-transfer tunnelling distance between the electrode and the ferrocene label. The resulting change in electron transfer efficiency is readily measured by cyclic voltammetry at target DNA concentrations as low as 10 pM.

The production of insoluble products was used by Patolsky et al., (2002), to detect DNA hybridisation. 5-bromo-4-chloro-3-indol phosphate is enzymatically converted to an insoluble indigo product. The DNA target was detected through a sandwich assay with a third oligonucleotide labelled with alkaline phosphatase (ALP). When ALP is attached, indigo product was precipitated and the electrochemical response of ferricyanide in solution decreased. A detection limit of 50 fM was achieved through this method.

DNA hybridisation on the electrode surface induced a variation of electron transfer resistance and capacitance of the surface that make it detectable a label-free target by impedance (Hason et al., 2002; Katz and Willner, 2003).

Moreover, field effect sensors were used to directly monitor the increase in surface charge when DNA was hybridised on the positively charged polymer modified electrode surface without any need of label (Fritz et al., 2002).

Table 1.1 Summary of electrochemical label-free methods for DNA detection

Transductor	Configuration	Sensitivity	Reference
CV	Sandwich with gold nanoparticles amplification	2 pM	Ozsoz et al., 2003
CV	Sandwich ALP labelled, detection of precipitated product	50 fM	Patolsky et al., (2002)
Chronocoulometry	Electrochemical detected displacement assay (EDDA)	1000 bacteria mL ⁻¹	Liepold et al., 2005
CV	Intercalator	600 fM	Tansil et al., 2005
DPV	Metal intercalator	20 μM	Maruyama et al., (2001)
Square wave voltammetry	Intercalator displacement	80 mM	Huey et al., (2005)
Adsorbative chronopotentiometry	Guanine oxidation with mediator and magnetic beads	800 pM	Wang and Kawde, (2002)
CV	Guanine oxidation with mediator	10 pM	Armistead and Thorp, (2000)
CV	Ferrocene-beacon	10 pM	Fan et al., (2003)
Impedance	Direct detection using mediator	0.8 fM	Berggren et al., (1999)

1.3 Aptasensors

1.3.1 Proteomic biosensors

DNA (Deoxyribonucleic acid) biosensors are the subject of intense research and development, which has yielded several commercial platforms. The results of the human genome project increase further the possible applications of these biosensors. However the DNA sequence information provides a static picture of the possibilities in which the cell might use its proteins but cell life is a dynamic process. Therefore an important value of the genetic information lies in its ability to predict the outcome, the phenotype. Nevertheless the translation of RNA (Ribonucleic acid) leads to a differential protein expression and in addition is the posttranslational modification of translated proteins that determines functional forms, so at the DNA level is difficult to assess the functionality of gene product.

Due to the discrepancy between the genotype and the phenotype it is desirable to detect also proteins to better understand the cellular function as well as for early detection of diseases and monitoring the progression of existing diseases or the effect produced by a drug in the organism

Microarray technology provides a tool to analyse a large number of molecules simultaneously. Antibody-based microarrays are being developed for the analysis of a large number of proteins (Dove, 1999). Randox laboratories launched the first protein array in 2003, nevertheless proteomics, the direct detection of gene expression products, poses a formidable technological problem. As is exposed in this section, microarrays based on aptamers could address this problems because of their combinatorial production, and possibility to generically transducer their affinity interactions.

1.3.2 Aptamers

Aptamers are small synthetic oligonucleotides (40-100 bases) isolated from random combinatorial libraries most commonly by exponential enrichment called SELEX (Systematic Evolution of Ligands by EXponential enrichment). As a result, a unique three-dimensional structure for the binding of their target can be detected. Aptamers can specifically recognise and bind to virtually any kind of target including, ions (Smironov and Shafer, 2000), whole cells (Famulok et al., 2000), drugs (Varani and Gallego, 2001), toxins (Jayasena, 1999), low molecular weight ligands (Famulok, 1999), peptides (Wilson and Szostak, 1999) and proteins (Mc Cauley, 2003).

The affinity of aptamers depends on the kind of target. Aptamers against small molecules have affinities in the micromolar range, as in the case of dopamine, 2.8 μM (Lorsch and Szostak, 1994) or ATP, 6 μM (Kiga et al., 1998). Affinities in the nanomolar and subnanomolar range are found against some large molecules as proteins, for example, vascular endothelial growth factor (VEGF) with an affinity of 100 pM (Ruckman et al., 1998), and keratinocyte growth factor, 1pM (Pagratis et al., 1997).

As well as high affinity aptamer also demonstrate high specificity. Using aptamers can discriminat targets on the basis of subtle structural differences such as the presence or absence of a hydroxyl group (Sassanfar and Szostak, 1993) or a methyl (Haller and Sanow, 1997). Enzymes with similar activity and structure can be distinguished, as is demonstrated with the detection of α -thrombin and γ -thrombin (Paborsky et al., 1996). More impressive is the ability of aptamers to distinguish between enantiomers, as was reported by Gieger et al, 1996, when L and D-arginine were discriminated. The high degree of specificity often seen in aptamers, sometimes even better than antibodies (Jenison et al., 1994), is a result of the selective process in the SELEX.

The aptamer generation emerged from the experimentation of three independent groups, all of whom published their work in 1990. First, the Joyce group (Robertson and Joyce, 1990) was looking for a new enzymatic activity of RNA. They used in vitro mutation, selection and amplification to isolate the enzymatic RNA, which became the basis for the current in vitro selection of aptamers. Then the Gold group was trying to identify in vitro the sequences of T4 DNA polymerase (Tuerk and Gold, 1990). The library they created was based on the natural structure but with the eight-loop randomised. They

were the first to baptise the process of in vitro selection as SELEX, and the process was able to identify the natural target of the enzyme as the predominant. The authors patented their process. A month later Szostak and Ellington reported the use of in vitro selection to isolate molecules with specific ligand binding activities (Ellington and Szostak, 1990). They created a library with 100 nucleotides of randomised sequences, related to any known oligonucleotide sequence. The targets had no previously identified nucleic acids ligand. This group coined the term aptamer, which comes from the Latin *aptus* meaning “to fit”.

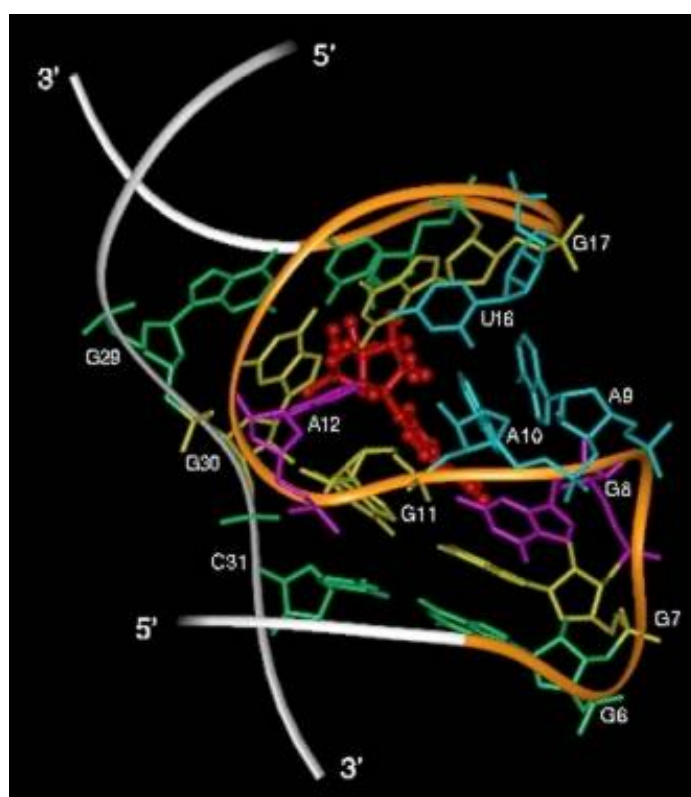


Figure 1. 2. NMR image of ATP binding RNA aptamer. (Protein data base ID: 1RAW) (Feigon et al., 1996)

1.3.3 Types of aptamers

Aptamers had been initially developed with DNA or RNA molecules for a direct interaction with the target. However, recently additional functionalities have been incorporated to aptamers:

- Spiegelmers

The word spiegelmer comes from the German word spiegel, which means “mirror”. These kinds of molecules are the mirror image of aptamers. In nature, nucleic acids are composed of D-nucleotides, and nucleases, the nucleic acid degrading enzyme, are L-amino acids. Consequently, the structure of nucleases is also inherently chiral, thus resulting in stereospecific substrate recognition. Hence, these enzymes only accept substrate molecules in the correct chiral configuration. Therefore L- oligonucleotides (spiegelmers) should escape from enzymatic recognition and subsequent degradation.

However due to this same principle nature developed no enzymatic activity to amplify such mirror image, thus it cannot be directly obtained by employing the SELEX process.

The first functional spiegelmers were designed to bind to the small molecules arginine and adenosine (Klussmann et al., 1996; Nolte et al., 1996).

- Aptamer beacons

Beacons are single stranded oligonucleotides designed to reveal the ligand interaction through a change in the 3-D structure of this strand, as explained in the previous section.

Aptamer beacons are based on the same principle. An additional sequence is added to the aptamer forming a stable stem-loop and destabilises the binding structure. Then the aptamer beacon exists in a quenched stem-loop structure in the absence of a target molecule. Formation of the aptamer beacon-target molecule complex would alter the equilibrium between quenched, and unquenched, structures generating a change in observed fluorescence intensity (Figure 1.3). The first aptamer beacon was developed by Yamamoto et al., 2000 to detect Tat protein of HIV-1.

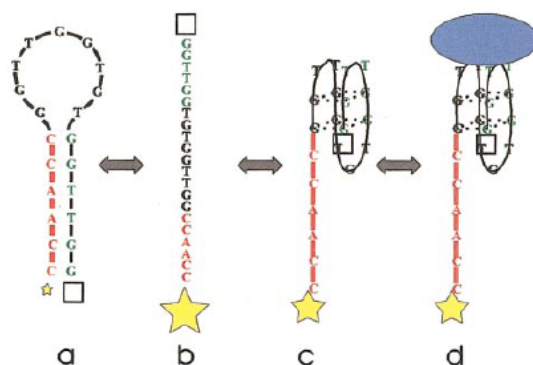


Figure 1. 3. Schematic draws of signalling mechanism by thrombin aptamer beacon. Figure acquired from the article Hamaguchi et al., 2001. (a) Aptamer beacon in quenched stem-loop conformation. (b) Unfolded conformation. (c) Aptamer in G-quartet conformation which allows thrombin binding. (d) Thrombin bound to aptamer beacon. Yellow stars represent the fluorophore, and the white square represents the quencher. The emission intensity of the fluorophore is represented by the size of the star, increases with the distance between the fluorophore and the quencher.

- Circular DNA aptamers

Circular DNA aptamers or captamers combine aptameric recognition with multitasking nucleic acid functions through the use of modular engineering principles derived from DNA nanotechnology.

DNA captamers have been demonstrated in 2-, 3- and 4-headed versions, focussing upon the pleiotropic activity that can be obtained by combining different functions together (Di Giusto and King, 2004). These scaffolds provide a framework for spatial orientation, allowing multiple binding activities to be combined into single molecules (Figure 1.4). Their circular structure imparts both enhanced thermal stability and exonuclease resistance



Figure 1. 4. Captamers for the detection of human thrombin by proximity extension. Figure obtained from the article Di Giusto et al., 2005.

- Aptazymes

The ribozyme or desoxyribozyme is an RNA or DNA molecule that catalyses a chemical reaction. Many natural ribozymes catalyse either their own cleavage or the cleavage of other RNAs, but synthetic ribozymes have also been found that function as polymerases, dephosphorylases and restriction endoribonucleases (Cech et al., 1997).

The ribozyme/deoxyribozyme linked to an aptamer is called allosteric ribozyme/deoxyribozyme or aptazyme (Figure 1.5). This system undergoes alteration of the catalytic activity in the presence of a molecule binding to a receptor site, the aptamer. In this way, aptazymes directly transduce molecular recognition into a quantifiable catalytic event. Aptazymes have been adapted to an array that discriminated between various metabolites (Seetharaman et al., 2001). Furthermore this kind of aptamer was used to construct catalytic molecular beacons (Stojanovic et al., 2000), which amplify the recognition event through cleavage of a doubly-labelled fluorescent substrate.

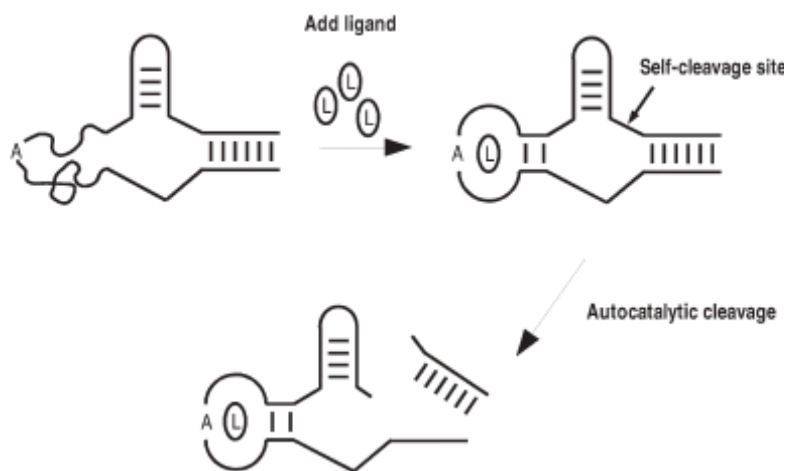


Figure 1. 5. This figure obtained from Koizumiet al., 1999, illustrates a simple self-cleaving aptazyme. The structure consists of a selfcleaving hammerhead ribozyme with an internal stem replaced by an aptamer sequence (“A”). Upon binding the ligand (“L”), the aptamer becomes well-ordered, reconstituting the disrupted hammerhead stem. Once the stem forms, the ribozyme can adopt an active conformation and undergo self-cleavage.

- Chemical modifications of DNA chain

Chemical modifications of DNA molecules have been carried out to increase their stability. PNA has been mentioned in a previous section.

Another chemical alternative to the ribose sugar backbone is the (3',2')- α -L-threose nucleic acid (TNA), with a four-carbon sugar backbone instead of two-carbon sugar backbone in DNA (Figure 1. 6).

TNA is capable of antiparallel, Watson-Crick base-pairing with complementary DNA, RNA, and TNA oligonucleotides (Schoning et al., 2000). This property is remarkable, given that the TNA repeat unit is one atom shorter than that of DNA or RNA. Furthermore protein polymerases can incorporate TNA monomers by primer extension on DNA templates (Chaput and Szostak, 2003), and can also use TNA to template DNA. A system for selecting functional TNA structures from libraries of random molecules was recently devised (Ichida et al., 2005).

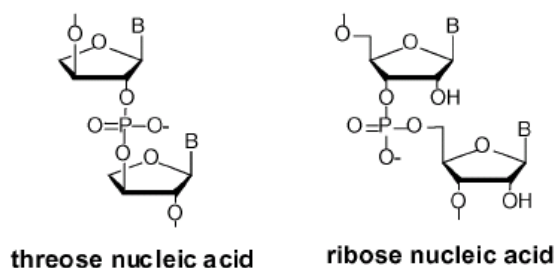


Figure 1. 6. Chemical structure of TNA and DNA. Adopted from Reference (Chaput et al., 2003)

Another way to modify the oligonucleotide structure is to introduce sulphur into the molecule by using phosphorothioate oligonucleotides (figure 1.7). Incorporation of a thioether into the 2'-substituent of ssDNA has resulted in improved binding to human serum albumin (Prakash et al., 2002). Kawakami and Sugimoto, 1997, carried out an in vitro selection of aptamers from an RNA library with phosphorothioate linkages instead of normal phosphodiester.

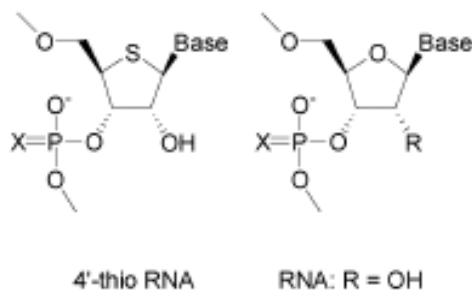


Figure I. 7. Chemical structure of thio-RNA and RNA. (Dande et al., 2003)

- Peptide aptamers

Peptide based combinatorial platforms are also mentioned here for clarity.

Peptide aptamers (paptamers, thioredoxin-insert proteins (TIPs)) are proteins that are designed to interfere with other protein interactions inside cells. These are also referred to as aptamers because they were developed through a combinatorial library to bind with proteins.

It consists of a variable peptide loop attached at both ends to a protein scaffold. The variable loop length is typically comprised of 10 to 20 amino acids, and the scaffold may be any protein, which has good solubility and compact folding. Currently, the bacterial protein Thioredoxin-A is the most used scaffold protein, the variable loop being inserted within the reducing active site, which is a -Cys-Gly-Pro-Cys- (Cysteine-Glycine-Prolamin-Cysteine) loop in the wild protein. Selection of Ligand Regulated Peptide Aptamers (LiRPAs) has been demonstrated by displaying 7 amino acid peptides from a novel scaffold protein based on the trimeric FKBP-rapamycin-FRB structure (Binkowski et al., 2005)

- Anticalins

Anticalins are ligand-binding proteins constructed on the basis of the lipocalin proteins as scaffolds. The principal element of this protein architecture is the β -barrel structure of eight antiparallel strands, which support four loops at its open end. These loops form the natural binding site of the lipocalins and can be reshaped *in vitro* by amino acid replacement, thus creating novel binding specificities. The bilin-binding protein

(BBP).was employed as a model system for the preparation of a random library with 16 selectively mutated residues. Several anticalins have been selected from this library, exhibiting binding activity for compounds like fluorescein or digoxigenin. (Schlehuber and Skerra, 2005)

1.3.4 SELEX

SELEX (Systematic Evolution of Ligands by EXponential enrichment) is the technique for isolating functional synthetic nucleic acids. This process is an in vitro screening of large random libraries of oligonucleotides by an iterative process of adsorption, recovery and amplification of the oligonucleotide sequences (Figure 1.8) (Spiridonova and Kopylov, 2000). A public database (HTPSELEX) provides access to primary and derived data from high-throughput SELEX experiments, this data base is freely accessible at <ftp://ftp.isrec.isb-sib.ch/pub/databases/htpselex/> and <http://www.isrec.isb-sib.ch/htpselex>.

The SELEX process starts with the synthesis of a single-stranded (ssDNA) random library of oligonucleotides. The starting round of a typical SELEX will contain around 10^{14} - 10^{15} of individual sequences. The ssDNA chemically synthesised are amplified by PCR in order to generate the corresponding double-stranded DNA (dsDNA). Depending on the kind of aptamer that is wanted, the library is converted into ssDNA by strand separation or into RNA by in vitro transcription. The ss nucleic acids are incubated with the target of interest. The nucleic acids that adopt a conformation that allow them to bind with the target are separated by filtration through a nitrocellulose column or by affinity column (for the small molecules). The aptamer-target duplex are eluted and amplified by RT-PCR, in the case of RNA aptamers or PCR in the case of DNA aptamers. This results in a smalls enriched pool of molecules with which to repeat the cycle. The process requires several iterations of the cycle, usually around 8-15 cycles, carried out under increasingly stringent conditions to achieve an aptamer of high affinity and specificity. SELEX takes a long time, around one month, nevertheless this process has been automated (Cox et al., 2002). Recently, Hybarger et al., (2006), developed a microfluidic SELEX prototype.

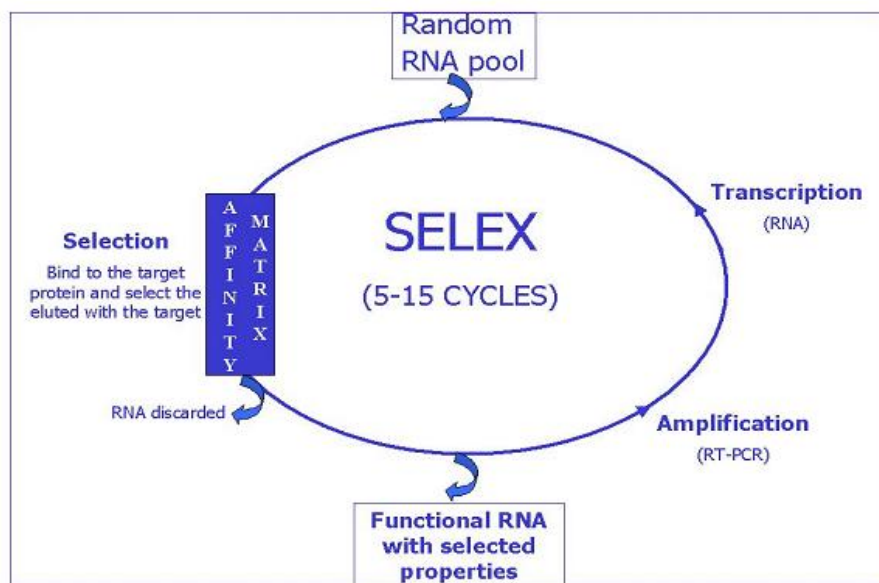


Figure I. 8. Scheme of SELEX process in the case of an RNA aptamer section.

Improvements upon around this process have increased binding efficiency of aptamers. One of the examples is PhotoSELEX, this technique substitutes one of the bases in the nucleic acid library with a photoactivatable nucleotide. In the presence of light this modified nucleotide is activated forming a photoinduced covalent bond to the target molecule, which provides an enhancement in the aptamer affinity (Golden et al., 2000)

Kinetic homogeneous affinity method termed non-equilibrium capillary electrophoresis of equilibrium mixtures (NECEEM). In NECEEM a short plug of the equilibrium mixture, containing a random library of ssDNA with the target, is injected into the inlet of a capillary tube. The ends of the tube are connected to a positive and negative potential and the free ssDNA, the free target and the complex ssDNA-target are dissociated during electrophoresis. This technique demonstrated an efficiency, which is at least two orders of magnitude higher than SELEX (Berezovski et al., 2003). The high efficiency of NECEEM allows for aptamer selection in as few as one round of enrichment and selection.

Counter-SELEX is a highly specific SELEX method that discards ligands that have the ability to bind the target as well as closely related structural analogue of the target (Jenison et al., 1994). During selection, the population of aptamers bound to the target is subjected to affinity elution with structural analogues and the sequences eluted are

discarded. Thus, the counter-SELEX strategy increases selectivity and could be a valuable tool in identifying aptamers aimed at a unique target in a complex mixture. Furthermore, in some diagnostic applications of small molecule targets, it may be important to measure the analyte as well as certain structural variants of the analyte. In that case, aptamers retained on the target could be specifically eluted.

FluMag-SELEX, incorporates fluorescent labels for DNA quantification and use of magnetic beads for target immobilisation in the SELEX process. The use of magnetic beads enables easy handling, use of very small amounts of target for the aptamer selection and a rapid and efficient separation of bound and unbound molecules. (Stoltenburg et al., 2005)

Another example is the post-SELEX process in which a modification of the ligand is carried out after the traditional SELEX process for the enhanced of the binding activity and other properties such as improved pharmacokinetics, tissue distribution, and nuclease resistance (Green et al., 1995)

1.3.5 Interactions between aptamer-target

The interactions between protein and aptamers include Van der Waals, hydrogen bonds and water mediated contacts (Gutfreund et al., 2005). About 30% of all interactions are non-specific bonds, mediated through Van der Waals forces; however, they are extremely important for the stability of the complex. The majority of the specific interactions involves hydrogen bonds (Schwabe, 1997) and demonstrates some amino acid- base preferences. Cowen et al., (2000), demonstrated that 80% of the binding energy was contributed by hydrogen bounds. The relative contributions of these and other forces, such as interaction with aromatic rings and Van der Waals forces have been also reported (Hermann and Patel, 2000). Water molecules also facilitate the contact by filling the empty spaces at the protein-aptamer interface and play an important role in complex formation (Tuerk and Gold, 1990).

The random nature of identifying or locking in a specific type of interaction results in a highly variable method of interaction.

1.3.6 Aptamer versus Antibodies

Aptamers, the nucleic acid equivalent to antibodies, possess numerous advantages over antibodies that make them ideal sensing elements for proteomic biosensors (Table 1.1). The antibody identification process is dependent on an animal host. The expression process is further complicated when the targets are toxins or low molecular weight molecules, which trigger minimal immunogenic response. The antibody's performance is not specific, and although monoclonal preparations have reduced the variability, the preparation still requires a lengthy purification protocol.

In contrast, aptamers are designed *in vitro*. They are independent of any animal host. Identification of aptamers utilises automated oligonucleotide synthesis and screening systems. The binding specificity, affinity and stability of aptamers can be improved by molecular evolution techniques or by rational design (Bacher and Ellington, 1998). Additionally, the identification process can be modified to obtain an aptamer that interacts with specific regions of the target or under differing binding condition. Once identified, aptamers are readily produced with extremely high reproducibility and purity using established chemical synthesis. Aptamers can also be easily labelled with reporter molecules without affecting their affinity. An aptamer sensor can support operation in a wide variety of sample matrices including non-physiological buffers and temperature conditions that would denature typical antibody formulations. Kinetic parameters in aptamer interaction can be changed on demand. Furthermore, antibodies are large and complex molecules that are sensitive to pH variations and temperature, which highly limit their use in reusable sensors. Aptamers can undergo repeated cycles of denaturation and renaturation without damaging their structure. In addition, they can be transported at ambient temperature, are stable for long-term storage and can be subjected to numerous freeze and thaw cycles.

Table 1. 2. Advantages of aptamers over antibodies.

Aptamers	Antibodies
- In vitro production	- Production requires the use of animals
- Automated synthesis and screening	- Production process complicated and expensive
- Identification of toxins, drugs and small molecules	- Limited to molecules that produce an immuno-response. Small molecules require conjugation to a hapten
- Can function at different temperatures, pH and buffers	- Can function only under physiological conditions
- Production is highly reproducible and produces a pure product	- Lot to lot variations are frequently observed
- Easily labeled in precise locations	- Labeling can cause loss of affinity
- Easy transportation and storage	- Sensitive to temperature and humidity changes

1.3.7 α -Thrombin

α -Thrombin is a two chain enzyme composed of an NH₂- terminal chain (MW=6000) and a COOH- terminal chain (MW=31000), which remain covalently associated through a disulphide bond. This enzyme is a highly specific serine protease generated by proteolytic activation of the zymogen prothrombin (Lundblad et al., 1976).

Thrombin is also responsible for feedback activation of the procofactors factor V and factor VIII, so thrombin has importance in anti-clotting therapeutics.

There is no known naturally occurring nucleic acid sequence that binds thrombin. The anti-thrombin aptamer sequence constitutes the first example of an in vitro designed oligonucleotide targeted towards protein binding. The identified thrombin-binding aptamer has a well-defined folded structure in solution (Bock et al., 1992, Macaya et al., 1993). α -thrombin binding affects two electropositive parts of the molecule, the fibrinogen-recognition and heparin-binding exosites. When thrombin is in contact with the aptamer, the aptamer adopts folded G-quadruplex structure, the central part of the structure is formed by two guanine quartets. The quartets are connected at one end by two TT loops, which span the two narrow grooves and at the other end by a TGT loop, which spans a wide groove of the mini-quadruplex.

The anti-thrombin aptamer can be applied as an inhibitor of thrombin activity (Tasset et al., 1997; Bock et al., 1992; Carrie et al., 2000). The aptamer drug ARC183 from Archemix Corporation is a thrombin inhibitor for use as an anticoagulant during coronary artery bypass graft procedures. Currently, herapin is used for this aim, however, the herapin treatment has serious side effects and requires a separate reversing agent. These limitations could be overcome with the use of the anti-thrombin aptamer. A further application of anti-thrombin aptamers is as an imaging agent to detect thrombus, since it distinguishes between actively growing clots and inactive clots. The thrombus imaging permits an accurate identification of pulmonary embolism, calf veins thrombi, vascular thrombus and other thrombotic disorders (Goldhaber, 1998; Knight, 1993; Worsley and Alavi, 2001). More recently, anti-thrombin aptamers have been used as biorecognition elements for thrombin detection in biosensors (Xu et al., 2001, Schlenso et al. 2004). Thrombin has been considered as a useful tumour marker in the diagnosis of pulmonary metastasis. The median concentration of thrombin in patients with metastasis was 5.4 pM (Rodríguez et al., 1997), thus an aptamer biosensor for thrombin detection, which could detect this concentration, could be a useful diagnostic tool.

1.3.8 Aptasensors

Aptasensor is the word to define biosensors using aptamers as the biorecognition element. The first examples of aptasensors date back to 1996, when Davis et al. investigated the feasibility of using aptamers to provide the selective component in an optical sensor application. They described a model system consisting of human neutrophil elastase coated on beads that interact with fluorescent tagged aptamers. Eight months later two new examples of aptasensors appeared. A radiolabeled aptamer was used for the detection of different protein kinase C isozymes (Conrad and Ellington, 1996) and Drolet et al, (1996), described an enzyme-linked sandwich assay that used a fluorescently labeled SELEX-derived oligonucleotide.

In the past decade hundreds of aptasensor papers have been published using an assortment of transducers. Table 1.2 provides a sampling of the potential targets, transduction methods and sensitivities of aptasensors. Fluorescence labels have been widely used in these applications. L-adenosine detection was transduced by evanescent wave-induced fluorescence (Hamaguchi et al., 2000). Thrombin detection was performed with aptamer-fluorescence-quenching pairs and by a competitive assay of fluorescently labeled thrombin with thrombin on an aptamer modified optical fiber (Kleijnung et al., 1998). Optical analysis has been also used to detect the catalytic activation of thrombin through the dissociation of a thrombin-aptamer complex (Pavlov et al., 2005).

For transduction and detection of non-labeled aptamers, quartz crystal microbalance (QCM) (Furtado et al., 1999; Pavlov et al., 2004; Liss et al., 2002) and surface plasmon resonance (SPR) (Fukusaki et al., 2001; Okumoto et al., 2002; Rhodes et al., 2001) are two widely described techniques. A label-free protein detection strategy using a microfabricated cantilever-based sensor that was functionalized with aptamers to act as receptors of Taq DNA polymerase was described by Savran et al., 2004. Atomic force microscopy (AFM) has been used to measure the specific interaction between a protein immunoglobulin E (IgE) and an aptamer (Jiang et al., 2003). A surface acoustic wave biosensor array was designed by coupling aptamers to detect thrombin and HIV-1 Rev peptide (Schlensog et al., 2004).

More recently, examples of electrochemical aptasensors have been reported. Ikebukuro et al., 2006, developed a biosensor using a two aptamer sandwich configuration. Impedance spectroscopy was used to detect a sensitive interaction of an aptamer with lysozyme and thrombin (Rodriguez et al., 2005; Radi et al., 2005). Applications of an “electrochemical beacon” have also been published. Beacons are oligonucleotide molecules able to undergo spontaneous conformation changes that can be detected. The first example was reported by Bang et al., 2005 where methylene blue was intercalated into the beacon sequence as an electrochemical label. The label is released when the protein interacts with the aptamer and is detected electrochemically. Two similar “beacon” approaches have been reported (Xiao et al., 2005; Radi et al., 2006), with conflicting results on the cause of signal switching. An electrochemical aptamer-based beacon was developed for cocaine detection by Baker et al, 2006.

Table 1. 3. Ultrasensitive aptasensors transducers.

Transducer	Technique	Label	Analyte	Sensitivity	Reference
Piezoelectric	QCM	No	IgE	500 pM	Liss et al., (2002)
Electrochemical	Differential pulse voltammetry	Ferrocene	Thrombin	500 pM	Radi et al, (2006)
	Impedance	No	IgE	100 pM	Xu et al., (2005)
	Square wave-stripping voltammetry	Semiconductor or nano-crystal	Thrombin	500 fM	Hansen et al., (2006)
Optical	SPR	No	Oligoadenylate sintetase	100 nM	Hartmann et al., (1998)

1.3.9 Applications

One of the first applications of aptamers was in the area of therapeutic drugs. Due to their high affinity and specificity, aptamers can block receptors and inhibit protein activity with high affinity and specificity. They have also shown a use in validating drug targets and screening drug candidates. Their advantages of small size, quick elimination, low production cost, biocompatibility, biodegradability and no cross reactivity with antibody binding receptors make them good candidates for therapeutic applications. However, because blood is rich in nucleases, an appropriate modification of the aptamer therapeutics is required to avoid nuclease attack.

One of the most successful therapeutic applications of an aptamer has been carried out for the treatment of age-related macular degeneration (Sassanfar and Szostak, 1993). Antivascular endothelial growth factor participates in the growth of abnormal new blood vessels in the eyes, which cause vision loss. An aptamer therapeutic developed to inhibit this abnormal growth has been developed by OSI Pharmaceuticals under the name Macugen®. The aptamer has been fully approved by the FDA for patients with neovascular age-related macular degeneration.

Another example is the Anti-thrombin aptamer, ARC183, which has been developed by Gilead. This aptamer inhibits most of the physiologic blood coagulation events (Tasset et al., 1997). It has passed phase I clinical trials. Other examples in the literature include an aptamer targeting C5 developed by Biesecker et al., (1999), which inhibits human serum hemolytic activity and an anti-tenascin C aptamer that was reported by Hicke et al, 2001. The later inhibits the activity of a trypsin like protease of non-structured protein (NS3) for the control of polyprotein secretin from the hepatitis C virus infections.

In addition to pharmaceuticals, Aptamers are also applied to the field of separation chemistry. Affinity chromatography is an established technique for the selection and separation of biomolecules from complex mixtures. Antibodies are frequently employed as receptor molecules in stationary phases due to their high affinity and selectivity. Nevertheless, a number of constraints limit their application in chromatography. In addition to some of the previously identified limitations (Table I.1), their large molecular size limits the surface loading on the stationary phase and

likewise limits the affinity binding capacity of the matrix. This is further compounded by the difficulty in obtaining antibodies for small molecules, especially toxins. As a result of their potential to overcome some of the antibody's limitations, aptamers have become a promising tool for affinity chromatography. A high affinity aptamer has been used by Romig et al., (1999) for purification of L-selectin. Adenosine and its analogues were successfully purified by Deng et al., (2001) using aptamers supported on a stationary phase. Furthermore aptamers have been used in a similar fashion to separate amino acids and polycyclic aromatic hydrocarbons (Kotia and Mc Gown, 2000).

In view of the advantages and simple structure of aptamers, they have been used as biorecognition elements in biosensor development. Due to the wide range of application of biosensors it has opened the possibility to apply aptamers in a number of fields such as environmental (Stratis-Cullum et al., 2005), industrial (Mann et al., 2005), defence (Kiel et al. 2004; Paddle, 2003), or medical (Dill and McShea, 2005; Gander and Brody, 2005).

1.4 Presentation of the thesis

The objective of this thesis is to demonstrate new concepts for the label-free detection of both proteins and oligonucleotides based-biosensors using electrochemical transduction.

The label-free oligonucleotide detection strategy is based on the displacement of a sub-optimum bound oligonucleotide by the target oligonucleotide, which is fully complementary to the immobilised capture probe. In the case where the sub-optimum sequence is labelled with an electrochemical reporter, positive detection would then be indicated by a decrease in signal, which is proportional to the concentration of the target.

It is expected that the use of the displacement platform will provide a reagentless and label free system with a decrease response time.

Ideally, the signal will only be displaced from the specific interaction with the target. The stability of pre-hybridised sub-optimum labelled oligonucleotide with the capture probe must be sufficient to prevent buffer or non-complementary oligonucleotide displacement.

Additionally a strong bond is required to link the label and the suboptimum oligonucleotide to avoid a decrease of the signal due to label degradation instead of specific displacement. To demonstrate the feasibility of these concepts, sub-optimum oligonucleotides were labelled with HRP and ferrocene and displaced by optimum targets demonstrating detection limits of 2 μM .

Label-free protein detection is based on aptamers. The target selected for these proof of concept was α -thrombin, and again the goal was to provide a generic label free platform for electrochemical detection. The anti-thrombin aptamer sequence constitutes the first example of an in vitro designed oligonucleotide targeted towards protein binding. The identified thrombin-binding aptamer has a well-defined folded structure.

For this purpose five strategies to electrochemically detect thrombin using a label-free aptamer-based biosensor were developed.

The first strategy used an immobilised capture probe aptamer that bound thrombin specifically. The transduction was achieved by the detection of an electroactive substrate for thrombin. Although this strategy is specific for thrombin, demonstrates for the first time an electrochemical aptasensor.

The second strategy exploits the two electropositive exosites of thrombin, to develop a sandwich assay with two aptamers. A thiolated aptamer was immobilised on a gold electrode and subsequently incubated with thrombin. In a second incubation step a biotin labelled aptamer was allowed to bind to the other thrombin exosite. The biotinylated aptamer was previously incubated with streptavidin-HRP forming a peroxidase labelled aptamer. The HRP thus attached at the electrode surface was quantified electrochemically using H_2O_2 and a diffusional osmium based mediator, providing a signal proportional to thrombin concentration.

Western blotting inspired the third strategy, where proteins immobilised on a membrane are detected by antibodies bearing reporter molecules. In these experiments, thrombin was immobilized on a modified gold electrode surface. The sensor was incubated first with biotin labelled aptamer and then with streptavidin-HRP, which was electrochemically detected as before.

The fourth strategy was based on fluorescent and electrochemical beacons. The beacon-like 3-D change of labelled aptamer structure when thrombin interacts with it can be transduced by observing the significant changes in the distance-dependent voltamperometric behaviour of an electrochemical label.

The last strategy is a modification of the aptamer-beacon based sensors of strategy four. In this case, the ferrocene labelled aptamer-beacon was co-immobilised with a monolayer of microperoxidase. The ferrocene label of the aptamer is forced closer to the electrode surface due to the effect of thrombin interaction. This allows electrochemical communication between the co-immobilised enzyme and the electrode surface mediated by ferrocene. In the presence of its substrate, the enzyme turns over and the ferrocene mediates the electron transfer of the enzyme to the electrode and produce the first reported molecularly engineering amperometric switch.

1.5 References

- Anderson G.P., Shriver-Lake L.C., Golden J.P., Ligler F.S., Proceedings of SPIE - The International Society for Optical Engineering, 1992, 1648, 39-43.
- Armistead P.M., Thorp H.H., Analytical Chemistry, 2000, 72, 3764-3770.
- Attridge J.W., Daniels P.B., Robinson G.A., Davidson G.P., Biosensors and Bioelectronics, 1991, 6, 201-214.
- Authier L., Grossiord C., Brossier P., Analytical Chemistry, 2001, 73, 18, 4450-4456.
- Bacher J.M., Ellington A.D., DDT, 1998, 3, 265.
- Baker B.R., Lai R.Y., Wood M.C.S., Heeger A.J., Plaxco K.W., Journal of American Chemical Society, 2006, 9, 128, 10, 3138- 3139.
- Bang G.S., Cho S., Kim B.G., Biosensors and Bioelectronics, 2005, 21, 863–870.
- Benson D.A., Boguski M.S., Lipman D.J., Ostell J., Nucleic Acids Research, 1997, 25, 1-6.
- Berggren C., Stalhandske P., Brundell J., Johansson G., Electroanalysis, 1999, 11, 156-160.
- Berezovski M., Nutiu R., Li Y., Krylov S.N., Analytical Chemistry, 2003, 75, 6, 1382-1386.
- Calvo-Muñoz M.L., Dupont-Filliard A., Billon M., Guillerez S., Bidan G., Marquette C., Blum L. Bioelectrochemistry, 2005, 66, 1-2, 139-143.
- Campàs M., Katakis I., TrAC - Trends in Analytical Chemistry, 2004, 23, 1, 49-62.
- Campbell C.N., Gal D., Cristler N., Banditrat C., Heller A., Analytical Chemistry, 2002, 74, 158-162.
- Caruthers M.H., Beaucage S.L., Becker C., Efcavitch J.W., Fisher E.F., Galluppi G., Chicharro M., Fernandes J., Palecek E., Bioelectrochemistry and Bioengineering, 1998, 45, 33–40.
- Bantel-Schaal U., Virology, 1991, 182, 1, 260-268.
- Chiorcea A.M., Brett A.M.O., Bioelectrochemistry , 2004, 63, 1-2, 229-232.

Cho S., Pak J.J., Hong J., KimPak Y., Journal of the Korean Physical Society, 2002, 41, 6, 1054-1057.

Crooke S.T., Biochimica Biophysic. Acta, 1999, 1489, 31-44

Geary R.S., Yu R.Z., Levin A.A., Current Opinion InVestetary Drugs, 2001, 2, 562-573.

Goldman R., McBride L., Gene amplification and analysis, 1983, 3, 1-26.

Del Pozo M.V., Alonso C., Pariente F., Lorenzo E., Analytical Chemistry , 2005, 77, 8, 2550-2557.

Dubois L.H., Nuzzo R.G., Annual Review of Physical Chemistry, 1992, 43, 437-442.

Bart J.C., Judd L.L., Kusterbeck A.W., Sensors and Actuators, B: Chemical, 1997, 39, 411-418.

Bianchi N., Rutigliano C., Tomassetti M., Feriotto G., Zorzato F., Gambari R., Clinical and Diagnostic Virology, 1997, 8, 3, 199-208.

Biesecker G., Dihel L., Enney K., Bendele R.A., Immunopharmacology, 1999, 42, 219-324.

Binkowski B.F., Miller R.A., Belshaw P.J., Chemistry and Biology., 2005, 12 ,7, 847-855.

Bock L.C., Griffin L.C., Lathan J.A., Vermaas E.H., Toole J.J., Nature, 1992, 355, 564-568.

Boozer C., Chen S., Jiang S., Langmuir, 2006, 22, 10, 4694-4698.

Breslauer K.J., Frank R., Blocker H., Marky L.A, Proceeding of the National Academy of Science U.S.A., 1986, 83, 3746-3750.

Brett C.M.A., Oliveira Brett A.M., Serrano S.H.P., Electrochimica Acta, 1999, 44, 24, 4233-4239.

Brown M., Ellington A.D, Combinatorial Chemistry, 2002, 5, 289-305.

Bryant M.A., Pemberton J.E., Journal of American Chemical Society, 1991, 113, 3629-3637.

Cech T.R., Arthur Z.J., Michael B., Biotechnology Advances, 1997, 15, 3-4, 666-669.

- Seetharaman S., Zivarts M., Sudarsan N., Breaker R.R., *Nature Biotechnology*, 2001, 19, 336-340.
- Chaput J.C., Szostak J.W., *Journal of American Chemical Society*, 2003, 125, 9274–9275.
- Chaput J.C., Ichida J.K., Szostak J.W., *Journal of American Chemical Society*, 2003, 125, 4, 856-857.
- Chiu N.H.L., Christopoulos T.K., *Analytical Chemistry*, 1996, 68, 2304-2308.
- Conrad R., Ellington A.D., *Analytical Biochemistry*, 1996, 242, 261–265.
- Cox J.C., Rajendram M., Riedel T., Davidson E.A., Sooter L.J., Bayer T.S., Schmitz-Cowan J.A., Ohyama T., Wang D., Natarajan K., *Nucleic acid Research*, 2000, 28, 2935-2942.
- Cullen D.C., Sethi R.S., Lowe C.R., *Analytical Chimica Acta*, 1990, 231, 33-39.
- Dande P., Prakash T.P., Sioufi N., Gaus H., Jarres R., Berdeja A., Swayze E.E., Griffey R.H., Bhat B., *Journal of Medical Chemistry*, 2006, 49, 1624-1634.
- Danielsson B., Hedberg U., Rank M., Xie B, *Sensors and Actuators, B*, 1992, 1-3, 138-142.
- Datta A.K., *Journal of Food Engineering*, 1990, 12, 223-238.
- Datta B., Armitage B.A., *Journal of American Chemical Society*, 2001, 123, 9612-9619.
- Davis K.A., Abrams B., Lin Y., Jayasena S.D., *Nucleic acid research*, 1996, 24, 702-706.
- Dill K., McShea A., *Drug Discovery Today: Technologies*, 2005, 2, 3, 253-258.
- Davis K.A., Abrams B., Lin Y., Jayasena S.D., *Nucleic Acids Research*, 1996, 24, 4, 702–706.
- DeYoung H., Garrett H., *High Technology*, 1983, 3 , 41-45.
- Deng Q. German I., Buchaman D., Kenedy R.T., *Analytical Chemistry*, 2001, 73, 5415-5420.
- Di Giusto D.G, King G.C., *Journal of Biological Chemistry*, 2004, 279, 46483–46489.

Di Giusto D.A., Wlassoff W.A., Gooding J.J., Messerle B.A., King G.C., *Nucleic Acids Research*, 2005, 33, 6, 1-7.

Dove A. *Nature Biotechnology*, 1999, 17, 233–239.

Eberson R.C., Miller J.A., Moran J.R., Ward M.D., *Journal of American Chemical Society*, 1990, 112, 3239-3243.

Egholm M., Buchardt O., Nielsen P.E., Berg R.H., *Journal of American Chemical Society*, 2002, 114, 1895–1897.

Ellington A.D., Szostak J.W., *Nature*, 1990, 346, 6287, 818–822.

Erdem A., Kerman K., Meric B., Akarca U.S., Ozsoz M., *Electroanalysis*, 1999, 11, 586–587.

Erdem A., Ozsoz M., *Analytical Chimica. Acta*, 2001, 437, 107–114.

Famulok M., *Current Opinion in Structural Biology*, 1999, 9, 324–329.

Famulok M., Mayer G., Blind M., *Accounting Chemical. Research*, 2000, 33, 591-599.

Fan C., Plaxco K.W., Heeger A.J., *Proceedings of the National Academy of Science USA*, 2003, 100, 9134–9137.

Farace G., Lillie G., Hianik T., Payne P., Vadgama P., *Bioelectrochemistry*, 2002, 55, 1-2, 1-3.

Farkas D.H., *Clinical Chemistry*, 2001, 47, 1871-1872.

Feigon J., Dieckmann T., Smith F.W., *Chemistry and Biology*, 1996, 3, 611-617.

Florin E.L., Rief M., Lehmann H., Ludwig M., Dornmair C., Moy V.T., Gaub H.E., *Biosensors and Bioelectronics*, 1995, 10, 895-901.

Fodor S.P.A., Read J.L., Pirrung M.C, Stryer L., Lu A.T., Solas, D., *Science*, 1991, 251, 767-777.

Fritz J., Cooper E.B., Gaudet S., Sorger P.K., Manalis S.R., *Proceedings of the National Academy of Science USA*, 2002, 99, 14142–14146.

Fukusaki E.I., Hasunuma T., Kajiyama S.I., Okazawa A., Itoh T.J., Kobayashi A., *Bioorganic and Medicinal Chemistry Letters* 1, 2001, 22, 2927-2930.

Furtado L.M., Su H., Thomson M., *Analytical Chemistry*, 1999, 71, 1167-1170.

- Holland C.A., Henry A.T., Whinna H.C., Church F.C., FEBS Letters, 2000, 484, 2, 87-91.
- Gallego J., Varani G., Accounting in Chemical Research, 2001, 34, 836-843.
- Gander T.R., Brody E.N., Expert Review of Molecular Diagnostics, 2005, 5, 1, 1-3.
- Geiger A., Burgstaller P., von der Eltz H., Roeder A., Famulok M., Nucleic Acids Research, 1996, 24, 6, 1029-1036.
- Goldhaber S.Z., New England Journal of Medicine, 1998, 339, 93-103.
- Golden M.C., Collins B.D., Willis M.C., Koch T.H., Journal of Biotechnology, 2000, 81, 167-178.
- Graham C.R., Leslie D., Squirrell D.J., Biosensors and Bioelectronics, 1992, 7, 7, 487-493.
- Green L.S., Jellinek D., Bell C., Beebe L.A., Feistner B.D., Gill S.C., Jucker F.M., Janji N., Chemical Biology, 1995, 2, 683-685.
- Gutfreund M.Y., Schueler O., Margalit H., Journal of Molecular Biology, 1995, 253, 370-382.
- Haller A.A., Sarnow P., Proceedings of the National Academy of Science U S A, 1997, 94, 8521-8527.
- Hamaguchi N., Ellington A., Stanton M., Analytical Biochemistry, 2001, 294, 126-131.
- Hansen J.A., Wang J., Kawde A.N., Xiang Y., Gothelf K.V., Collins G., Journal of American Chemical Society, 2006, 128, 2228-2229.
- Hartmann R., Nørby P.L., Martensen P.M., Jørgensen P., James M.C., Jacobsen C., Moestrup S.K., Journal of Biological Chemistry, 1998, 273, 3236-3246.
- Hashimoto K., Ito K., Ishimori Y., Analytical Chemistry, 1994, 66, 3830-3833.
- Hason S., Dvorak J., Jelen F., Vetterl V., Talanta, 2002, 56, 905-913.
- Hermann T., Patel D.J., Science, 2000, 287, 820-825.
- Hernández-Rodríguez N.A., Correa E., Contreras-Paredes A., Reviews of the Institute of Nat. Cancerology, 1997, 43, 2, 65-75.

- Herron J.N., Tolley S.E., Smith R., Christensen D.A., Proceedings of SPIE - The International Society for Optical Engineering, 2006, 60, 6080-6089.
- Hicke B.J., Marion C., Chang Y.F., Gould T., Lynott C.K., Parma D., Schmidt P.G., Warren S., Journal of Biological Chemistry, 2001, 276, 52, 48644-48654.
- Horvath S.J., Firca J.R., Hunkapiller T., Hunkapiller M.W., Hood L., Methods of Enzymology, 1987, 154, 314-326.
- Howley P.M., Israel M.A., Law M.F., Martin M.A., Journal of Biological Chemistry, 1979, 254, 11, 4876-4883
- Horrocks B.R., Mirkin M.V., Analytical Chemistry, 1998, 70, 22, 4653-4660.
- Huey F.T., Gong H., Dong X.D., Zeng X., Tan A.L., Yang X., Swee N.T., Analytica Chimica Acta, 2005, 551, 23-29.
- Hunkapiller M., Kent S., Caruthers M., Dreyer W., Firca J., Giffin C., Nature 1984, 310, 105-11.
- Hybarger G., Bynum J., Williams R.F., Valdes J.J., Chambers J.P., Analytical and Bioanalytical Chemistry, 2006, 384, 191-198.
- Ichida J.K., Zou K., Horhota A., Yu B., McLaughlin L.W., Szostak J.W., Journal of American Chemical Society, 2005, 127, 2802-2803.
- Ikebukuro K., Kiyohara C., Sode K., Biosensors and Bioelectronics, 2005, 20, 2168-2172.
- Jelen F., Erdem A., Palecek E., Bioelectrochemistry, 2002, 55, 165-167.
- Jenison R.D., Gill S.C., Pardi A., Polisky B., Science, 1994, 263, 1425-1434.
- Jiang Y., Zhu C., Ling L., Wan L., Fang X., Bai C., Analytical Chemistry, 2003, 75, 2112-2116.
- Jonsson U., Malmqvist, M., Ronnber, I., Berghe, L., Progress in Colloid and Polymer Science, 1985, 70, 96-100.
- Kajima S., Okazawa A., Itoh T., Kobayashi A., Bioorganic and Medical Chemistry Letters, 2001, 1, 2927-2935.
- Karube I., Kubo I., Suzuki S., Annals of the New York Academy of Sciences, 1984, 434, 508-511.

- Katz E., Willner I., *Electroanalysis*, 2003, 15, 913–947.
- Kawakami J., Sugimoto N., *Nucleic acids symposium series*, 1997, 37, 201-202.
- Keese C.R., Giaever I., *Proceedings of the Annual Conference on Engineering in Medicine and Biology*, 1990, 2, 500-501.
- Kiga D., Futamura Y., Sakamoto K., Yokoyama S., *Nucleic Acids Research*, 1998, 26, 7, 1755–1760.
- Kindervater R., Kunnecke W., Schmid R.D., *Analytica Chimica Acta*, 1990, 234, 113-117.
- Kingdon C.F.M., *Applied Microbiology and Biotechnology*, 1985, 22, 165-168.
- Kleinjung F., Klussmann S., Erdmann V.A., Scheller F.W, Bier F.F., *Analytical Chemistry*, 1998, 70, 328-331.
- Kocum C., Ulgens S.D., Cubukcu E., Piskin E., *Ultramicroscopy*, 2006, 106, 4-5, 326-333.
- Kopylov A.M., Spiridonova V.A., *Molecular Biology*, 2000, 34, 6, 940-954.
- Klussmann S., Nolte A., Bald R., Erdmann V.A., Furste J.P., *Nature Biotechnology*, 1996, 14, 1112-1115.
- Knight L.C., *Journal of Nuclear Medicine*, 1993, 34, 554-561.
- Koizumi M., Soukup G.A., Kerr J.N., Breaker R.R., *Natural Structures in Biology* 1999, 6, 1062–1071.
- Kopylov A.M., Spiridonova V.A., *Molecular Biology*, 2000, 34, 6, 940-954.
- Kotia R.B., Li L., McGown L.B., *Analytical Chemistry*, 2000, 72, 827-832.
- Kurreck J., *European Journal of Biochemistry*, 2003, 1628-1644.
- Kwon Y., Roh Y., *Ultrasonics*, 2004, 42, 1-9, 409-411.
- Lausted C., Dahl T., Warren C., King K., Smith K., Johnson M., *Genome Biology*, 2004, 5, R58.
- Lee M., Walt D.R., *Analytical Biochemistry*, 2000, 282, 142-146.
- Lee Y., Lim G., Moon W., *NSTI Nanotechnology Conference and Trade Show - NSTI Nanotech 2005 Technical Proceedings*, 2005, 477-480.

- Levicky R., Herne T.M., Tarlov M.J., Satija S.K., *Journal of American Chemical Society*, 1998, 120, 9787-9792.
- Li B., Zhang Z., Jin Y., *Analytical Chemistry*, 2001, 73, 6, 1203-1206.
- Li D., Frey M.W., Baeumner A.J., *Journal of Membrane Science*, 2006, 279, 1-2, 354-363.
- Li H., Rothberg L., *Proceedings of the National Academy of Science USA*, 2004, 101, 39, 14037-14039.
- Liebold P., Wieder H., Hillebrandt H., Friebel A., Hartwich G., *Bioelectrochemistry*, 2005, 67, 2, 143-150.
- Liss M., Petersen B., Wolf H., Prohaska E., *Analytical Chemistry*, 2002, 74, 4488-4495.
- Liu S., Ye L., He P., Fang Y., *Analytical Chimica Acta*, 1996, 335, 239-243.
- Liu S.F., Li J.R., Jiang L., *Colloids and Surfaces A: Physicochemical and Engineering Aspects*, 2005, 257-258, 57-62.
- Livache T., Roget A., Dejean E., Barthet C., Bidan G., Teoule R., *Nucleic Acids Research*, 1994, 22, 2915-2921.
- Lorsch J.R., Szostak J.W., *Biochemistry*, 1994, 33, 4, 973-982.
- Lowe C.R., *Biosensors*, 1985, 1, 3-16.
- Lundblad R.L., Kingdon, H.S., Mann, K.G., *Methods of Enzymology*, 1976, 45, 156-176.
- Fukusaki E., Hasunuma T., Macaya R.F., Schultze P., Smith F.W., Roe J.A., Feigon J., *Proc. Natl. Acad. Sci. USA*, 1993, 90, 3745-749.
- Ma K.S., Zhou H., Zoval J., Madou M., *Sensors and Actuators, B: Chemical*, 2006, 114, 1, 58-64.
- Major A., Barzda V., Piunno P.A.E., Musikhin S., Krull U.J., *Progress in Biomedical Optics and Imaging - Proceedings of SPIE*, 2005, 5969-5976.
- Maniatis T., Fritsh E.F., Sambrook J., *Molecular cloning: a laboratory manual*. Cold Spring Harbor University Press, 11.45-11.57.
- Mao X., Yang L., Su X.-L., Li Y. *Biosensors and Bioelectronics*, 2005, 21, 7, 1178-1185.

- Marcus A., *Molecular biology*, New York, Academic Press, 1989.
- Maruyama K., Mishima Y., Minagawa K., Motonaka J., *Journal of electroanalysis*, 2001, 510, 96-102.
- Matz B., *Journal of Virology*, 1987, 61, 5, 1427-1434.
- McCauley T.G., Hanaguchi N., Stanton M., *Analytical biochemical*, 2003, 319, 244-250.
- Meade T.J., *Journal of American Chemical Society*, 2001, 123, 45, 11155-11161.
- Mebrahatu T., Berry G.M., Bravo G.M., Michelhaugh S.L., Soriaga M.P., *Langmuir*, 1988, 4, 1147-1151.
- Meric B., Kerman K., Ozkan D., Kara P., Erensoy S., Akarca U.S., Mascini M., Ozsoz M., *Talanta*, 2002, 56, 837-846.
- Mikkelsen S.K., *Electroanalysis*, 1996, 8, 15-19.
- Millan K.M., Saraullo A. Mikkelsen S.R., *Analytical Chemistry*, 1993, 65, 2317-2319.
- Millan K.M., Mikkelsen S.R., *Analytical Chemistry*, 1993, 65, 2317-2323.(b)
- Mir M., Katakis I. *Analytical and Bioanalytical Chemistry*, 2005, 381, 5, 1033-1035.
- Mir M., Vreeke M., Katakis I., *Electrochemical Communication*, 2006, 8, 505-511.
- Nolte A., Klusmann S., Bald R., Erdmann V.A., Furste J.P., *Nature Biotechnology* 1996, 14, 1116-1119.
- Nuwaysir E.F., Huang W., Albert T.J., Singh J., Nuwaysir K., Pitas A., *Genome Research*, 2002,12, 1749-1755.
- Okumoto Y., Ohmichi T., Sugimoto N., *Biochemistry*, 2002, 41, 2769-2775.
- Olofsson L., Rindzevicius T., Pfeiffer I., Kall M., Hook F., *Langmuir*, 2006, 19, 24, 10414-10419.
- Oretskaya T.S., Romanova E.A., Andreev S.Yu., Antsyovich S.I., Tóth C., Gajdos V., Hianik T. *Bioelectrochemistry*, 2002, 56, 1-2, 47-51.
- Oyama M., Ikeda T., Lim T.-K., Ikebukuro K., Masuda Y., Karube I., *Biotechnology and Bioengineering*, 2000, 71, 3, 217-222.

Ozsoz M., Erdem A., Kerman K., Ozkan D., Tugrul B., Topcuoglu N., Ekren H., Taylan M., *Analytical Chemistry*, 2003, 75, 9, 2181-2187.

Paborsky L.R, McCurdy S.N., Griffin L.C., Toole J.J., Leung L.L., *Journal of Biological Chemistry*, 1993, 268, 28, 808-811.

Pace S.J., *Medical Instrumentation*, 1985, 19, 168-172.

Pagratis N.C., Fitzwater T., Jellinek D., Dang C., *Nature Biotechnology*, 1997, 15, 1, 68-73.

Palecek E., *Nature*, 1960, 188, 656-657.

Palecek E., *Analytical Biochemistry*, 1988, 170, 421-431.

Palecek E., Fojta M., Tomschik M., Wang L., *Biosensors and Bioelectronics*, 1998, 13, 621-628.

Palecek E., *Talanta*, 2002, 56, 809-819.

Pang D.W., Abruña H.D., *Analytical Chemistry*, 1998, 70, 3162-3169.

Parellada J., Narváez A., López M.A., Domínguez E., Fernández J.J., Pavlov V., Katakis I., *Analytica Chimica Acta*, 1998, 362, 1, 47-57.

Park J.W., Jung H.S., Lee H.Y., Kawai T., *Biotechnology and Bioprocess Engineering*, 2005, 10, 6, 505-509.

Patolsky F., Katz E., Bardea A., Willner I., *Langmuir*, 1999, 15, 11, 3703-3706.

Patolsky F., Lichtenstein A., Willner I., *Nature Biotechnology*, 2001, 19, 253-257.

Patolsky F., Weizmann Y., Willner I., *Journal of American Chemical Society*, 2002, 124, 770-772.

Patolsky F., Lichstein F., Willner I., *Chemical European Journal*, 2003, 9, 1137-1145.

Pavlov V., Shlyahovsky B., Willner I., *Journal of American Chemical Society*, 2005, 127, 6522-6523.

Pavlov V., Xiao Y., Shlyahovsky B., Willner I., *Journal of American Chemical Society*, 2004, 126, 11768-11769.

Peng H., Soeller C., Cannell M.B., Bowmaker G.A., Cooney R.P., Travas-Sejdic J., *Biosensors and Bioelectronics*, 2006, 21, 9, 1727-1736.

- Pividori M.I., Merkoçi A., Alegret S., *Biosensors and bioelectronics*, 2001, 16, 1133-1142.
- Popovich N., Thorp H.H., *Interface*, 2002, 11, 30–34.
- Potyrailo R.A., Conrad R.C., Ellington A.D., Hieftje G.M., *Analytical Chemistry*, 1998, 70, 3419-3425.
- Pournaghi-Azar M.H., Hejazi M.S., Alipour E., *Analytica Chimica Acta*, 2006, 570, 2, 144-150.
- Prakash T.P., Manoharan M., Kawasaki A.M., Fraser A.S., Lesnik E.A., Sioufi N., Leeds J.M., Teplova M., Egli M., *Biochemistry*, 2002, 41, 11642-11648.
- Radi A.E., Acero J.L., Baldrich E., O'Sullivan C.K., *Journal of American Chemical Society*, 2006, 128, 117-124.
- Radi A.E., Sanchez J.L.A., Baldrich E., O'Sullivan C.K., *Analytical Chemistry*, 2005, 77, 19, 6320-632.
- Rampi M.A., Schueller O.J., Whitesides G.M., *Appl. Phys. Lett.*, 1998, 72, 1781-1783.
- Ray A., Norden B., *FASEB Journal*, 2000, 14, 9, 1041-1060.
- Rhodes A., Smither N., Chapman T., Parson S., Rees S., *FEBS. Letters*, 2001, 506, 85-93.
- Riepl M., Mirsky V.M., Ostblöm M., Liedberg B., 53rd Annual meeting in international society of electrochemistry, Düsseldorf, 2002.
- Robertson D.L., Joyce G.F., *Nature*, 1990, 344, 6265, 467–468.
- Rodriguez M.C., Kawde A., Wang J., *Chemical Communications*, 2005, 4267–4269.
- Romig T.S., Bell C., Drolet D.W., *J. Chromatography B*, 1999, 731, 275-282.
- Ruckman J., Green L.S., Waugh S., Gillette W.L., Henninger D.D., Claesson-Welsh L., Sagiv J., *Journal of American Chemical Society*, 1980, 102, 92-105.
- Samuelson L.A., Kaplan D.L., Lim J.O., Kamath M., Marx K.A., Tripathy S.K., *Thin Solid Films*, 1994, 242, 50-55.
- Sassanfar M., Szostak J.W., *Nature*, 1993, 364, 550–553.

Savran C.A., Knudsen S.M., Ellington A.D., Manalis S.R., *Analytical Chemistry*, 2004, 76, 3194-3198.

Sawata S., Kai E., Ikebukuro K., Iida T., Honda T., Karube I., *Nucleic acids symposium series*, 1997, 37, 247-248.

Schlehuber, S., Skerra, A. *Expert Opinion on Biological Therap*, 2005, 5, 11, 1453-1462

Schlensoog M.D., Gronewold T.M.A., Tewes M., Famulok M., Quandt E., *Sensors and Actuators, B: Chemical*, 2004, 101, 3, 308-315.

Schubert F., Renneberg R., Scheller F. W., Kirstein L., *Analytical Chemistry*, 1984, 56, 1677-1682.

Schuler G.D., Boguski M.S., Stewart E.A., Stein L.D., Gyapay G., Rice K., White R.E., Cox D.R., *Science*, 1996, 274, 540-546.

Schwabe J.W., *Current Opinion on Structural Biology*, 1997, 7, 1, 126-34.

Schoning K.U., Scholz P., Guntha S., Wu X., Krishnamurthy R., Eschenmoser A., *Science*, 2000, 290, 1347-1351.

Singh-Gasson S., Green R.D., Yue Y., Nelson C., Blattner F., Sussman M.R., *Nature Biotechnology*, 1999, 17, 974-978.

Singhal P., Kuhr W.G., *Analytical Chemistry*, 1997, 69, 23, 4828-4832.

Smironov I., Shafer R.H., *Biochemistry*, 2000, 39, 1462-68.

Stojanovic M.N., de Prada P., Landry D.W., *Nucleic Acids Research*, 2000, 28, 2915-2919.

Stoltenburg R., Reinemann E.C., Strehlitz E.B., *Analytical and Bioanalytical Chemistry*, 2005, 383, 83-91.

Stratis-Cullum D.N., Wade K.L., Pellegrino P.M., *Proceedings of SPIE - The International Society for Optical Engineering*, 2005, 5994-5999.

Tanjic N., *Journal of Biological Chemistry*, 1998, 273, 32, 556-567.

Tansil N.C., Xie H., Xie F., Gao Z., *Analytical Chemistry*, 2005, 77, 126-134.

Tasset D.M., Kubik M.F., Steiner W., *J. Mol. Biol.*, 1997, 272, 688-698.

Tessier L., Patat F., Schmitt N., Pourcelot L., Frangin Y., Guilloteau D., *Proceedings of the Ultrasonics International Conference*, 1993, 627-630.

- Thevenot D.R., Toth K., Durst R.A., Wilson G.S., Pure Applied Chemistry, 1999, 71, 12, 2333-2348.
- Thorp H.H., Trends in Biotechnology, 2003, 21, 12, 522-524.
- Tuerk C., Gold L., Science, 1990, 249, 4968, 505-510.
- Tuerk C., Gold L., Science, 1990, 249, 505-510.
- Ulman A., Chemical Review, 1996, 96, 1533-1542.
- Valdes J.J., Wall J.G, Chambers J.P., Eldefrawi M.E, Johns Hopkins APL Technical Digest (Applied Physics Laboratory), 1988, 9, 4-9.
- Varani G., Gallego J.A., Accounting Chemical Research, 2001, 34, 836-843.
- Vincke B.J., Devleeschouwer M.J., Patriarche G.J., Analytical Letters, 1985, 18, 593-607.
- Vo-Dinh T., Tromberg B.J., Griffin G.D., Ambrose K.R., Sepaniak M.J., Gardenhire E.M., Applied Spectroscopy, 1987, 41, 735-738.
- Wang H.Y., Biotechnology and Bioengineering Symposium, 1984, 14, 601-610.
- Wang J., Kawde A.B., Analyst, 2002, 127, 383-386.
- Wang J., Cai X., Rivas G., Shiraishi H., Farias P.A.M., Dontha N., Analytical Chemistry, 1996, 68, 2629-2634.
- Wang J., Cai X., Rivas G., Shiraishi H., Analytica Chimica Acta, 1996, 326, 1-3, 141-147. (b)
- Wang J., Cai X., Fernandes J.R., Grant D.H., Ozsoz M., Analytical Chemistry, 1997, 69, 4056-4059.
- Wang J., Jiang M, Journal of American Chemical Society, 1998, 120, 8281-8282.
- Wang J., Ozsoz M., Cai X., Rivas G., Shiraishi H., Grant D H., Yang I.V., Ropp P.A, Thorp H.H., Analytical Chemistry, 2002, 74, 347-354.
- Warren S.J., Biological Chemistry, 2001, 276, 48644-48649
- Watanabe E., Toyama K., Karube I., Matsuoka H., Suzuki S., Enzyme Engineering: Proceedings of the International Enzyme Engineering Conference, 1984, 529-532.

- Watson L.D., Maynard P., Cullen D.C., Sethi R.S., Brettle J., Lowe C.R., *Biosensors*, 1987, 3, 101-115.
- Wilson D.S., Szostak J.W., *Annual Review of Biochemistry*, 1999, 68, 611-647.
- Worsley D.F., Alavi A., *Radiologic Clinics of North America*, 2001, 39, 1035-1052.
- Wrobel N., Deininger W., Hegeman P., Mirsky V.M., *Colloids and surfaces B: Biointerfaces*, 2003, 32, 157-162.
- Xiao Y., Lubin A.A., Heeger A.J., Plaxco K.W., *Angewante Chemie*, 2005, 117, 5592 – 5595.
- Xu S., Cai X., Tan X., Zhu Y., Lu B., *Proceedings of SPIE - The International Society for Optical Engineering*, 2001, 4414, 35-37.
- Xu D., Yu X., Liu Z., He W., Ma Z., *Analytical Chemistry*, 2005, 77, 5107-5113
- Xu Y., Jiang Y., Yang L., He P.G., Fang Y.Z., *Chinese Journal of Chemistry*, 2005, 23, 12, 1665-1670.
- Yamamoto R., Kumar P.K.R., *Genes to Cells*, 2000, 5, 5, 389-396.
- Yang D.F., Wilde C.P., Morin M., *Langmuir*, 1996, 12, 6570-6579.
- Yao G., Fang X., Yokota H., Yanagida T., Tan W., *Chemistry - A European Journal*, 2003, 19, 22, 5686-5692.
- Yao G., Tan W., *Analytical Biochemistry*, 2004, 331, 2, 216-223.
- Yu C.J., Wan Y., Yowanto H., Li J., Tao C., James M.D., Tan C.L., Meade T.J., *Journal of the American Chemical Society*, 2001, 123, 45, 11155-11161.
- Yu C. J., Wan Y., Yowanto H., Li J., Tao C., James M.D., Tan C.L., Blackburn G.F.,
- Zhang Y., Kim H.H., Heller A., *Analytical Chemistry*, 2003, 75, 3267-3269.
- Zhang G., Zhou Y., Yuan J., Ren S., *Analytical Letters*, 1999, 32, 14, 2725-2736.

Chapter 2. Detection of direct DNA hybridisation

2.1 Introduction

The information generated by the Human Genome Project has resulted an increased value of DNA chips in clinical setting for the diagnosis, diseases analysis and drug elopement.

The most generalised readout method for DNA chips is fluorescence. Fluorescence transduction involves expensive instrumentation. An overlooked area of application of DNA detection is the point-of-care and home setting. For such applications limited number of sensors is sufficient although miniaturisation is important to limit the sample volume. In such settings electrochemical DNA sensors are competitive and can provide a fast responding and inexpensive diagnostic platform.

In this thesis different platforms for electrochemical DNA detection at macro and micro scale are developed

The first challenge is to ascertain that direct DNA hybridisation can be detected. In what follows, a diffusional mediator was used to transduce the catalytic signal obtained from a HRP labelled oligonucleotide hybridised with an immobilised capture probe on gold electrodes. The immobilisation of a redox polymer on the surface and the transduction of the signal by the redox polymer, improved the system's response time, lower sample volume and provided a quasi-reagentless system which was easy to use.

A test system using a 255-mer oligonucleotide amplified by PCR was electrochemically detected through a non-diffusional transduction. The oligonucleotide was selective for the *Micobacterium tuberculosis* rpoB gene region containing the mutation that confers resistance to rifampicin.

Furthermore, biocompatible photolithography has been used for the demonstration of electrochemical microarray manufacture. Oligonucleotides specific for breast cancer were electrochemically detected on this platform.

2.2 Materials and methods

2.2.1 Materials

The synthetic oligonucleotide sequences were purchased from Eurogentec (Belgium), with the exception of the synthetic oligonucleotide used for breast cancer detection that were supplied by the Institute of Radioisotopes and Radiodiagnostics Products, NCSR Demokritos. The sequences are shown below:

19-mer biotin-labelled capture probe oligonucleotide (*biotin-capture probe*):

5'-Biotin-AGCCAGCTGAGCCAATTCA-3'

19-mer thiol-labelled capture probe oligonucleotide (*thiol-capture probe*):

5'-Thiol-C₆-AGC CAGCTGAGCCAATTCA-3'

19-mer complementary oligonucleotide (*complementary target*)

5'-TGAATTGGCTCAGCTGGCT-3'

19-mer thiol-labelled complementary oligonucleotide. This oligonucleotide strand was subsequently bioconjugate with maleimide horseradish peroxidase activated (maleimide-HRP) to lead a HRP-labelled oligonucleotide, therefore this sequence is coined (*complementary-HRP*)

5'-Thiol- C₆-TGAATTGGCTCAGCTGGCT -3'

Primers were used for the amplification of the fragment of the *Mycobacterium Tuberculosis* rpoB gene region containing the mutation that confers resistance to rifampicin. They were:

Forward primer

5'-GAGGCGATCACACCGCAGACG T-3'

Reverse primer

5'-Digoxigenin-GATGTTGGGCCCTCAGGGGT T-3'

19-mer thiol digoxigenin-labelled capture probe oligonucleotide (*thiol-capture probe-Dig*):

5'-thiol-AGCCAGCTGAGCCAATTC A-Digoxigenin-3'

18-mer biotin-labelled complementary capture probe oligonucleotide for breast cancer detection (*biotin-wild BC capture probe*):

5'-biotin-AAACTAAATGTAAGAAAA-3'

18-mer Biotin-labelled mutated capture probe oligonucleotide for breast cancer detection (*biotin-mutated BC capture probe*):

5'-biotin-AAACTAAAGTAAGAAAA-3'

22-mer biotin-labelled breast cancer target oligonucleotide (*biotin-BC target*):

5'-Biotin-AAAATTTTCTTACATTTAGTTT-3'

All oligonucleotide solutions were made at 1 mg mL⁻¹ with autoclaved milliQ water and stored at -20 °C.

Maleimide-HRP (P1709), 3,3',5,5'-Tetramethylbenzidine Liquid Substrate (TMB) (T0440), Denhardt's solution (D9905), sodium citrate salt buffer (SSC) (S6639), Trizma hydrochloride (Tris-HCl) (T3253), 2-mercaptoethanol (M6250), Polyethylene glycol sorbitan monolaurate (Tween 20) (P1379) and Ethylenedinitril tetraacetic acid (EDTA) (E5134) were purchased from Sigma. NaCl (131659), and H₂O₂ (131072.12) were supplied from Panreac and NaH₂PO₄ (33,198-8) from Aldrich. Streptavidin coated plates were obtained from Thermo Labsystems. Anti-digoxigenin horseradish peroxidase (α -Dig-HRP) (1207733) and anti-digoxigenin-Alkaline phosphatase (α -Dig-ALP) (1093274) were acquired from Roche. p-aminophenyl phosphate (A5030) was purchased from LKT Laboratories Inc. Sephadex G25 DNA grade resin (17-0853-01) was supplied from Amersham Pharmacia Biotech. Gold silicon wafers and biocompatible photoresist polymer were hand over from Institute of Microelectronics, NCSR Demokritos. AZ 5214 photoresist, AZ MIF726 developer and tetramethyl ammonium hydroxide (TMAH) were purchased from Clariant, etching of the chromium UTE-1 was supplied from Cyantek and photoacid generator UVI 6974 from Union Carbide. The electron-conducting diffusional redox mediator ([Os(bpy)₂(pyr-CH₂-NH₂)]Cl) and the redox polymer (Poly-vinylpyridine-Os(bipyridine)₂Cl) were synthesised as reported in the literature (Gregg and Heller, 1991; Katakis and Heller, 1992). All the reagents for PCR amplification, Taq DNA polymerase (M1661), and deoxynucleoside triphosphates (dNTPs) (U1330) were supplied from Promega.

Aqueous solutions were prepared with Milli Q water (Milli Q system, Millipore). All other chemicals were of analytical grade

2.2.2 Instrumentation

The hybridisation of oligonucleotide was detected colourimetrically with an ELISA reader SpectraMax 340PC from Molecular Devices with SoftMax Pro software. The bioconjugation was monitored with the spectrophotometer 8453 from Hewlett Packard with the software HP845x UV-Visible system. Electrochemical measurements were carried out using an Autolab PGSTAT10 electrochemical analysis system and GPE management software from Eco Chemie. Electrochemistry was performed in a home made 20 μ L two electrode thin layer cell with a 18 mm² square gold sheet as a working electrode opposite to a solid state Ag/AgCl reference/counter painted on a plastic substrate. Ag/AgCl ink from Dupont (5874 conductor) was used and this is called a “quasi Ag/AgCl reference” since its potential was modulated by the contact solution. To keep potentials consistent throughout this work, this electrode has been calibrated for each solution used against a standard Ag/AgCl. 3-electrode cell setup was used with a carbon electrode as working electrode, Ag/AgCl as reference electrode and stainless steel as counter electrode.

The thermal cycler to amplify DNA was a Mini-gene from Bibby Stuart Scientific. Photolithography process was performed with MG 1410 mask aligner supplied from Carl Suss and WS-400B spin coater purchased from Laurel Technologies.

2.2.3 Real DNA sample amplification by PCR

PCR for the selective amplification of the *Micobacterium (M) tuberculosis* rpoB gene region containing the mutation that confers resistance to rifampicin was carried out as described by Genomica (Garcia et al., 2001). For the amplification of the rpoB gene in

M. tuberculosis complex, including *M. tuberculosis* and *M. bovis*, forward and reverse primer were used. The reverse primer was digoxigenin labelled at the 5' end to allow further detection of the PCR product. This pair of primers amplified a 255-bp fragment of the *rpoB* gene including the region containing the mutation conferring rifampicin resistance.

PCR reactions were carried out in a 25 μ L final volume containing 71 nM forward primer and 0.5 μ M reverse digoxigenin labelled primer, 1 \times Taq DNA polymerase buffer without $MgCl_2$, 1.5 mM $MgCl_2$, 200 μ M each of dATP, dCTP, dGTP and dTTP, 1.25 Units of Taq DNA polymerase and 2.5 μ L of oligonucleotide target. Amplifications started with a denaturation step of 2 minutes at 94 $^{\circ}C$, followed by 45 cycles each consisting on 20 seconds at 94 $^{\circ}C$, 30 seconds at 65 $^{\circ}C$ and 40 seconds at 72 $^{\circ}C$, and completed with a 4 minutes final step at 72 $^{\circ}C$.

The final product of this asymmetric amplification is a digoxigenin-labelled predominantly single stranded 255-mer oligonucleotide.

2.2.4 Bioconjugation: Synthetic 19-mer DNA labelling with HRP

The 19-mer complementary oligonucleotide and the 19-mer mutated oligonucleotide were purchased with a 5'-thiol and a 6-atom carbon spacer. They were labelled with horseradish peroxidase (HRP) using maleimide activation (Hermanson, 1995). The maleimide activated peroxidase was dissolved in phosphate buffer salt (PBS) 100 mM, 30 mM EDTA and 10 mM NaCl at pH 6.5 and mixed with a ten-fold molar excess of thiol labelled oligonucleotide solution. The solution was left to stand for 12 hours in the dark and then separated with a Sephadex G25 gel filtration column. The concentration of the resulting HRP labelled oligonucleotide and the activity of the labelled enzyme was determined spectrophotometrically.

2.2.5 Optimisation of hybridisation conditions by ELONA

- Colourimetric detection of 19-mer complementary-HRP

Streptavidin coated plates were incubated with 50 μL of 0.2 $\mu\text{g mL}^{-1}$ *biotin-capture probe* for 15 minutes at 25 °C. Plates were washed three times with 100 mM Tris-HCl pH 7.5, 150 mM NaCl and 1% Tween (wash solution). The hybridisation was performed by incubating with 50 μL of 18 $\mu\text{g mL}^{-1}$ *complementary-HRP* in 10 mM Tris-HCl, 1 mM EDTA, 0.3 x SSC and 2 x Denhardt's solution at pH 7.5 (hybridisation buffer) for 1 hour at 55 °C. The hybridisation was followed by a washing step and detected adding 50 μL of TMB incubated for 30 minutes at 25 °C. Coloured product from the reaction between HRP and TMB was obtained. The absorbance is directly related to HRP concentration and it was detected spectrophotometrically at 405 nm.

- Colourimetric detection of 22-mer oligonucleotide specific for breast cancer.

Streptavidin plates were first incubated with 5 $\mu\text{g mL}^{-1}$ of *biotin-wild BC capture probe* oligonucleotide in 50 mM phosphate buffer pH 6.5 for 30 minutes at 25 °C, and followed by 7 $\mu\text{g mL}^{-1}$ of *biotin-BC target* in 50 mM HEPES buffer, 50 mM NaCl, 1 mM EDTA, pH 8.0 for 30 minutes at 25 °C. Hybridisation was detected with streptavidin-HRP 0.25 $\mu\text{g mL}^{-1}$ in 50 mM HEPES buffer, 50 mM NaCl, 1 mM EDTA, pH 8.0 for 30 minutes at 25 °C, with the subsequent addition of the peroxidase colorimetric substrate, TMB, for 15 minutes. The change of colour of the TMB was detected spectrophotometrically at 405 nm.

Between each stage a washing procedure was carried out with the wash buffer.

2.2.6 Colourimetric detection of direct hybridisation of PCR products by ELONA

Streptavidin coated plates were incubated with 50 μL of 0.2 $\mu\text{g mL}^{-1}$ of *biotin-capture probe* for 15 minutes at 25 °C. Plates were washed three times with wash solution. The

hybridisation was performed by incubating with 10 μL of 255mer- PCR amplified target in hybridisation buffer for 1 hour at 55 $^{\circ}\text{C}$. The hybridisation was followed by an incubation of 1:1000 (dilution with respect to the original product) of α -Dig-HRP for 1 hour at 25 $^{\circ}\text{C}$. Afterwards a washing step and detection adding 50 μL of TMB incubated for 30 minutes at 25 $^{\circ}\text{C}$ was carried out, with the subsequent detection of the coloured product obtained from the TMB-HRP reaction at 405 nm.

2.2.7 Electrode preparation

Before use, gold electrode surfaces were cleaned with piranha solution (70% (v/v) 10 M H_2SO_4 , 30% (V/V) 10 M H_2O_2) for 2 hours at 60 $^{\circ}\text{C}$ and then with 10 M KOH for 1 hour at 60 $^{\circ}\text{C}$. Extreme caution should be used with this solution since it reacts violently with organic material and all work should be carried out in the fume hood. Electrodes were stored in a 10 M H_2SO_4 solution. Before use they were cleaned with concentrated HNO_3 solution for 10 minutes and rinsed with distilled water.

In the case of microarrays only 2 minutes in piranha solution were employed for cleaning since prolonged incubation in piranha may strip the gold off the electrode surface. Microarrays were rinsed with distilled water and afterwards dried and kept under argon atmosphere.

Graphite rods (3 mm diameter) were sealed in an insulating heat-shrink plastic. The rods were then cut to expose a disc of carbon. Electrodes were polished with two grits of sand paper and sonicated to remove graphite powder. Electrodes were further polished using three particle size of alumina oxide solutions (10 μm , 1.0 μm , 0.3 μm) and sonicated to remove all traces of alumina. Clean electrodes were stored in the dark under vacuum until use.

Before use the electrodes were checked with cyclic voltamperometry (CV) to verify their real area and that their capacitance was within an acceptable range. A satisfactory value of capacitance for gold electrodes is below 20 μFcm^{-2} and carbon electrode below 60 μFcm^{-2} .

Gold sheet electrodes were tested in 2 M sulphuric acid. CV between -0.2 and 1.8 V (vs. Ag/AgCl) at 0.2 V s⁻¹ were carried out. Platinum electrode was also tested with the same solution between -0.2 and 1.2V (vs. Ag/AgCl) at the same scan rate.

The area of carbon electrodes was measured in 2.5 mM ferricyanide, 150 mM NaCl by CV between -0.5 and 0.5 V (vs. Ag/AgCl) at 0.050 V s⁻¹scan rate.

Capacitance was tested in 10mM PBS 50mM, pH 8 by CV between -0.5 and 0.5 V (vs. Ag/AgCl) at 0.050 V s⁻¹scan rate.

2.2.8 Electrochemical detection of direct hybridisation with diffusional mediators

Best results for the immobilisation of the *thiol-capture probe* were obtained from a mixed monolayer immobilisation. This was preparing by incubating the electrode in 12 µg mL⁻¹ of *thiol-capture probe* in 1 M KH₂PO₄ for 2 hours at room temperature, followed by incubation for 1 hour at 25 °C in 1 mM mercaptoethanol to displace all the oligonucleotides that have been adsorbed on to the surface instead of through the thiol group, and also to block the free gold surface. Between steps the electrodes were washed with wash buffer.

Hybridisation was accomplished with 12 µg mL⁻¹ concentration of the *complementary-HRP* in hybridisation buffer.

Electrochemical measurements took place in a thin layer cell with Ag/AgCl reference/counter in a total volume of 20 µL. At time zero 13.3 µL of 0.5 mM mediator [Os(bpy)₂(pyr-CH₂-NH₂)]Cl in 50 mM SSC buffer, 0.2 M NaCl pH 5.5 was injected. A potential of -0.1 V (vs. Ag/AgCl) was applied for 100 seconds. After this time and addition of 6.6 µL of 6 mM H₂O₂ was made and the cell was switched off for 5 minutes before the application of -0.1 V and the amperometric monitoring of the response.

2.2.9 Electrochemical detection of direct hybridisation with non-diffusional mediator

The immobilisation of osmium polymer was accomplished by crosslinking with streptavidin and polyethyleneglycol diglycidyl ether (PEG-DE). 40 µg of redox polymer, 5 µg of PEG-DE and 2 µg of streptavidin were mixed. 10.5 µL of the mixture was deposited on the electrode and left to dry in the dark under vacuum for 12 hours. Afterwards the electrode was incubated for 1 hour at 25 °C in 20 µL of 15 µg mL⁻¹ *biotin-capture probe*. 18 µg mL⁻¹ *complementary-HRP* in hybridisation buffer was left to react with the immobilised capture probe for one hour at 55 °C. Electrodes were washed between steps.

Detection was carried out in a 5 mL electrochemical cell with Ag/AgCl reference, and stainless steel counter electrode. The modified carbon electrode was immersed in 300 µL of 50 mM SCC buffer, 0.2 M NaCl pH 5.5 and a potential of +0.1 V was applied. 100 µL of 6 mM was added after 150 seconds. 200 seconds after the H₂O₂ injection the current was recorded.

2.2.10 Electrochemical detection of direct hybridisation of PCR products with non-diffusional mediator

The electrochemical detection of the selective amplification of the *M.tuberculosis* rpoB gene region containing the mutation that confers resistance to rifampicin was carried out on carbon electrodes using an osmium polymer crosslinked on the electrode surface. A similar protocol as the used in the amperometric detection of 19-mer synthetic oligonucleotide with redox polymer transduction was followed. However, after hybridisation an additional step was necessary for detection, because in this case the amplified oligonucleotide was labelled with digoxigenin instead of the HRP. Incubation for one hour at 25 °C in 1:250 with α-Dig-HRP was required. Electrochemical detection was performed in the same manner as explained in 2.2.9.

2.2.11 Interdigitated electrodes as demostartion of electrochemical microarrays.

- Microarray fabrication by photolithography.

For the patterning of gold electrodes, sputtered gold silicon wafers and three 5 inches diameter quartz-chromium masks were required. With the first mask the gold electrodes were patterned on the silicon surface. To delimitate the electrodes surfaces, the connections between the electrodes and the pads were insulated and to this end a second mask was used. With the third mask one of the two sets of electrodes was opened for the attachment of the biomolecules.

In order to pattern the gold electrodes with the first mask, AZ 5214 photoresist was deposited on the wafer. The spin speed was set in 7000 rpm giving a film thickness of 1 μm . Then the wafer was pre-baked at 95 °C for 10 minutes and exposed in a mask aligner at 310 nm with a resulted dose of 22 mJ cm^{-2} . The polymer not exposed to the ultraviolet (UV) light was removed after incubation with AZ MIF726 for 1 minute. Then the wafer was baked on a hotplate at 120°C for 10 minutes. The etching of the gold was made with *Aqua Regia*, afterwards the polymer that protected the patterned gold was removed with acetone in an ultrasonic bath. The insulator layer was attained with the same photoresist and the same procedure, only after the development the wafer was baked at 200°C for 1 hour in order to fully crosslink the photoresist. The result was a gold interdigitated electrode (IDE) consisted of two sets of 50 microelectrodes with 20 μm gap-width and band-width (Figure 2.1).

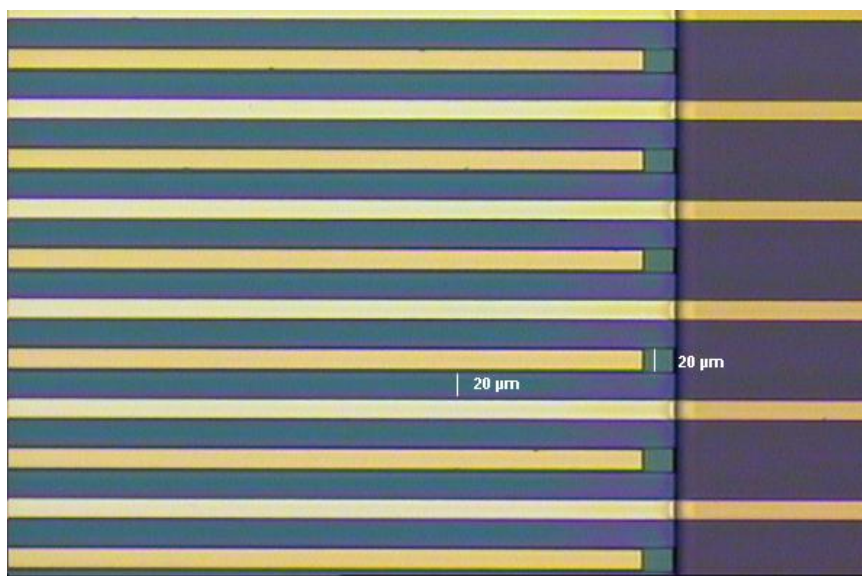


Figure 2.1. Gold IDE array picture. Each set of electrodes consist on 50 microelectrodes with a width of 20 μ m and a distance between electrodes of 20 μ m.

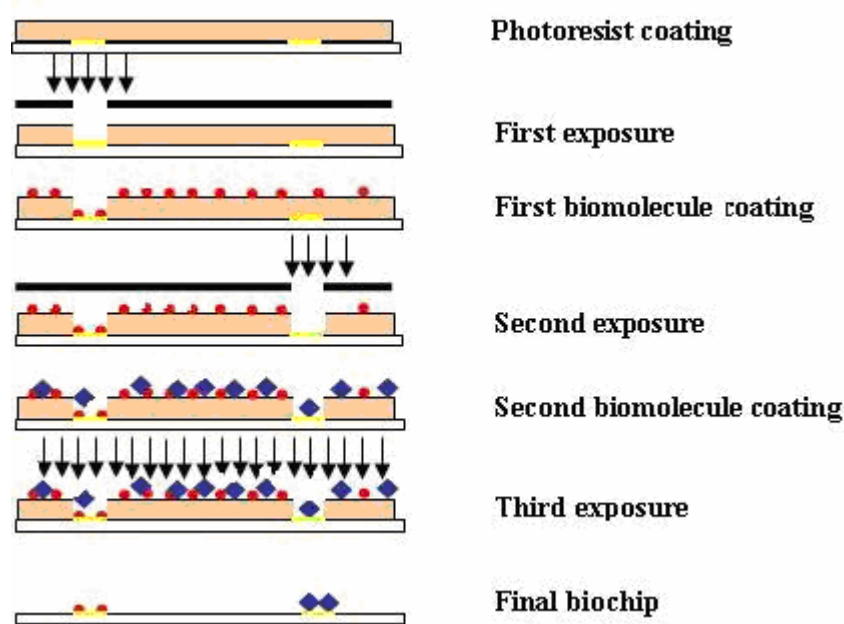
A biocompatible photoresist polymer was used in order to open first one set of electrodes and after the biomolecules attachment on the opened set of electrodes, the second set of electrodes were exposed for its attachment with a different biomolecule. The photoresist polymer used for this application should fulfil certain requirements in order to be able to give two successive lithographies under biocompatible conditions. The process after the biomolecules deposition should be carried out below 50 $^{\circ}$ C in dilute aqueous base solution, concentration lower than 0.26×10^{-3} N and in wavelengths above 300 nm. The photoresist polymer used (Douvas et al., 2001) is a copolymer synthesized from four methacrylate monomers using free radical polymerization. The monomers participating in the polymer were tert-butyl methacrylate where its tert-butyl ester group is the acid cleavable group, hydroxyethyl methacrylate and acrylic acid where their carboxyl and alcoholic groups turn the resist more hydrophilic, improving polymer adhesion to the substrate and isobornyl methacrylate where its hydrophobic isobornyl group keeps the unexposed polymer insoluble. The photoresist polymer contains also a photoacid generator.

The biocompatible polymer was spin-coated on the gold patterned wafer by spinning at 3000 rpm for 1 minute. The pre-baking was performed on a hotplate at 120 $^{\circ}$ C for 5 minutes and the exposure was made on the same mask-aligner with a dose of 160 mJ cm^{-2} . Afterwards the wafer was post-exposure bake at 50 $^{\circ}$ C for 3 minutes and

developed in TMAH 1.04×10^{-3} N for 3 minutes. Before this procedure the first set of electrodes were opened and prepared to be covered with the biomolecules.

After the biomolecules attachment the exposure, post-exposure bake and development steps were repeated in order to open the second set of electrodes.

Once the second biomolecule was immobilised the wafer was flood exposed in mask-aligner using a glass as a filter in order to cut all the wavelengths below 300 nm. The exposure dose was 720 mJ cm^{-2} . Finally the wafer was thermally treated at 50°C for 5 minutes and developed in TMAH 2.6×10^{-3} N for 5 minutes. Following this procedure all the photoresist film was stripped away, leaving the gold electrodes with the attached biomolecules ready for use. The scheme below shows the steps for the biocompatible patterning of two biomolecules on an array (scheme 2.1).



Scheme 2. 1: Scheme of biocompatible lithography biomolecules patterning on array.

Two experiments were carried out on microarrays:

- Bi-enzyme-oligonucleotide patterning detection on array.

Gold IDE arrays were coated with photosensitive biocompatible polymer. After the UV light exposure, one set of electrodes left deprotected while the other remained protected

by the polymer. A mixture of $0.2 \mu\text{g mL}^{-1}$ of *thiol-capture probe-dig* and 1:2000 of α -Dig-HRP was left to react for 1 hour at 37°C . Once the mixture was incubated, $20 \mu\text{L}$ of this solution was combined with $10 \mu\text{L}$ of 2 mg mL^{-1} redox polymer and was placed on the working electrode surface. Electrodes were incubated 2 hours at room temperature to allow for the redox polymer adsorption and the formation of dative binding between thiol-oligonucleotide and gold electrodes. The wafer was soaked in wash solution and blocked with an incubation of 1 mM mercaptoethanol for 1 hour at room temperature. The second set of electrodes was exposed at 320 nm and developed with 1 mM of TMAH. This opened electrode surface was incubated with pre-reacted *thiol-capture probe-Dig* with α -Dig-ALP and redox polymer at the same concentration as before and then blocked in the same manner

After each biomolecule attachment the array was interrogated amperometrically with a bipotentiostat. Ag/AgCl was the reference electrode and platinum the counter electrode. The electrochemical cell was a drop of $100 \mu\text{l}$ of 50 mM Hepes buffer pH 7.5, 200 mM NaCl on the array working electrode, which was in contact with the reference and counter electrode. -0.1 V was applied in the first set of electrodes where HRP labelled oligonucleotide was immobilized, and 0.3 V in the second set of electrode where alkaline phosphatase (ALP) labelled oligonucleotide was deposited. Both substrates, H_2O_2 for HRP detection and p-aminophenyl phosphate for the catalysis of ALP were added.

- Breast cancer gene patterning detection on array.

When one set of electrodes was deprotected, $40 \mu\text{g}$ osmium redox polymer, $5 \mu\text{g}$ PEG-DE and $2 \mu\text{g}$ streptavidin was placed on the working electrode surface. Electrodes were incubated for 1 hour at 25°C . The wafer was washed and incubated with $5 \mu\text{g mL}^{-1}$ *biotin-mutated BC capture probe* in 50 mM phosphate buffer pH 6.5 for 30 minutes at 25°C and then the free streptavidin was blocked with $1 \mu\text{M}$ biotin in 50 mM phosphate buffer pH 6.5 for 30 minutes at room temperature. Then the second set of electrodes was deprotected. This set of electrodes was modified with the same mixture of copolymer, PEG-DE and streptavidin and then incubated with $5 \mu\text{g mL}^{-1}$ *biotin-wild BC capture probe* and finally blocked in the same manner. $7 \mu\text{g mL}^{-1}$ of *BC target* in 50 mM HEPES buffer, 50 mM NaCl, 1 mM EDTA, pH 8.0 was incubated on the array for

30 minutes at 25 °C and afterwards 0.25 $\mu\text{g mL}^{-1}$ streptavidin-HRP in 50 mM HEPES buffer, 50 mM NaCl, 1 mM EDTA, pH 8.0 was incubated for 30 minutes at 25 °C. After each step the array was washed with the buffer.

The arrays were interrogated amperometrically in the same manner as previously. -0.1 V was applied in both set of electrodes, to detect the target which was labelled with HRP, 1 μL of 100 mM H_2O_2 was injected into the electrochemical cell and a reduction current was recorded.

2.3 Results and Discussion

2.3.1 Optimisation of hybridisation conditions by optical ELONA

In order to determine the optimum conditions for the hybridisation of the complementary oligonucleotide, enzyme-linked oligonucleotide assay ELONA was performed to optimise time, concentration and temperature of hybridisation (results not shown). It was found that the best signal/noise ratio was obtained with 18 $\mu\text{g mL}^{-1}$ of *complementary target* incubated 1 hour at 55 °C. Under these optimal conditions a hybridisation signal of 1.35 absorbance was obtained with a background of 0.08 absorbance (Figure 2. 2).

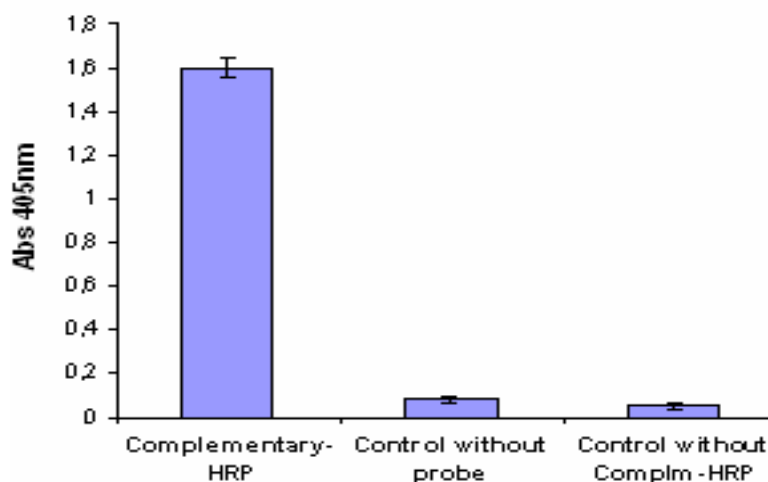


Figure 2. 2. Colourimetric detection of $18 \mu\text{g mL}^{-1}$ 19-mer HRP labelled oligonucleotide hybridised for 1 hour at $55 \text{ }^\circ\text{C}$ in hybridisation buffer (see experimental part). Colourimetric substrate of HRP, TMB, was incubated for 30 minutes at $25 \text{ }^\circ\text{C}$. Coloured product from the reaction between HRP and TMB was read at 405 nm by spectrophotometry. (n=3)

2.3.2 Colourimetric detection of oligonucleotide specific for breast cancer

Colourimetric detection of oligonucleotide hybridisation, for sequences corresponding to a certain region of the breast cancer gene, was detected next to controls.

As shows Figure 2. 3 there were clear differences between sample and control, though comparing with the previous 19-mer oligonucleotide detection, higher background was obtained in this experiment, 40% of background from the higher control signal.

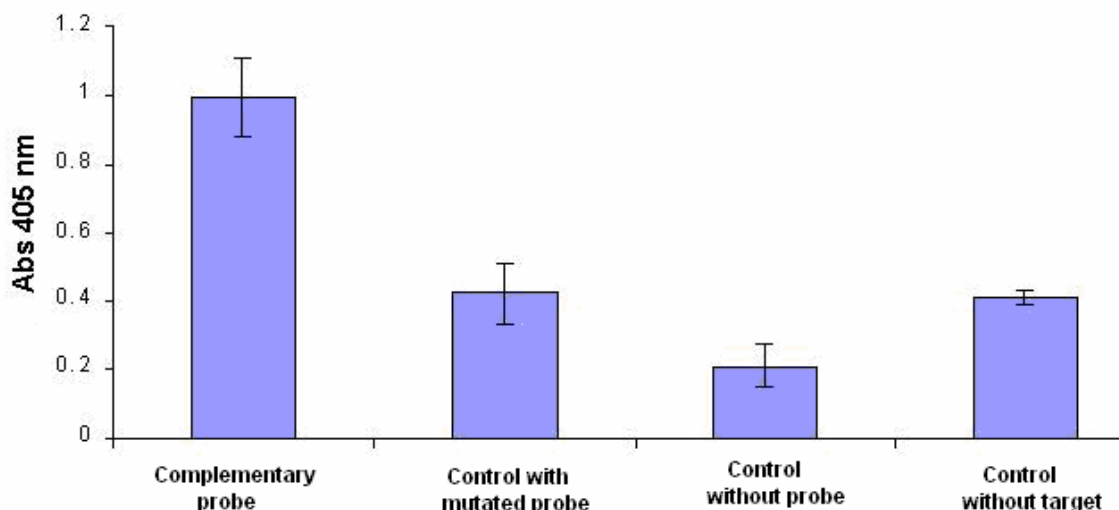


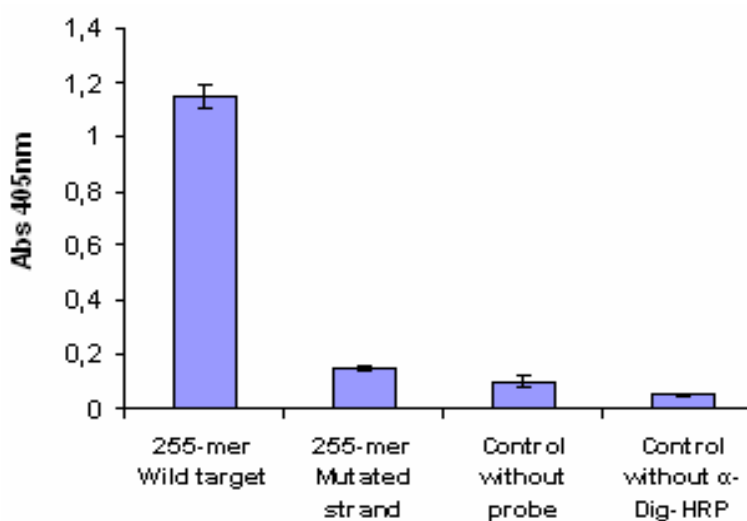
Figure 2. 3. Colorimetric detection of $5 \mu\text{g mL}^{-1}$ of breast cancer oligonucleotide hybridisation in hybridisation buffer. Peroxidase colorimetric substrate was incubated for 15 minutes and the change of colour was detected spectrophotometrically at 405 nm . (n=3)

The high background obtained in this system may be due to the streptavidin-HRP incubation that is required in this system. In the previous experiments the complementary oligonucleotide was directly bioconjugated with HRP. In contrast, in

this system complementary oligonucleotide was labelled with a biotin molecule and is necessary to bind this molecule with the reporter enzyme. Thus an extra step is required to link biotin with streptavidin-HRP, however streptavidin-HRP also binds non-specifically with the solid support, increasing the background response. From the results, it appears tht streptavidin-HRPinteracts non-specificallywith the probe and the EONA system appears not to be able to distinguish the mutations. The system was not further optimised since the translation of these experiments to the electrochemical system needed only demonstrate that a two-electrode “array” can be manufactured.

2.3.3 Colourimetric detection of direct hybridisation of PCR products

Once amplification of the *M.tuberculosis* rpoB gene region was finished, the predominant ss 255-mer oligonucleotide obtained was detected by ELONA. Low background signal was observed, 0.05 absorbance units was obtained when no α -Dig-HRP was used, 0.1 absorbance were detected with the control without capture probe immobilised and 0.15 absorbance when a mutated 255-mer oligonucleotide was hybridised, while the signal obtained from the target hybridisation was 1.15 absorbance units (Figure 2.4).



Chapter 2. Detection of direct DNA hybridisation

Figure 2. 4. Colourimetric detection of 255-mer oligonucleotide amplified by PCR. Peroxidase colorimetric substrate was incubated for 15 minutes and the change of colour was detected spectrophotometrically at 405 nm. (n=3)

In this system as well an extra step was also required to bind the 255-mer digoxigenin labelled oligonucleotide with the reporter enzyme (α -Dig-HRP). However in this case the increase of background was not detected presumably due to the different nature of the labelled antibody as compared to streptavidin. In fact, streptavidin has been reported in the literature to non-specifically interact with oligonucleotides. The lower background also marginally permits the detection of mutations in the ELONA system. Therefore, in the case when a direct labelling of the oligonucleotide with the enzyme is not possible, it is preferable to use a digoxigenin rather than a biotin label.

Various concentrations of the oligonucleotide target were amplified by PCR and then detected by ELONA following the same protocol.

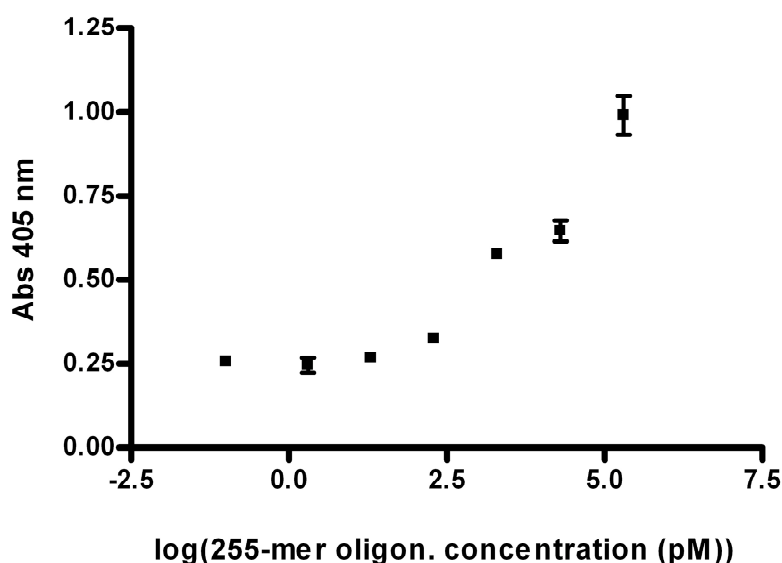


Figure 2. 5. Colorimetric detection of different concentrations of 255-mer oligonucleotide hybridisation by colourimetric detection. 255-mer oligonucleotide concentration (200000, 20000, 2000, 200, 20, 2, 0 pM) were plotted logarithmically. (n=3)

To determine measure the limit of detection the non-quantifiable signals were discarded and the values that have a linear response were fit in a linear regression line. The standard deviation of the line was measured and multiplied by 3, in order to reduce the

probability of a false non-detection to 5%, this value was added to the signal value distinguishable from noise response. Detection limit obtained for this system was equal to 201.4 ± 0.2 pM (Figure 2.5).

These experiments performed with the “standard” methods of DNA detection allowed the establishment of condition for the electrochemical detection and provided a basis for comparison of the two methods.

2.3.4 Electrode preparation

The real surface area of an electrode can be orders of magnitude greater than the geometrical area, so knowing the active area is meaningful because current depends on it. The roughness factor shows the ratio of the real surface area to the geometrical area of the electrode. The roughness factor changes depending on material, chemical and electrochemical treatment of the electrode surface.

- Gold sheet electrode

Cyclic voltamperometric determination of gold electrode real surface is based on the electrochemically induced deposition of oxide monolayer on the electrode surface and measurement of the charge corresponding to this monolayer. The integration of the peak area associated with the electrochemical reduction of the oxide monolayer produced at 0.8 V versus Ag/AgCl was used to find the real electrode area. The measurements were performed in 2 M H₂SO₄ at the potential scan rate 0.2 V s⁻¹, scanning between -0.2 and 1.8 V versus Ag/AgCl. The charge/area ratio is different for the different planes of a gold crystal, but it is usually considered to be 400 μC cm⁻² for a polycrystalline gold electrode (Bard and Dekker, 1976).

This gold sheet electrode has been used as working electrode in the thin layer cell accompanied with a plastic substrate Ag/AgCl ink or platinum reference/counter electrode.

This electrode has a geometrical area of 0.18 cm^2 and $0.26 \pm 0.1 \text{ cm}^2$ was the experimental value obtained.

- Platinum electrode

Determination of the real surface area of bare platinum electrodes is based on the formation of a hydride monolayer electrochemically adsorbed at the electrode surface. The measurements were performed in $2 \text{ M H}_2\text{SO}_4$ at the potential scan rate 0.2 V s^{-1} , scanning between -0.2 and 1.2 V versus Ag/AgCl . $210 \mu\text{C cm}^{-2}$ was the conversion factor used to calculate the real platinum electrode area (Trasatti and Petrii, 1991).

This electrode has been used as reference/counter electrode in a two-electrode cell or as counter electrode in a three-electrode cell. This electrode consists on a 0.5 mm platinum wire coiled in spiral to increase its area.

The experimental value of platinum area was 2 cm^2 . This Pt electrode was used as counter/reference electrode in a two-electrode cell with the gold sheet electrode. In order to support the current through electrodes and to maintain its inherent potential, the area of the complementary electrode must be greater than working electrode. In this case the Pt electrode is 10 times larger than working electrode, which is an appropriate area for this purpose.

- Carbon electrode

This electrode with an exposed disc-shaped area of 3 mm diameter, it has been used as working electrode in 3-electrode cell setup.

The analyte used for the carbon electrode area measurement was the ferricyanide anion, $\text{Fe}(\text{CN})_6^{3-}$, it has a very fast one electron reversible exchange. $\text{Fe}(\text{CN})_6^{3-}$ has a diffusion coefficient, $D = 0.72 \times 10^{-5} \text{ cm}^2 \text{ s}^{-1}$ (Petrovic, 2000), which allows through the Randles-Sevcik equation (Bard and Faulkner, 1980) the relation of the electrode area with the peak height and the scan rate of the CV.

$$i_p = 0.4463 n F A C (n F v D / R T)^{1/2} \quad (\text{Equation 2.1})$$

Where, i_p is the peak height current (A), n is the number of electrons involved in the redox couple, v is the rate at which the potential is swept ($V s^{-1}$), A is the electrode area (cm^2), C is the analyte concentration, D is the analyte diffusion coefficient ($cm^2 s^{-1}$), R is the gas constant ($8.3 J mol K^{-1}$), and T is the temperature (273 K).

This electrode has a theoretical area of $0.07 cm^2$ and 5 times higher was the experimental area obtained. This difference between experimental and theoretical value is due to the porosity of this material.

- Capacitance measurements.

At a given potential, the electrode solution interface is characterized by a double layer capacitance. The electrical double layer is the array of charges particles and oriented dipoles that exists at every material interface. In electrochemistry such layer reflects the ionic zones formed in the solution to compensate for the excess of charge on the electrode. Thus a negatively charged electrode attracts a layer of positively charged ions.

Capacitance is a crucial factor in electrochemical experiments because it gives rise to current during the charging of the capacitor. To calculate the magnitude of this current, we differentiate this equation respect to t and assume that capacitance is constant: (Bard and Faulkner, 1980) (Equation 2.2)

$$\frac{dQ}{dt} = C \frac{dE}{dt}$$

dQ/dt is an expression for current (Δi) and dE/dt is the potential scan rate v . Finally is obtained a relation between current and scan rate; $\Delta i = C v$

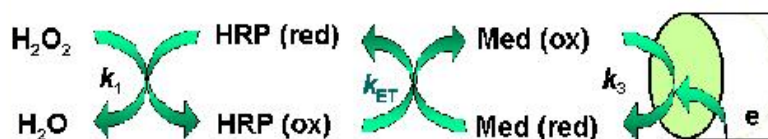
Thus by measuring a solution of 10mM PBS 50mM, pH 8 by cyclic voltamperometry the charging current at a given scan rate, we determine the capacitance of the system.

The capacitance obtained for gold electrodes was below $20 \mu F cm^{-2}$ and carbon electrode below $60 \mu F cm^{-2}$.

2.3.5 Electrochemical detection of direct hybridisation with diffusional mediator

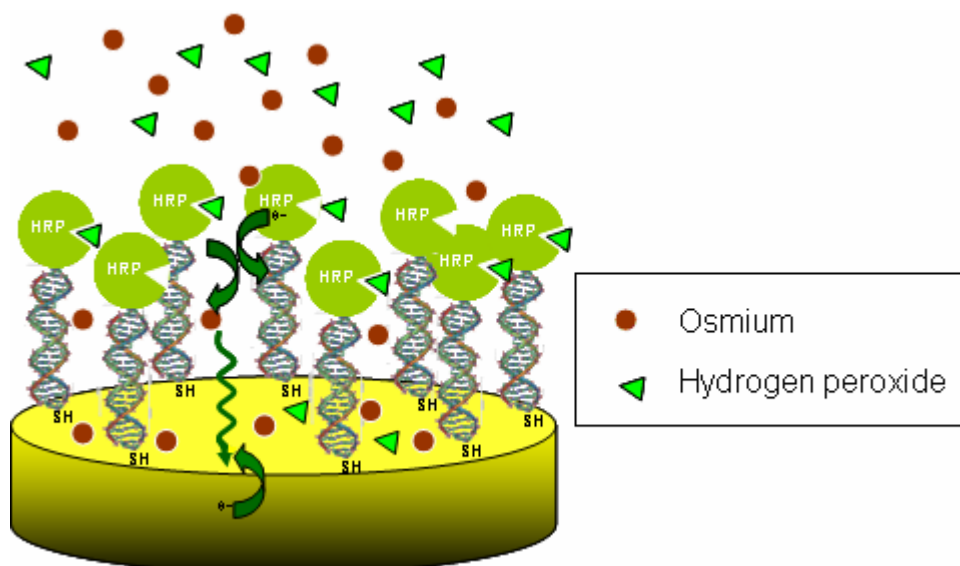
Following the determination of appropriate range of parameters with ELONA, the electrochemical detection of hybridisation on immobilised capture probes on gold was optimised.

In all the systems where HRP was involved as reporter molecule, the following reaction was produced (scheme 2.2). HRP catalyses the reduction of H_2O_2 to H_2O and becomes oxidised. Electrons formed at the electrode are transferred to the enzyme by a mediator (Gregg and Heller, 1992), which is recycled through an electrochemical scheme that is shown schematically below.



Scheme 2.2. Electrocatalysis of HRP through a mediator.

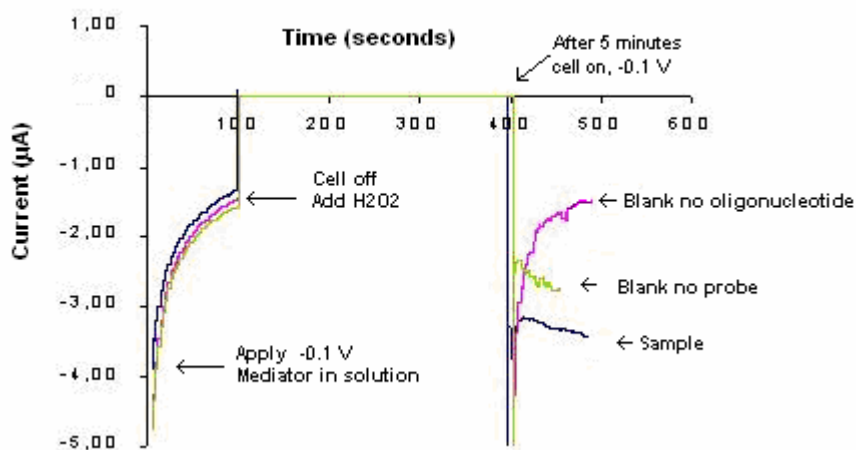
As shown in scheme 2.3, in these experiments DNA capture probe was attached on the surface through a dative bond with the gold surface and complementary-HRP hybridisation was chronoamperometrically detected with the addition of H_2O_2 and diffusional mediator, $([\text{Os}(\text{bpy})_2(\text{pyr}-\text{CH}_2-\text{NH}_2)]\text{Cl})$.



Scheme 2.3. Chronoamperometric detection of hybridisation by way of a diffusional mediator.

This catalytic reaction gives rise to a catalytic current, which can demonstrate itself as a steady state current if the cell is thin enough. Although an effort was made to create thin film cell, after some preliminary optimisations (results not shown) the detection protocol that was chosen was a bulk electroreduction of the mediator. This scheme has the disadvantage of higher detection limit and magnification of non-specific background current but demonstrates beyond doubt that the signal is produced from the phenomena depicted in scheme 2.3.

The plot of these currents achieved for hybridisation of the complementary-HRP sequence through diffusional mediation and the controls measured for this system are shown in Figure 2.6.



Chapter 2. Detection of direct DNA hybridisation

Figure 2. 6. Chronoamperometric plots for the detection of DNA hybridisation by diffusional mediator. At time zero with mediator in solution a potential of -0.1 V vs. Ag/Ag/Cl was applied. The potential was switched off after 100 seconds at which time 2 mM H_2O_2 was injected. After 5 minutes incubation, -0.1 V was applied.

As can be appreciated in Figure 2.6, the control without complementary-HRP has a different shape comparing with control without capture probe or sample response. The system where HRP was not added has a positive sloping towards the base line, while the chronoamperogram obtained from the system without capture probe show a negative slope due to the enzyme response, which accumulates the oxidised mediator in the cell. However in the case of the control without capture probe, HRP response comes from the non-specific adsorption on the surface.

The catalytic current achieved for hybridisation of the complementary-HRP sequence was 2.54 μA , which was significantly higher than the controls (Figure 2.7). Background currents for the control experiments of 1.30 μA was obtained when complementary-HRP was not used, to test the current that could be obtained from the mediator. However, as shows Figure 2. 6 this reduction current decreased exponentially with time. To gauge the non-specific adsorption of complementary-HRP, the capture probe was not immobilised on the surface, obtaining 1.39 μA . Furthermore results obtained from experiments, in which no incubation after H_2O_2 injection was performed, lowers the current to 0.7 μA , demonstrating that the accumulation of oxidased mediator in te cell is important although it comes at the cost of longer detection times.

Although the colorimetric results showed better reproducibility and lower background, the electrochemical detection allows faster detection in small volumes and minimum manipulation steps

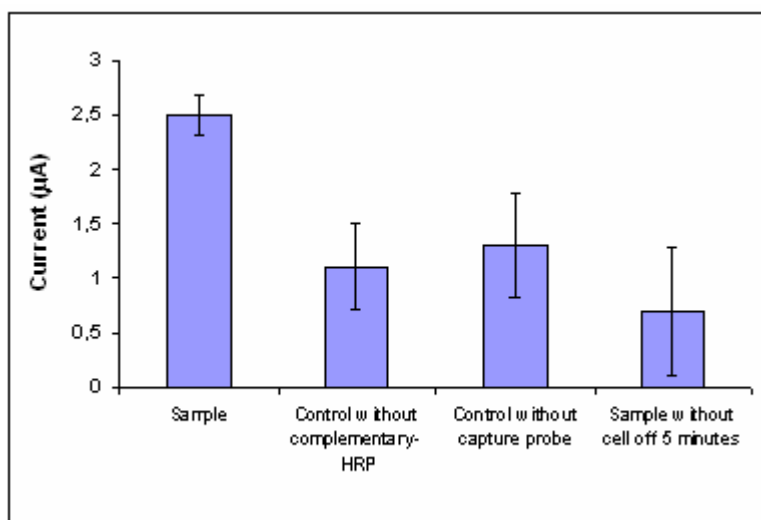


Figure 2. 7. Amperometric detection of 19-mer complementary-HRP hybridisation by diffusional mediator was plotted with control. Experimental conditions as in figure 2. 6. The resulting current was recorded after 5 seconds from the H_2O_2 injection. (n=3)

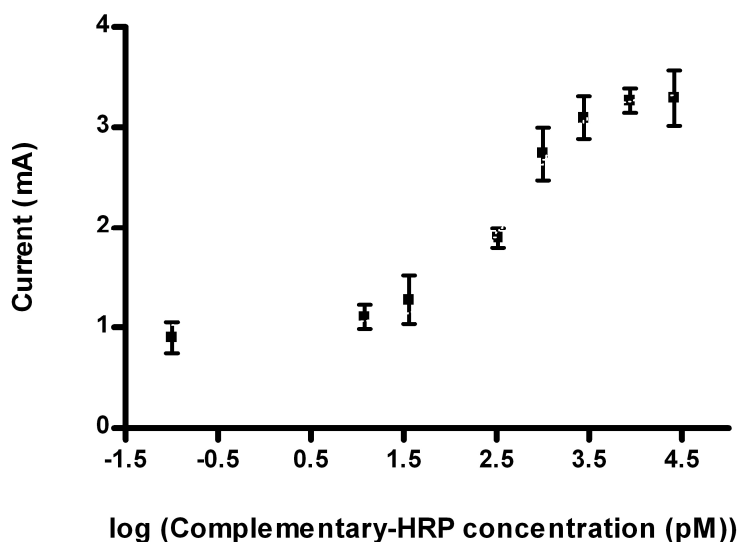


Figure 2. 8. Amperometric response of 0.18 cm^2 gold electrode modified with thiolated capture probe to detect complementary-HRP concentrations; 0, 12, 36, 330, 1000, 2760, 8686, 26200 pM, concentrations plotted logarithmically. Detection through diffusional mediator. (n=3)

The limit of detection was calculated as before measuring different concentrations of complementary-HRP (0, 12, 36, 330, 1000, 2760, 8686, 26200 pM), following the same detection protocol explained before in this section. A detection limit of $331 \pm 0.3 \text{ pM}$ was achieved (Figure 2. 8).

2.3.6 Electrochemical detection of direct hybridisation with non-diffusional mediator

Replacing the diffusional mediator with a redox polymer for the transduction of reducing equivalents from the electrode surface to the peroxidase label of hybrids confers several advantages to the detection platform: The system becomes quasi reagentless because only the addition of the enzyme substrate is needed; the detection can be performed in real time because pre-conditioning of the mediator is not needed; the response is potentially independent of hydrodynamics of the cell; smaller volumes can be used; electron transfer can become more efficient allowing higher signal noise ratio. For these reasons detection of hybridisation with a redox polymer (Narvaez et al., 2000) (Figure 2.9) immobilised on the surface was subsequently attempted.

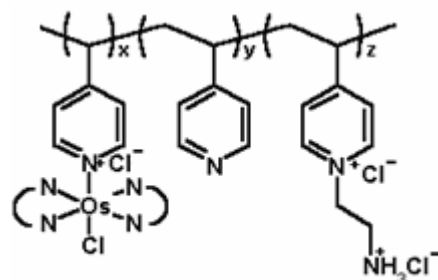
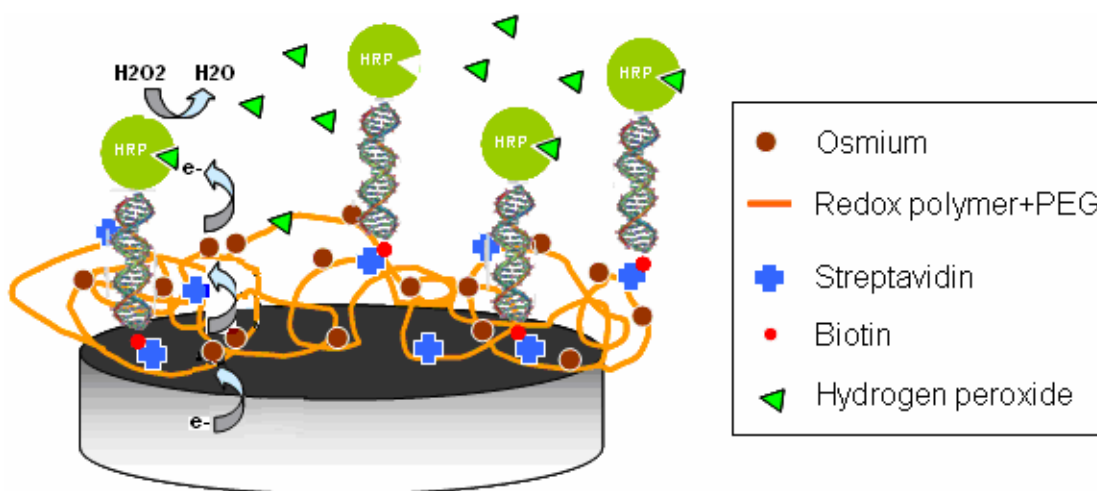


Figure 2. 9. Redox polymer used in the DNA detection ($x = 1$, $y = 3.5$, $z = 0.5$)

In this electrode configuration streptavidin is co-immobilised with the crosslinked with PEG-DE . A biotinilated capture probe is subsequently incubated with the electrode providing the sensor on which complementary-HRP hybridisation can be chronoamperometrically detected with the simple addition of H_2O_2 (Scheme 2.4).



Scheme 2. 4. Chronoamperometric detection of hybridisation with redox polymer. Electrones are transferred through a hopping mechanism and the mediator is immobilised.

However the probe-redox polymer hydrogel electron transfer capacity depends strongly on the films composition. It will also affect the non-specific adsorption events since the redox polymer is a polycation. For this reason it is fairly important to optimise the relation between redox polymer, PEG-DE and streptavidin in the film.

The film composition was optimised with respect to the amount of redox polymer and crosslinker. Redox pymer was varied from 88 to 98 % (w/w) in the film and the crosslinked PEG-DE from 1.2 to 33 % (w/w). It should be noted that as the percentatge of redox polymer or PEG-DE was increased , the film tickness was also increased. This can have two opposite effects on one hand it provides more efficient electrone transfer because the HRP is closer to the redox mediator and on the other hand it causes slower electron hoping through the ever increasing distance for electron transfer. Usually the two effects balance each other at an optimum film thickness. The result of this optmisation are summarised in Figures 2.10 and 2.11.

As shown in Figure 2.10, higher amount of redox polymer cause an increase of the current, and also improve the difference between specific and non-specific signal. This is an unexpected results since the polycationic polymer should attract non-specifically the *complementary-HRP* and is probably due to the film morphology: non-specific adsorption occurs at the outer more distant layer of the hydrogel whereas specific interactions occure closer to the surface providing faster electron transfer.

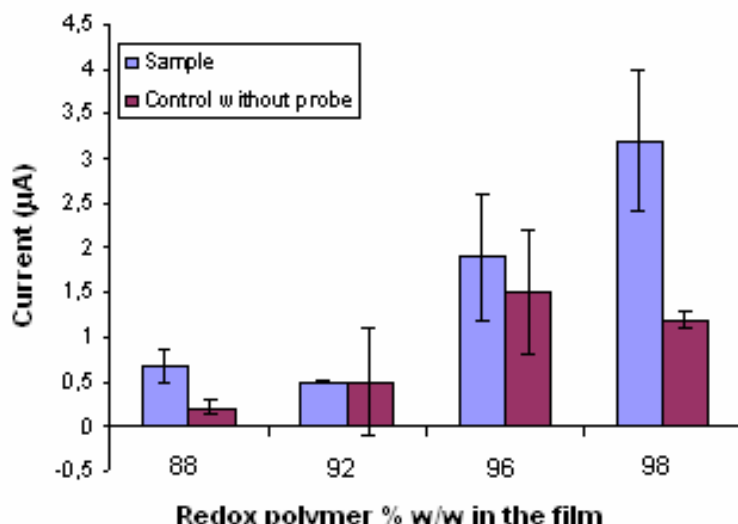


Figure 2. 10. Amperometric response of 3 mm diameter carbon electrodes modified with redox polymer as a function of redox polymer present (w/w) in the film. Columns shown response in the presence of 2 mM H₂O₂ of electrode incubated for one hour at 55 °C with 18 µg mL⁻¹ of complementary-HRP in hybridisation buffer. (n=3)

PEG-DE optimisation is shown in Figure 2.11. it had a less dramatic effect in response and non-specific currents. At high concentrations the crosslinking probably limits the accessibility of the capture probe and the mobility of the polymer chains. Both effects lower the electron transfer efficiency and limit the response.

From the above there appears to be an optimum film composition at the ratio 40:5:2 w/w of redox polymer: PEG-DE: streptavidin. This composition was used for further experiment.

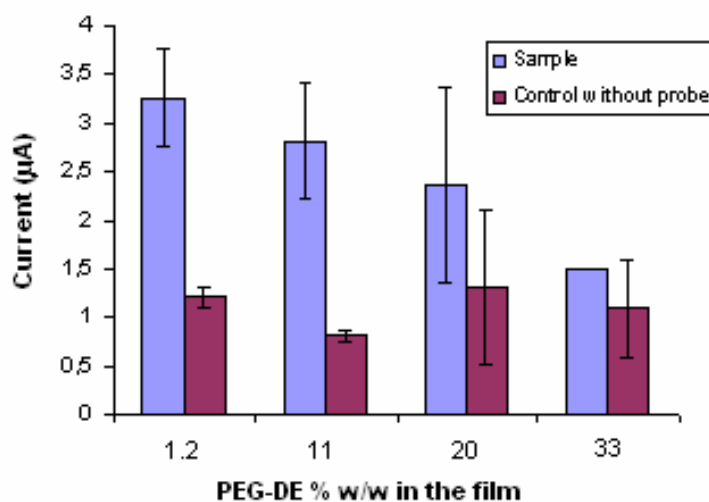


Figure 2. 11. Amperometric response of 3mm diameter carbon electrodes modified with redox polymer as a function of PEG-DE percentatge in the film. Columns depict response in the presence of 2 mM H₂O₂ of electrode incubated for one hour at 55 °C with 18 µg mL⁻¹ of complementary-HRP in hybridisation buffer. Blue columns are the response of electrodes with capture probe whereas dark red columns depict response of the control electrode without probe. (n=3)

The optimised electrodes showed almost no response to H₂O₂ in the absence of complementary-HRP. It is observed from the results that non-diffusional transduction results to similar current density as the diffusional and similar non-specific currents (36 and 44 % respectively) under the same conditions. The high background currents made immaterial the determination of detection limit. It was decided that this type of sensors could only be used for the detection of labelled PCR products where the concentration is usually not a problem.

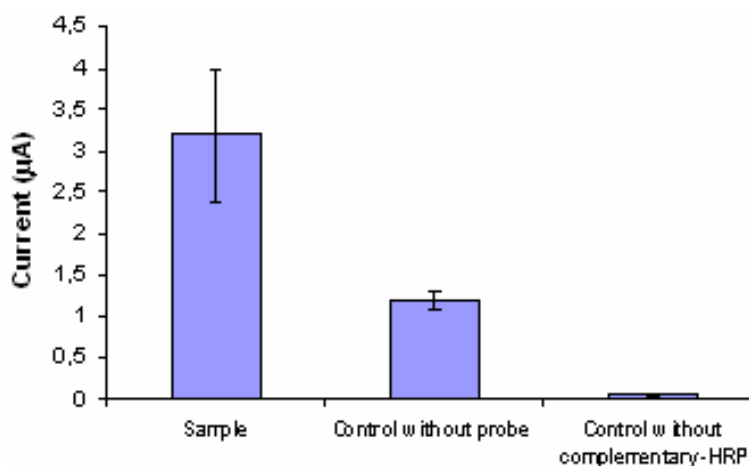


Figure 2. 12. Amperometric detection of 19-mer complementary-HRP hybridisation by redox polymer immobilised on the electrode. Chronoamperometry was carried out in a 3-cell electrode setup. At time zero in 50 mM SCC buffer, 0.2 M NaCl pH 5.5 a potential of +0.1 V was applied. 2 mM H₂O₂ was added after 150 seconds. Before 200 seconds of the injection the current was recorded. (n=3)

2.3.7 Electrochemical detection of direct hybridisation of PCR product with non-diffusional mediator

To examine the feasibility of using the DNA sensors to detect labelled PCR products asymmetric PCR for the specific amplification of *Mycobacterium tuberculosis* rpoB

gene region containing mutations that confer resistance to rifampicin was carried out. Predominantly single stranded 255-mer digoxigenin-labelled oligonucleotide was obtained. This amplified oligonucleotide sequence was detected following a similar protocol as for the non-diffusional detection of 19-mer oligonucleotides, using the electrodes optimised as described. The amplified product was labelled with digoxigenin. The electrodes were incubated in the PCR product solution for one hour at 55 °C in hybridisation buffer. Antibody was added and after an additional one hour incubation and washing the response to 2 mM of H₂O₂ was observed.

Control electrodes were used to quantify non-specific adsorption of the α -Dig-HRP. Typically responses are depicted in Figure 2.13 and the results are summarised in Figure 2.14.

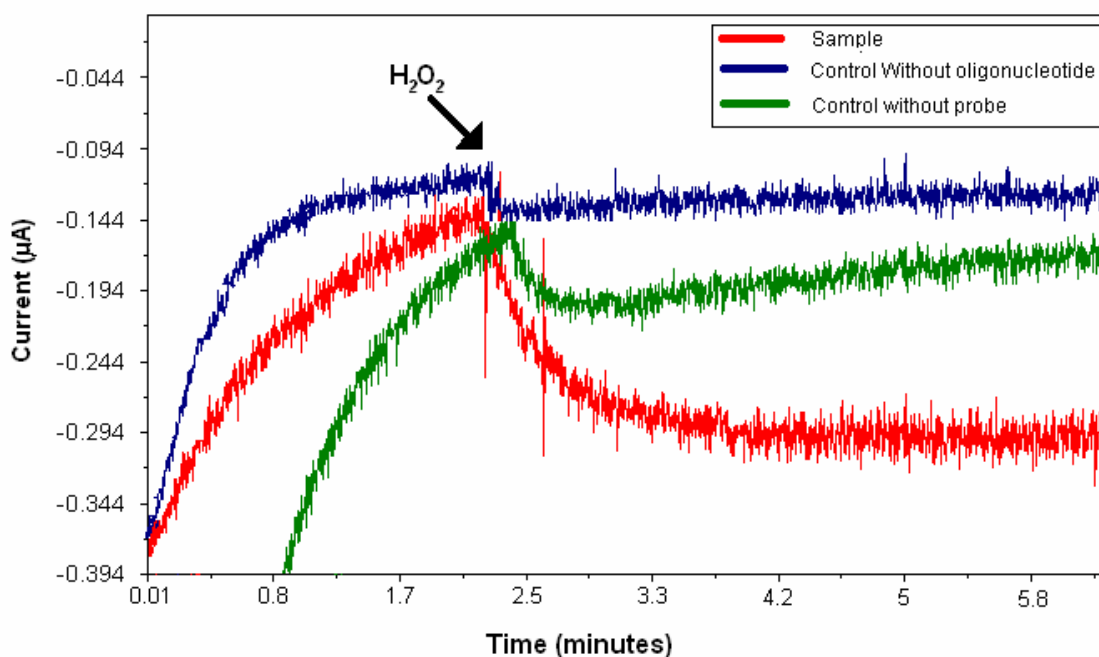


Figure 2.13. Typical chronoamperometric response of electrodes with capture probe after incubation with 255-mer amplified oligonucleotide and α -Dig-HRP (see text). Chronoamperometry was carried out in a 3-electrode cell with redox-polymer modified electrodes in 50 mM SCC buffer, 0.2 M NaCl pH 5.5. Applied potential +0.1 V. Arrow indicates addition of 2 mM H₂O₂. (n=3)

The catalytic currents observed were more than an order of magnitude lower than in the case of 19-mer detection (87 ± 8 nA) whereas the non-specific currents increased reaching approximately 50 % of the specific response. The high non-specific currents

are more likely due to the non-specific adsorption of α -Dig-HRP since in this case a second incubation is needed with the reporter enzyme.

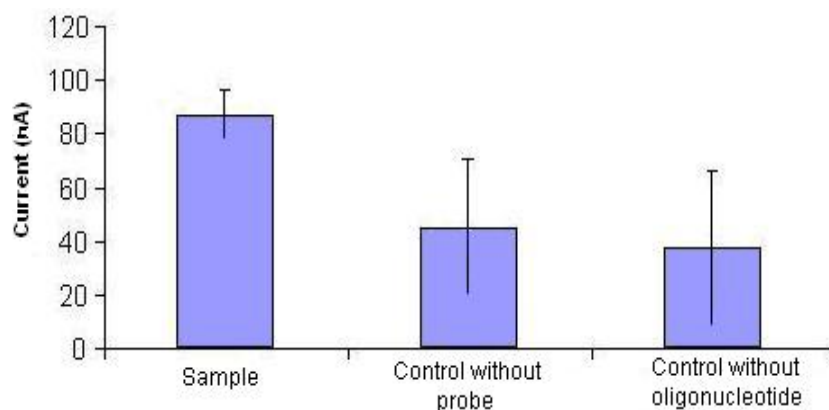


Figure 2. 14. Average amperometric response and background currents for detection of amplified 255-mer oligonucleotide hybridisation. Experimental conditions as in figure 2. 13. (n = 3)

Several factors contribute to the lower currents obtained with the 255-mer oligonucleotides. The enzyme label for the 19-mer oligonucleotide was much closer to the redox centres of the polymer than that of the 255-mer. This is so because in the case of 19-mer oligonucleotide the distance between the 5' label and the electrode surface was 65 Å, while was 870 Å for the 255-mer oligonucleotide. Since the redox polymer was surface bound, the electrons produced in the label of the 255-mer oligonucleotide covered the distance from the enzyme to the first available redox centre was much higher than in the case of the covalently bound label in the 5' end of the 19-mer. The low currents could also be explained due to the low efficiency of the additional step of the binding of the digoxigenin-oligonucleotide with the α -Dig-HRP.

Finally, it is very likely that the bulky and electrically insulating 255-mer caused a general sluggishness of the electron hopping in the redox polymer film.

Cyclic voltamperometry of the films resulting after 19-mer and 255-mer oligonucleotide hybridisation (Figure 2. 15) demonstrated lower peak currents and peak separation for the 255-mer containing redox polymer films including slower electron transfer.

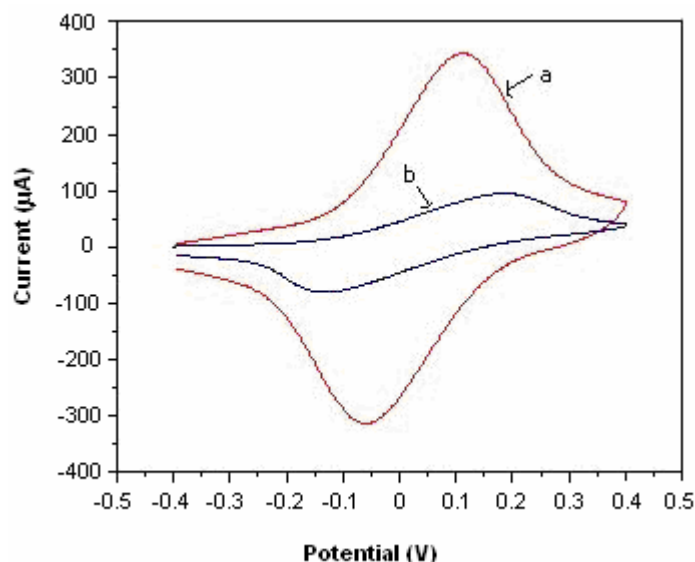


Figure 2. 15. Cyclic voltammperometry of redox polymer modified electrodes after hybridisation with the 19-mer (a) and 255-mer oligonucleotide (b). Cyclic voltammperometry was carried out in a 3-electrode cell, at a scan rate of 0.05 V s^{-1} , using 3 mm diameter carbon electrodes in hybridisation buffer.

2.3.8 Interdigitated electrodes as demonstration of electrochemical microarrays.

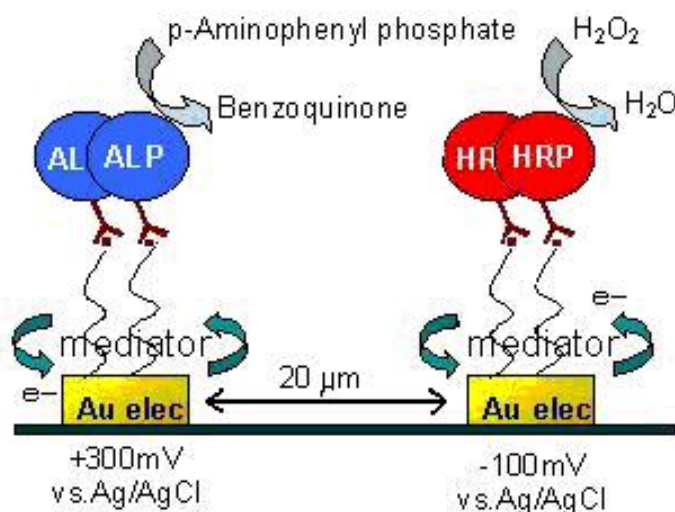
To demonstrate that several electrochemical DNA biosensors can be integrated in a multianalyte detection device a two-electrode feasibility exercise was undertaken. The use of interdigitated electrodes guarantees high enough currents, which at the same time demonstrates that a $20 \mu\text{m}$ resolution for arraying can be achieved. Biocompatible photolithography was the method of choice for arraying.

The photolithographic patterning process exposes one set of electrodes by removing the photosensitive polymer over it, while the other remained protected by the polymer. On the deprotected electrodes biomolecules were immobilised, and then the photopolymer was removed from the second set of electrodes. A second incubation with a different biomolecule would allow the construction of an array with closely spaced functionalities. However, during the second incubation both electrodes are exposed, which could bring about a non desire adsorption of the second biomolecule on the first

set of electrodes. Due to the close spacing of electrodes an effect of crosstalk could be detected.

To determine the extend of these two problems, before detection of DNA hybridisation, the non-specific adsorption of the second oligonucleotide on the first specifically adsorbed oligonucleotide was quantified. To this end, two enzyme labelled oligonucleotides were used, HRP and ALP.

Scheme 2.5 depicts the expected resulting architecture and the conditions for detection of each enzymatic product.



Scheme 2. 5. Scheme of catalytic current production for HRP and ALP enzymes.

After the sequential modification of the electrodes that was carried out as described in the experimental part, measurement of the enzyme response as amperometric current with each substrate separately and with both substrates at the same time was carried out. Figure 2.16 shows the response obtained after the addition of both substrates on the bi-enzyme patterned array. It can be seen that after the second addition of 2.5 mM of H₂O₂ only the electrode with peroxidase responded to the addition of the substrate, even when a third higher addition was made. When 0.3 mM of p-aminophenyl phosphate was added into the cell after the H₂O₂, no response was detected from the HRP electrode, while an oxidation response was measured for the electrode with oligonucleotide-ALP, a response that was repeated after a second injection. Therefore it can be concluded that no crosstalk occurs between the electrodes and that the non-specific adsorption of the second oligonucleotide if its occurs, is low and it cannot be detected electrochemically.

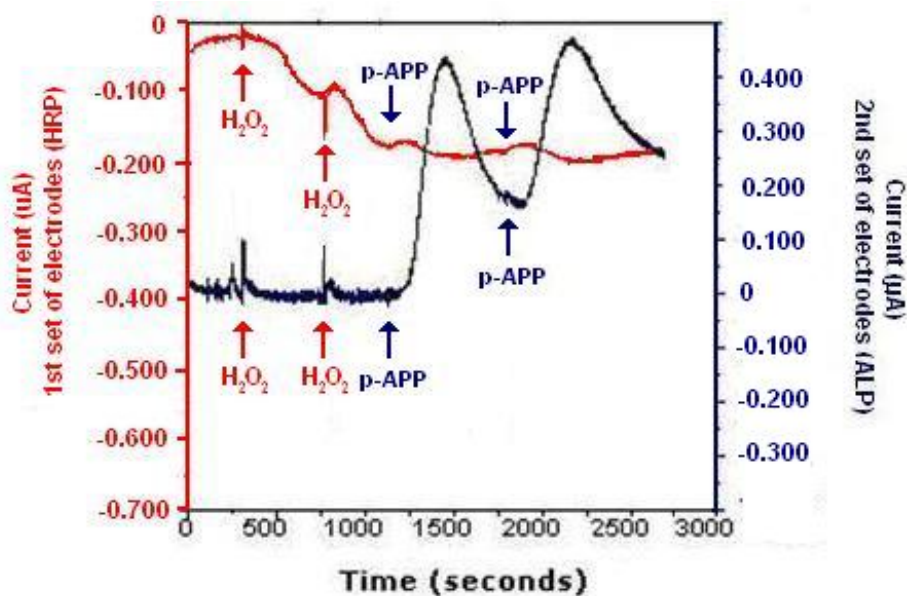


Figure 2. 16. Amperometric response of IDE photolithographically defined array with two electrodes immobilized. (Red) On the first set of electrodes oligonucleotide-HRP was immobilized and a potential of -0.1 V was applied, current response is plotted in the left red axis, (blue) and oligonucleotide-ALP was immobilized on the second set of electrodes where 0.3 V potential was used, current response is plotted in the right blue axis. Cell setup and conditions described in experimental part.

Once verified that non-specific adsorption of oligonucleotides did not occur, the electrochemical detection of hybridisation of the breast cancer gene was attempted with the immobilisation of a mutated capture probe (control) and a complementary capture probe on different electrode sets by biocompatible photolithography. In a separate IDE array a second control was carried out immobilising complementary capture probe but without the addition of the target.

Figure 2.17 shows the amperometric results and the response for different concentrations of H₂O₂ obtained from the patterned arrays. On this array the target labelled with biotin was incubated and subsequent incubation with streptavidin-HRP was made. After washing this interaction was detected amperometrically with the addition of H₂O₂. The signal obtained from the set of electrodes with complementary probe was higher, 1.7 µA for 6 mM H₂O₂, while in the set of electrodes where the mutated probe was immobilised only 0.4 µA was observed for the same concentration of substrate. The array where the target was not incubated shows that the H₂O₂ does not produce any current by itself in the conditions of the experiment.

The experiment demonstrates that in the same array, a mutated gene can be detected with certainty by electrochemical transduction.

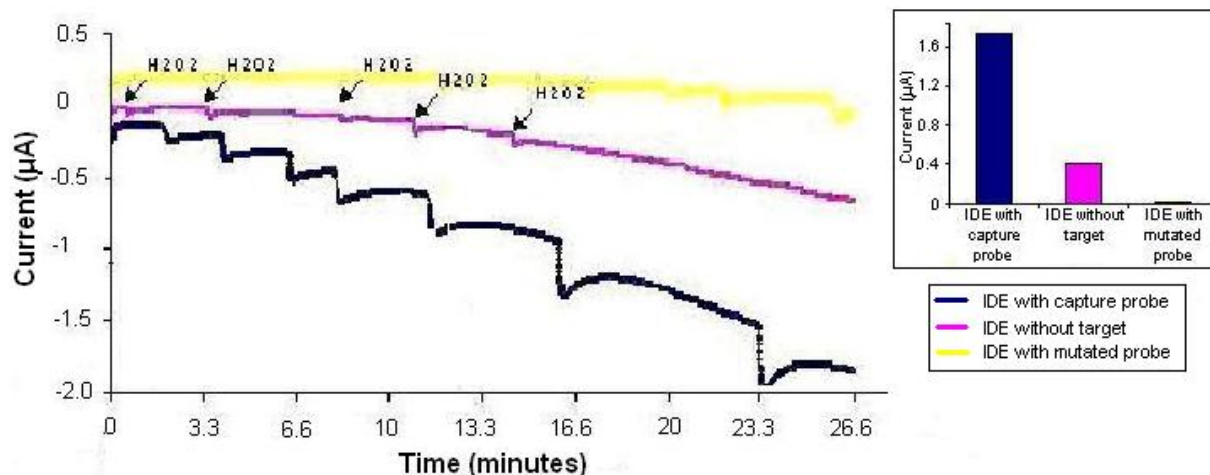


Figure 2. 17. Amperometric response of IDE array modified with $5 \mu\text{g mL}^{-1}$ complementary (blue line) and mutated probe (yellow line) with the subsequent hybridisation with $7 \mu\text{g mL}^{-1}$ target. Pink line represents the response to H_2O_2 . Electrochemical cell was a $100 \mu\text{L}$ drop as described in experimental part.

Breast cancer oligonucleotide amperometric detection on IDE using biocompatible photolithography. Complementary capture probe was immobilized on the electrode to detect the target, control with complementary capture probe but without target, control with mutated capture probe immobilized.

2.4 Conclusions

This chapter describes the feasibility of electrochemical DNA hybridisation detection of labelled PCR oligonucleotide products. Two different transduction schemes are described, diffusional and non-diffusional and they both showed similar reliability and sensitivity. The electrochemical detection compares well the “standard” optical ELONA detection both in terms of reliability and facile use. However,

electrochemical is amenable to simultaneous multianalyte analysis in small sample volumes. It remains to be seen if real time monitoring of hybridisation is possible.

2.5 References

Bard A.J., Dekker M., Electroanalytical Chemistry, New York, 9, 1976.

Bard A.J., Faulkner L.R., Electrochemical methods, John Wiley and sons, 1980.

Douvas A, Argitis P, Diakoumakos C.D., Misiakos K., Dimotikali D., Kakabakos S.E., Journal of vacuum science and technologie B, 2001, 19, 6, 2820-2824.

Garcia L., Alonso-Sanz M., Rebollo M.J., Tercero J.C., Chaves F., Journal of Clinical Microbiology, 2001, 20, 1813-1818.

Gregg B.A., Heller A., Journal of Physical Chemistry, 1991, 95, 5970-5975.

Hermanson G.T., Bioconjugated techniques, Academic Press, 1995.

Kong Y.T., Boopathi M., Shim Y.B., Biosensors and Bioelectronics, 2003, 30, 19, 3, 227-232.

Li J., Chu X., Liu Y., Jiang J., He Z., Zhang Z., Shen G., Yu R., Nucleic Acids Research, 2005, 33, 19, 168-177.

Narvaez A., Suarez G., Popescu I.C., Katakis I., Dominguez E., Biosensors and Bioelectronics, 2000, 15, 1-2, 43-52

Petrovic S., The Chemical Educator, Vol. 5, No. 5, Springer-Verlag New York, Inc.

Trasatti S., Petrii O.A., Pure Applied Chemistry, 1991, 63, 711-717.

Chapter 2. Detection of direct DNA hybridisation

Chapter 3. Detection of DNA hybridisation by Displacement.

3.1 Introduction

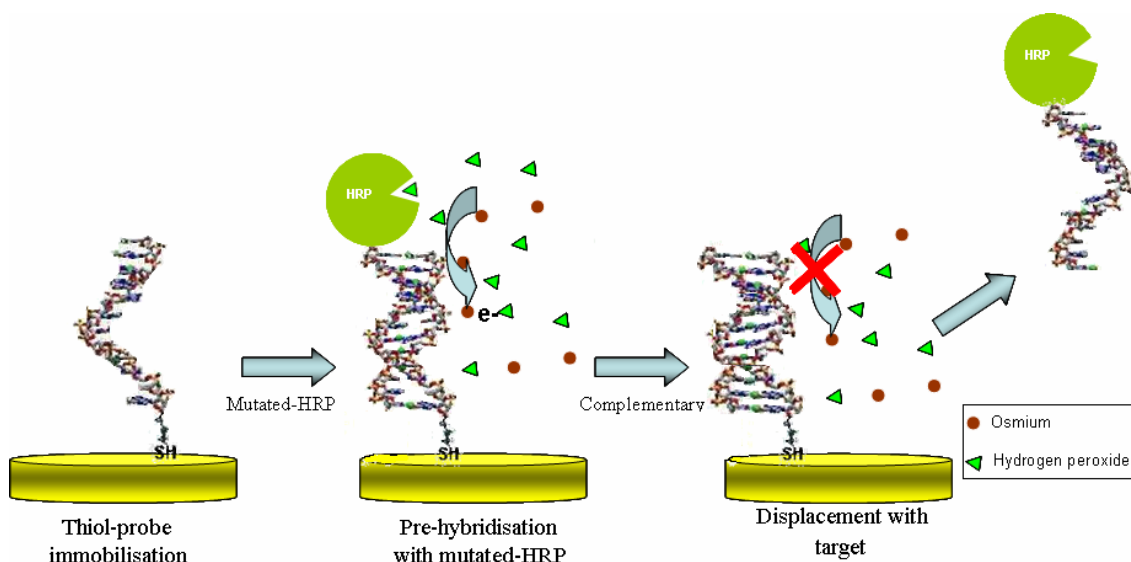
In chapter 2 it was demonstrated that electrochemical reporting of DNA hybridisation is possible. However, the detection was based on labelling the target, an operation that in today's molecular biology laboratories is routine (through PCR) but that from the point of view of biosensors developments adds to the complexity of the detection procedure and therefore to the attractiveness of the method. Essentially the work exposed in chapter 2 demonstrated that an electrochemical ELONA can be implemented. However, its attractiveness is limited because it competes with the industry "standard" that is optimised and gives reliable results when the cost and time of sample pre-treatment and labelling are assumed.

In this part of the thesis are described the effort to develop a label-free electrochemical DNA sensor. This biosensor is based on the displacement of a labelled pre-hybridised sub-optimum sequence by the target oligonucleotide.

The method of detection by displacement requires the pre-hybridisation of the capture probe immobilised on the electrode surface with a sub-optimum mutated oligonucleotide labelled with a redox molecule that produce an electrochemical signal. Due to the higher affinity of the target that is fully complementary to the capture probe, the sub-optimum label can be displaced when the complementary target is introduced in the system. A decrease of the signal should be produced that verifies the presence of the target and this decrease should be proportional to its concentration.

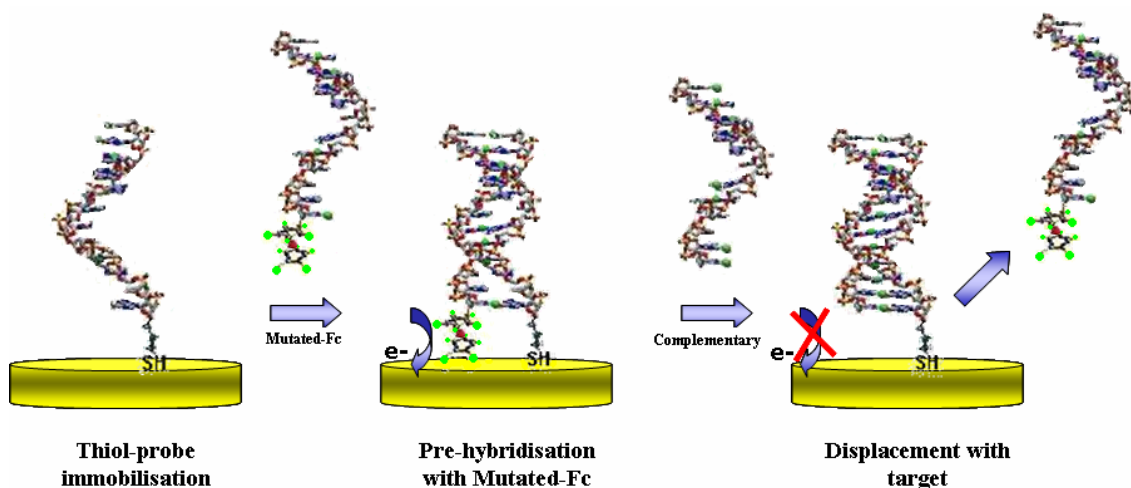
Two different suboptimum labels were developed corresponding to two different electrochemical detection strategies. The first is depicted in Scheme 3.1 and involves labelling of the suboptimum sequences with HRP in the hope of achieving signal amplification, which would provide a higher margin for displacement detection and therefore lower detection limits. Suboptimum sequences and displacement conditions were optimised colourimetric methods and electrochemical detection demonstrated only with the diffusional mediator-based platform developed in chapter 2.

Chapter 3. Detection of DNA hybridisation by displacement



Scheme 3. 1. Conceptual schematic of sub-optimum HRP labelled mutated oligonucleotide displacement detection.

The second is depicted in Scheme 3.2 and involves labelling of suboptimum sequences with ferrocene reporter molecules that were detected with a variety of electrochemical techniques in order to decide on one that could confer higher sensitivity. This second suboptimum sequence was designed to detect the cystic fibrosis gene and therefore optimisation of the mismatched base pairs was limited.



Scheme 3. 2. Conceptual schematic of sub-optimum ferrocene labelled mutated oligonucleotide displacement detection.

3.2 Materials and methods

3.2.1 Materials

a. HRP-labelled displacement sequences.

HPLC purified oligonucleotide were ordered from Eurogentec (Belgium) as follows.

19-mer biotin-labelled capture probe oligonucleotide (*biotin-capture probe*):

5'-Biotin-AGCCAGCTGAGCCAATTCA-3'

19-mer thiol-labelled capture probe oligonucleotide (*thiol-capture probe*):

5'-Thiol-C₆-AGCCAGCTGAGCCAATTCA-3'

19-mer complementary oligonucleotide (*complementary target*):

5'-TGAATTGGCTCAGCTGGCT-3'

19-mer thiol-labelled complementary oligonucleotide. This oligonucleotide strand was subsequently bioconjugate with maleimide activated horseradish peroxidase (maleimide-HRP) leading to a HRP-labelled oligonucleotide. This sequence is coined (*complementary-HRP*)

5'-Thiol- C₆-TGAATTGGCTCAGCTGGCT-3'

19-mer thiol-labelled mutated oligonucleotide. This oligonucleotide strand was also subsequently bioconjugated with maleimide activated horseradish peroxidase (maleimide-HRP) leading to a HRP-labelled oligonucleotide, (*Mutated-HRP*). This sequence has 4 mutations with respect to total complementarily.

5'- Thiol- C₆-TGAGTGGGCTCGGGTGGCT-3'

b. Ferrocene-labelled displacement sequences.

The 15-mer oligonucleotide sequence specific for detection of the cystic fibrosis (CF) gene. These oligonucleotides were purchased from VBC Biotech Service GmbH (Austria) and Eurogentec (Belgium).

15-mer amine labelled mutated oligonucleotide, for its bioconjugation with ferrocene (*ferrocene-CF mutated*):

Amine-C₆-5'-AATATCATTGGTGTT-3'

15-mer thiol labelled capture probe oligonucleotide (*thiol-CF capture probe*):

5'-ACACCAAAGATGATA- C₆-Thiol-3'

15-mer complementary oligonucleotide (*CF complementary target*):

5'- TATCATCTTTGGTGT-3'

22-mer non-complementary oligonucleotide (*non-complementary*) used for controls.

5'- GAGGCGATCACACCGCAGACGT-3'

All stock oligonucleotide solutions were made at 1mg mL⁻¹ with autoclaved milliQ water and stored at -20°C.

c. Other chemical.

Maleimide-HRP (P1709), 3,3',5,5'-Tetramethylbenzidine liquid Substrate (TMB) (T0440), Denhardt's solution (D9905), N, N'-dicyclohexylcarbodiimide (EDC) (D3128), Sodium tetraborate (12687), DNA salmon testes (D2389), bovine serum albumin (BSA) (B6917), tris(hydroxymethyl) aminomethane-acetic (Tris-Ac) (T3647), tris(hydroxymethyl)aminomethane-hydrochloride acid (Tris-HCl) (T2367), Polyethylene glycol sorbitan monolaurate (tween) (T2389), Ethylenedinitril tetraacetic acid (EDTA) (E5134), diammonium citrate (C1883), streptavidin peroxidase labelled (S5512), saline sodium citrate buffer (SSC) (S6639), ferrocyanide (P3289), ferricyanide (P8131) and 2-mercaptoethanol (M6250) were purchased from Sigma. NaCl (131659), HCl (131020), KOH (131515), KH₂PO₄ (121509), H₂SO₄ (131056) and H₂O₂ (131072.12) were supplied from Panreac. Sodium tetraborate (22,173-2), dimethylformamide (27,054-7), ferroceneacetic acid (335045), dithiothreitol (DTT) (64656-3), and N-Hydroxysuccinimide (NHS) (13067) were from Aldrich and 3-hydroxypicolinic acid (HPA) (36197) from Fluka. The Sephadex G25 DNA grade resin (17-0853-01) was purchased from Amersham Pharmacia Biotech. Streptavidin coated plates were purchased from Labsystems. The electron-conducting diffusional redox mediator ([Os(bpy)₂(pyr-CH₂-NH₂)]Cl) was synthesised as reported in the literature (Gregg and Heller, 1991).

3.2.2 Instrumentation

a. HRP-labelled displacement.

Colourimetric detection of DNA hybridisation by enzyme-linked oligonucleotide assay (ELONA) was performed with an ELISA plate reader SpectraMax 340PC from Molecular Devices running SoftMax Pro software.

Electrochemical measurements were carried out using an Autolab PGSTAT10 electrochemical analysis system running GPES management software from Eco Chemie. Electrochemistry was performed using a carbon screen-printed working electrode (SPE) with 0.78 mm^2 area and Ag/AgCl ink as reference and counter electrode or in a home-made $20 \text{ }\mu\text{L}$ two electrode thin layer cell with a 18 mm^2 square gold sheet as a working electrode opposite to a platinum reference and counter electrode. To keep potentials consistent throughout this work, this electrode has been calibrated for each solution against a standard Ag/AgCl.

b. Ferrocene-labelled displacement.

For characterisation of ferrocene labelled oligonucleotide, matrix assisted laser desorption ionisation-time-of-flight mass spectrometry (MALDI-TOF) detection was carried out in a stainless steel plate with a Voyager DE-STR from Applied Biosystems.

The e-SPR electrochemical cell is a two-electrode system, with a 4.8 mm^2 gold layer sensor disk working electrode that is defined by a gasket when the cell is assembled. The $35 \text{ }\mu\text{L}$ cell has platinum reference and counter electrode. The instrument can be programmed for automatic injection and washing steps.

Impedance measurements were carried out in the same e-SPR electrochemical cell with a CH Instruments Inc. potentiostat. The curve fitting was performed with ZView 2 software.

3.2.3 Procedures involved in HRP-displacement detection

3.2.3.1 Biocojugation of 19-mer DNA labelling with HRP

The 19-mer complementary oligonucleotide and the 19-mer mutated oligonucleotide were purchased with a 5'-thiol and a 6-atom carbon spacer. They were labelled with HRP using maleimide activation (Hermanson, 1995). The maleimide activated peroxidase was dissolved in sodium phosphate buffer (PBS) 100 mM, 30 mM EDTA and 10 mM NaCl at pH 6.5 and mixed with a ten-fold molar excess of thiol labelled oligonucleotide solution with respect to maleimide-HRP. The solution was left to stand for 12 hours in the dark and then separated with a Sephadex G25 gel filtration column. The concentration of the resulting HRP labelled oligonucleotide and the activity of enzyme labelled was determined spectrophotometrically.

3.2.3.2 Optimisation of displacement conditions by ELONA

Streptavidin plates were used to immobilise the biotin-labelled capture probe. 50 μL of 0.2 $\mu\text{g mL}^{-1}$ capture probe solution was left to bind for 15 minutes at 25 $^{\circ}\text{C}$. 50 μL of 10 $\mu\text{g mL}^{-1}$ *mutated-HRP* oligonucleotide in hybridisation buffer was added and left to incubate for 1 hour at 50 $^{\circ}\text{C}$. Hybridisation of *mutated-HRP* and *complementary -HRP* were optimised for various concentrations, times and temperatures to obtain the best conditions for pre-hybridisation of mutated-HRP and its subsequent displacement.

The background signal was established with the pre-hybridised HRP-labelled mutated oligonucleotide, which was measured after addition of 50 μL of TMB and incubation for 30 minutes at 25 $^{\circ}\text{C}$. In wells where displacement was evaluated, after the pre-hybridisation step with *mutated-HRP* oligonucleotide, 50 μL of 30 $\mu\text{g mL}^{-1}$ *complementary* target in hybridisation buffer was incubated for different times and at varying temperatures as indicated, followed by the detection with TMB. Washing with wash buffer (100 mM Tris-HCl pH 7.5, 150 mM NaCl and 1% Tween) was performed between all incubation steps.

3.2.3.3. Electrochemical monitoring of displacement of HRP-labelled sequences.

The electrochemical detection of displacement was carried out on screen-printed electrodes.

The biotin-capture probe was immobilised through biotin-streptavidin linkage. Streptavidin was adsorbed on the surface by incubating the SPE for 30 minutes at room temperature in $100 \mu\text{g mL}^{-1}$ streptavidin. The electrode was exposed to a $10 \mu\text{g mL}^{-1}$ of biotin-capture probe for 15 minutes at room temperature. This was followed by a blocking step, incubating the SPE for 1 hour at 37°C in 10 mM Tris-HCl pH 7.5, 1% BSA, to block any remaining active streptavidin surface.

To hybridise the capture probe with *mutated-HRP*, the SPE was immersed in hybridisation buffer containing $10 \mu\text{g mL}^{-1}$ *mutated-HRP* for 1 hour at 50°C .

The electrochemical cell was a drop of $2 \mu\text{l}$ of solution on the SPE that covered working and reference electrode.

$1 \mu\text{l}$ of 0.1 mg mL^{-1} $[\text{Os}(\text{bpy})_2(\text{pyr-CH}_2\text{-NH}_2)]\text{Cl}$ (Os bpy) mediator in 10 mM Tris-HCl pH 7 and $1 \mu\text{l}$ of 2 mM of fresh hydrogen peroxide solution in 10 mM Tris-HCl pH 7 were mixed on the electrode surface, allowing 2 minutes of resting time before -0.050 V was applied to detect the pre-hybridisation electrochemically. Between each step the electrodes were washed with wash buffer.

$0.5 \mu\text{l}$ of 0.2 mg mL^{-1} of Os bpy mediator in 10 mM Tris-HCl pH 7, $0.5 \mu\text{l}$ of 4 mM hydrogen peroxide in the same buffer and $1 \mu\text{l}$ of $30 \mu\text{g mL}^{-1}$ complementary target were mixed on the electrode surface, allowing 2 minutes of incubation time before -0.050 V was applied to detect displacement.

The control measurement was done following the same steps except that in the last one $1 \mu\text{l}$ of 10 mM Tris-HCl pH 7 instead of complementary target was used.

3.2.4 Procedures involved in ferrocene displacement detection

3.2.4.1 Bioconjugation of DNA labelling with ferrocene

Amine-C₆-5'-AATATCATTGGTGTT-3' was the mutated sequence of the DNA conjugated with ferrocene. Its synthesis was contracted to Eurogentec (Belgium) and was HPLC-purified. It contains a 5' hexamethylene amine. The oligonucleotide solution was made at 1 mg mL⁻¹ with autoclaved milliQ water and stored at -20 °C. A freshly prepared solution of 125 nmol of N-hydroxysuccinimide ester (NHS) and 250 nmol of N,N'-dicyclohexylcarbodiimide (EDC) in anhydrous dimethylformamide were added to a solution of 100 nmol of ferrocene acetic acid in the same solvent. The final volume was 300 µL. The reaction mixture was stirred at room temperature under argon until appearance of a precipitate. EDC forms an active ester functional group with carboxylate group using NHS. In this reaction a precipitate of o-acylurea is formed that was removed by centrifugation and the supernatant was added to 90 µL of 0.1 M sodium tetraborate buffer at pH 8.5 containing 10 nmol of the amino modified oligonucleotide and it was left to react for 6 hours at room temperature. The active ester group in the presence of amine nucleophiles is attacked, the NHS group leaves as a precipitate, creating a stable amide linkage with the amine. The white precipitate was separated by centrifugation. The supernatant contained a disulphide-ferrocene-labelled oligonucleotide. The disulphide bond was broken with 10 molar excess of dithiothreitol (DTT) to leave free a thiol group linked to the oligonucleotide. The modified oligonucleotide was purified with G-25 Shephadex column. UV Spectrophotometry was used to collect the appropriate fraction from the column. The elution profile is depicted in Figure 3.1. The product was characterised by UV spectrometry, cyclic voltammetry and MALDI-TOF.

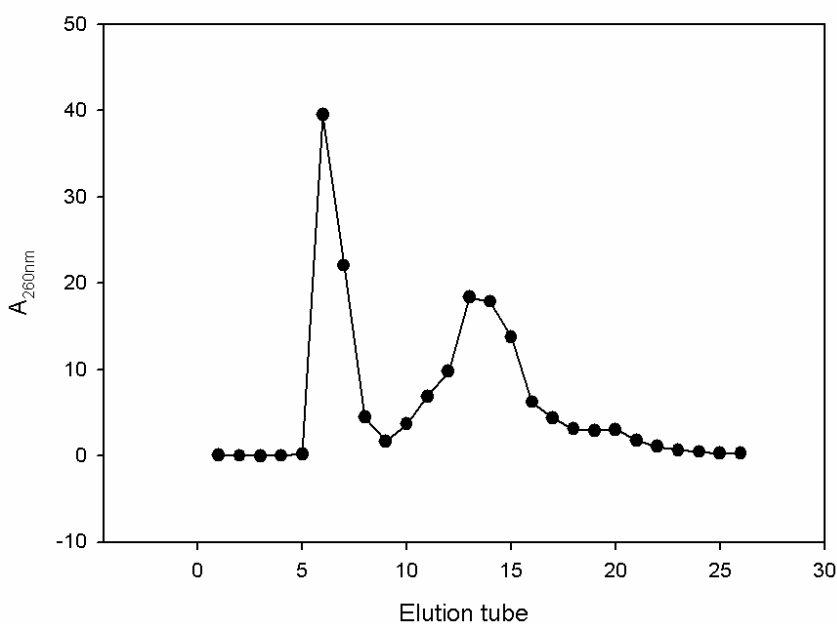


Figure 3.1. Tubes eluted from a size exclusion chromatography to separate ferrocene labelled oligonucleotide from ferroceneacetic acid.

UV spectrophotometry measurements were carried out using 1cm path-length quartz cuvettes. This technique was used to measure the absorbance at 265 nm of ferroceneacetic acid and the 260 nm of the oligonucleotide bases of the fractions eluted from the separation column.

MALDI-TOF characterisation was carried out using a 3-hydroxypicolinic acid (HPA) matrix. A 50 g L⁻¹ solution of 3-HPA in Milli-Q water and 50 g L⁻¹ solution of diammonium citrate were prepared and both reagents were combined in a ratio of 3-HPA:NH₄Citrate (9:1). The mixture was stirred for 1 minute and centrifuged to separate the white precipitate. The same volume of supernatant was mixed with ferrocene-oligonucleotide, in a final concentration of 12 pmol μL⁻¹. 2 μL of the mixture was allowed to air-dry on a stainless steel plate. 20000V of accelerating voltage, 92% of grid voltage, 400 nseconds of extraction delay time, 1715 of laser intensity and 50 of shots were applied in a linear mode for the measurement. Amine-C₆-5'-AATATCATTGGTGTT-3' was used as a primary standard and the same protocol was used for their detection by MALDI-TOF. The MALDI-TOF spectra are depicted in Figure 2 and 3.

Chapter 3. Detection of DNA hybridisation by displacement

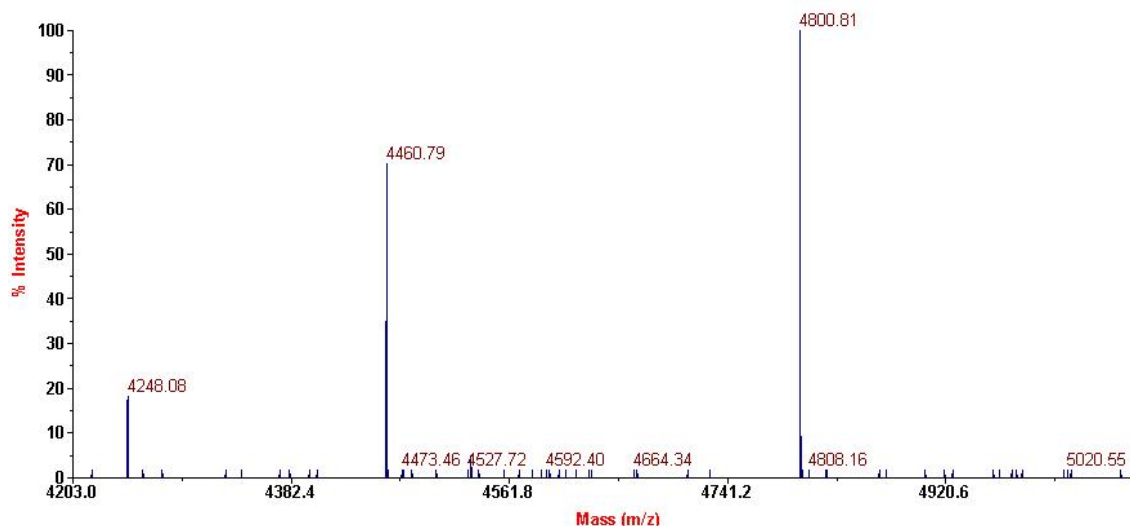


Figure 3. 2. MALDI-TOF graph of amino-oligonucleotide at 25000V of accelerating voltage, 92% of grid voltage, 400 nseconds of extraction delay time, 1865 of laser intensity and 50 of shots in a linear mode.

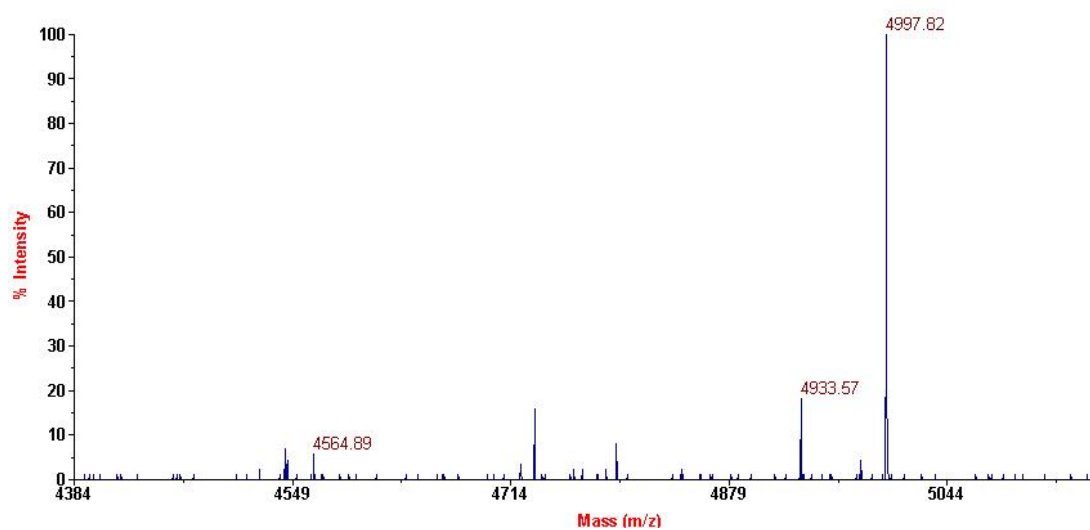


Figure 3. 3. MALDI-TOF graph of ferrocene-oligonucleotide. Detection was carried out in the same way as amino-oligonucleotide.

3.2.4.2. Electrochemical monitoring of displacement of ferrocene labelled sequences

35 μL of 10 mM PBS, 150 mM NaCl pH 7.5 on clean bare gold e-SPR chip was used to measure the background response of the bare surface with buffer by cyclic voltamperometry (CV), differential pulse voltammetry (DPV) and impedance. The conditions used for CV measurements were; scan rate of 0.1 V s^{-1} , between -0.5 V and 0.5 V , DPV was scanned between -0.2 and 0.2 V , with an increment of potential of 0.005 V , an amplitude of 0.05 V , a pulse width of 0.05 seconds and a pulse period of 0.5 seconds. Conditions for impedance experiments were; initial potential of 0.015 V , frequencies from 0.1 MHz to 0.1 Hz and amplitude of 0.005 V . The same measurements were carried out with an equimolar mixture of ferrocyanide and ferricyanide in a final concentration of 1 mM in 10 mM PBS, 150 mM NaCl pH 7.5. Afterwards the cell was cleaned with wash buffer and cleanliness was verified by CV in buffer. The same CV shape as before the detection of ferrocyanide/ferricyanide should be obtained to assure the cleanliness of the surface.

$12 \mu\text{g mL}^{-1}$ of *thiol-CF capture probe* in $1 \text{ M KH}_2\text{PO}_4$ was immobilised for one hour at room temperature on the gold chips. 1 mM of mercaptoethanol was used for 1 hour at room temperature to block the remained gold surface non-occupied by the capture probe. Pre-hybridisation of *ferrocene-CF mutated* oligonucleotide was performed incubating $48 \mu\text{g mL}^{-1}$ of this oligonucleotide in hybridisation buffer for 60 minutes at room temperature. After pre-hybridisation CV, DPV and impedance were carried out in buffer and in ferrocyanide/ferricyanide. Afterwards $30 \mu\text{g mL}^{-1}$ of CF-complementary target in hybridisation buffer was incubated for 30 minutes at room temperature. After displacement CV, DPV and impedance were recorded in the same manner.

3.2.4.3. Amplification of ferricyanide signal by ferrocene

$12 \mu\text{g mL}^{-1}$ of *thiol-CF capture probe* in $1 \text{ M KH}_2\text{PO}_4$ was immobilised for one hour at room temperature on 18 mm^2 gold electrodes. 1 mM of mercaptoethanol was used for 1

hour at room temperature to block the surface. One electrode was incubated for 1 hour at room temperature with $48 \mu\text{g mL}^{-1}$ of *ferrocene-CF mutated* oligonucleotide, while the other was incubated with $30 \mu\text{g mL}^{-1}$ of *complementary oligonucleotide* in the same manner. The immobilised electrodes were immersed in $15 \mu\text{L}$ of 10 mM PBS , 150 mM NaCl pH 7.5 into a 2 electrodes cell set up with platinum as reference and counter electrode. A potential of -0.2 V was applied to record reduction of ferrocene and when the current arrived at the base line, 100 seconds, $5 \mu\text{L}$ 4 mM of $\text{Fe}(\text{CN})_6^{-3}$ in 10 mM PBS , 150 mM NaCl pH 7.5 was injected into the cell to record the effect of ferrocyanide in the reduction of ferrocene.

3.3. Results and Discussion

3.3.4. Displacement of HRP-labelled sub-optimum sequences

3.3.4.1 Optimisation of sub-optimum probes and displacement conditions by ELONA

The method of detection by displacement requires the pre-hybridisation of the capture probe immobilised on the surface with a sub-optimum HRP-mutated oligonucleotide. Due to the higher affinity of the target that is fully complementary to the capture probe, the sub-optimum label can be displaced when the complementary target is introduced in the system. The decrease of the signal should verify the presence of the target and should be proportional to its concentration.

In order to obtain a functional displacement system it is important to have a pre-hybridisation of the *mutated-HRP* that is stable enough to maintain the duplex until the target can come into contact with the capture probe. This prevents the displacement of *mutated-HRP* by buffer or other non-complementary oligonucleotides. At the same time, this duplex should be unstable enough to be displaced by the target that is fully complementary to the capture probe.

Chapter 3. Detection of DNA hybridisation by displacement

Affinity drives the duplex formation between two oligonucleotide strands and clearly depends on the number of mutations, the type and position of the mismatched base pair (Aboul-ela et al., 1985). In a mutated duplex, dissociation kinetic constant (k_{diss}) was affected more than association constant (k_{ass}) by the presence of mismatched base pairs (Gotoh et al., 1995).

Santa Lucia and co-workers (Peyret et al., 1999; Allawi and Santa Lucia, 1997; Allawi and Santa Lucia, 1998) reported the stability conferred by base pairs obtained from statistical simulation, according to the following sequence: $G-C > A-T > G-G > G-T = G-A > T-T = A-A > T-C > A-C > C-C$. These results were experimentally confirmed by Tawa and Knoll, (2004), who obtained more stable duplexes from a T-G mismatch than from a T-C pair. Aboul-ela et al., (1985), found that G-A, G-G and G-T were less destabilising mismatches than C-C and C-T and Gotoh et al., (1995), detected better stability of the duplex with G-A and G-T mismatches rather than A-A, T-T, C-T and C-A. In contrast with Santa Lucia and co-workers results, Ke and Wartell, (1996), found better stability from A-G mismatch compared to A-T Watson and Crick pair or G-G and G-T mismatches, however they all coincided with the lower stability of C-C and C-T mismatches.

Furthermore the relative stability of duplexes with two internal adjacent mismatches was studied. It was found that the stability series follows the order: $GA-GA > AA-TT > TA-TA > AA-GC > GT-GA > AA-GA > GG-GA > GG-TA > GT-TA > GG-TG > GG-TG = CA-GC = CA-GA = GC-TA = TA-GC > GT-TG > AA-AC = GT-TT > GC-TG > CA-CC = CA-AC = TA-AC = TC-TG = AA-CC = GC-TT > TA-CC > TC-TT = TC-AC > TC-TC = TC-CC$ (Ke and Wartell, 1996).

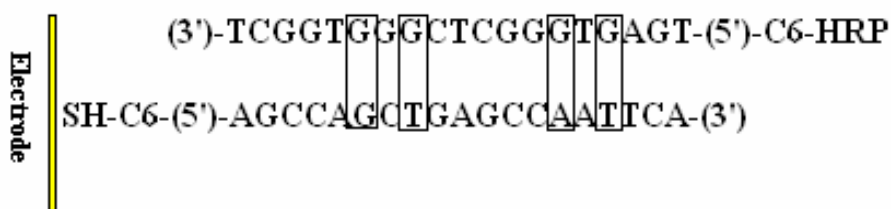
Additionally the neighbouring bases to the mismatch can destabilise the duplex. Two duplexes with the same bases mutated in the same position can be more destabilised by A or T neighbour than a C or G base. Moreover duplexes T_m with identical neighbour sequences but different next-neighbours are also different, therefore the next neighbour stacking interactions can also influence DNA stability (Ke and Wartell, 1996).

The affinity for the duplex formation also depends on the position of the mismatching base pair along the sequence. For oligonucleotide strands of short lengths, a commonly accepted model for duplex formation is that of nucleation followed by helix “zipping” (Craig et al., 1971; Cantor and Schimmel, 1980), so mismatches near the surface are expected to affect the efficiency of duplex formation. However DNA duplexes with the

Chapter 3. Detection of DNA hybridisation by displacement

mismatching base pair located near the 5' end of the duplex (far from the surface) suffered stronger destabilising effect as compared to mismatches closer to the 3' end. Internal mismatches destabilise the duplex more significantly than terminal mismatches (Tawa and Knoll, 2004). Gotoh et al., (1995), arrived to a similar conclusion. In addition their results suggested that the distance between the immobilised end and the location of the mismatch do not affect the kinetic parameters. Also their results suggest that the number of consecutive matched bases in the sequence stabilise the duplex even if the number of mismatched base pairs are the same.

Having these observations in mind and the type of application in question, the sequence shown in Scheme 3.2 was eventually synthesised. The rationale behind its selection was that a high thermodynamic stability was needed that could still however be disturbed kinetically. Four mutations; G-G, T-G, A-G and T-G, has been incorporated for this reason. Three of these four mutations have great stability in the ranking of Santa Lucia and co-workers (Peyret et al., 1999; Allawi and Santa Lucia, 1997; Allawi and Santa Lucia, 1998), while A-G is in the middle of the ranking, although Ke and Wartell, (1996), found this mismatch more stable than A-T Watson-Crick match. So, although four mutations were introduced in the suboptimum, they confer thermodynamic stability to the capture probe. In addition, the mismatches are positioned both near to the extremes and closer to the center of the sequence having in both cases two groups of five matches together in the 19-mer sequence, which can stabilise the duplex (Scheme 3.3). However, the presence of mismatches to the 3' end of the capture probe can promote the “unzipping” of the



Scheme 3.3. Representation of capture probe sequence and mutated HRP labelled oligonucleotide. The four mutations inside the rectangles.

An additional complication arises from the fact that the mutated sequence needs to be labelled with a reporter molecule, which could destabilise the duplex. Fotin et al.,

Chapter 3. Detection of DNA hybridisation by displacement

(1998), compared the signal obtained from the same sequence labelled and unlabelled that hybridise with an immobilised capture probe. A slight decrease of ΔG° for the labelled sequence was obtained, which was close to the experimental error. However Fotin's experiments were carried out with a small fluorescent label, (hexachlorofluorescein phosphoramidite), which may not be representative of HRP-C₆ molecule used here for the labelling of the mutated oligonucleotide.

I was thought that the fine-tuning of the conditions where displacement could be achieved could be achieved by optimising the temperature and time of the interaction, so a first experimental was done to obtain a rough indication of the affinity of the capture probe and establish the conditions of the ELONA experiments.

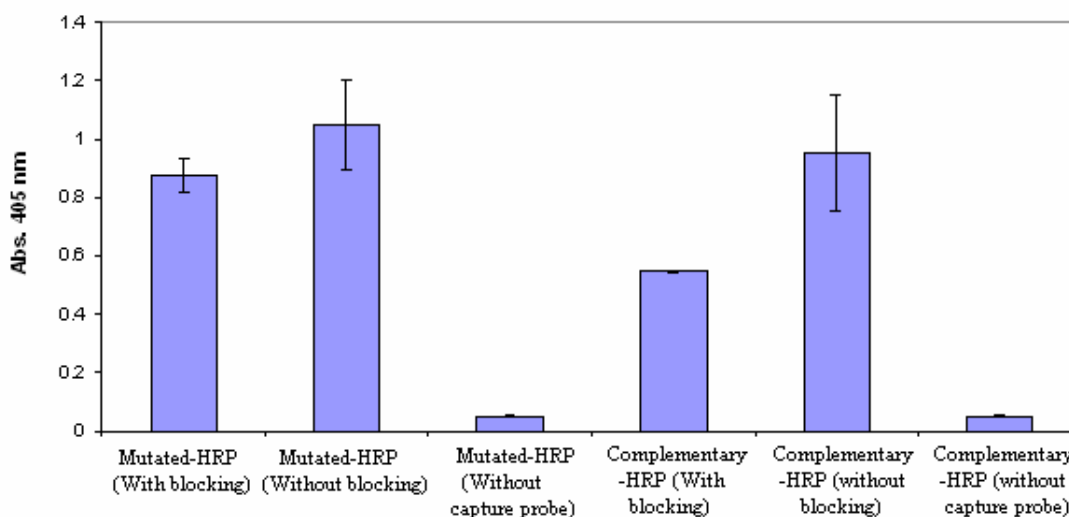


Figure 3.4. Colourimetric response from *mutated-HRP* and *complementary-HRP* with immobilised capture probe. Establishment of blocking conditions and controls. Hybridisation was carried out at 25 °C for 1 hour with 30 $\mu\text{g mL}^{-1}$ of oligonucleotide-HRP. Colourimetric detection was performed after 30 minutes incubation with at 405 nm. (n=3)

Figure 3.4 shows these results and also provides a first indication of thermodynamic equilibrium of the complementary and suboptimum target. The results showed higher response from the system without blocking (10 mM Tris-HCl buffer pH 7.5 with 5 % milk), although this response is less reliable (higher error bars).

Control experiments without capture probe and with and without blocking (results not shown) verify the same low non-specific adsorption of labelled oligonucleotide HRP

on the surface, obviating the necessity of use of blocking. For these reasons subsequent experiments were done without blocking to reduce steps and to increase sensitivity.

These results also show the high thermodynamic stability of the *mutated*-HRP duplex with the capture probe. The response from the *mutated*-HRP:capture probe duplex is for all intents and purposes equal (if anything, it is higher when blocking is used) to the response from the *complementary*-HRP:capture probe duplex under the conditions of the experimental (long hybridisation time and low temperature). This behaviour illustrates that the first goal (of a strong duplex with the suboptimum sequence) of the probe design has been achieved, however the question remains if the label could be displaced. This behaviour could also suggest that hybridisation on solid supports is more complex than as discussed in several publications (Peterson et al., 2002; Naef et al., 2002; Pozhitkov et al., 2003).

In order to give answer to these questions, the time and temperature dependence of the response were examined.

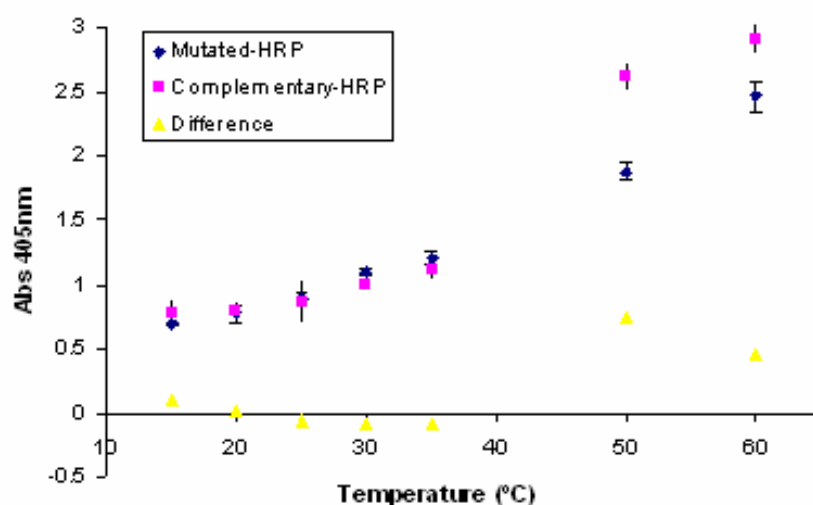


Figure 3.5. Absorbance resulting from the interaction of $30 \mu\text{g mL}^{-1}$ *mutated*-HRP and $30 \mu\text{g mL}^{-1}$ *complementary*-HRP hybridisation with immobilised capture probe for 60 minutes as a function of the temperature of incubation. Colourimetric detection was performed in all cases after 30 minutes incubation with TMB at room temperature at 405 nm. Hybridisation buffer and procedure described in materials and methods. (n=3)

Figure 3.5 shows the response obtained from hybridisation detection of *mutated*-HRP and *complementary*-HRP with an immobilised capture probe. In both cases increasing signal with increasing temperature was obtained. Similar response was obtained from

Chapter 3. Detection of DNA hybridisation by displacement

both between 15 and 35 °C, but at higher temperatures higher response from the *complementary-HRP*, around 20 – 28 %, as compared to the *mutated-HRP* signal was obtained.

These results could be explained taking into account the T_m values of both duplexes.

T_m is defined as the temperature at which 50 % of the DNA molecules form a stable double helix and the other 50 % have been separated to single strand molecules. It can be calculated by (Howley et al., 1979) (Equation 3.1);

$$T_m = 81.5 C + 16.6 (\log_{10} [Na^+]) + 0.41 (\% G+C) - (600 / \text{strand length})$$

Or using the relation of the nearest-neighbouring bases (Breslaur et al., 1986). For achieving efficient hybridisation while maintaining the stringency required for ELONA a rule of thumb indicates that 5-10°C below the T_m should be used in ELONA.

T_m obtained for complementary-HRP sequence was 57 °C with the Howley equation and 54 °C with the neighbouring bases relation. A reduction of 1 °C in the T_m for every 1 % of bases pair mutations in dsDNA (Maniatis et al., 1982) is described. Accordingly, the mutated-HRP sequence T_m might be around 36 °C. Therefore at 50 °C, the *complementary-HRP* is close to its T_m , and while the *mutated-HRP* should not hybridise so much at 14 °C above its T_m .

However, the T_m values and the assumption of the percentage of temperature decrease with mismatches were calculated for hybridisation duplexes in solution. Some examples in the literature demonstrate that the theory applicable to DNA hybridisation in solution can not be applied for heterogeneous hybridisation.

Markly and Breslauer, (1987), demonstrated that classical equation of melting curve analysis could no be applied in the case of hybridisation of target with an immobilised capture probe on solid support, because it is valid only for equal concentrations of both strands. But in the case of complementary-HRP and mutated-HRP hybridised with an immobilised capture probe, an excess of free oligonucleotide interact with a limited concentration of capture probe on the surface.

Fotin et al., (1998), observed a decrease in the stability of duplexes formed on a solid support compared with the stability of the same duplexes in solution. These differences

Chapter 3. Detection of DNA hybridisation by displacement

of stability change the T_m values for immobilised duplexes and the Howley equation cannot be applied in these cases.

Furthermore, the literature for solid-phase DNA oligonucleotide duplex formations suggests that the pre-nucleation state is greatly affected by temperature. At this time is not clear whether mild heating overcomes a nucleation barrier or facilitates another part of the hybridisation process such as zippering, base stacking or structural reorientation. However an increase of temperature resulted in all cases easier and faster hybridisation (Bloomfield et al., 2000.)

Ke and Wartell, (1996), observed a different relation between the mutations and the decrease of T_m with duplexes immobilised on solid phase. T_m of DNA with adjacent mismatches showed a decrease of 1 °C in the T_m for every 0.5 % mutations of base pairs in double stranded DNA. However as discussed; Peyret et al., (1999); Allawi and Santa Lucia, (1997); Allawi and Santa Lucia, (1998); Ke and Wartell, (1995); Tawa and Knoll, (2004); Aboul-ela et al., (1985); Gotoh et al., (1995), all mismatches can not be treated in the same way, due to the dependence on the type of mismatch and its position on the kinetics and thermodynamics stability of the DNA duplex. Whatever that real T_m of the immobilised duplex, Figure 3.5 suggest that a critical point is reached between 35 and 50 C either because the thermodynamics or because the nucleation od ippering kinetics are affected.

To shed light to the mechanism that limits the response experiments probing the kinetics of the processes were need. These were performed at 50°C and 60 °C and are depicted in Figure 3.6 and Figure 3.7. It should be noted that ELONA is a limited technique to examine kinetics since several steps of washing and colour development are needs, but still, the results can provide some insight.

Figure 3.6. shows the results obtained from mutated-HRP and complementary-HRP hybridised with capture probe at 50 °C as a function of incubation. It can be seen that at short times higher signal is obtained *mutated-HRP* while *complementary-HRP* gave higher signal at long incubation times.

Chapter 3. Detection of DNA hybridisation by displacement

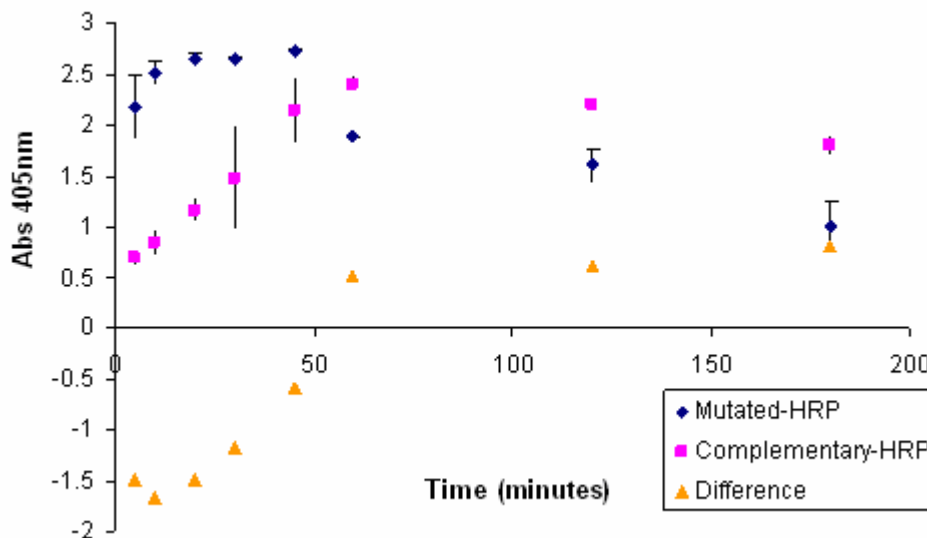


Figure 3. 6. Absorbance resulting from the interaction of $30 \mu\text{g mL}^{-1}$ *mutated-HRP* and $30 \mu\text{g mL}^{-1}$ *complementary-HRP* with immobilised capture probe at $50 \text{ }^\circ\text{C}$ as a function of incubation time. Colourimetric detection was performed after 30 minutes incubation with TMB at room temperature and at 405 nm. Conditions as in Figure 3.5. (n=3)

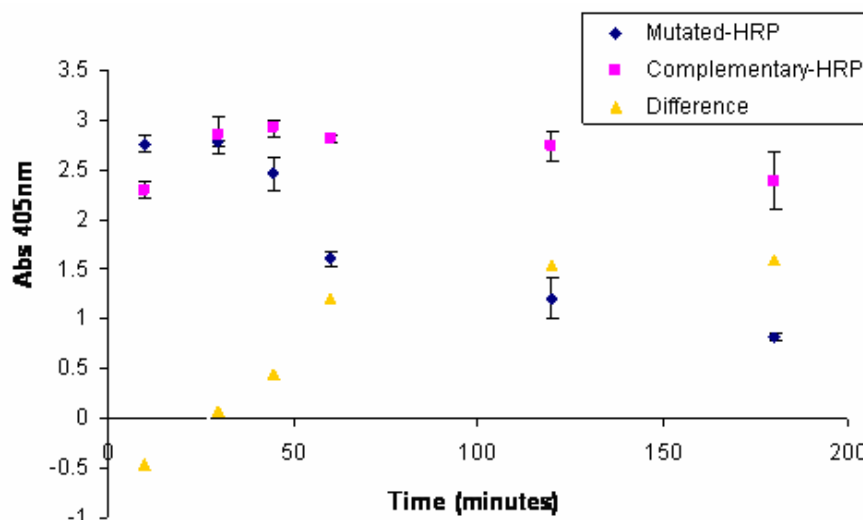


Figure 3. 7. Absorbance resulting from the interaction of $30 \mu\text{g mL}^{-1}$ *mutated-HRP* and $30 \mu\text{g mL}^{-1}$ *complementary-HRP* with immobilised capture probe at $60 \text{ }^\circ\text{C}$ as a function of time of incubation. Colourimetric detection was performed after 30 minutes incubation with TMB at room temperature at 405 nm. Conditions as in Figure 3.5. (n=3)

Figure 3.7 is a repeated of the experiments described in figure 3.6 but at this higher temperature the signal difference between *mutated-HRP* and at short times is smaller and the *complementary-HRP* signal becomes higher at shorter times. In addition, the

difference of the signal is higher at long times. It appears therefore that the hybridisation of the *complementary-HRP* is favored at higher temperatures.

These results coincide with the ones obtained by Dai et al., 2002. They found that hybridisation kinetics was significantly different for specific and non-specific binding of labelled DNA to surface-bound oligonucleotides. They showed that specific binding takes longer to reach hybridisation equilibrium than the mismatched oligonucleotide. Increasing hybridisation time generally increased the specificity of the hybridisation. Moreover, Sorokin et al., (2005), arrived to a similar conclusion. They observed that since mismatched duplexes hybridise faster than their perfect counterparts, the complementary signal was higher at long incubation time.

This behaviour could be partially explained with the model of oligonucleotide hybridisation on solid support done by Chan et al., (1995). Capture of the perfectly complementary target is modelled as a combined reaction-diffusion process. In this model there are two different mechanisms by which targets can hybridise with the complementary probes: direct hybridisation from the solution and hybridisation by molecules that adsorb non-specifically and then surface-diffuse to the probe. The results indicate that non-specific adsorption of ssDNA on the surface and subsequent 2-D diffusion can significantly enhance the overall reaction rate. Heterogeneous hybridisation depends strongly on the rate constant of DNA adsorption/desorption in the non-probe-covered regions of the surface (Adam and Delbruck, 1968). Bloomfield et al., (1974), measured a rate constant for oligonucleotides association in solution to be about three orders of magnitude smaller than the diffusion limited rate. Then it could be possible that *mutated-HRP*, due to its lack of complementarity, has more tendency to the non-specific adsorption on the surface, which enhance their higher and faster hybridisation with the immobilised capture probe at short times through surface diffusion. It should also be remembered that mismatched sequences will predominate at shorter times and lower temperatures, it “zippering” is the most activated process. Under this light the results presented so far could be explained as follows: (a) The apparent T_m immobilised capture probe with *mutated-HRP* and *complementary-HRP* duplex is higher than the calculated in solution and is in both cases higher than 50°C. (b) In both cases hybridisation is a complex phenomenon that involves diffusion to the surface, adsorption/desorption equilibrium, surface diffusion, nucleation and zippering. Thermodynamics plays an important role on the stability on the zippered duplex only

Chapter 3. Detection of DNA hybridisation by displacement

and therefore, the displacement could occur only if both suboptimum and optimum duplex compete for this state. (c) It appears that the most activated process (highest energy of activation) is the zippering. Zippering is most extensive for the *complementary-HRP:capture probe* duplex and for this reason when the temperature is raised, even at short times the *complementary-HRP:capture probe* predominates. However it appears that this advantage is gained only at temperatures above 50°C. Another postulate is that concentrations of the target probe would be affect all this processes and therefore could probably tip the balance at some concentrations.

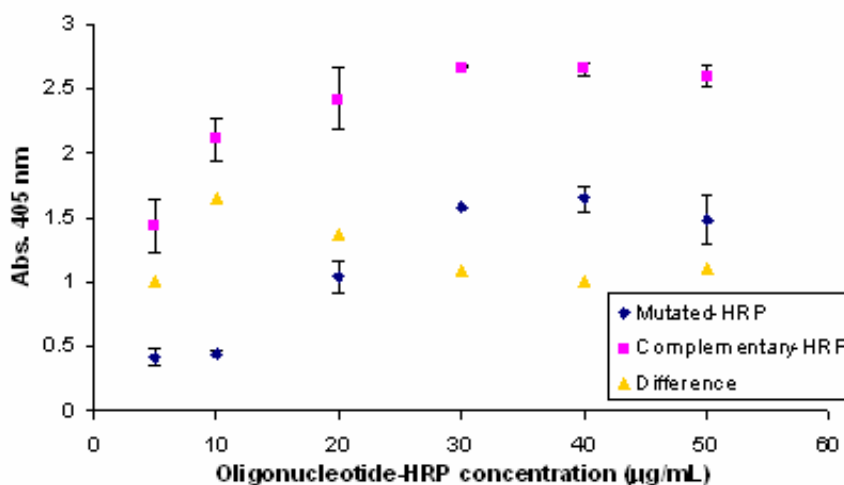


Figure 3. 8. Absorbance resulting from the interaction of different concentrations of *mutated-HRP* and *complementary-HRP* with immobilised capture probe for 60 minutes at 50 °C. Colourimetric detection was performed after 30 minutes incubation with TMB at room temperature at 405 nm. Other conditions as in Figure 3.5 (n=3)

For this reasons the experiments described in Figure 3.8 were performed. Figure 3.8, shows the results obtained from the hybridisation of different concentration of *complementary-HRP* and *mutated-HRP* with captures probe immobilised on the support. At lower concentrations of target, lower adsorbance for the *mutated-HRP* duplex was detected, although there appears to be a limit at 10 µg mL⁻¹ where probably starts limiting both responses. Above 30 µg mL⁻¹ a saturated signal for both targets was obtained. Although the concentration of the target cannot be controlled in a displacement assay (it is precicely what the response is supposed to detect), assuming that the equilibrium is fully reversible, this experiment sets the optimum conditions for the pre- hybridisation of the sub-optimum label: The optimum conditions for pre-

Chapter 3. Detection of DNA hybridisation by displacement

hybridisation were chosen $10 \mu\text{g mL}^{-1}$ of *mutated-HRP* in 10 mM Tris-HCl, 1 mM EDTA, 0.3 x SSC and 2 x Denhardt's solution at pH 7.5 for 1 hour at 50 °C, since under these conditions the maximum difference could be obtained for displacement.

Once a stable pre-hybridisation of *mutated-HRP* was obtained, optimisation of displacement with *complementary oligonucleotide* was carried out. To detect displacement two colourimetric detections were performed, the first after pre-hybridisation of *mutated-HRP* to establish the base-lines and the second after displacement with *complementary oligonucleotide*. Both colourimetric detections were carried out in the same manner; 30 minutes incubation with TMB detection at 405 nm. Background displacement could occur with buffer due to displacement of the equilibrium. For this reason for every measurement the "zero concentration" displacement was established by incubating under the same conditions in the absence of target.

The time of displacement incubation was the first variable to optimise. Figure 3. 9, shows the percentage of displacement obtained with the target, (*complementary oligonucleotide*) and with the buffer as control. The signal obtained after displacement with *complementary* or buffer was converted to a percentage of displacement considering the signal from the pre-hybridised *mutated-HRP* as 100 % of the signal in each case and the signal obtained after displacement with *complementary* or buffer was converted to a percentage of displacement of the original signal from the pre-hybridised *mutated-HRP*.

Chapter 3. Detection of DNA hybridisation by displacement

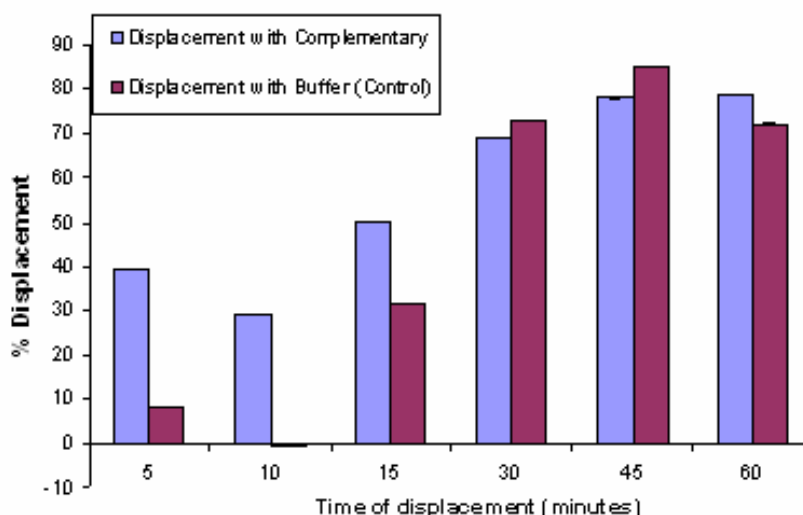


Figure 3. 9. Absorbance resulting from the displacement of pre-hybridised *mutated-HRP* with *complementary* or buffer (control). Conditions of pre-hybridisation; $10 \mu\text{g mL}^{-1}$ of *mutated-HRP* for 1 hour at 50°C . Conditions of displacement; $30 \mu\text{g mL}^{-1}$ of *complementary* at 55°C for various time of incubation. Colourimetric detection was performed after 30 minutes incubation with TMB at room temperature and 405 nm. (n=3)

When the time of incubation, with *complementary oligonucleotide* for displacement of the pre-hybridised sub-optimum *mutated-HRP* oligonucleotide. Increases the percentage of displacement is enhanced, 79 % after 60 minutes, however the non-specific displacement with buffer increases in the same manner. (72 % after 60 minutes). In contrast, at shorter time of displacement incubation greater difference between the non-specific and specific displacement was detected. At 5 minutes while the *complementary oligonucleotide* displaces 39.3 % of the signal from the pre-hybridised mutated-HRP, only 7.8 % of signal was displaced by the buffer, so a 31.5 % of specific signal was displaced after 5 minutes of incubation with complementary oligonucleotide at 55°C .

Therefore the displacement incubation time was optimised at 5 minutes and this value was fixed to examine the effect of temperature on the displacement efficiency.

Chapter 3. Detection of DNA hybridisation by displacement

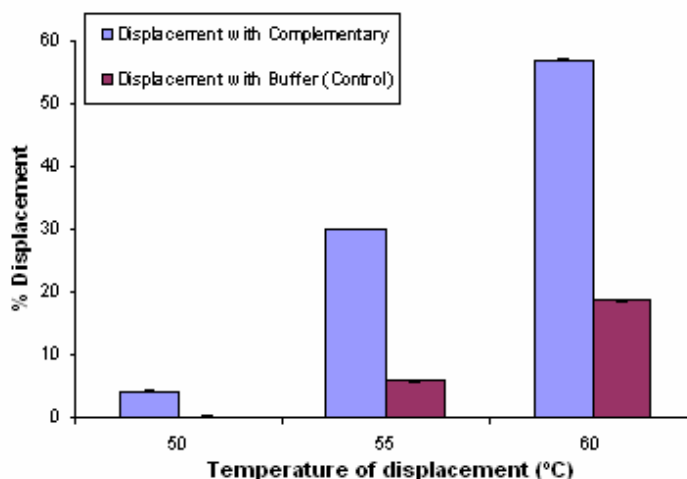


Figure 3. 10. Absorbance resulting from the displacement of pre-hybridised *mutated-HRP* with *complementary* or buffer (control). Conditions of pre-hybridisation; $10 \mu\text{g mL}^{-1}$ of *mutated-HRP* for 1 hour at $50 \text{ }^\circ\text{C}$. Conditions of displacement; $30 \mu\text{g mL}^{-1}$ of *complementary* for 5 minutes at various temperatures of incubation. Colourimetric detection was performed after 30 minutes incubation with TMB at room temperature and 405 nm ($n=3$)

Figure 3.10 shows the results obtained for *mutated-HRP* displacement by *complementary oligonucleotide* at different temperatures of incubation. As expected, increasing the incubation temperature higher destabilisation of pre-hybridised *mutated-HRP* was produced, however non-specific displacement by the buffer also profit from this destabilisation. Subtracting the value of this “zero” displacement, the highest specific displacement (38.3 %) was achieved at $60 \text{ }^\circ\text{C}$.

The proportionality of the signal displaced with the concentration of the target, *complementary oligonucleotide*, was verified with the experiments described in Figure 3.11.

Chapter 3. Detection of DNA hybridisation by displacement

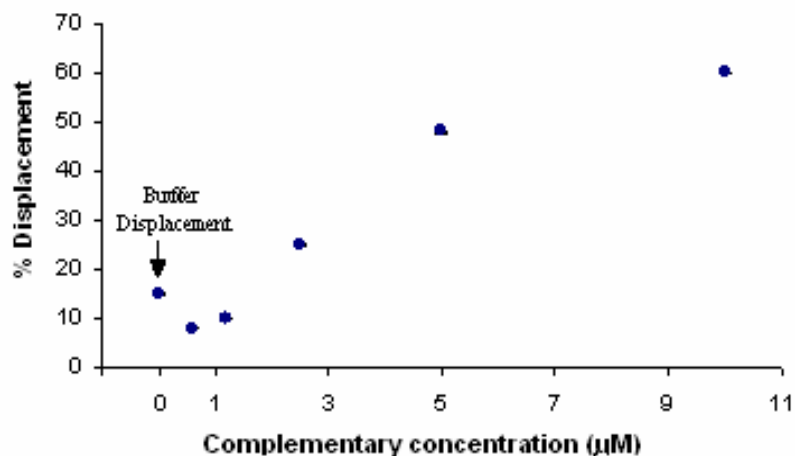


Figure 3. 11. Absorbance resulting from the displacement of pre-hybridised *mutated-HRP* with *complementary* or buffer (control). Conditions of pre-hybridisation; $10 \mu\text{g mL}^{-1}$ of *mutated-HRP* for 1 hour at 50°C . Conditions of displacement; Incubation at 60°C for 5 minutes at various concentrations of *complementary*. Colourimetric detection was performed after 30 minutes incubation with TMB at room temperature at 405 nm. (n=3)

Higher percentage of displaced signal was detected at higher concentrations of target, which demonstrates that this displacement configuration is appropriate to detect label free oligonucleotide. However below $2.5 \mu\text{M}$ of target the displacement from low concentrations of target cannot be differentiated from the non-specific displacement by the buffer (Figure 3. 11).

The displacement detection that has been optimised colourimetry achieved the objective of decreasing the time of detection from 1 hour in direct hybridisation of 19-mer oligonucleotides to 5 minutes in the case of displacement detection, at least in an ELONA system. Additionally this system can be used to detect label-free oligonucleotide targets in the range of μM . Although this part was developed to determine the conditions that could be used for electrochemical detection, and describes the development of a fast and label free method to detect specific oligonucleotide sequences

3.3.4.2 Electrochemical detection of displacement of HRP-labelled sequences

The displacement method optimised with ELONA was transferred to an electrode to be detected electrochemically. For this purpose, the diffusional mediator detection described in the experimental section was used. As shown in Figure 3.12, 23.2 % of the signal was displaced by the complementary oligonucleotide. Essentially no displacement was observed by the buffer. However, it has to be noted that with electrochemical detection the relative standard deviation ($0.12 + 0.03 \mu\text{A}$) was higher than that obtained in colourimetric detection ($0.59 + 0.02$).

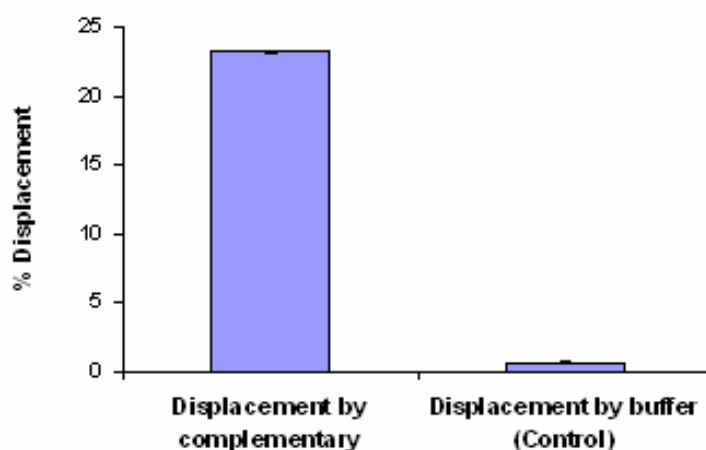


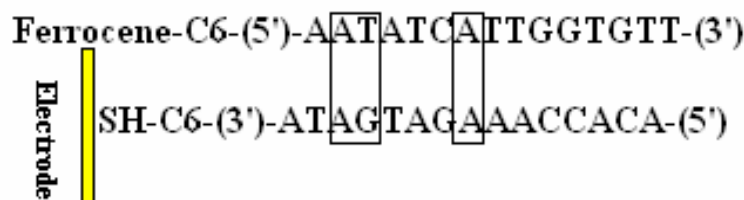
Figure 3. 12. Displacement percentage of current decrease for the displacement of mutated-HRP by $30 \mu\text{g mL}^{-1}$ of *complementary-HRP*. The conditions of the experiment are described in the experimental section. (n=3)

The experimental setup to maintain the concentration of mediator constant and to control the temperature at 60°C proved to be impossible to control to a degree that could yield reproducible measurements. For this reasons displacement had to be done at room temperature with SPE. It is expected that these results could be improved by applying the optimal conditions or changing the sub-optimum oligonucleotide sequence to achieve improved displacement at room temperature.

3.3.5 Displacement of ferrocene labelled suboptimum sequence for cystic fibrosis detection

The experience with the HRP modified suboptimum probe led to the conception of a simpler detection scheme based on displacement for the detection of the cystic fibrosis gene. In this configuration a ferrocene label was used that could hopefully lead to a reagentless and labelless detection (see scheme 3.5).

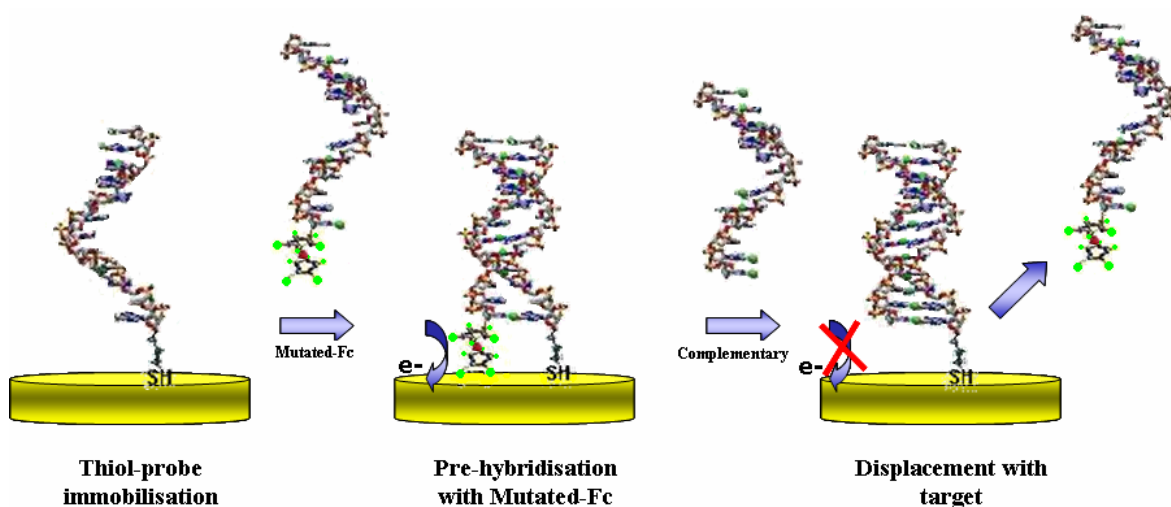
For this purpose the sequence of the oligonucleotides had to be changed. A capture probe to recognise specifically the cystic fibrosis (CF) gene region, indicative of this disease was used. The sub-optimum sequence used for displacement detection had three mutations, A-A and G-T together and A-A (Scheme 3.4). Although this sub-optimum sequence had one mutation less than the previous sequence, it should result in lower stability of the sub-optimum duplex, because there are 11 matches as compared to the 15 matches of the previous sequence, two of these three mutations being A-A mismatches, that are considered by Peyret et al., (1999); Allawi and Santa Lucia, (1997); Allawi and Santa Lucia, (1998); Ke and Wartell, (1995); Tawa and Knoll, (2004); Aboul-ela et al., (1985); Gotoh et al., (1995) most destabilising to the duplex. In addition, the sub-optimum duplex left the first base of the capture probe free a fact that might enhance zipping at the complementary oligonucleotide contributing to easier displacement. The lower stability of the sub-optimum duplex might afford displacement at room temperature.



Scheme 3.4. Representations of capture probe sequence and mutated ferrocene labelled oligonucleotide. The three mutations of the sub-optimum oligonucleotide are inside the rectangles.

Chapter 3. Detection of DNA hybridisation by displacement

The label of the mutated oligonucleotide was also changed. A redox molecule, ferrocene, was attached to the 5' end of mutated oligonucleotide. Ferrocene is a smaller molecule compared to HRP, which should not affect so much the hybridisation of the duplex, and allows the label to be close to the electrode surface increasing the electrochemical response. Although this redox label is not in principle amenable to signal amplification an advantage is that a reagentless system would in principle results due to the fact that in this case it was not necessary to add the substrate or the mediator to obtain a response (scheme 3.5).



Scheme 3. 5. Conceptual schematic of sub-optimum ferrocene labelled mutated oligonucleotide displacement detection.

The first step was the bioconjugation of the mutated oligonucleotide with the ferrocene molecule. A 5' hexamethylene amine oligonucleotide was conjugated with a ferrocenacetic acid as was explained in section 3.2.4.1.

After the conjugation of amine-oligonucleotide ($MW=4776 \text{ g mol}^{-1}$) with EDC ($MW=155 \text{ g mol}^{-1}$), NHS ($MW=115 \text{ g mol}^{-1}$), DTT ($MW=154 \text{ g mol}^{-1}$) and ferrocenacetic acid ($MW=244 \text{ g mol}^{-1}$) to obtain a ferrocene-labelled oligonucleotide ($MW=5003 \text{ g mol}^{-1}$), the excess reagents were separated. Due to the 10 fold excess of the acid it was assumed that all oligonucleotide had reacted. The rest of reagents were separated from the thiol-ferrocene-labelled sequence by size exclusion chromatography with a G-25 Sephadex column. The components were separated in two major groups according to their size, ferrocene-labelled oligonucleotide eluting first and next the low

Chapter 3. Detection of DNA hybridisation by displacement

molecular weight molecules (EDC, NHS, DTT). UV Spectrophotometry was used to collect the appropriate fractions from the column. The fractions collected combined the ferroceneacetic acid moiety absorbance as a broad peak at 265 nm and the 260 nm peak of the oligonucleotide bases. The two peaks overlap, therefore it was not possible to make a quantitative determination of ferrocene-oligonucleotide molecule by spectrophotometry. For this reason MALDI-TOF spectra of the product were obtained. MALDI-TOF analysis confirmed that a ferrocene molecule was attached to the oligonucleotide.

3.3.5.1 Electrochemical displacement detection of ferrocene labelled oligonucleotide

In order to develop the reagentless and labelless detection of the cystic fibrosis (CF) gene, series of questions need to be answered: from the various electrochemical techniques available, one has to be chosen that provides the maximum advantage for detection. Since each technique is based on different principles, advantages of sensitivity signal/ratio etc. can be discovered by a survey of techniques. Additionally SPR and e-SPR are techniques that can give us information of surface processes without the need of labelling. Therefore, CV, DPV, impedance and e-SPR were evaluated for detection, but at the same time were used to optimise the molecular architecture constructed on the electrode surface. In this sense, the following parameters that affect both detections and surface architecture were examined.

- The concentration of the capture probe in solution during electrode modification which will decide the surface coverage.
- The concentration of *ferrocene-CF mutated* which will determine the zero current and the efficiency of displacement.
- The NaCl concentration in the hybridisation buffer both with the *ferrocene-CF mutated* pre-hybridisation and during displacement

The criteria that was used for optimisation was the efficiency of displacement as percentage of the initial signal after 30 minutes of displacement incubation at 30 $\mu\text{g mL}^{-1}$

Chapter 3. Detection of DNA hybridisation by displacement

¹ concentration of *CF-complementary*. At a second level the inferred (as explained below) non-specific or “zero” displacement by buffer was used as a criterion (such “zero” displacement was minimised).

Surface plasmon resonance (SPR) was used to monitor in real time the immobilisation of the *thiol-CF capture probe* on gold chips, the pre-hybridisation of *ferrocene-CF mutated* oligonucleotide, and displacement of this pre-hybridised by *CF-complementary* target. Electrochemical methods were then difference of signal before and after displacement.

The non-specific or “zero” displacement due to the presence of buffer can be calculated from the degrees of change expected in SPR. According to the rule of thumb used for the calculation of surface coverage (120 m° of change corresponds to 1 ng mm⁻²) the coverage of a monolayer of oligonucleotide yields about 180 m° of response. When the *ferrocene-CF mutated* oligonucleotide is displaced a very small difference in molecular weight and probably also in refractive index results. Considering that the typical response for the hybridisation of the suboptimum is in the range of 70-80 m°, and only a 20 m° for a monolayer that does not contain ferrocene (results not shown). It appears logical to consider that any SPR results that show after displacement an angle change much higher than this value, are due to the non-specific displacement by buffer. Obviously, the higher this value, the higher the non-specific displacement is, and the less reliable the architecture. Thus, this criterion (displacement value over 20 m°) was used for the qualitative exclusion of configuration if other criteria were similar.

First of all the position of the label was decided. Ferrocene label in the 5' end of the mutated oligonucleotide (close to the surface) offers higher electrochemical signal due to its proximity to the electrode surface, however because of steric impediments ferrocene the label might cause problems in the hybridisation event. So the pre-hybridisation of the *ferrocene-CF mutated* with the immobilised capture probe and the signal produced by the ferrocene in this pre-hybridisation were tested with two different *ferrocene-CF mutated* oligonucleotides, one labelled in the 5' and another labelled in the 3' end.

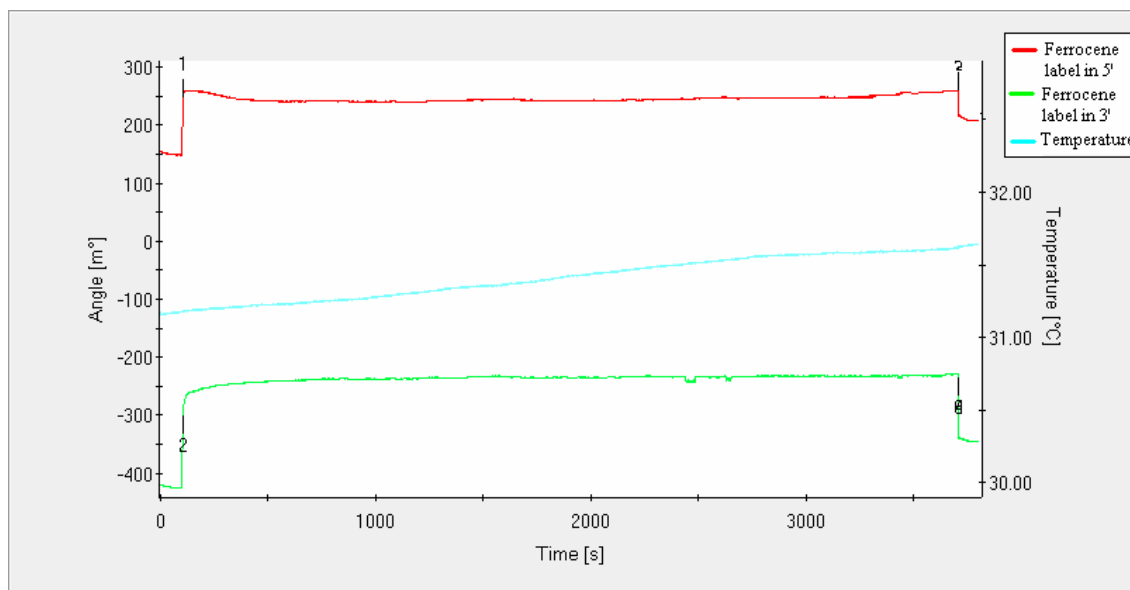


Figure 3.13. e-SPR-ogram of pre-hybridisation of *ferrocene-CF mutated* oligonucleotide at 5' (in red) and in 3' (in green). $24 \mu\text{g mL}^{-1}$ *Ferrocene-CF mutated* oligonucleotide in hybridisation buffer was incubated for 1 h at room temperature on a chip modified with capture probe. At arrow 1 and 2 the ferrocene-CF mutated was injected followed by buffer injection at arrow 3 and 4.

As shown in Figure 3.13 the surface plasmon angle change corresponding to the *ferrocene-CF mutated* hybridisation with the capture probe, is almost the same regardless of the 5' or 3' position of the label. Labelling at 3' produced a slightly more hybridisation (79 m°), than the 5' label led (70 m°), so hybridisation might be slightly affected by the position of the label. However a large difference was obtained with the electrochemical detection of the duplex. CV in buffer carried out after the hybridisation of ferrocene-CF mutated with the capture probe showed ferrocene peaks in the case of ferrocene label at 5', while no peaks were detected in the case of ferrocene label at 3'. For this reason in subsequent experiments the ferrocene label was at the 5' end.

In continuation the typical results observed with the three electrochemical techniques for detection of displacement event are described. First Cyclic voltamperometry (CV) in buffer was used. After pre-hybridisation of *ferrocene-CF mutated* this technique detected the redox peak of the ferrocene molecule. When complementary oligonucleotide displaced ferrocene-CF mutated oligonucleotide, the height of the peak decreases depending on the amount of ferrocene molecules that are removed close to the electrode, which is proportional to the concentration of target added into the cell (Figure 3.14).

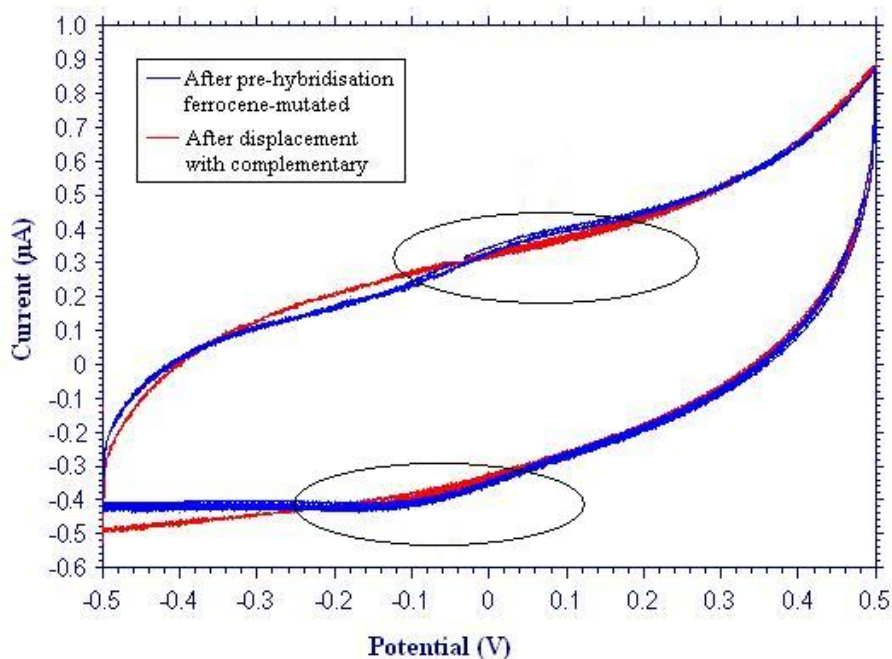


Figure 3. 14. Typical CV before and after displacement of *ferrocene-CF mutated* oligonucleotide. CV was performed at 0.1 V s^{-1} between -0.5 and 0.5 V in the presence of 10 mM PBS , 150 mM NaCl , $\text{pH } 7.5$. The highlighted differences in the peakcurrent is indicative of displacement.

Since CV results in small changes, differential pulse voltammetry (DPV) in buffer was used as an alternative. As in CV, the height of the peak is directly related with the amount of ferrocene molecules immobilised, so after displacement the peak decreases in comparison to the peak before displacement. Current DPV allows for a very effective correction of the charging background current, which should allow better sensitivity. Figure 3.15, shows a typical DPV.

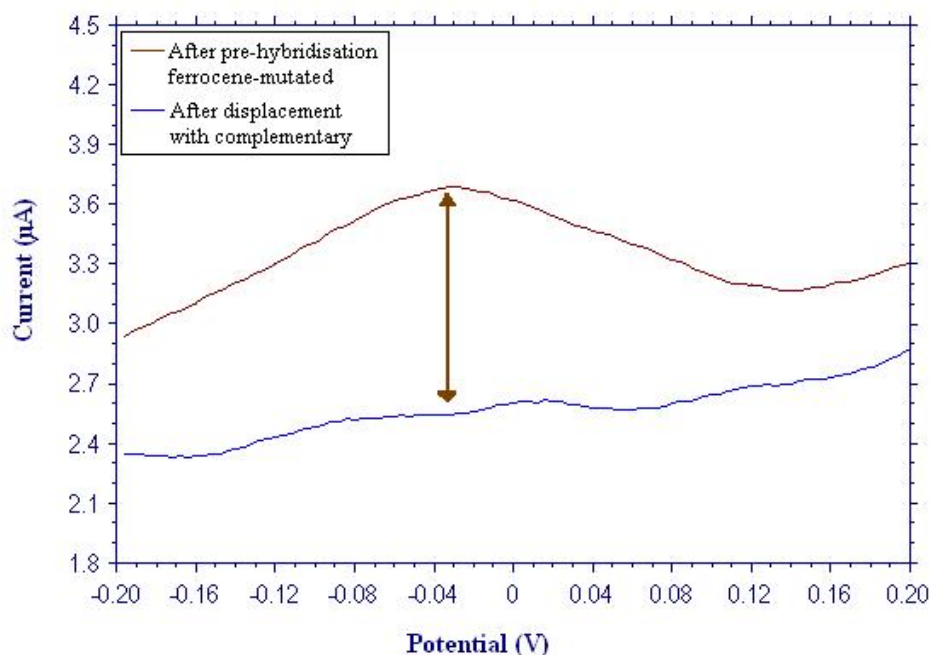


Figure 3.15. Typical DPV before and after displacement of *ferrocene-CF mutated* oligonucleotide. DPV was performed between -0.2 and 0.2 V, with an increment of potential of 0.005 V, an amplitude of 0.05 V, a pulse width of 0.05 seconds and a pulse period of 0.5 seconds in the presence of 10 mM PBS, 150 mM NaCl, pH 7.5. The highlighted signal difference is indicative of displacement.

Finally impedance spectroscopy in buffer was also used to try to discern differences of the spectrum before and after displacement. The change of ferrocene concentration close to the electrode surface affects the electron transfer resistance (R_{et}) value. When the amount of ferrocene molecule increases, enhancement of electron transfer between the label and the electrode is observed, and decrease on the R_{et} is obtained. After displacement the amount of ferrocene molecules decreases with the subsequent increase of R_{et} (Figure 3.16).

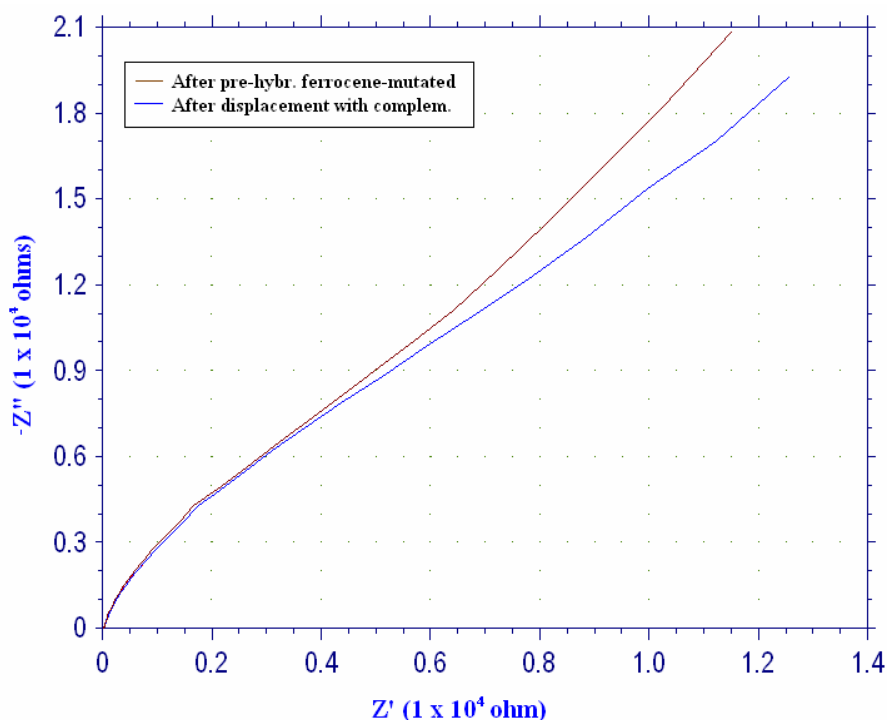


Figure 3. 16. typical Nyquist plot of ferrocene-CF mutated displacement by complementary oligonucleotide. Impedance measurements were performed in the presence of 10 mM PBS, 150 mM NaCl, pH 7.5. An AC voltage of 0.05 V in amplitude and 0.015 V in potential within the frequency range of 100000 – 0.1 Hz. The differences in response can be read in one only frequency where the effect of displacement is more important.

Laviron, (1979), related the parameters of R_{et} and capacitance of the immobilised layer (C_{ads}) with the heterogeneous electron transfer rate constant (k_f) through equation 3.2;

$$k_f = (2 R_{et} C_{ads})^{-1} \quad (\text{Equation 3.2})$$

In this case an increase of displacement, that produces a decrease of ferrocene molecules immobilised and therefore a decrease of electron transfer, produces a decrease of k_f .

The common graphs to represent the data in impedance spectroscopy are Nyquist and Bode plots. Nyquist plot consists in a real and an imaginary part. Usually the impedance real part is plotted on the X axis and the imaginary part on the Y axis of a chart and Bode plots represent the log frequency on the X axis and both the absolute

Chapter 3. Detection of DNA hybridisation by displacement

value of the impedance and phase-shift on the Y axis. However impedance data is commonly analysed by fitting it to an equivalent electrical circuit model, which is required to obtain the values of R_{et} and C_{ads} that are the elements of the circuit. Impedance values detected in displacement of ferrocene-CF mutated system in buffer were fitted to the next circuit (Figure 3. 17).

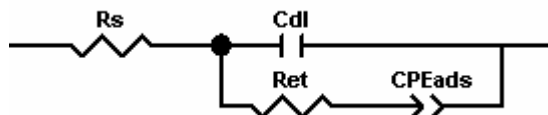


Figure 3. 17. Equivalent circuit for displacement of ferrocene-CF mutated oligonucleotide system in buffer.

In this circuit, R_s is the solution resistance, C_{dl} is the double-layer capacitance, R_{et} is the electron transfer resistance and CPE_{ads} is a constant phase element (CPE) of immobilised molecules. CPE is capacitor that does not behave ideally, due to surface roughness and/or different ion adsorption/desorption kinetics.

Initial observations indicate that these three techniques were not very sensitive and/or reproducible. For this reason they were repeated adding ferrocyanide/ferricyanide in solution. In this case, not only the effect of the ferrocene label was detected, but also the effect of another redox molecule in solution. Ferrocyanide/ferricyanide in CV and DPV can help to transfer the electrons produced in the redox reaction of ferrocene label to the electrode surface enhancing the signal. An effort is made to explain this catalytic effect later in the chapter (section 3.3.4.2).

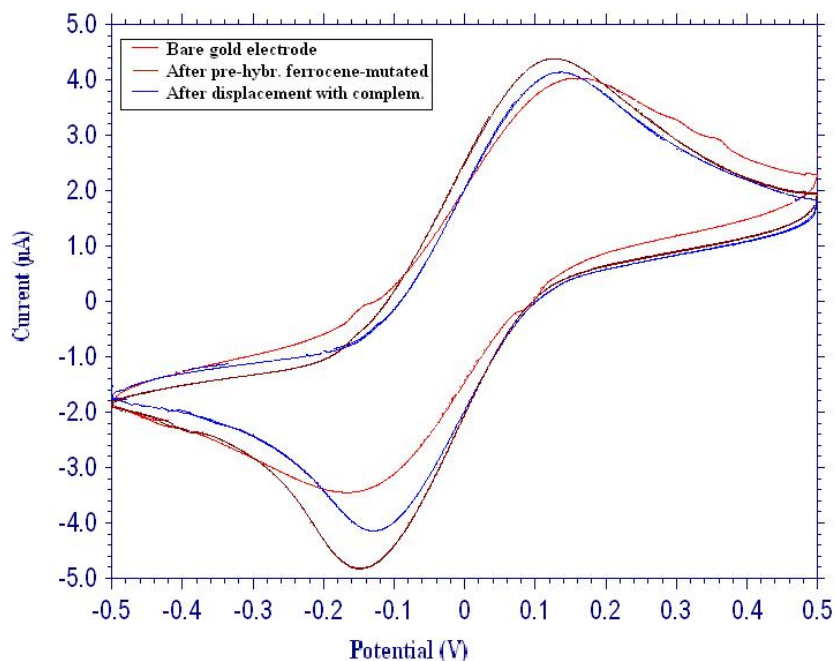


Figure 3. 18 Typical CV before and after displacement of ferrocene-CF mutated oligonucleotide. CV was performed at 0.1 V s^{-1} between -0.5 and 0.5 V in the presence of 1 mM of ferrocyanide/ferricyanide in 10 mM PBS, 150 mM NaCl, pH 7.5.

In the presence of ferrocyanide/ferricyanide in solution the CVmetry showed an enhancement in signal as observed in Figure 3.18. Pre-hybridisation of *ferrocene-CF mutated* oligonucleotide resulted to a higher reduction current comparing with to the signal after displacement or with the bare gold electrode. It is believed that the ferrocene electron transfer is catalysed by ferrocyanide/ferricyanide increasing the current and after displacement this effect is reduced due to the relative absence of ferrocene molecules. It also should be noted that this effect is more pronounced for the reduction reaction of ferrocene as explained later in the chapter.

Similar effects were observed in the case of DPV in the presence of $\text{Fe}(\text{CN})_6^{-3}$ couple.

Chapter 3. Detection of DNA hybridisation by displacement

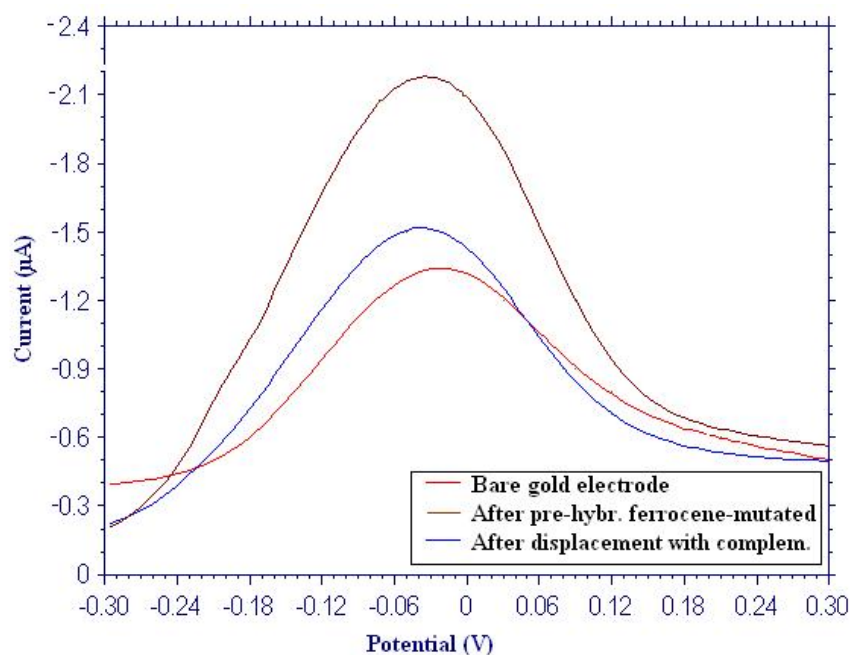


Figure 3.19. Typical DPV before and after displacement of ferrocene-CF mutated oligonucleotide. DPV was performed between -0.2 and 0.2 V, with an increment of potential of 0.005 V, an amplitude of 0.05 V, a pulse width of 0.05 seconds and a pulse period of 0.5 seconds in the presence of 1 mM of ferrocyanide/ferricyanide in 10 mM PBS, 150 mM NaCl, pH 7.5.

The use of ferrocyanide/ferricyanide in impedance spectroscopy has been widely used for the detection of biomolecules interactions. The change on the electrode surface due to the hybridisation event reveals an increase in the electron-transfer resistance at the electrode surface upon the construction of the double-stranded assembly. This is attributed to the electrostatic repulsion of ferrocyanide upon formation of the negatively charged double-stranded superstructure (Patolsky et al., 1999; Park et al., 2005). However in this case the ferrocene molecule immobilised on the surface has to be taken into account in the system. Thus, when *ferrocene-CF mutated* was hybridised on the surface, $\text{Fe}(\text{CN})_6^{-4} / \text{Fe}(\text{CN})_6^{-3}$ ions suffered two electrostatic effects, the repulsion by the negative charged phosphate backbone of the DNA and an attraction by the positive charged ferrocene molecule, to this effect was added the electron transfer produced by the ferrocene molecules on the electrode surface. Whereas after displacement only the repulsion produced by the double stranded DNA to the $\text{Fe}(\text{CN})_6^{-4} / \text{Fe}(\text{CN})_6^{-3}$ ions increased the electron transfer resistance value (Figure 3.20). In this Figure the diameter of the semicircles in each case are proportional to R_{et} .

Chapter 3. Detection of DNA hybridisation by displacement

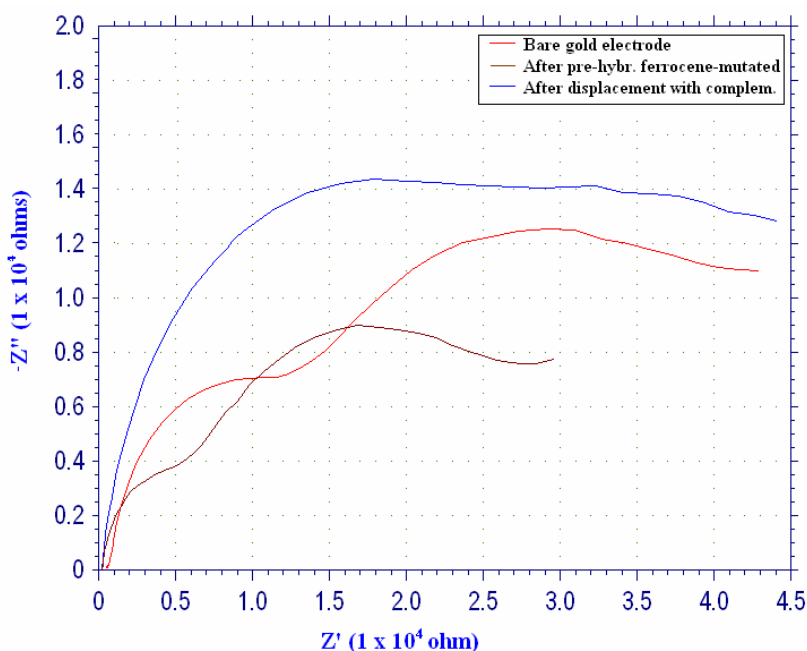


Figure 3.20. Typical Nyquist plot of ferrocene-CF mutated displacement by complementary oligonucleotide. Impedance measurements were performed in the presence of 1 mM of ferrocyanide/ferricyanide in 10 mM PBS, 150 mM NaCl, pH 7.5. An AC voltage of 0.05 V in amplitude and 0.015 V in potential within the frequency range of 100000 – 0.1 Hz.

The results obtained with *ferrocene-CF mutated* displacement with ferrocyanide/ferricyanide in solution were fitted to the next circuit (Figure 3.21);

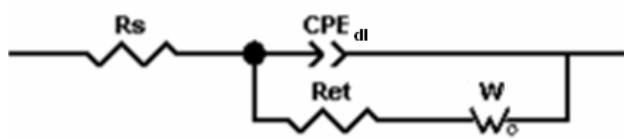


Figure 3. 21. Equivalent circuit for displacement of ferrocene-CF mutated oligonucleotide system in ferrocyanide/ferricyanide.

Where R_s is the solution resistance, CPE_{dl} is the double-layer pseudo-capacitance, R_{et} is the electron transfer resistance and W is the Warburg element, which is related with the diffusion of the $Fe(CN)_6^{-4}$ and $Fe(CN)_6^{-3}$ ions.

Chapter 3. Detection of DNA hybridisation by displacement

With the previous procedure the concentration of capture probe immobilised on the gold surface was optimised. The density of capture probe on the surface has importance due to that it should represent an optimal distance between strands to allow for high hybridisation efficiencies, but at the same time high amount of capture probes for the highest possible hybridisation signals. Maximum hybridisation signal and maximum hybridisation efficiency is not necessarily obtained at the same probe density (Fixe et al., 2004). The reason is that DNA probes that are too closely packed cannot participate in the hybridisation reaction due to steric hindrance or electrostatic interactions (Vainrub and Pettitt, 2003; Shchepinov et al., 1997).

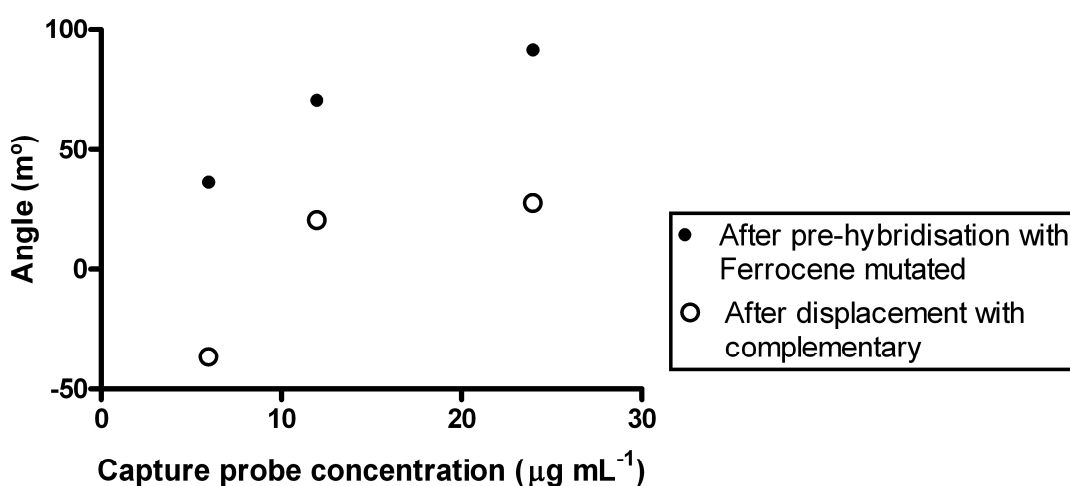


Figure 3. 22. Results obtained by SPR from the pre-hybridisation of $12 \mu\text{g mL}^{-1}$ *ferrocene-CF mutated* oligonucleotide and the subsequent displacement with $30 \mu\text{g mL}^{-1}$ *complementary-CF* oligonucleotide at different concentrations of capture probe (6, 12, 24 $\mu\text{g mL}^{-1}$) in 1 M KH_2PO_4 .

As shown in figure 3.22, the increase of capture probe concentration in solution presumably increases the amount of immobilised probe on the surface producing a higher amount of hybridisation of *ferrocene-CF mutated*-oligonucleotide, which is demonstrated by the increase of m° signal in SPR. With a concentration of $24 \mu\text{g mL}^{-1}$ capture probe was close to the hybridisation saturation.

However, concentration of $24 \mu\text{g mL}^{-1}$ a higher hybridisation was observed and a very high no-specific or “zero” displacement was also observed. Following this reason it appears that $12 \mu\text{g mL}^{-1}$ of capture probe is the best concentration.

Chapter 3. Detection of DNA hybridisation by displacement

Additionally optimisation of the capture probe concentration was made as mentioned by means of the different electrochemistry techniques. The results obtained are summarised (Table 3.1).

Table 3.1 Effect of the capture probe concentration on electrochemical methods of pre-hybridisation of *ferrocene-Cf mutated* and displacement detection.

Technique	Immobilisation	Capture probe concentration ($\mu\text{g mL}^{-1}$)		
		6	12	24
CV in buffer (Peak height, μA)	After pre-hybrid.(fc-mutated)	0	4×10^{-2}	4.9×10^{-2}
	After displacement	0	3.1×10^{-2}	5×10^{-4}
DPV in buffer (Peak height, μA)	After pre-hybrid.(fc-mutated)	4×10^{-3}	5.4×10^{-2}	6.3×10^{-2}
	After displacement	5.1×10^{-3}	4.8×10^{-3}	5.9×10^{-3}
Impedance in buffer (K_f)	After pre-hybrid.(fc-mutated)	12050	14100	1960
	After displacement	1002	10400	1860
CV in $\text{Fe}(\text{CN})_6^{4-}/\text{Fe}(\text{CN})_6^{3-}$ (Peak height, μA)	After pre-hybrid.(fc-mutated)	1.3	2.4	1.3
	After displacement	0.8	1.4	1.6
DPV in $\text{Fe}(\text{CN})_6^{4-}/$ $\text{Fe}(\text{CN})_6^{3-}$ (Peak height, μA)	After pre-hybrid.(fc-mutated)	0.9	1.3	0.67
	After displacement	0.66	0.77	0.81
Impedance in $\text{Fe}(\text{CN})_6^{4-}/$ $\text{Fe}(\text{CN})_6^{3-}$ (R_{et} , ohms)	After pre-hybrid.(fc-mutated)	7050	2706	136
	After displacement	7258	6854	2823

The results obtained by CV in buffer showed an increase of peak height at higher concentrations of capture probe, which was also corroborated with SPR results. It is assumed that this increase corresponds to higher amount of *ferrocene-CF mutated* hybridised. After displacement of *ferrocene-CF mutated* by the target a decrease of peak height was obtained, which demonstrate the functionality of the system. Best signal displacement was obtained with $24 \mu\text{g mL}^{-1}$ of capture probe. Similar results were obtained with DPV in buffer.

Chapter 3. Detection of DNA hybridisation by displacement

While impedance in buffer demonstrated higher electron transfer rate constant at higher concentrations of ferrocene on the surface and this value decreased after displacement. Again at a concentration of $24 \mu\text{g mL}^{-1}$ the most pronounced effect of displacement was observed.

CV and DPV in the presence of ferrocyanide/ferricyanide showed in general also an increase of signal with an increase of capture probe concentration. However now the The best displacement effect was seen at $12 \mu\text{g mL}^{-1}$ of capture probe.

Impedance in ferrocyanide/ferricyanide detected a decrease of R_{et} was when the concentration of ferrocene on the surface increases, so after displacement an increase of R_{et} was detected as expected. In this case, the most pronounced displacement effect was detected at $24 \mu\text{g mL}^{-1}$ of capture probe.

Although most of cases $24 \mu\text{g mL}^{-1}$ appeared to be the optimum concentration, taking into account the possible non-specific adsorption detected by SPR, $12 \mu\text{g mL}^{-1}$ of capture probe was chosen as optimum concentration to enhance specific displacement.

The next variable optimised was the concentration of *ferrocene-CF mutated* oligonucleotide that was used for pre-hybridisation with the capture probe. An increase of signal in the pre-hybridisation of the *ferrocene-CF mutated* contributes to a system with high signal a high sensitivity.

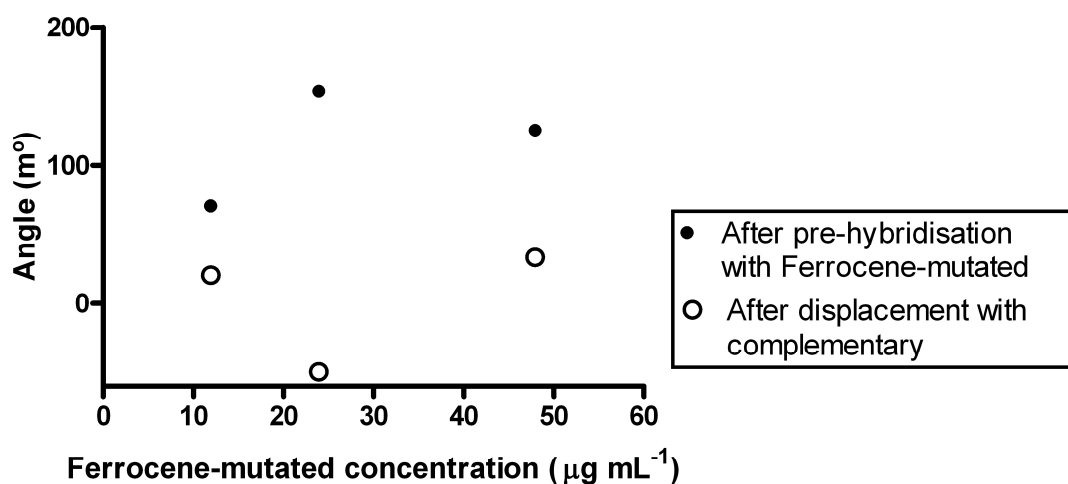


Figure 3. 23. Results obtained by SPR from the pre-hybridisation of ferrocene-mutated oligonucleotide and the subsequent displacement with complementary oligonucleotide at different concentrations of ferrocene-CF mutated ($12, 24, 48 \mu\text{g mL}^{-1}$) in hybridisation buffer. $12 \mu\text{g mL}^{-1}$ of capture probe and $30 \mu\text{g mL}^{-1}$ of *CF-complementary* was used in these experiments.

Chapter 3. Detection of DNA hybridisation by displacement

Figure 3.23 shows the SPR signal as a function of *ferrocene-CF mutated* concentration hybridised. It appears that with a concentration of $48 \mu\text{g mL}^{-1}$ *ferrocene-CF mutated* the system arrives to the hybridisation saturation.

Again although a concentration of $24 \mu\text{g mL}^{-1}$ shows a higher hybridisation signal, a higher non-specific displacement was observed, therefore $48 \mu\text{g mL}^{-1}$ of ferrocene-CF mutated was chosen as the optimum concentration by this technique.

Optimisation of *ferrocene-CF mutated* concentration was attempted by means of different electrochemistry techniques. The results obtained are summarised in Table 3.2.

Table 3.2 Effect of sub-optimum level on the performance of electrochemical methods for displacement detection.

		Ferrocene-CF mutated concentration ($\mu\text{g mL}^{-1}$)		
Technique	Immobilisation	12	24	48
CV in buffer (Peak height, μA)	After pre-hybrid.(fc-mutated)	4×10^{-2}	4.4×10^{-2}	5.3×10^{-2}
	After displacement	3.1×10^{-2}	3.8×10^{-2}	2.7×10^{-2}
DPV in buffer (Peak height, μA)	After pre-hybrid.(fc-mutated)	5.4×10^{-2}	5.8×10^{-2}	7.8×10^{-2}
	After displacement	4.8×10^{-3}	2.3×10^{-2}	3.9×10^{-2}
Impedance in buffer (K_f)	After pre-hybrid.(fc-mutated)	14100	17500	30800
	After displacement	10400	12000	22000
CV in $\text{Fe}(\text{CN})_6^{-4}/\text{Fe}(\text{CN})_6^{-3}$ (Peak height, μA)	After pre-hybrid.(fc-mutated)	2.4	3.9	4.8
	After displacement	1.4	3.5	3.8
DPV in $\text{Fe}(\text{CN})_6^{-4}/\text{Fe}(\text{CN})_6^{-3}$ (Peak height, μA)	After pre-hybrid.(fc-mutated)	1.3	1.9	2.4
	After displacement	0.77	1.5	1.8
Impedance in $\text{Fe}(\text{CN})_6^{-4}/\text{Fe}(\text{CN})_6^{-3}$ (R_{et} , ohms)	After pre-hybrid.(fc-mutated)	2706	218	175
	After displacement	6854	218	97

In *ferrocene-CF mutated* oligonucleotide concentration optimisation similar trends but higher signals were obtained as with the capture probe concentration optimisation. In this case also an increase of concentration of *ferrocene-CF mutated* oligonucleotide showed an increase of electrochemical signal and a decrease of signal after displacement.

CV and DPV in buffer or ferrocyanide/ferricyanide showed an increase of peak height at higher concentrations of *ferrocene-CF mutated*, due to the higher amount of ferrocene immobilised on the surface. For the same reason an increase of K_f response was obtained by impedance in buffer when the *ferrocene-CF mutated* concentration increased and a decrease after displacement. The optimum concentration for all these techniques was $48 \mu\text{g mL}^{-1}$ of *ferrocene-CF mutated* concentration. Results in the presence of in ferrocyanide/ferricyanide. Led to the same conclusion. Therefore, taking into account all techniques a concentration of *ferrocene-CF mutated* oligonucleotide of $48 \mu\text{g mL}^{-1}$ was chosen for the subsequent experiments.

The last variable to be optimised was the concentration of sodium chloride in the hybridisation buffer. An increase of cations in the hybridisation environment might stabilise the duplex because both strands in the duplex are negatively charged and suffer mutual repulsion.

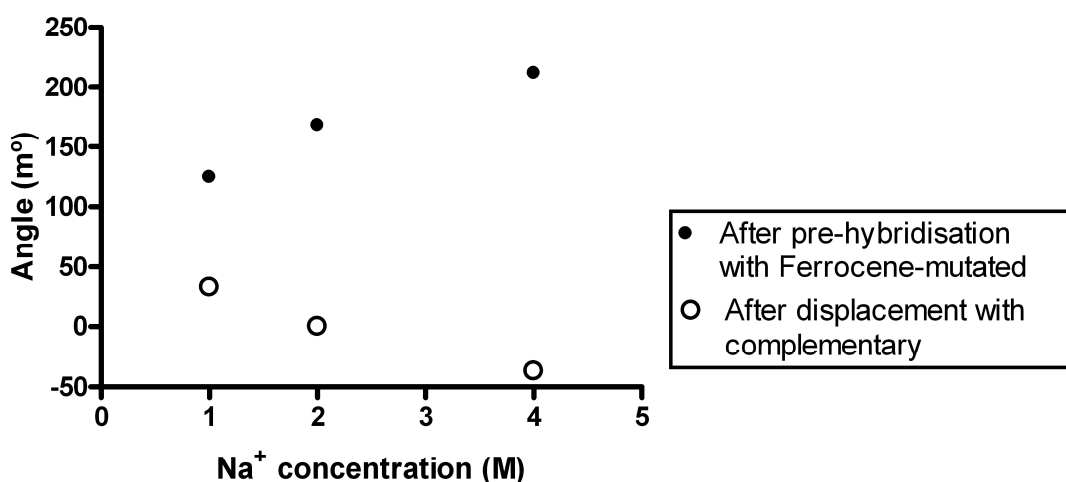


Figure 3. 24. Results obtained by SPR from the pre-hybridisation of *ferrocene-CF mutated* oligonucleotide and the subsequent displacement with *complementary-CF* oligonucleotide at different concentrations of NaCl (1, 2, 4 M) in hybridisation buffer during the pre-hybridisation of *ferrocene-CF mutated* oligonucleotide. Electrodes modified with $12 \mu\text{g mL}^{-1}$ of capture probe and $48 \mu\text{g mL}^{-1}$ of *ferrocene-CF mutated*.

Chapter 3. Detection of DNA hybridisation by displacement

Figure 3.24. shows a high enhancement of hybridisation of *ferrocene-FC mutated* oligonucleotide with the capture probe when the concentration of NaCl in hybridisation buffer increased. So it seems correct the hypothesis that higher concentrations of salt during hybridisation stabilise the duplex, however at the same time, it appears that extreme non-specific displacement also is enhanced by it.

For this reason, 1 M of NaCl in pre-hybridisation and displacement was chosen as optimum.

NaCl concentration was also optimised by means of different electrochemistry techniques. The results obtained are summarised in table 3.3.

Table 3.3 Effect of NaCl concentration in pre-hybridisation and displacement buffers on the performance of electrochemicals methods for displacement detection.

Technique	Immobilisation	NaCl concentration (M)		
		1	2	4
CV in buffer (Peak height, μA)	After pre-hybrid.(fc-mutated)	5.3×10^{-2}	0	0
	After displacement	2.7×10^{-2}	1.1×10^{-2}	0
DPV in buffer (Peak height, μA)	After pre-hybrid.(fc-mutated)	7.8×10^{-2}	1.3×10^{-2}	1×10^{-2}
	After displacement	3.9×10^{-2}	1.6×10^{-2}	0.6×10^{-2}
Impedance in buffer (K_f)	After pre-hybrid.(fc-mutated)	30800	7280	11200
	After displacement	22000	13700	11500
CV in $\text{Fe}(\text{CN})_6^{-4}/\text{Fe}(\text{CN})_6^{-3}$ (Peak height, μA)	After pre-hybrid.(fc-mutated)	4.8	9.5	10
	After displacement	3.8	9.8	11
DPV in $\text{Fe}(\text{CN})_6^{-4}/\text{Fe}(\text{CN})_6^{-3}$ (Peak height, μA)	After pre-hybrid.(fc-mutated)	2.4	4.3	4.8
	After displacement	1.8	5	4.9
Impedance in $\text{Fe}(\text{CN})_6^{-4}/\text{Fe}(\text{CN})_6^{-3}$ (R_{et} , ohms)	After pre-hybrid.(fc-mutated)	175	200	159
	After displacement	97	220	510

Chapter 3. Detection of DNA hybridisation by displacement

Results were obtained with CV, DPV and impedance in buffer when compared to the SPR results. By SPR an increasing hybridisation of *ferrocene-FC mutated* was obtained with increasing concentration of NaCl, whereas by CV, DPV and impedance in buffer a decrease of electrochemical signal was detected at increasing concentration of salt. The reasons for this behaviour might be the formation of chloride film on the electrode surface due to the high concentration of NaCl during the pre-hybridisation incubation, which might affect electron transfer.

However CV and DPV in ferrocyanide/ferricyanide show the same trend as SPR, probably because mixture of ferrocyanide/ferricyanide, competed with the metal-chloride in the surface compensating the effect that this film produced in the electrochemically active surface area.

It is also significant the low values of R_{et} were obtained in impedance with ferrocyanide/ferricyanide in solution compared to previous optimisations. At higher concentrations of NaCl, high concentrations of ions were free in the solution, so the increase in the concentration of electrolyte enhances the electron transfer, decreasing the electron transfer resistance.

Comparing electrochemical signals before and after displacement with CV, DPV and impedance in buffer or in ferrocyanide/ferricyanide, as expected, showed lower values after displacement.

After optimisation, the best conditions for pre-hybridisation of *ferrocene-FC mutated* oligonucleotide and subsequent displacement with *complementary* oligonucleotide, were: incubation of $12 \mu\text{g mL}^{-1}$ *capture probe*, pre-hybridisation with of $48 \mu\text{g mL}^{-1}$ *ferrocene-CF mutated* and 1M of NaCl in hybridisation buffer.

The reproducibility of the detection of *ferrocene-CF mutated* displacement was evaluated in a home made $20 \mu\text{L}$ two electrode thin layer cell with a 18 mm^2 square gold sheet as a working electrode opposite to a solid state platinum reference and counter electrode by CV and DPV with ferrocyanide/ferricyanide in solution. Peak height of CV was measured before and after displacement obtaining $12.2 \pm 1.3 \mu\text{A}$ after the pre-hybridisation of *ferrocene-CF mutated* and $6.2 \pm 0.3 \mu\text{A}$ after displacement with complementary. Similar results were obtained by DPV: $9.9 \pm 0.7 \mu\text{A}$ after the pre-hybridisation of *ferrocene-CF mutated* and $4.5 \pm 0.8 \mu\text{A}$ after displacement with complementary

Chapter 3. Detection of DNA hybridisation by displacement

Non-specific displacement signal was shown in next figure 3.25. Displacement of pre-hybridised ferrocene-CF mutated oligonucleotide was detected by DPV in ferrocyanide/ferricyanide. Displacement was carried out with a complementary oligonucleotide as target, with buffer as control and another control was performed with a 22-mer non-complementary oligonucleotide.

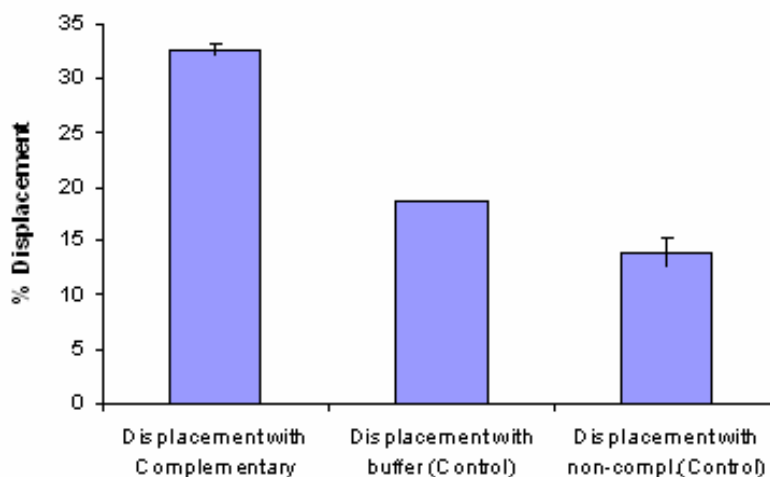


Figure 3. 25. Percentage of electrochemical displacement detection of pre-hybridised ferrocene-CF mutated by complementary oligonucleotide target. The controls were carried out displacing with buffer or with a non-complementary oligonucleotide instead of complementary. These results were obtained with DPV in ferrocyanide/ferricyanide. The electrode was modified with $12 \mu\text{g mL}^{-1}$ of capture probe, $48 \mu\text{g mL}^{-1}$ of *ferrocene-CF mutated* and the signal was displaced with $16 \mu\text{g mL}^{-1}$ of complementary target. (n=3)

The results were presented as percentage of displacement obtained with the target, complementary oligonucleotide, and with the buffer and non-complementary oligonucleotide as control. The signal from the pre-hybridised mutated-HRP was considered the 100 % of the signal and the signal obtained after displacement with complementary or controls was converted to a percentage of displacement.

32.6 % of *ferrocene-FC mutated* displacement with complementary oligonucleotide was achieved while 18.7 % was obtained with buffer and 13.9 % with a non-complementary oligonucleotide. So the specific displacement was equal to 14% (Figure 3.25).

Proportionality of signal displaced with the concentration of the target, *complementary oligonucleotide*, was tested and plotted in Figure 3.26.

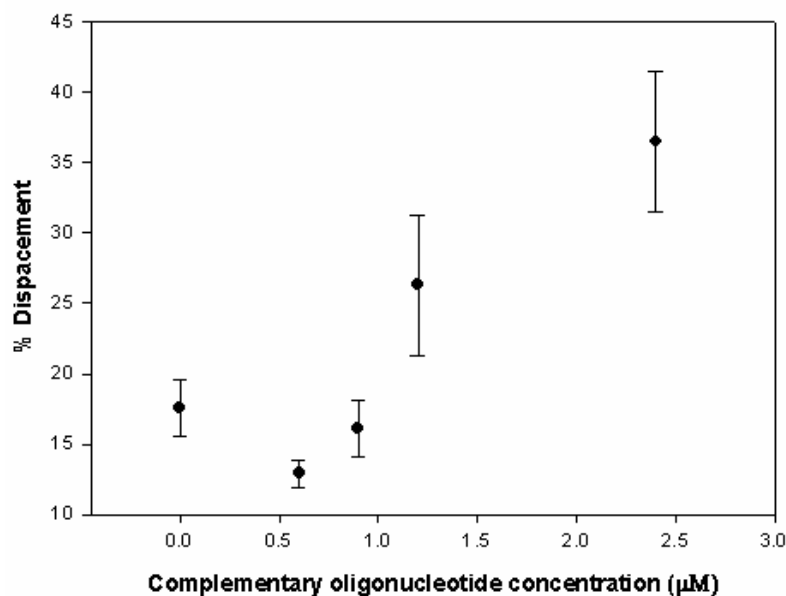


Figure 3. 26. Electrochemical detection of displacement of pre-hybridised *ferrocene-CF mutated* with different concentrations of *complementary oligonucleotide*. These results were obtained with DPV in ferrocyanide/ferricyanide. The electrode was modified with $12 \mu\text{g mL}^{-1}$ of *capture probe*, $48 \mu\text{g mL}^{-1}$ of *ferrocene-CF mutated*. (n=2)

Higher percentage of displaced signal was detected at higher concentrations of target, a fact that demonstrates the functionality of the system to detect label free oligonucleotide hybridisation in a reagentless system. However below $1.2 \mu\text{M}$ of target the displacement cannot be differentiated from the non-specific displacement by the buffer.

Comparing this with the previous electrochemical system that uses HRP label for the displacement detection, lower percentage of displacement was obtained with ferrocene labelled, 14 % *versus* 22 % of HRP displacement and a similar range of detection was obtained with both systems. However in this case a completely reagentless system was achieved and lower relative standard deviation was obtained ($6.2 \pm 0.3 \mu\text{A}$ *versus* $0.12 \pm 0.03 \mu\text{A}$ with HRP system).

3.3.5.2 Amplification of ferricyanide signal by ferrocene

As mentioned unexpected enhancement of ferricyanide signal was obtained with ferrocene label.

Stell et al., (1998); Choi et al., (2005), used ferricyanide in solution and CV to detect changes in the surface charge of gold electrodes and the consequent electrochemical interaction between $\text{Fe}(\text{CN})_6^{-3}$ and the electrode when a dsDNA was hybridised on the electrode surface. Because when hybridisation was done the reduction/oxidation of negative charges on the sugar-phosphate backbone of dsDNA cover the electrode surface, which prevents $\text{Fe}(\text{CN})_6^{-3}$ from approaching the surface, decreasing current signal was observed. So a similar decrease of current might be obtained in the displacement system. However this system can not be directly compared with the Stell and Choi experiments because a ferrocene label was attached to the 5' end of the hybridised species. The positively charged ferrocene molecule linked to the negatively charged oligonucleotide, produced an opposite effect of $\text{Fe}(\text{CN})_6^{-4} / \text{Fe}(\text{CN})_6^{-3}$ attraction, hence increasing the current signal.

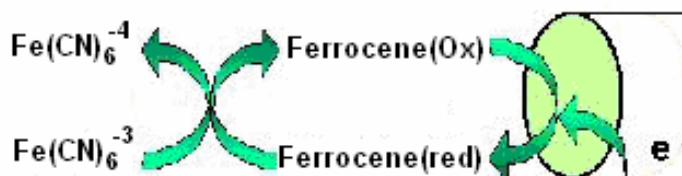
The effect of the attraction of ferricyanide to a positively charged molecule attached to DNA was already reported by Park and Hahn, (2004). A dsDNA-modified electrode was treated with an intercalating agent, proflavine, then the negative charges on the duplex strands were compensated with the positive charges of intercalator molecules, which provides a surface-charge condition that facilitates the approach of $\text{Fe}(\text{CN})_6^{-3}$ to the electrode surface, detecting an increase of signal when proflavine was intercalated in the dsDNA.

Furthermore an effect of enhancement of ferricyanide signal with a ferrocene label was reported by Heeger et al., 2004. Their approach worked by the addition of an electrochemical mediator, ferricyanide, that was reduced by the ferrocene label, thus in the presence of ferricyanide the electrode repeatedly reduced each ferrocene increasing the peak currents. A similar system was reported by Ostatna et al., (2005) and Boon et al., (2000), in this case the reduction of methylene blue was considerably improved in the presence of an electron acceptor, $\text{Fe}(\text{CN})_6^{-3}$.

Chapter 3. Detection of DNA hybridisation by displacement

So a double effect of attraction and enhancement of the signal is produced by the ferrocene label to ferrocyanide/ferricyanide, which allows more sensitive detection of the pre-hybridisation of ferrocene-CF mutated and the subsequent displacement.

The redox reaction produced between ferrocene label and ferricyanide is shown in next scheme (Scheme 3.6).



Scheme 3. 6. Redox catalytic reaction produced between ferrocene label and ferricyanide.

As the scheme shows, this system is based on transfer of the electrons from the reduced form of ferrocene to $\text{Fe}(\text{CN})_6^{-3}$ resulting in the conversion of $\text{Fe}(\text{CN})_6^{-3}$ to $\text{Fe}(\text{CN})_6^{-4}$ and the oxidation of ferrocene, which is reduced on the electrode surface. So in the presence of ferricyanide the electrode repeatedly reduces each ferrocene molecules immobilised on the electrode surface increasing the current signal. As shown in Figure 3.27, in CV the increase of current appeared in the reduction peak, because the reaction produced on the electrode surface was the reduction of ferrocene.

To demonstrate this hypothesis chronoamperometry of a modified electrode with complementary oligonucleotide hybridised with capture probe immobilised on the surface and other electrodes with *ferrocene-CF mutated* oligonucleotide hybridised with immobilised *capture probe* was carried out.

Each electrode was immersed in 15 μL of 10 mM PBS, 150 mM NaCl pH 7.5 in a 2 electrode cell set up with platinum as reference and counter electrode. A potential of -0.2 V was applied to record reduction of ferrocene. when the current arrived at the base line. After 100 seconds, 5 μL 4 mM of $\text{Fe}(\text{CN})_6^{-3}$ in 10 mM PBS, 150 mM NaCl pH 7.5 was injected into the cell to record the effect of ferrocyanide in the reduction of ferrocene.

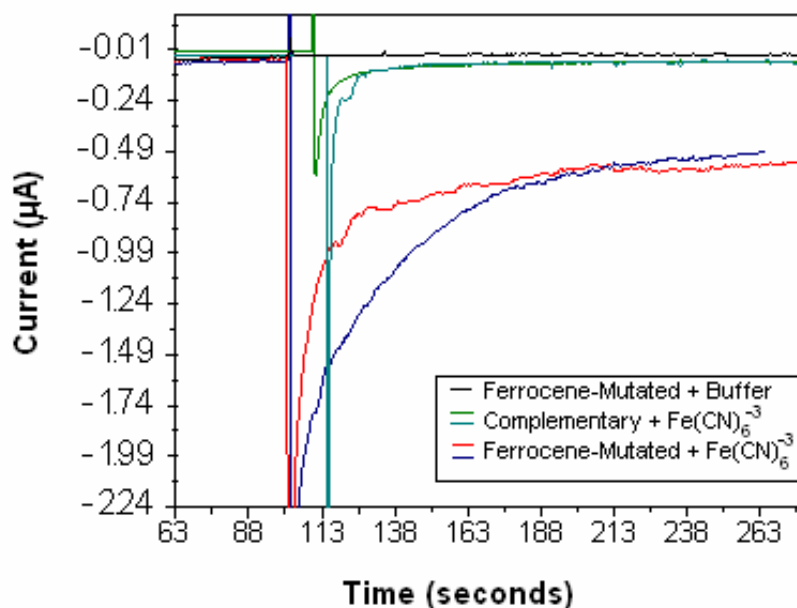


Figure 3. 27. Chronoamperometry of ferrocene-CF mutated oligonucleotide hybridised with immobilised capture probe (red and blue line) and complementary oligonucleotide hybridised with immobilised capture probe (sky-blue and green line) with 1 mM ferrocyanide in solution. Ferrocene-CF mutated hybridised electrodes were also detected in buffer without ferrocyanide as control (black line).

Figure 3.27. shows the results obtained in the chronoamperometry. Red and blue lines show a sustained reduction current of about 0.47 μA due to the cycle between ferrocene and ferrocyanide shown in scheme 3.5. This cycle was not produced in the absence of ferrocyanide (black line) or of ferrocene (green line)

These experiments demonstrate an electrocatalytic cycle that results in signal amplification when ferrocyanide was present in the system with a ferrocene label. However this approach leads to a sensor that is no longer reagentless.

3.4 Conclusions

This chapter describes different sub-optimum displacement assays to detect a label-free oligonucleotide target. A pre-hybridisation of a sub-optimum labelled mutated oligonucleotide results in the production of ready to use label-free biosensor. Due to the higher affinity of the target that is fully complementary to the capture probe, the pre-

hybridised mutated labelled is displaced and the decrease of the signal verified the presence of the target and was proportional to its concentration.

Two sub-optimum displacement systems were demonstrated with HRP label. The first was optimised resulting to a 5 minutes ELONA. It used an HRP-labelled mutated sub-optimum in the hope to achieve amplification. However HRP electrochemical transduced was not amenable to the hybridisation conditions and this work was limited to a proof of concept. Still electrochemical detection of sub-optimum displacement with HRP label shows a specific displacement of 22.5 % at 4 μM of the target.

Sub-optimum hybridisation displacement for detection of cystic fibrosis gene region was demonstrated by seven methods, SPR, CV in buffer, DPV in buffer, impedance in buffer, CV in ferrocyanide/ferricyanide, DPV in ferrocyanide/ferricyanide and impedance in ferrocyanide/ferricyanide. Comparing with the previous electrochemical system using HRP labelled for the displacement detection, lower percentage of displacement was obtained with ferrocene labelled, 14 % *versus* 22 % of HRP displacement and a similar range of detection was demonstrated with both systems. However in this case a completely reagentless system was achieved and lower relative standard deviation was obtained ($6.2 + 0.3 \mu\text{A}$ *versus* $0.12 + 0.03 \mu\text{A}$ with HRP system). Furthermore this system demonstrated the benefit of signal amplification when ferrocyanide was inserted in a system with a ferrocene label.

3.5 References

Aboul-ela F., Koh A., Tinoco I., Martin F.H., *Nucleic Acids Research*, 1985, 13, 4811-4824.

Adam G., Delbruck M., *Reduction of dimensionality in biological diffusion process. In structural chemistry and molecular biology.* W.H. Freeman and Company, San Francisco, 1968.

Allawi H.T., Santa Lucia J.Jr., *Nucleic acids Research*, 1998, 26, 2694-2701.

Allawi H.T., Santa Lucia J.Jr., *Biochemistry*, 1997, 36, 10581-10594.

Chapter 3. Detection of DNA hybridisation by displacement

Bloomfield V.A., Crothers D.M., Tinoco I., *The physical chemistry of nucleic acids*, 1974, Harper and Row, New York

Bloomfield V.A., Crothers D.M., Tinoco I., *Nucleic acid structures, properties and functions*. University Science Books, Sausalito, 2000.

Boon E.M, Ceres D.M., Drummond T.G., Hill M.G., Barton J.K, *Nature biotechnology*, 2000, 18, 1096-1100.

Breslauer K.J., Frank R., Blocker H., Marky L.A., *Proceedings of the National Academy of Science U.S.A.*, 1986, 83, 3746-3750.

Cantor R.C., Schimmel P., *Biophysical chemistry I*, W.H. Freeman, New York, 1980.

Choi Y.S., Lee K.S., Park D.H., *Bulletin of the Korean Chemical Society*, 2005, 26, 3, 379-383.

Craig M.E., Crothers D.M., Doty P., *Journal of Molecular Biology*, 1971, 62, 383-401.

Dai H., Meyer M., Stepaniants S., Ziman M., Stoughton R., *Nucleic acid Research*, 2002, 30, 16, 86-93.

Fixe F., Dufva M., Telleman P., Christensen C.B., *Nucleic Acids Research*, 2004, 32, e9.

Fotin A.V., Drobyshev A.L., Proudnikov D.Y., Perov A.N., Mirzabekov A.D., *Nucleic Acid Research*, 1998, 26, 6, 1515-1521.

Gotoh M., Hasegawa Y., Shinohara Y., Shimizu M., Tosu M., *DNA research*, 1995, 2, 285-293.

Gryadurov D.A., Lapa S.A., Zasedatev A.S., *J. Biomol. Structural Dynamics*, 2005, 22, 6, 725-734.

Heeger A.J., Fan C., Plaxcon K., *US Patent*, 435006000, 2004.

Hermanson G.T., *Bioconjugated techniques*, Academic Press, 1995.

Howley P.M., Israel M.A., Law M.F., Martin M.A., *Journal of Biological Chemistry*, 1979, 254,11, 4876-4883.

Ke S.H., Wartell R.M., *Nucleic Acids Research*, 1993, 21, 5137-5143.

Ke S.H., Wartell R.M., *Nucleic Acids Research*, 1996, 24, 4, 707-712.

Laviron E., *J. Electroanalytical Chemistry*, 1979, 97, 135-149.

Chapter 3. Detection of DNA hybridisation by displacement

Li J., Chu X., Liu Y., Jiang J., He Z., Zhang Z., Shen G., Yu R., *Nucleic Acids Research*, 2005, 33, 19, 168-177.

Markly L.A., Breslauer K.J., *Biopolymers*, 1987, 26, 1601-1620

Maniatis T., Fritsh E.F., Sambrook J., *Molecular cloning: a laboratory manual*. Cold Spring Harbor University Press, 11.45-11.57.

Marcus A., *Molecular biology*, New York, Academic Press, 1989.

Naef F., Lim D.A., Patil N., Magnasco M., *Physical Review E*, 2002, 65, 40901-40904.

Ostatná V., Dolinnaya N., Andreev S., Oretskaya T., Wang J., Hianik T. *Bioelectrochemistry*, 2005, 67, 2, 205-210.

Park N.K., Hahn J.H., *Analytical Chemistry*, 2004, 76, 900-905.

Peterson A.W., Wolf L.K., Georgiadis R.S., *Journal of American Chemical Society*, 2002, 124, 14601-14607.

Peyret N., Seneviratnet P.A., Allawi H.T., Santa Lucia J.Jr., *Biochemisry*, 1999, 38, 3468-3477.

Pozhitkov A., *Molecular taxonomy. Bioinformatics and practical evaluation*. Ph.D. Thesis, Institute of Genetics, University of Cologne, 2003.

Shchepinov M.S., Case-Green S.C., Southern E.M., *Nucleic Acids Research.*, 1997, 25, 1155–1161.

Sorokin N.V., Chechetkin V.R., Livshits M.A., Pankov S.V., Donnikov M.Y., *J.Biomolecular Structures*, 2005, 22, 725-734.

Steel A.B., Herne T.M., Tarlov M.J., *Analytical Chemistry*, 1998, 70, 4670-4675.

Vainrub A., Pettitt B.M., *Biopolymers*. 2003, 68, 265–270.

Chapter 3. Detection of DNA hybridisation by displacement

Chapter 4. Electrochemical aptasensors

4.1 Introduction

The advent of proteomics obligates to the availability of combinatorial protein-recognition elements and the generic transduction of their biorecognition reaction.

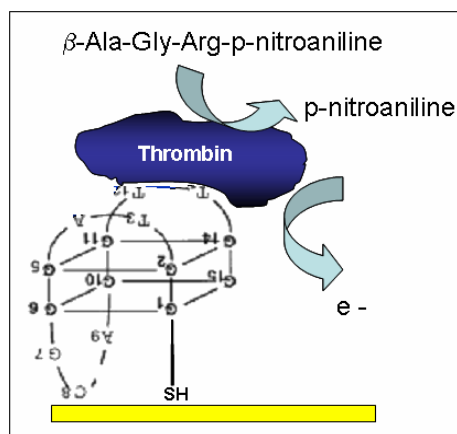
As mentioned in the first chapter, some examples of antibody arrays have been commercialised, although aptamers are the molecules of choice to create combinatorial proteomic chips.

Although electrochemical transducers offer substantial advantages over other transducers typically used in microarrays, such as high sensitivity, fast response, robustness, low cost of mass production and the possibility for miniaturisation, electrochemical transducers applied in aptamer based sensors are rarely reported.

Thrombin was selected as a target for this work because of its wide spread reporting in the literature.

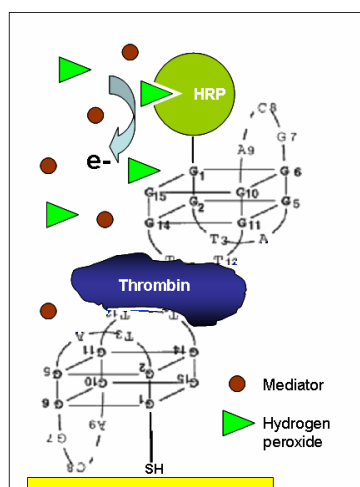
In this thesis different strategies to realise an electrochemical aptamer based sensor for thrombin detection are described.

In the most straightforward configuration a thiol-terminated aptamer was immobilised on a gold electrode. After incubation with thrombin, the aptamer bound thrombin was detected by quantification of a reaction that it catalyses the production of p-nitroaniline. While the p-nitroaniline product could be detected optically, electrochemical detection proved faster and more sensitive. (Scheme 4.1)



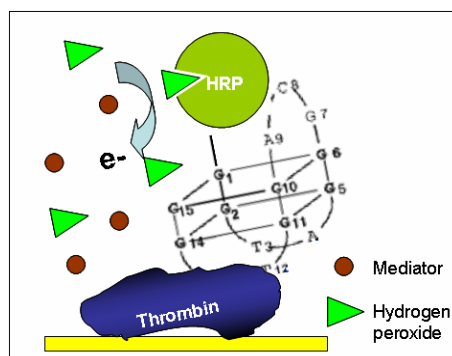
Scheme 4. 1. Schematic representation of thrombin-aptamer interaction detection through a specific thrombin substrate.

In a second configuration, thrombin was detected using a sandwich format. Thrombin has two electropositive exosites, both of which are capable of binding the aptamer. The thiolated aptamer was again immobilised on a gold electrode and incubated with thrombin. In a second incubation step a biotin labelled aptamer was allowed to bind to the other thrombin exosite. The biotin aptamer was previously incubated with streptavidin-HRP (Horseshoe peroxidase) effectively forming a peroxidase labelled aptamer. The HRP thus immobilised at the electrode surface was measured electrochemically using H_2O_2 and a diffusional osmium mediator. The current resulting for the activity of HRP was related through calibration to the quantity of thrombin (Scheme 4.2).



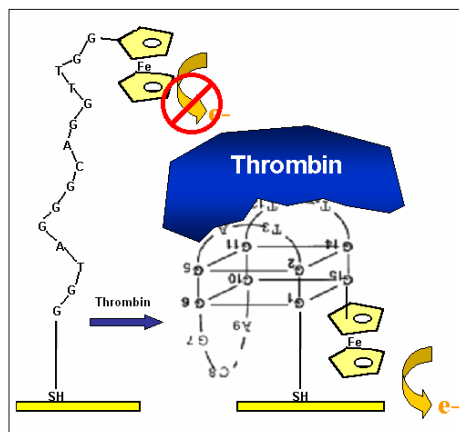
Scheme 4. 2. Aptamer base sensor in a sandwich manner.

Western blotting inspired the third strategy, where proteins immobilised on a membrane are detected by antibodies bearing reporter molecules (Lin et al. 1996). In these experiments, thrombin was immobilised on a modified gold electrode surface. The sensor was incubated first with biotin labelled aptamer and then with streptavidin-HRP. Electrochemical detection of HRP was again performed, using H_2O_2 and a diffusional osmium based mediator (Scheme 4.3).



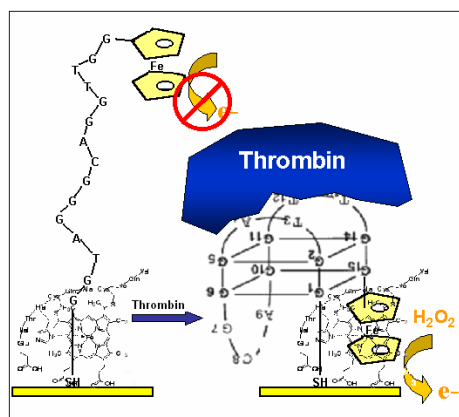
Scheme 4.3. Scheme of thrombin detection through its surface adsorption.

In the fourth strategy thrombin aptamer was used as a model to demonstrate the simple reagentless and label-free electrochemical transduction of its molecular beacon-like transition upon molecular recognition because it is well characterised and extensively studied with fluorescence label (Hamaguchi et al., 2001). The beacon-like 3-D change of the aptamer structure can be transduced by observing the significant change in the distance-dependent voltamperometric behaviour of the label as demonstrated by Fan et al, 2003, for a molecular beacon. We show that the phenomena observed are specific (Scheme 4.4).



Scheme 4.4. Schematic presentation of aptabeacon strategy.

In the last strategy, a modification of the previous aptamer-beacon based sensor was carried out. In this case the gold surface, where the aptamer-beacon was immobilised, was also covered with a monolayer of microperoxidase. Hence, the redox centre of the co-immobilised enzyme recognises the ferrocene end of the aptamer approached to the electrode surface due to the effect of thrombin interaction, so in the presence of its substrate, the enzyme mediates the electron transfer. This catalytic reaction also serves for signal amplification (Scheme 4.5).



Scheme 4.5. This scheme shows an approximation of aptabeacon with MP-11 system.

4.2 Materials and methods

4.2.1 Materials

The sequences of the HPLC purified 20-mer oligonucleotide for thrombin detection are shown below:

20-mer biotin labelled aptamer (*biotin-aptamer*):

5'-Biotin-C₁₂- CCAACGGTTGGTGTGGTTGG -3'.

20-mer thiol labelled aptamer (*thiol-aptamer*):

5'-Thiol-C₉- CCAACGGTTGGTGTGGTTGG -3'.

20-mer disulphide amine labelled oligonucleotide, for its modification with ferrocene in the 3' end (*aptabeacon*):

Thiol-C₉-5'- CCAACGGTTGGTGTGGTTGG -3'-C7-Amine

The oligonucleotides were purchased from Quiagen (Spain). All stock oligonucleotide solutions were made at 1mg mL⁻¹ with autoclaved milliQ water and stored at -20 °C.

N, N'-dicyclohexylcarbodiimide (EDC) (D3128), Sodium tetraborate (12687), DNA Salmon testes (D2389), bovine serum albumin (BSA) (B6917), tris(hydroxymethyl)aminomethane-acetic (Tris-Ac) (T3647), tris-HCL (T2367), Polyethylene glycol sorbitan monolaurate (tween) (T2389), Thrombin substrate β-Ala-Gly-Arg-p-nitroaniline (T3018), diammonium citrate (C1883), thrombin (T7009), streptavidin peroxidase labelled (S5512), p-nitroaniline (N2128), Microperoxidase-11 (M6756), saline sodium citrate buffer (S6639) and 2-mercaptoethanol (M6250) were purchased from Sigma. NaCl (131659), HCl (131020), KOH (131515), KH₂PO₄ (121509), H₂SO₄ (131056) and H₂O₂ (131072.12) were supplied from Panreac. Sodium tetraborate (22,173-2), dimethylformamide (27,054-7), ferroceneacetic acid (335045), dithiothreitol (DTT) (64656-3), and N-Hydroxysuccinimide (NHS) (13067) were from Aldrich and 3-hydroxipicolinic acid (HPA) (36197) from Fluka. The Sephadex G25 DNA grade resin (17-0853-01) was purchased from Amersham Pharmacia Biotech. Streptavidin coated plates were purchased from Labsystems. The electron-conducting

diffusional redox mediator ($[\text{Os}(\text{bpy})_2(\text{pyr-CH}_2\text{-NH}_2)]\text{Cl}$) was synthesised as reported in the literature (Gregg and Heller, 1991).

4.2.2 Instrumentation

The colourimetric detection of thrombin by enzyme-linked oligonucleotide assay (ELONA) was detected with an ELISA reader SpectraMax 340PC from Molecular Devices running SoftMax Pro software. Measurements were carried out using 1cm path-length quartz cuvettes.

Electrochemical measurements were carried out using an Autolab PGSTAT10 electrochemical analysis system running GPES management software from Eco Chemie. Electrochemistry was performed in a home made 20 μL two electrode thin layer cell with a 18 mm^2 square gold sheet as a working electrode opposite to a platinum electrode or a solid state Ag/AgCl reference/counter painted on a plastic substrate. Ag/AgCl ink from Dupont (5874 conductor) was used and this is called a “quasi Ag/AgCl reference” since its potential was modulated by the contact solution. To keep potentials consistent throughout this work, this electrode has been calibrated for each solution used against a standard Ag/AgCl.

Matrix assisted laser desorption ionisation-time-of-flight mass spectrometry (MALDI-TOF) detection was carried out in a stainless steel plate with a Voyager DE-STR from Applied Biosystems.

The electrochemical surface plasmon resonance (e-SPR) measurements were performed with double channel Autolab ESPRIT™ equipment from Eco Chemie. The e-SPR electrochemical cell is a two-electrode system, with a 4.8 mm^2 gold layer sensor disk working electrode that is defined when the cell is tightened. The 35 μL cell has platinum counter-reference electrode. The instrument can be programmed for automatic injection and washing steps.

4.2.3 Aptamer bioconjugation with ferrocene.

The sequence of the aptamer for thrombin (5'-CCAACGGTTGGTGTGGTTGG-3') was reported in the literature (Bock et al., Nature). Its synthesis was contracted to Qiagen (Germany) and was HPLC-purified. It contains a 5' nonamethylene disulphide and a 3' heptamethylene amino-spacer giving as final structure: (Disulfur-C₉-5'-CCAACGGTTGGTGTGGTTGG-3'-C₇-Amine). The aptamer solution was made at 1 mg mL⁻¹ with autoclaved milliQ water and stored at -20 °C. A freshly prepared solution of 125 nmol of N-hydroxysuccinimide ester (NHS) and 250 nmol of N,N'-dicyclohexylcarbodiimide (EDC) in anhydrous dimethylformamide were added to a solution of 100 nmol of ferrocene acetic acid in the same solvent. The final volume was 300 µL. The reaction mixture was stirred at room temperature under argon atmosphere until appearance of a precipitate. EDC forms an active ester functional group with carboxylate group using NHS. In this reaction is formed a precipitate of o-acylurea that was removed by centrifugation and the supernatant was added to 90 µL of 0.1 M sodium tetraborate buffer at pH 8.5 containing 10 nmol of the amino modified aptamer and it was left to react for 6 hours at room temperature. The active ester group in the presence of amine nucleophiles is attacked, the NHS group leaves as a precipitate, creating a stable amide linkage with the amine. The white precipitate was separated by centrifugation. The supernatant contained a disulphide-ferrocene-labelled aptamer. The disulphide bound was broken with 10 molar excess of dithiothreitol (DTT) to leave free a thiol group linked to the aptamer. The modified aptamer was purified with G-25 Sephadex column. UV Spectrophotometry was used to collect the appropriate fraction from the column. The product was characterised by UV spectrometry, cyclic voltammetry and MALDI-TOF.

UV spectrophotometry measurements were carried out using 1cm path-length quartz cuvettes. This technique was used to measure the absorbance at 265 nm of ferroceneacetic acid and the 260 nm of the oligonucleotide bases of the fractions eluted from the separation column.

Cyclic voltammetry of ferrocene-aptamer was performed in 10 mM Tris HCl buffer, 150 mM NaCl (pH 7.5) at 0.025 V s⁻¹ with a 18 mm² gold electrode and a Ag/AgCl quasi reference electrode.

MALDI-TOF characterisation was carried out using a 3-hydroxypicolinic acid (HPA) matrix. A 50 g L⁻¹ solution of 3-HPA in Milli-Q water and 50 g L⁻¹ solution of diammonium citrate were prepared and both reagents were combined in a ratio of 3-HPA : NH₄Citrate (9:1). The mixture was stirred for 1 minute and centrifuged to separate the white precipitate. The same volume of supernatant was mixed with ferrocene-aptamer, in a final concentration of 12 pmol μL⁻¹. 2 μL of the mixture was allowed to air-dry on a stainless steel plate. 20000V of accelerating voltage, 92% of grid voltage, 400 nseconds of extraction delay time, 1715 of laser intensity and 50 of shots were applied in a linear mode for the measurement.

4.2.4 Electrochemical detection of thrombin reaction product

- Colourimetric detection:

Streptavidin coated plates were incubated with 100 μL of 12 μg mL⁻¹ *biotin-aptamer* for 30 minutes at 25 °C. The plates were washed three times with 100 mM Tris-HCl pH 7.5, 150 mM NaCl and 1 % Tween (wash solution). The thrombin interaction was performed by incubating with 100 μL of 18 μg mL⁻¹ thrombin in 10 mM Tris-Ac for 1 hour at 37 °C. The thrombin-aptamer binding was followed by a washing step. Bound thrombin was detected by adding 50 μL of 5 mM thrombin chromogenic substrate allowing the reaction to proceed at 37 °C and following the formation of p-nitroaniline at 405 nm.

- Electrochemical detection:

A mixed self-assembled monolayer was used for the aptamer immobilisation on the gold electrode. The electrode was incubated for two hours at room temperature in 12 μg mL⁻¹ *thiol-aptamer* dissolved in 1 M KH₂PO₄. This was followed by an incubation in 1 mM mercaptoethanol for one hour at room temperature to displace the oligonucleotides that had randomly adsorbed onto the surface instead of through the thiol group and to block any free surface sites. Between incubation steps the electrodes were washed three times with wash solution for 5 minutes.

The aptamer modified electrodes were incubated in $18 \mu\text{g mL}^{-1}$ of thrombin in 10 mM Tris-Ac, 50 mM NaCl pH 7.5 for one hour at 37 °C.

Electrochemical measurements were recorded in the thin layer cell configured to contain a total volume of 20 μL . 5 mM of thrombin chromogenic substrate in 100 mM Tris-Ac, 50 mM NaCl pH7.5 was injected into the cell and a differential pulse polarography between -0.2 V and -1 V with a pulse height of -0.05 V and a pulse duration of 70 ms was recorded every 5 minutes for the 30 minute duration of the experiment.

4.2.5 Thrombin-aptamer binding assay using a sandwich format

The *thiol-aptamer* immobilisation and the subsequent interaction with thrombin were performed following the same steps detailed for the previous system. 65 μL of a pre-mixed solution containing $2 \mu\text{g mL}^{-1}$ streptavidin-horseradish peroxidase (SA-HRP) and $12 \mu\text{g mL}^{-1}$ *biotin-aptamer* was used to bind labelled aptamer at the second thrombin binding site. The incubation was done at 37 °C for 1 hour. Between steps the electrodes were washed with wash solution.

The interaction of aptamer-thrombin-aptamer was detected by chronoamperometry, using the thin layer cell. 13.3 μL of 0.5 mM mediator $[\text{Os}(\text{bpy})_2(\text{pyr-CH}_2\text{-NH}_2)]\text{Cl}$ in 50 mM citrate buffer, 0.2 M NaCl pH 6.5 were injected into the cell. A potential of -0.1 V vs. Ag/AgCl was applied for 100 seconds. The cell was switched off, and 6 mM H_2O_2 solution was added to the cell. The reaction was allowed to proceed 5 minutes before the reapplication of the -0.1 V potential and the amperometric monitoring of the response.

4.2.6 Thrombin immobilisation on electrode surface for its detection in an aptasensor

Modification of the gold electrode was necessary for the immobilisation of thrombin on the surface. To activate the surface the gold electrodes were immersed in 65 μL of 1 mM mercaptoethanol in 1 M KH_2PO_4 for 1 hour at room temperature. The thrombin was immobilised by incubation in an 18 $\mu\text{g mL}^{-1}$ of thrombin buffer solution (10 mM Tris-Ac, 50mM NaCl pH 7.5) for one hour at 37 °C. A blocking step was necessary to avoid non-specific adsorption of other biomolecules. This was accomplished by incubation in a 1% bovine serum albumin (BSA) solution for one hour at 37 °C. The thrombin bound on the surface was detected with a pre-mixed solution of 2 $\mu\text{g mL}^{-1}$ streptavidin-HRP and 12 $\mu\text{g mL}^{-1}$ *biotin-aptamer* which was incubated with the electrode for one hour at 37 °C. Between incubation steps the electrodes were washed with wash solution. The same protocol explained in the previous assay was followed for the chronoamperometric detection of *HRP-aptamer* bound with thrombin.

4.2.7 Electrochemical aptabeacon

- Electrochemical experiments

A self-assembled monolayer was used for the aptamer immobilisation on the gold electrode. The electrode was incubated for two hours at room temperature in 0.25 $\mu\text{g mL}^{-1}$ *thiol-aptamer-ferrocen* dissolved in 1 M NaH_2PO_4 . The aptamer modified electrodes were incubated in 18 $\mu\text{g mL}^{-1}$ of thrombin in 10 mM Tris-Ac, 50 mM NaCl pH 7.5 for one hour at 37 °C.

Cyclic voltamperometry was recorded in 50 mM citrate buffer pH 6.5, 100 mM NaCl, before and after the addition of thrombin (0.05 V s^{-1} , between -0.05 V to 0.050 V , vs. Ag/AgCl). Two-electrode system with a 18 mm^2 square bio-modified gold sheet as a working electrode opposite to a solid state Ag/AgCl reference/counter painted on a plastic substrate was used. The thin layer cell configured to contain a total volume of 20 μL was employed for these experiments.

- e-SPR experiments

In the e-SPR experiments, 35 μL of 10 mM HEPES, 50 mM NaCl pH 8 was added into the cell to set the baseline, 0.25 $\mu\text{g mL}^{-1}$ of *thiol-aptamer-ferrocen* in 1 M NaH_2PO_4 was immobilised for one hour on the gold coated glass surface. The interaction with thrombin was performed with incubation of 18 $\mu\text{g mL}^{-1}$ thrombin in 50 mM citrate buffer pH 6.5, 100 mM NaCl during 20 minutes. Regeneration of thrombin was carried out with three incubations of 100 mM glycine, 150 mM HCl for 15 minutes each. As a control, 2.5 μM of BSA in 50 mM citrate buffer pH 5, 100 mM NaCl was injected under the same conditions as the thrombin. After each immobilisation a cyclic voltammogram was recorded with a scan rate of 0.01 V s^{-1} between -0.2 V and 0.2 V (vs. platinum). The e-SPR electrochemical cell is a two-electrode system, with a 4.8 mm^2 gold layer sensor disk working electrode that is defined when the cell is tightened. The 35 μL cell has a platinum reference-counter electrode.

4.2.8 Chronoamperometric aptabeacon

- Electrochemical experiments

18 mm^2 square gold electrodes were modified with a mixed self-assembled monolayer exposing it to 0.25 $\mu\text{g mL}^{-1}$ of *thiol-aptamer-ferrocene* in 1 M NaH_2PO_4 and 160 μM MP-11. Then the interaction with the different concentrations of thrombin or BSA in the case of controls was performed in 50 mM citrate buffer pH 5, 100 mM NaCl was detected by cyclic voltammetry (scan rate of 0.01 V s^{-1} , scan between -0.3 V and 0.4 V) and chronoamperometry -0.1 V was applied in a solution of 1 mM H_2O_2 in 50 mM citrate buffer pH 6.5, 100 mM NaCl, after 100 seconds different concentrations of thrombin or BSA (control) was added. The interaction was detected in real time.

- **e-SPR experiments**

35 μL of 10 mM HEPES, 50 mM NaCl pH 8 was added into the cell to set the baseline, a mixture of 0.25 $\mu\text{g mL}^{-1}$ of *thiol-aptamer-ferrocene* in 1 M NaH_2PO_4 and 160 μM MP-11 was immobilised for one hour on the gold chips. 35 μL of thrombin concentrations between (270 nM to 34.5 fM) in 50 mM citrate buffer pH 6.5, 100 mM NaCl were incubated with the sensor for 1 hour at 25 °C. The same concentrations BSA under the same conditions to qualify non-specific response were also injected. The excess of thrombin or BSA incubated with the mixed monolayer of the redox-labelled aptamer and MP-11 was subsequently washed.

After SPR detection the same interaction was detected electrochemically on the same gold chip used as working electrode and with a platinum wire used as counter-reference electrode. Two electrochemical techniques were used to detect this interaction, impedance spectroscopy and chronoamperometry.

Impedance measurements were carried out in 50 mM citrate buffer pH 6.5, 100 mM NaCl using a frequency sweep between 50 MHz and 0.1 Hz, and a sinusoidal ac potential perturbation of 0.005 V.

The same electrochemical cell used for impedance measurements was used for chronoamperometry detection. 35 μL of 50 mM citrate buffer pH 6.5, 100 mM NaCl was added into the cell, a potential of -0.1 V *versus* Ag/AgCl was applied and when the base line was stabilised (at 100 seconds), 1 mM H_2O_2 was injected into the electrochemical cell. The response could be observed at 20 seconds but the current obtained after the first steady state at 150 seconds after the H_2O_2 injection was more recorded.

4.3 Results and Discussion

4.3.1 Aptamer bioconjugation with ferrocene

After the conjugation of the disulphide-amine-labelled-aptamer ($MW=6837 \text{ g mol}^{-1}$) with EDC ($MW=155 \text{ g mol}^{-1}$), NHS ($MW=115 \text{ g mol}^{-1}$), DTT ($MW=154 \text{ g mol}^{-1}$) and ferrocenacetic acid ($MW=244 \text{ g mol}^{-1}$) to obtain a thiol-ferrocene-labelled aptamer ($MW=7063 \text{ g mol}^{-1}$), the excess of reagents were separated. Due to a 10 fold excess of ferrocenacetic acid, it is assumed that all aptamer was modified entire. The rest of reagents were separated from the thiol-ferrocene-labelled aptamer by size exclusion chromatography with a G-25 Sephadex column. The components were separated in two major groups according to the size range, thiol-ferrocene-labelled aptamer was eluted first and next the low molecular weight molecules (EDC, NHS, DTT and ferrocenacetic acid).

UV Spectrophotometry was used to collect the appropriate fraction from the column. The fraction collected combined the ferrocenacetic acid moiety absorbance as a broad peak at 265 nm and the 260 nm peak of the oligonucleotide bases. Figure 4.1 shows the elution profile of the reaction mixture. Good peak resolution was observed showing the separation between ferrocenacetic acid and ferrocene-aptamer.

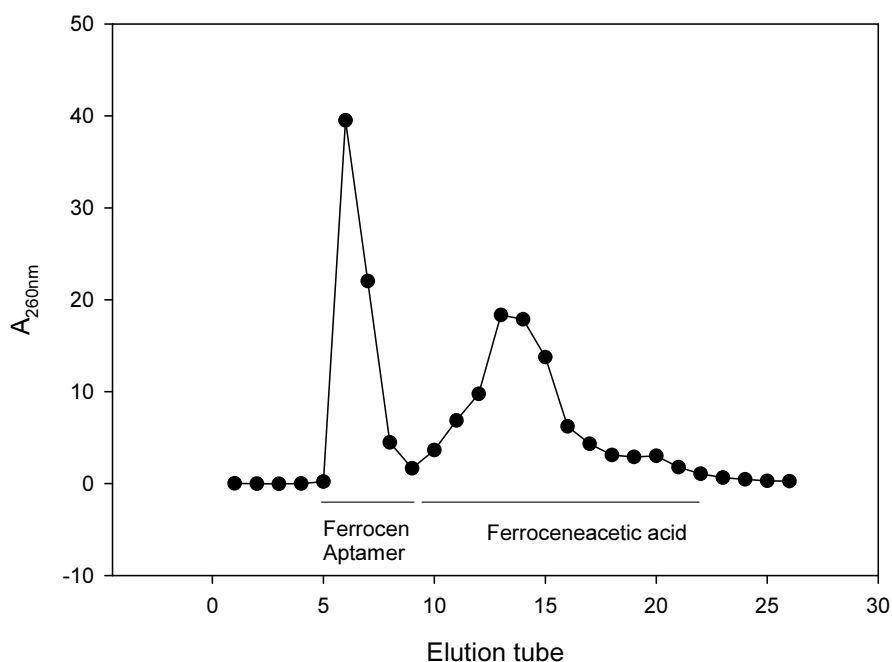


Figure 4. 1. Elution profile monitored spectrophotometrically at 260 nm of the reaction mixture to prepare thiol-ferrocene aptamer. A G25 size exclusion chromatography columns was used.

Cyclic voltammetry verified that the product had an apparent redox potential of about 0.1 V vs. the Ag/AgCl reference used (Figure 4.2). This potential, which was negatively shifted from the one of the starting ferroceneacetic acid as expected from the reaction of the carboxylic group, agreed well with the 0.09 V redox potential reported by Brazil and Kuhr, 2002, authors who describe a synthesis procedure most closely resembling the one followed here. In this work it is therefore assumed that the above characteristic values indicate the successful synthesis of the redox-modified aptamer.

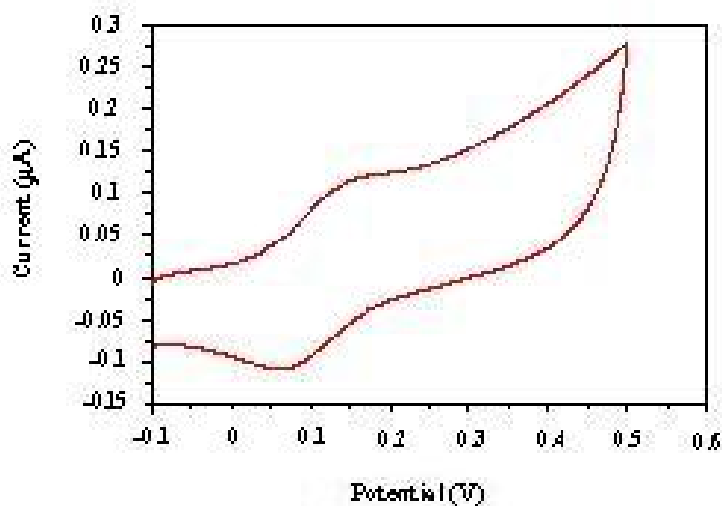


Figure 4. 2. Cyclic voltammetry of aptamer-ferrocene at 0.025 V s^{-1} scanned between -0.1 and 0.5 V in 10 mM Tris HCl buffer, 150 mM NaCl (pH 7.5).

MALDI-TOF detection confirmed that ferrocene molecule was attached to the aptamer and is shown in Figure 4.3.

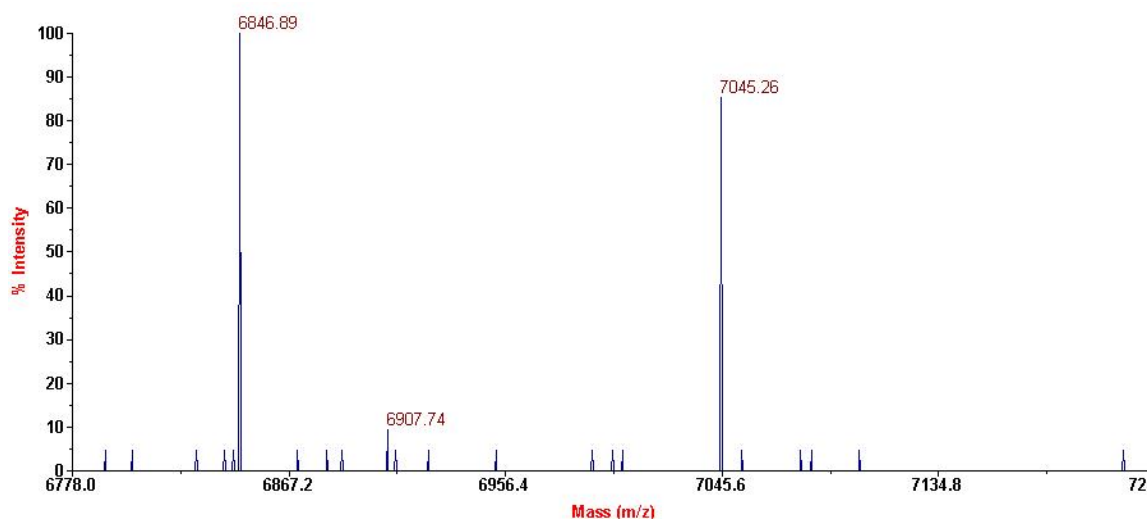


Figure 4. 3. MALDI-TOF spectrum of aptamer-ferrocene product. Detection was carried out at 20000V of accelerating voltage, 92% of grid voltage, 400 nseconds of extraction delay time, 1715 of laser intensity and 50 of shots in a linear mode.

4.3.2 Electrochemical detection of thrombin reaction product

α -human thrombin is a highly specific serine protease that catalyses the hydrolysis of the thrombin chromogenic substrate, β -Ala-Gly-Arg-p-nitroaniline producing p-nitroaniline. The rate of yellow coloured p-nitroaniline formation can be followed by its UV adsorption at 405 nm, or electrochemically by the reduction of its nitro group. When saturated by enzyme substrate the formation rate of p-nitroaniline is proportional to the enzyme concentration.

In the basic ELONA configuration biotin-aptamer was immobilised on a streptavidin plate and incubated with thrombin. The bound thrombin was detected by incubation with the chromogenic substrate. A slow response was obtained from the colourimetric detection of thrombin by ELONA. After one hour of incubation it was impossible to differentiate the background (controls; without thrombin addition and without biotin-aptamer incubation) from the aptamer-thrombin signal (sample). After three hours of incubation a signal only 20% greater than the background was detected. 24 hour incubation was necessary to clearly differentiate between controls and sample (Figure 4.4).

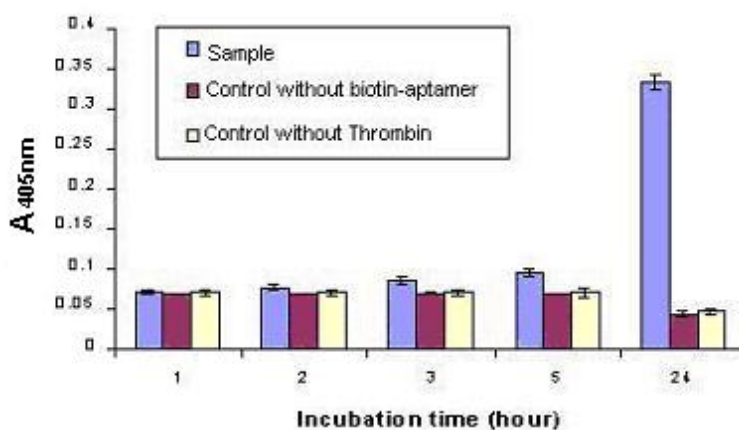


Figure 4. 4. Colourimetric detection (ELONA) of thrombin bound with *biotin-aptamer* through a chromogenic thrombin substrate. Thrombin substrate was incubated at different times and controls without *biotin-aptamer* and without thrombin were carried out. Response obtained spectrophotometrically at 405 nm. ELONA plate was modified with $12 \mu\text{g mL}^{-1}$ of *biotin-aptamer* and $18 \mu\text{g mL}^{-1}$ of thrombin, the interaction was detected with 5 mM of thrombin substrate.

However when a similar approach was used to detect colourimetrically the thrombin-aptamer complex in a homogeneous solution format, instead of immobilised on a plate a response was obtained in a little over 30 minutes (Liu et al., 2002). The Fibrinogen exosite is important for thrombin recognition of substrates, cofactors and inhibitors (Padmanabhan et al., 1993). The different response between the surface immobilised thrombin-aptamer and the homogeneous solution thrombin-aptamer complex is probably due to blocking of the substrates access to the fibrinogen exosite by the solid support, or simply due to less amount of immobilised thrombin

Since both the substrate and the p-nitroaniline released during hydrolysis have different redox potentials they can be detected by differential pulse voltammetry (DPV) (Heiduschka and Dittrich, 1990). β -Ala-Gly-Arg-p-nitroaniline and p-nitroaniline solutions were measured separately by DPV. The polarographic peaks potential for the free and the peptide bound p-nitroaniline at pH 7.5 is -0.77 V and -0.55 V vs. Ag/AgCl respectively. Different concentrations (0 μ M, 86 μ M, 107 μ M, 128 μ M, 150 μ M) of each solution was detected. At the same concentration the current obtained from the p-nitroaniline was 2.5 times higher than the substrate current peak, owing to the adsorption of the peptide (β -Ala-Gly-Arg-p-nitroaniline) on the electrode surface (Heiduschka and Dittrich, 1990), which produces a decrease in the diffusion constant with a consequent decrease of current (Figure 4.5).

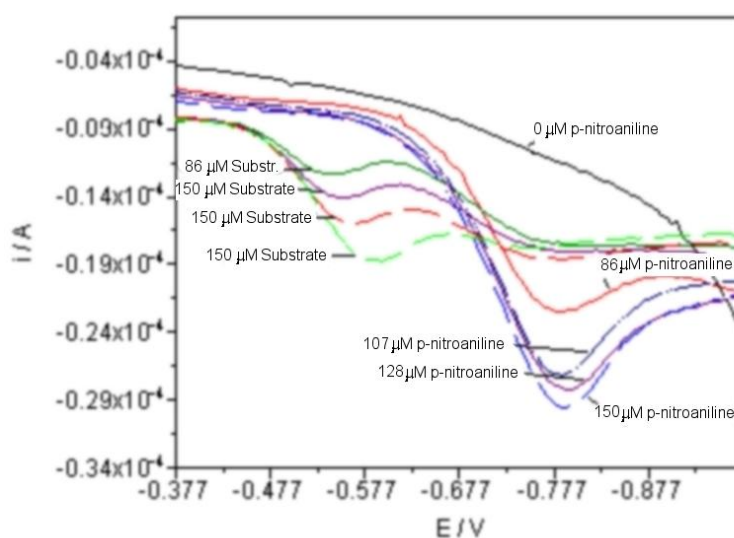


Figure 4. 5. DPV of thrombin product and substrate between -0.2 V and -1 V with a pulse height of -0.05 V and pulse duration of 70 ms. (A) Different concentrations ($0\mu\text{M}$, $86\mu\text{M}$, $107\mu\text{M}$, $128\mu\text{M}$, $150\mu\text{M}$) of thrombin substrate ($\beta\text{-Ala-Gly-Arg-p-nitroaniline}$) in solution (peak at 0.5 V) and different concentrations of p-nitroaniline (not produced by catalytic reaction) (peak at 0.7 V) was detected. Electrochemical detection was carried out in a 5 mL electrochemical cell with a Ag/AgCl reference, gold working electrode and a stainless steel counter electrode

In the electrochemical format thiol-aptamer immobilised on gold working electrode binds thrombin during an incubation step. The bound thrombin was detected by quantification of p-nitroaniline produced by the thrombin. The DPV experiments showed a current peak at -0.45 V in the presence of the thrombin substrate. After 5 minutes the peak at -0.45 V decreased and a new peak was detected at -0.70 V indicating the formation of p-nitroaniline. The same measurements carried out on a control electrode where BSA was substituted for thrombin, showed only a peak at 0.45 V. The electrochemical measurement were carried out in a $20\ \mu\text{l}$ cell using a system with two electrodes, a plastic substrate painted with Ag/AgCl ink was utilised as reference-counter electrode. The potentials of substrate and p-nitroaniline were shifted 0.1V in the negative direction comparing with the obtained with the p-nitroaniline and substrate detection in solution, however the detection of the p-nitroaniline and substrate in solution was carried out in a three-electrodes cell with a Ag/AgCl KCl saturated reference electrode and detection of p-nitroaniline produced in an immobilised aptamer-thrombin complex was carried out in a two-electrode cell set-up using a solid state Ag/AgCl reference/counter painted on a plastic substrate. (Figure 4.6)

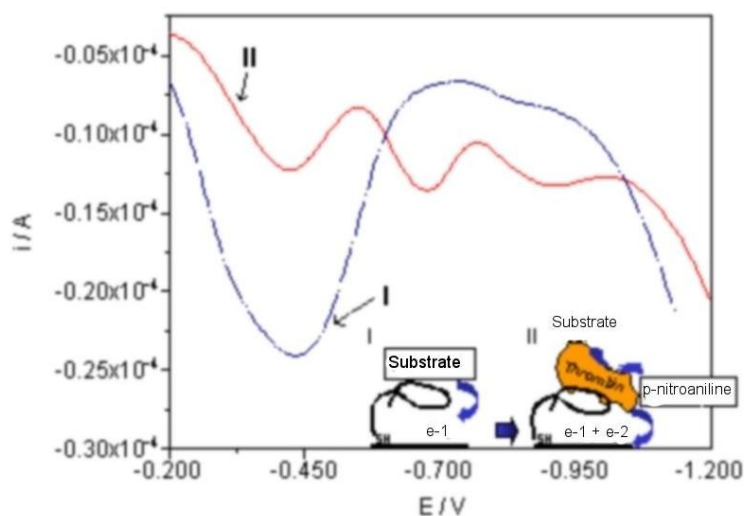


Figure 4. 6. DPV run under the same conditions of Figure 4.5. Thiol-aptamer-thrombin modified gold electrode was used in a 20 μL cell with a two electrodes system using a plastic substrate painted with Ag/AgCl ink as reference-counter electrode. (II) After 5 minutes of thrombin substrate injection and (I) control with BSA instead of thrombin.

Figure 4.7, shows the response average of the aptasensors with thrombin and with BSA as control after 5 minutes of thrombin substrate incubation. This figure shows the peak current of thrombin substrate at 0.45 V and the peak current of the product from thrombin catalysis at -0.7 V. From the system with BSA no consumption of substrate was observed and no current was detected at -0.7 V, in contrast to the system with thrombin attached to aptamer where a current of 3.15 μA at -0.7 V and a decrease of 77 % of peak current from the substrate at 0.45 V were detected.

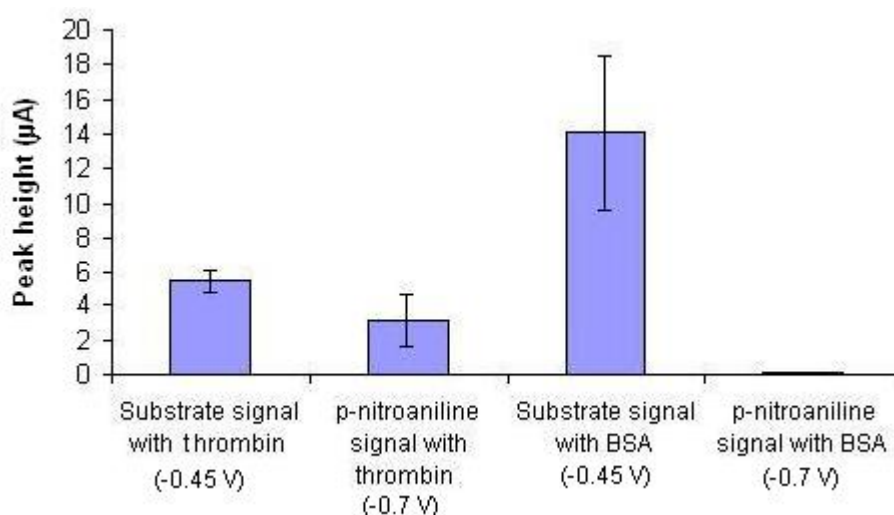


Figure 4. 7. DPV detection of thrombin substrate and p-nitroaniline produced from the thrombin catalysis after 5 minutes of substrate incubation in the aptamer-based sensor. The electrochemical measurements reported are the peak currents, measure in the same conditions as explained in figure 4.5.

A calibration graph was plotted with the curves shown in Figure 4.5. Interpolating the peak height obtained with the product of the thrombin catalysis and from the thrombin substrate, was calculated the concentration of product generated and the concentration of substrate consumed. An average of 38 μM of substrate was hydrolysed by thrombin and a similar value of 24 μM of p-nitroaniline was produced in the same reaction.

Differential pulse voltammetry was recorded for different times of thrombin substrate incubation. Figure 4.8, shows the current decreasing tendency of the thrombin substrate peak currents for the aptasensor exposed to thrombin as function of time, while the control with BSA shows a constant current in time.

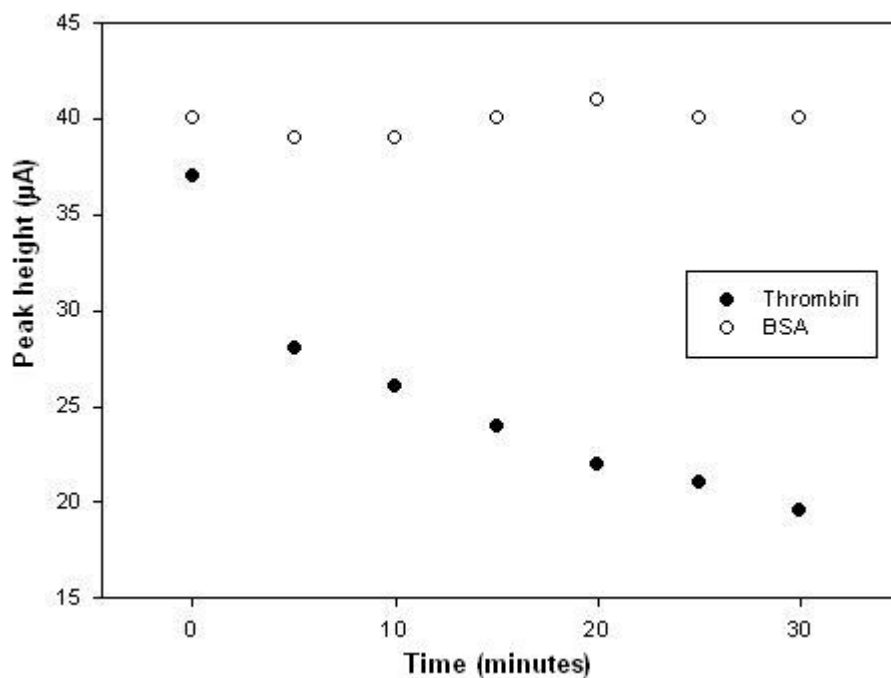


Figure 4. 8. Variation of the substrate peak current as a function of time during the hydrolysis of the substrate by thrombin detected in the aptamer-based sensor and measured by differential pulse voltammetry following the same conditions as explained in figure 4.5.

The peak current obtained in differential pulse voltamperometry is directly proportional to the concentration of the analyte measured. The following equation relates these values: (Equation 4.1)

$$i_p = \frac{nFAD^{1/2}C}{\sqrt{\pi t_m}} \left(\frac{1 - \sigma}{1 + \sigma} \right)$$

Where i_p is the current, n the number of electrons transferred, which in this reaction is equal to 4, F is the faraday constant (96485 C mol^{-1}), A is the electrode area (0.018

cm²), D is the diffusion coefficient (for a similar molecule, 3,5 dinitrobenzoate in aqueous solution at 25 °C diffusion coefficient is equal to $0.754 \times 10^{-5} \text{ cm}^2 \text{ sec}^{-1}$, (Lide, 2005)), C is the analyte concentration, t_m is the transition time (0.07 seconds), and $\sigma = \exp(nF/RT)(\Delta E/2)$ where ΔE is the pulse amplitude (0.05V), R is the gas constant (8.3 J mol K⁻¹), and T is the temperature (273 K).

110 μM of thrombin substrate concentration was used for the experiments, which is equivalent to a theoretical current of 85 μA, while the experimental current obtained from this reagent at the same concentration was 23 μA.

An important reduction in the assay time from 3 hours to 5 minutes was demonstrated on going from an optical to an electrochemical measurement. Electrochemistry is inherently surface associated techniques while the optical detection is dependent on detection of the reaction product in the bulk of the sample. For this reason it was possible to reduce assay time.

4.3.3 Thrombin-aptamer binding assay using a sandwich format

Human α-thrombin X-ray structure data (Rydell et al., 1990) (Figure 4. 9) reveals a protein with multiple functional regions. In addition to the active site and the adjacent hydrophobic site (the apolar binding site), there are two electropositive exosites. The fibrinogen-recognition exosite at the base of the active-site cleft consists of Arginine 73, Arginine 75 and Arginine 77. It can bind with the wide groove formed by the TGT loop of the aptamer. The second exosite is a more strongly electropositive heparin-binding domain composed of Arginine 126, Lysine 236, Lysine 240 and Arginine 93. It can bind the two narrow grooves formed by two loops of TT bases. The thrombin's multiple binding sites allow it to be detected by a sandwich assay.

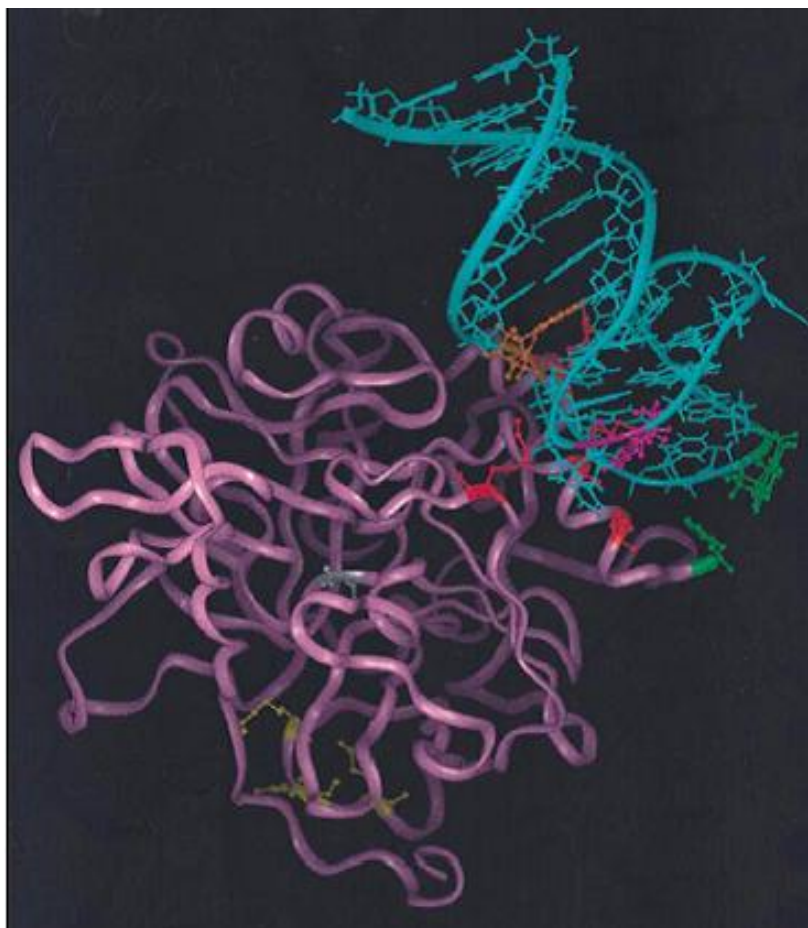
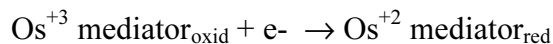
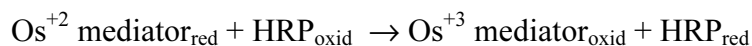
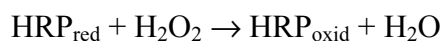


Figure 4. 9. The interaction between aptamer and thrombin is illustrated in this image (Rydel et al., 1990). α -human thrombin, shown in purple, the orientation is toward the active site cleft with the active site Ser is shown in white. The strongest positive electrostatic field is observed for the heparin-binding exosite on the top of the molecule (shown in red). The second surface region of high positive charge is shown in yellow. The diagram of the anti-thrombin aptamer, shown in turquoise, is positioned such that nucleotide T12 (green) in the second loop of the G-quadruplex can establish a contact with Phe245 (green) of thrombin. The A at position 4 of the G-quadruplex (pink) which plays a role in determining the binding site of this DNA and the first G of the strand (orange) which contributes to high-affinity binding are shown directed toward the positive charged residues (red) of the heparin-binding exosite.

To complete the sandwich assay a second aptamer bearing HRP, was incubated with previously bound thrombin. HRP is readily detected electrochemically through its enzymatic reaction. HRP catalyses the non-specific oxidation of a variety of species using H_2O_2 as oxidising agent. Previously the use of an efficient mediator and the addition of H_2O_2 allowed electrochemical detection of peroxidase through the electrocatalytic reaction (Katakis and Heller, 1992; Vreeke et al., 1995; Vreeke et al., 1992)



Different strategies to incubate thrombin and the second aptamer with the first immobilised aptamer were attempted. Separated 1 hour incubation steps for thrombin, biotin-aptamer and SA-HRP were carried out at 37 °C. Doing three separate incubations gives an increase of chronoamperometric signal from the control without thrombin, because of a higher non-specific adsorption of SA-HRP. A pre-incubation of thrombin, biotin-aptamer and SA-HRP in a tube for 1 hour at 37 °C with the subsequent interaction of the pre-incubated mixture with the immobilised aptamer was tested. In this case, a decrease of sample signal was obtained. The reason could be that thrombin was already bound with the second aptamer-HRP, which produced a decrease of binding sites combined with steric impediment for thrombin to bind with the immobilised aptamer. Higher sample response and a decrease of the controls response was obtained with a pre-incubation of biotin-aptamer and SA-HRP for 1 hour at 37 °C. Thrombin was incubated with the immobilised aptamer for 1 hour at 37 °C, and subsequent the pre-incubated mixture of biotin aptamer and SA-HRP was incubated 1 hour at 37 °C with the immobilised aptamer-thrombin.

A control without mercaptoethanol incubation was made however a reduction of sample signal was obtained without blocking layer. The monolayer of mercaptoethanol plays an important role in the correct thiol-aptamer immobilisation displacing the aptamer that was immobilised on gold surface through the amino groups instead of the thiol groups and also blocking the rest of the gold surface that was not occupied by the aptamer (Levichy et al., 1998).

Optimisation of incubation temperature and time of thrombin and biotin-aptamer-HRP interaction was carried out. The increase of temperature in the interaction between thrombin and biotin-aptamer-HRP negatively affects the non-specific binding of SA-HRP, nevertheless a decrease in the incubation time reduces this problem.

The catalytic current achieved for the optimised configuration of aptamer-thrombin-aptamer interaction was 4.5 μA . Negative controls were carried out to verify that the observed signal was not due to non-specific adsorption. A negative controls without the base aptamer immobilised on the electrode surface resulted in a 1.8 μA catalytic current and the same current was obtained from the control with thrombin, however it had lower reproducibility. A third negative control, this one without HRP labelled aptamer, resulted in a 0.2 μA current (Figure 4.10).

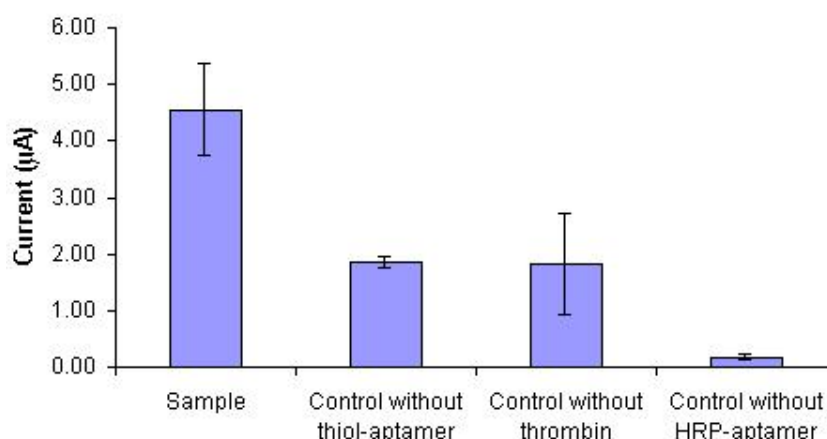


Figure 4. 10 Amperometric detection of thrombin through a sandwich format. The electrochemical measurement reported is the difference in current at -0.1 V (vs. Ag/AgCl) before and after addition of 6 mM H_2O_2 . Electrode was modified with 12 $\mu\text{g mL}^{-1}$ of *biotin-aptamer*, 18 $\mu\text{g mL}^{-1}$ of thrombin and 12 $\mu\text{g mL}^{-1}$ of the second *biotin-aptamer* pre-incubated with 2 mg mL^{-1} of SA-HRP,. (n = 5)

While the assay as designed suffered from significant non-specific adsorption of HRP labelled aptamer, the limit of detection for this system was still 92 ± 0.4 nM (Figure 4.11). To measure the limit of detection the non-quantifiable or saturated points were discarded and the values that have a linear response were fitted in a linear regression line. The standard deviation of the line was measured and multiplied by 3, in order to reduce the probability of a false non-detection to 5 %. This value was added to the signal value distinguishable from noise response.

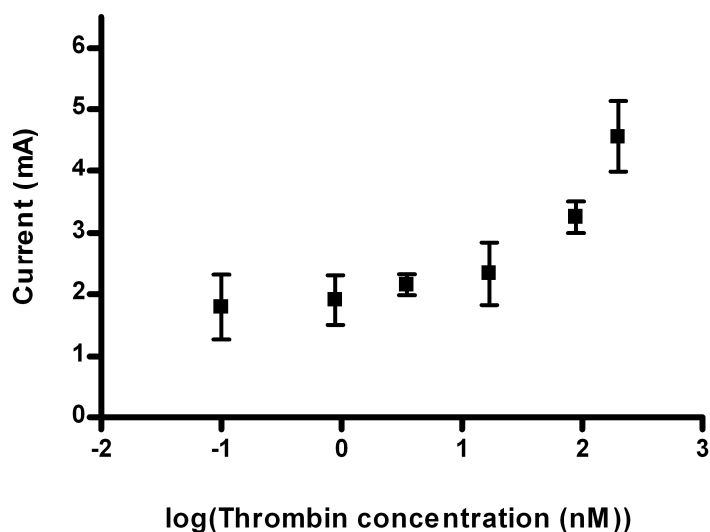


Figure 4.11 Chronoamperometric response of different concentration of thrombin in a sandwich format. Conditions as explained in Figure 4.10.

4.3.4 Thrombin adsorption on electrode surface for its detection in an aptasensor

The direct adsorption of thrombin on bare gold electrodes, mercaptoethanol modified gold electrodes and polystyrene surface (ELONA plates) was tested. Thrombin was only detected on the mercapto treated surface and was not detectable on the unmodified surfaces. Gold, polystyrene and gold modified with mercaptoethanol have a respective positive, neutral and negative charge. It is likely that the negatively charged gold surface interacted through hydrogen bonds or van der Waals interactions with the electropositive binding site of thrombin. However, it is also possible that on the other surfaces the adsorption position of thrombin created steric impediments preventing subsequent aptamer binding. Alternatively thrombin might have denatured and lost its aptamer binding capability.

The first electrochemical assays of thrombin immobilised on the surface showed large amperometric currents, 23 μA . However these experiments were performed without the benefit of a blocking agent. In fact, the non-specific adsorption of aptamer-HRP showed an even higher signal, 37.6 μA . Different blocking agents, ($1 \mu\text{g mL}^{-1}$ DNA

salmon testes, 1% tween, 5% powdered milk, and 1% BSA), incubation times for aptamer-HRP conjugation (10, 30, 45, 60 minutes) and concentrations of streptavidin-HRP ($2 \mu\text{g mL}^{-1}$, $1 \mu\text{g mL}^{-1}$, $0.5 \mu\text{g mL}^{-1}$) were tested to avoid the non-specific binding of aptamer-HRP on the electrode surface. BSA was the only blocking that shows higher response from the sample than from the control without thrombin. (Figure 4.12)

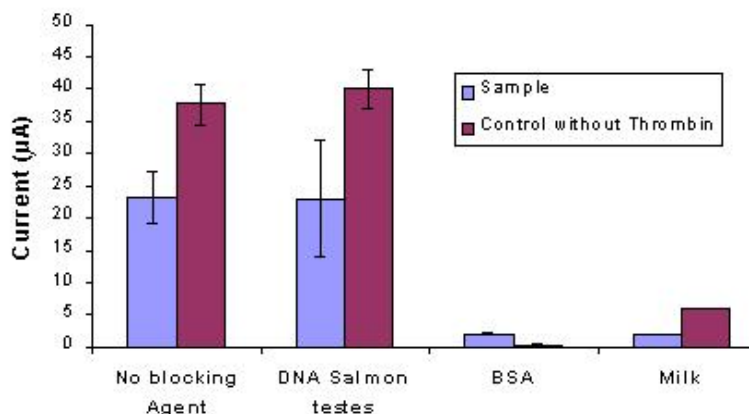


Figure 4. 12 Chronoamperometric response of aptamer-HRP interacted with thrombin immobilised on modified gold (18 nm^2). Test of different blocking agent to reduce the non-specific adsorption of aptamer-HRP. Chronoamperometric response was the difference in current at -0.1 V (vs. Ag/AgCl) before and after addition of $6 \text{ mM H}_2\text{O}_2$. ($n = 5$)

Incorporating the blocking step in the protocol, the concentration of SA-HRP was optimised. Higher concentration of SA-HRP produced more or less the same average response than lower SA-HRP concentration but caused high irreproducibility in the response.

The effect of the duration of aptamer-HRP incubation was also optimised. As shown in figure 4.13 at short incubation times the non-specific adsorption of aptamer-HRP is higher. An incubation of 60 minutes is necessary to assure a clear difference between the sample and the control.

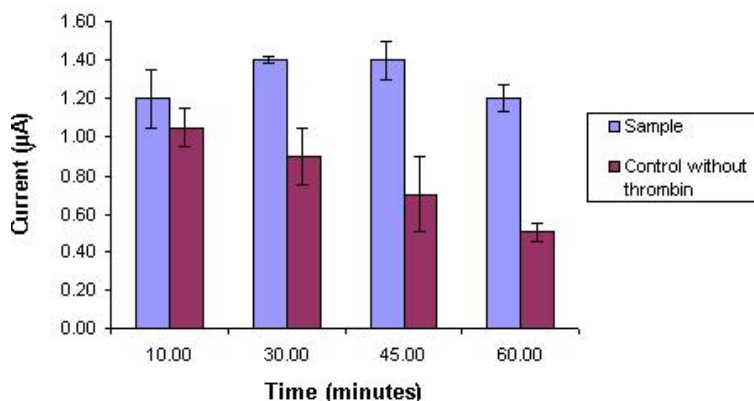


Figure 4.13. Test of different incubation times of aptamer-HRP with thrombin adsorbed on the modified gold surface. Experimental conditions as in figure 4.12.

The best results were achieved with 1% BSA and incubation for 60 minutes in a mixture of $2 \mu\text{g mL}^{-1}$ streptavidin-HRP and $12 \mu\text{g mL}^{-1}$ biotin-aptamer. Under these conditions the catalytic current was $1.2 \mu\text{A}$. The controls without thrombin, without aptamer-HRP and without surface modification were $0.5 \mu\text{A}$, $0.12 \mu\text{A}$ and $0.1 \mu\text{A}$ respectively. (Figure 4.14)

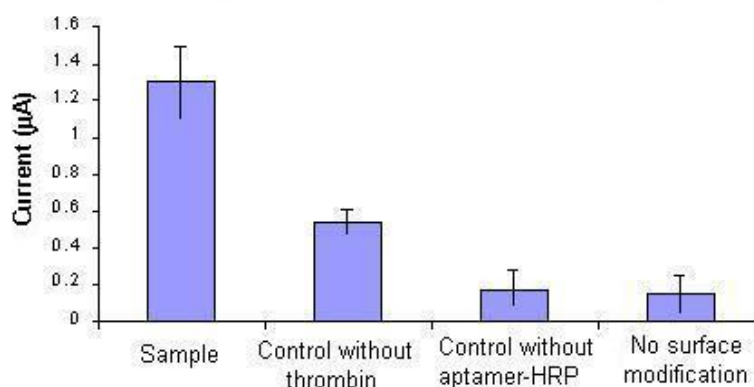


Figure 4.14. Amperometric detection of aptamer-HRP interacted with thrombin adsorbed on the gold modified surface. The electrochemical measurement reported is the difference in current at -0.1 V (vs. Ag/AgCl) before and after addition of $6 \text{ mM H}_2\text{O}_2$. Electrode was modified with $18 \mu\text{g mL}^{-1}$ of thrombin and $12 \mu\text{g mL}^{-1}$ of *biotin-aptamer* pre-incubated with 2 mg mL^{-1} of SA-HRP. ($n = 5$)

Again the assay was limited by non-specific adsorption. The limit of detection for this configuration was calculated as explained in 4.3.3 and was $2.75 \pm 0.3 \text{ nM}$ (Figure 4.15), which might allow use in cases of detection of metastasis of lung cancer.

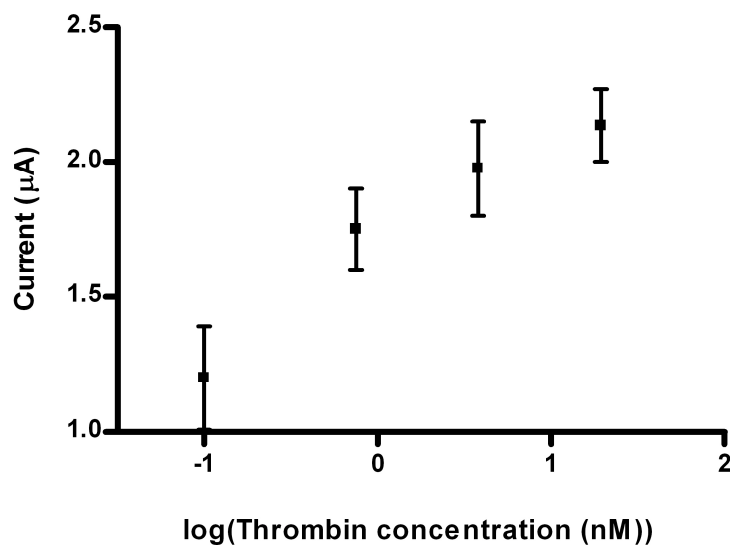


Figure 4. 15. Chronoamperometric response of different concentration of thrombin immobilised on electrode surface and detected with specific aptamer. Experimental conditions as explained in Figure 4.14.

This configuration is based on the capacity of thrombin to be adsorbed on the electrode surface even when present at low concentrations. Most of the non-specific signal was obtained as a result of the non-specific interaction of the aptamer with the surface, which was avoided by an appropriate blocking agent. Since a wash step is incorporated between aptamer interaction and detection, electrochemical interference in blood or plasma should not cause significant problems in the application of this technique. However it should be examined if thrombin can be successfully adsorbed on the electrode in the presence of other blood proteins.

4.3.5 Electrochemical aptabeacon

The anti-thrombin aptamers has a well studied change of conformation when it is bound with thrombin. When binding occurs anti-thrombin aptamers are folded in a G-quadruplex structure with a central part of the structure formed by two guanine quartets (Padmanabhan et al, 1993) (Figure 4.16)

protein immobilised ($120 \text{ m}^{\circ} = 1 \text{ ng of protein mm}^{-2}$) (User manual for Autolab SPIRIT, 2003). However this relationship has limits of application, because on the lower side the smallest assumed hydrodynamic radius of protein that can produce a change (the manufacturer calculates this to correspond to a protein with molecular weight of 5000 g mol^{-1}) and on the upper side the penetration depth of the evanescent wave which they calculate to be 300-400 nm. Obviously, in our calculations we have assumed additionally that molecular weight is directly proportional to biomolecule size and that the same relationship holds true for our redox-modified thiolated aptamer. Still, after seeing the results of the calculation we thought it was interesting to mention them since they gave a reasonable correlation with what we assume is the architecture built on the surface of the e-SPR disc. We must caution however that especially in the case of the aptamer, we have been also working at the limit of size that the manufacturer assumes is the lowest limit of detection of the instrument (5000 g mol^{-1}).

The immobilisation of the redox labelled aptamer was simultaneously evidenced by cyclic voltammetry at a scan rate of 0.01 V s^{-1} , as shown in inset (a) of Figure 4.17. A faint signal is obtained probably due to the fact that some of the redox aptamer is flatly lying on the electrode surface or simply by statistical approach of the unfolded form of the aptamer to the surface. Using next equation, CV peaks were integrated to obtain the charge passed, which showed apparent surface coverage of $2.6 \times 10^{-14} \text{ mol mm}^{-2}$.

$$Q = nFA\Gamma \quad (\text{Equation 4.2})$$

Where Q is the charge, n is the number of electrons produced in the redox reaction, A is the electrode area, F is the Faraday constant (96485 C mol^{-1}) and Γ is the surface coverage.

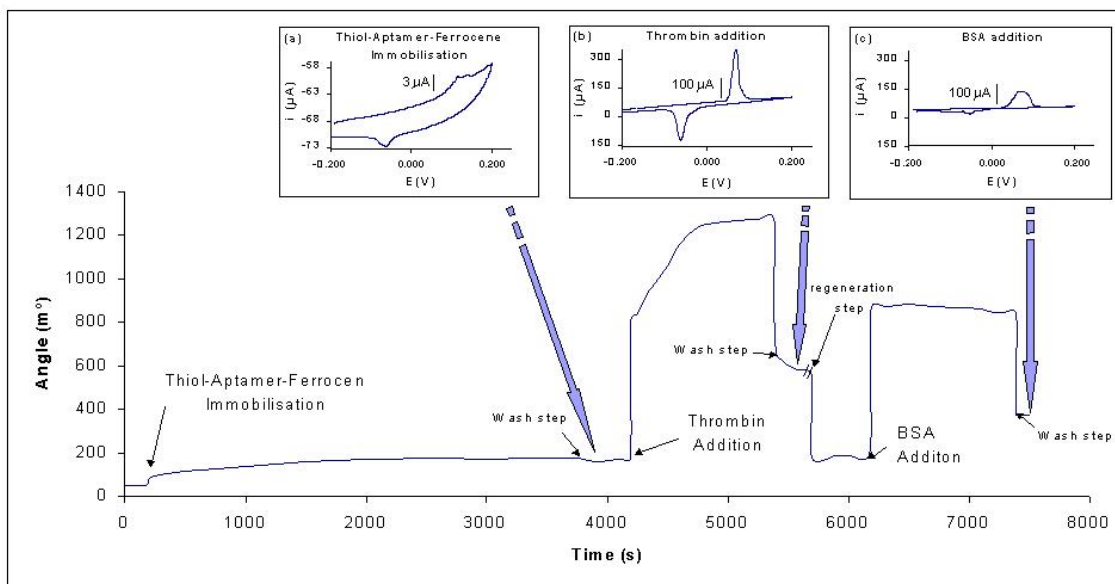


Figure 4. 17. e-SPR-ogram of the aptasensor demonstration. In the insets in situ cyclic voltammetry of e-SPR disc at points indicated by the arrows, CV was carried out at scan rate of 0.05 V s^{-1} , between -0.2 and 0.2 V .

In a second step, the aptamer-modified disc was exposed to $2.5 \mu\text{M}$ of thrombin in 50 mM citrate buffer pH 5, 100 mM NaCl for 20 minutes. As shown in Figure 4.17, after the washing step, a residual 415 m° shift is observed in the reflectance angle which corresponds to $9.3 \times 10^{-14} \text{ mol mm}^{-2}$ of thrombin remaining attached to the aptasensor. This would correspond to 72% of the sites capturing the target thrombin at this high concentration. Simultaneous voltammetry of the resulting molecular architecture revealed an almost 200-fold increase in peak current. This indicates that the ferrocene labelled aptamer's conformation has changed to bring the ferrocene in close proximity to the electrode surface as is shown in the inset (b) of Figure 4.17. Now, cyclic voltammetry at different scan rates was more consistent with a surface wave although the unusual peak to peak separation indicates strong and probably different interactions of the reduced and oxidised species or a strong ion exclusion effect as suggested in Radi et al., 2006. Integration of the charge showed an apparent surface coverage of $9.5 \times 10^{-13} \text{ mol mm}^{-2}$, which is close (within an order of magnitude) to the approximate empirical calculation mentioned.

These results demonstrate a strong 3-D change that is dependent upon target recognition, and corroborate that said change can be detected by cyclic voltammetry. It should be noted that the electrochemical signal increase upon the recognition event

appears to provide higher sensitivity than SPR. BSA was used as a non-specific target under the same conditions (2.5 μM for 20 minutes, in the same buffer as for the thrombin interaction). The residual reflectance angle change was in this case 110 m° , value that corresponds to about $1.5 \times 10^{-14} \text{ mol mm}^{-2}$. This would correspond to about 10% of the aptamer sites binding with BSA. However, the electrochemistry of the resulting structure showed significantly different behaviour as response to this non-specific interaction and integration of charge showed about 15% surface coverage as compared to the specific interaction. More importantly the shape of the voltammogram was significantly different. The peak width at half height (ΔE_{FWHM}) was almost three times larger in the case of the non-specific interaction as compared to the interaction with the target. It is therefore shown that other proteins that may modulate the approach of the redox label to the surface, non-specific adsorption can be distinguished when the electrochemical behaviour is analysed in its totality.

To demonstrate the possibility of a re-usable biosensor, the regeneration of thrombin-aptamer interaction was attempted. Regeneration experiments were carried out in a home made 20 μL two electrode thin layer cell with an 18 mm^2 square gold sheet as a working electrode opposite to a solid state Ag/AgCl reference/counter painted on a plastic substrate. Ag/AgCl ink. EDTA and NaOH with ethanol have been reported as efficient regenerators in aptamer-protein interaction (Liss et al., 2002, Minunni et al., 2004). Three incubations of 15 minutes with 50 mM of EDTA were carried out, however no decrease in signal was detected. In contrast interaction regeneration was achieved after the second incubation with 12 mM NaOH with 1,2 % Ethanol. After regeneration a new interaction between aptamer and thrombin was achieved, however the second interaction resulted to 13 % lower signal as compared to the previous. (Figure 4.18)

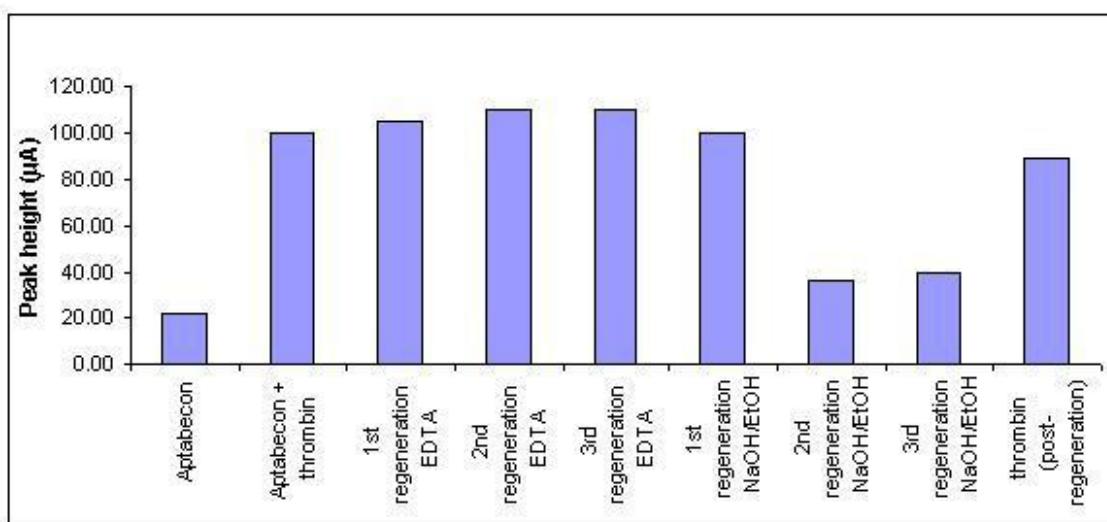
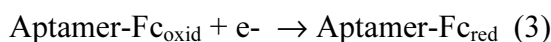
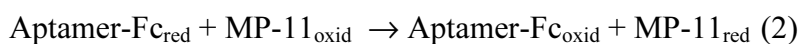
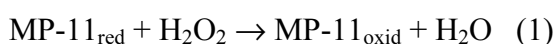


Figure 4. 18. Thrombin-aptabeacon interaction regeneration. The peak height of the CV was plotted. CV was carried out at scan rate of 0.05 V s^{-1} , between -0.2 and 0.2 V .

The reproducibility of the aptabeacon sensor was tested in the same $20 \mu\text{L}$ two electrode thin layer cell. The same protocol was followed on five replicate electrodes. With $1 \mu\text{M}$ of thrombin was obtained a reproducibility of $218 \pm 0.25 \mu\text{A}$.

4.3.6 Chronoamperometric aptabeacon

The results obtained in the previous aptabeacon experiments suggested that indeed, upon thrombin recognition the ferrocene labelled end of the aptamer approached the electrode surface. It was hypothesised that one could use the now readily available redox centre to mediate electron transfer from a co-immobilised redox enzyme in the presence of its substrate. If true, a catalytic current would be observed according to the catalytic cycle:



Reaction (2) would not occur when the unfolded form of the aptamer distances the Fc from the surface bound enzyme. This catalytic sequence would also serve for signal amplification.

To test this hypothesis a mixed monolayer of the redox-labelled aptamer and microperoxidase (MP-11) was constructed. This configuration should translate the distance modulation to a steady state amperometric current that could also be more quantifiable.

To achieve this, the mixed self-assembled monolayer was constructed by incubating the e-SPR gold chip simultaneously in redox labelled aptamer and MP-11. Various concentrations of this mixture were tested to optimise this layer. Incubation of 1.5 μM of analyte (thrombin) for 1 hour at 25 $^{\circ}\text{C}$ was used to detect the optimum mixture concentration. Interaction was detected by SPR and chronoamperometry. Chronoamperometric measurements were carried out in 35 μL of 50 mM citrate buffer pH 6.5, 100 mM NaCl was added into the cell, a potential of -0.1 V versus Ag/AgCl was applied and when the base line was stabilised (at 100 seconds), 1 mM H_2O_2 was injected into the electrochemical cell. Response was recorded after 150 seconds.

A higher response and higher specificity, using bovine serum albumin (BSA) as non-specific target, was obtained with a mixture of 4.5 μM redox labelled aptamer and 1.8 μM MP-11 in 1 M NaH_2PO_4 , incubated for 1 hour at 25 $^{\circ}\text{C}$. Therefore this mixture concentration was used in subsequent experiments (Figure 4.19)

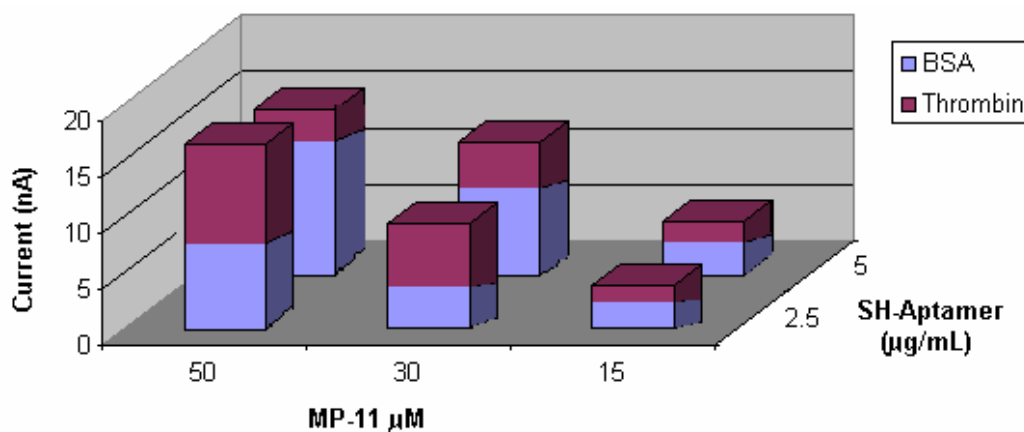


Figure 4. 19. Chronoamperometry results from the aptabeacon with MP-11 system in the optimisation of aptamer-ferrocene and enzyme concentrations. Chronoamperometry was detected at a potential of -0.1 V versus Ag/AgCl.

After the first layer immobilisation, SPR measurements showed a 180 m° shift in the angle of reflectance, this shift corresponds to a 1.7×10^{-13} mol mm⁻² of surface coverage, calculated by employing the empirical relationship explained previously.

In a second step, the aptamer-MP11-modified disc was exposed to 35 µL of thrombin concentrations between (270 nM to 34.5 fM) in 50 mM citrate buffer pH 6.5, 100 mM NaCl for 1 hour at 25 °C. The same concentrations of BSA under the same conditions were used to stablish the background response. Additional control measurements without thrombin and control without redox labelled aptamer were carried out. As shown in Figure 4.20, for a concentration of 540 pM thrombin, a residual 27 m° shift was observed in the reflectance angle which corresponds to 6.7×10^{-15} mol mm⁻² of thrombin remaining attached to the aptasensor. Comparing with the previous aptabeacon system, aptabeacon with MP-11 has a 23 % more surface coverage than the previous system with a self-assembled monolayer of aptabeacon, however in this case the large part of this coverage is due to the MP-11, so less amount of aptamers strands were immobilised. For this reason only a 4 % of thrombin interacted with this aptabeacon+MP11 layer while in the previous system 72 % of thrombin interacted.

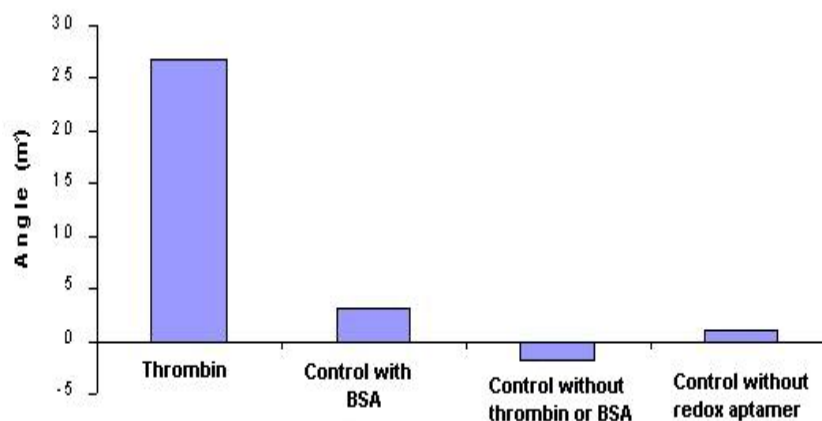


Figure 4. 20. Surface plasmon resonance response from the aptabeacon with MP-11 sensor. Response to thrombin, control with BSA, control with buffer and control without Fc-aptamer. Electrode was modified with a mixture of $0.25 \mu\text{g mL}^{-1}$ of *thiol-aptamer-ferrocene* and $160 \mu\text{M}$ of MP-11 and $18 \mu\text{g mL}^{-1}$ of thrombin.

For the same concentration of BSA a 3 m° shift in the angle of reflectance was detected. This response corresponds to an 18 times less interaction (3.7×10^{-16} mol mm⁻² BSA) compared to thrombin. When no thrombin or BSA was incubated a negative shift of -2 m° was obtained, corresponding to a small amount of desorption of the first layer after 1 hour of buffer (50 mM citrate buffer pH 6.5, 100 mM NaCl) incubation. A control without aptamer-Fc was measured to check the effectiveness of the ferrocene label as electron transfer mediator, in the case of electrochemical detection and in the case of SPR to check the specificity of the analyte to the aptamer. In this case a low response of 1 m° was obtained. This signal is related to a non-specific binding of thrombin.

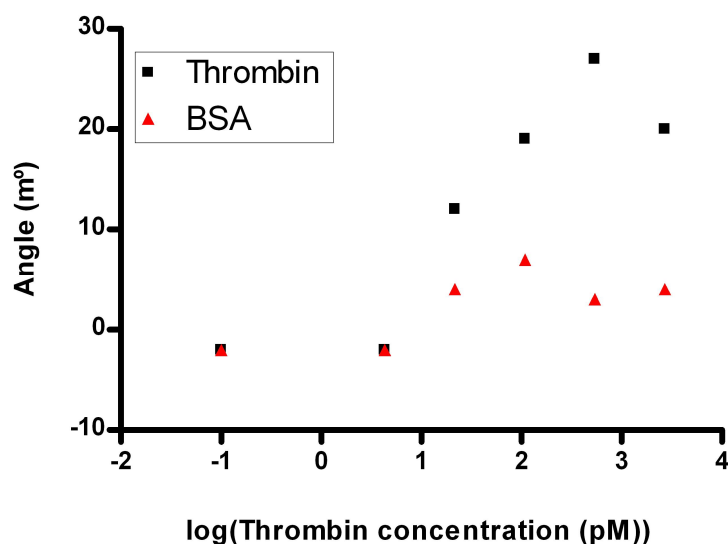


Figure 4. 21. SPR response of different concentrations of thrombin and BSA in an aptabeacon with MP-11 format. Thrombin and BSA concentration were plotted logarithmically.

Various concentrations of thrombin and BSA were measured following the same conditions explained in this section. The limit of thrombin detection of this aptamer-MP-11 based sensor transduced with SPR was 23.8 pM (Figure 4.21).

After SPR detection the same interaction was detected electrochemically on the same gold chip used now as working electrode. The electrochemical circuit was closed with platinum electrode used as counter-reference electrode. Two electrochemical techniques were used to detect this interaction, impedance spectroscopy and chronoamperometry.

Impedance spectroscopy was used first because this technique perturbed the cell with an alternate voltage of small magnitude at around the open circuit potential of the system. The chronoamperometry study electrode reaction through large perturbation of the system, by imposing a potential that drives the electrode to a condition far from equilibrium, so this technique could produce a disturbance on the surface that could change the results obtained with the next technique.

Impedance measurements were collected before and after the interaction of thrombin with the co-immobilised aptabeacon. The impedance data obtained with this system were fitted to a Randles modified equivalent circuit to determine electrical parameter values. This circuit has been chosen based on Vorotyntsev theoretical model of a surface confined redox system (Vorotyntsev et al., 1994). The circuit, presented in the inset of figure 4.17, includes a solution resistance between working and reference electrode (R_s), a double layer capacitance produced by the layer of aptamer-thrombin (C_p) MP-11 film resistance (R_f), an aptamer-thrombin resistance (R_p) a constant phase element (CPE) that is a capacitor that does not behave ideally and it is related to the capacitance of the rough gold surface, and a Warburg impedance element (Z_w) resulting from the diffusion of the ferrocene-label. For all the samples measured, an estimated error of the R_f fitted in this circuit was between 3%-10%.

The association of thrombin with the co-immobilised aptamer-ferrocene might produces significant changes in the circuit element values, except for solution resistance that has a stable value around 80 ohms. The circuit element that undergoes a more significant change is the film resistance. When the interaction occurs the ferrocene label approaches to the MP-11 layer transferring electrons to the electrode surface, which create a decrease in the film electron transfer resistance. Hence it has been the element chosen to be compared with different concentrations of target and controls measurements.

Figure 4.22 shows the Nyquist plots obtained with 270 nM thrombin with the aptabeacon with MP-11 and the control of this system. High electron transfer resistance ($R_f=51$ kohm) was obtained on the system where the absence of redox labelled aptamer was detected, due to the lack of ferrocene molecule to help in the electron transfer. An electron transfer resistance of 43 kohm was obtained with the control without thrombin. In this case the ferrocene molecule attached to the aptamer was present in the system but it is far to the electrode surface. When 270 nM thrombin interacted with the co-

immobilised film of ferrocene-aptamer and MP-11 lower electron transfer resistance was obtained ($R_{ct} = 11 \text{ kohm}$). The specificity of the method was demonstrated using a similar protein (BSA), but that does not show specific binding to this aptamer, at the same concentration used for thrombin. In this case the electron transfer resistance is 61 % higher than the obtained with thrombin and 37% lower that the obtained with the control without analyte. These results suggest that thrombin binds specifically with the thrombin binding aptamer, but some non-specific binding of BSA was observed, causing a small conformational change in the aptamer-ferrocene molecule.

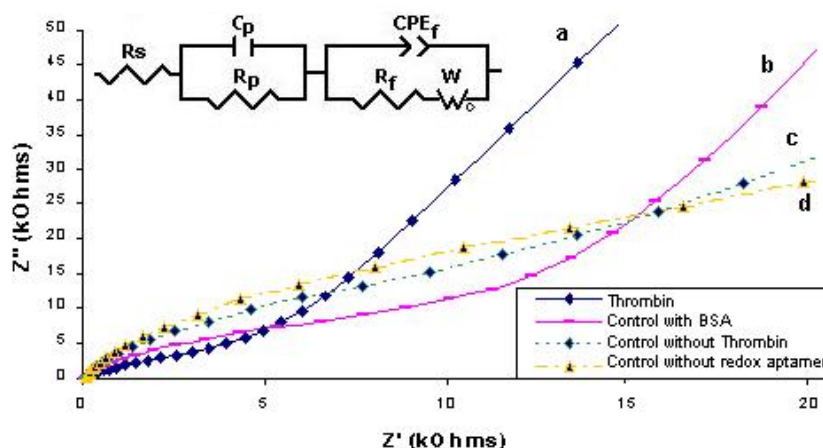


Figure 4. 22. Nyquist plots obtained from a ferrocene labelled aptamer and MP-11 modified electrode to detect thrombin. a) Detection of 270 nM Thrombin, b) Control with 270 nM BSA instead of thrombin, c) Control without thrombin or BSA, d) Control without ferrocene labelled aptamer. On the top of the figure representation of the equivalent circuit used to fit the frequency scans.

To check the proportionality of the thrombin-aptamer interaction response to the concentration of the target, various concentrations of thrombin and BSA were tested. In Figure 4.23 shows higher electron transfer observed with thrombin interaction comparing with BSA and these differences increase when thrombin concentration is increased. The limit of thrombin detection of this aptamer-MP-11 based sensor transduced with impedance spectroscopy was 30 fM.

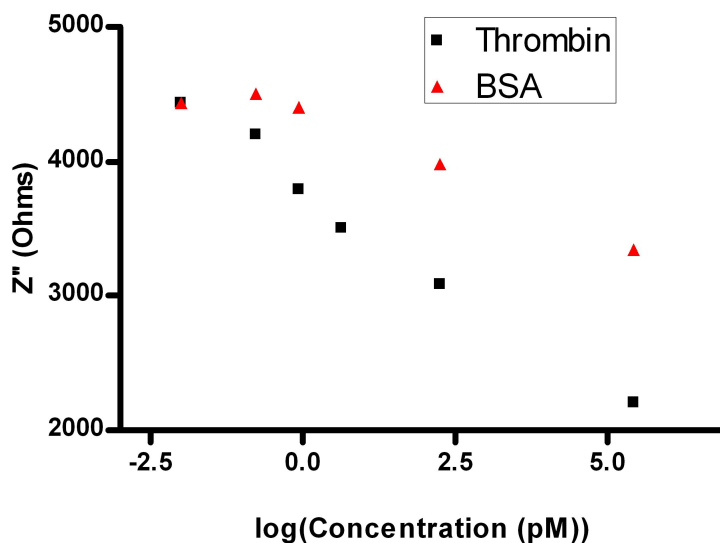


Figure 4. 23. Impedance response of different concentration of thrombin and BSA in an aptabeacon with MP-11 format. Thrombin and BSA concentrations were plotted logarithmically.

Once impedance measurements were carried out, the interaction of thrombin with ferrocene labelled aptamer and MP-11 modified electrode was observed with chronoamperometry to detect the biomolecular recognition event translating the distance modulation to a steady state amperometric current.

The same electrochemical cell used for impedance measurements was used for chronoamperometry detection.

After washing the excess of thrombin incubated with the mixed monolayer of the redox-labelled aptamer and MP-11, 35 μL of 50 mM citrate buffer pH 6.5, 100 mM NaCl was added into the cell, a potential of -0.1 V versus Ag/AgCl was applied and when the base line was stabilised (at 100 seconds), 1 mM H_2O_2 was injected into the electrochemical cell. The response can be measured in 20 seconds however the current obtained after the first steady state at 150 seconds was more reproducible. Thrombin interacts specifically with ferrocene labelled aptamer, and due to the chair conformation that adopt the aptamer when bound with thrombin, the ferrocene label was closer to the MP-11 which allows the ferrocene molecule to transfer the electrons produced in the redox reaction between peroxidase (MP-11) and H_2O_2 to the electrode surface

A reduction current of 35 nA, was obtained after 1.3 μM thrombin incubation with the aptasensor. When BSA was incubated instead of thrombin some reduction was detected

(15 nA with 1.3 μ M BSA). This response came from BSA non-specifically adsorbed over the Fc-aptamer, which changes slightly the redox aptamer conformation. From the control without thrombin or BSA and the control without redox labelled aptamer very low current was obtained (0.4 nA and 0.2 nA respectively) (Figure 4.24).

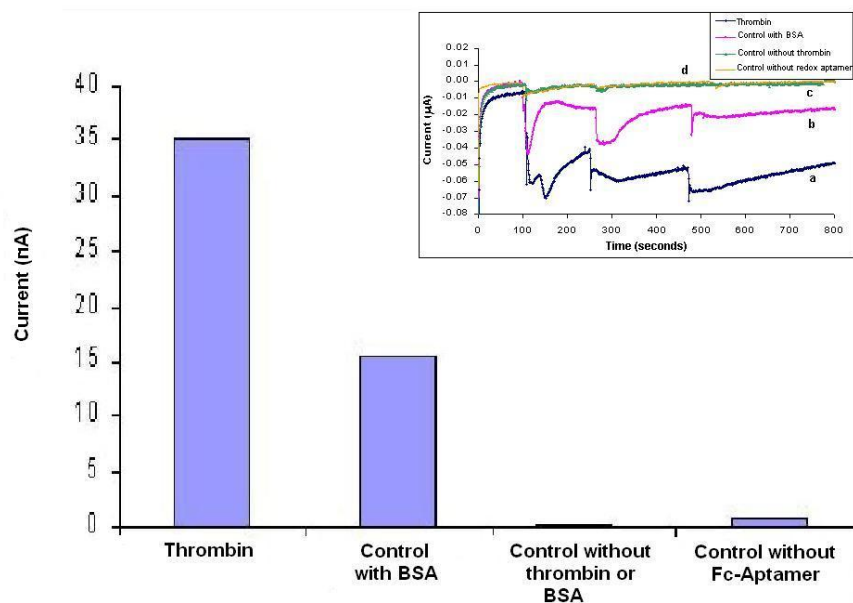


Figure 4. 24. Amperometric aptasensor response to thrombin and controls. In the inset the amperometry is shown. Applied potential -0.1 V vs. Ag/AgCl, injection of 1mM H_2O_2 at 100 seconds. Response measured at 250 seconds. Electrode area 4.8 mm².

As is shown in Figure 4.25, chronoamperometry response was recorded with redox aptamer and MP-11 modified gold electrode in the presence of decreasing concentrations of thrombin and BSA. The limit of thrombin detection for this aptamer-MP-11 based sensor transduced with chronoamperometry was 5 nM.

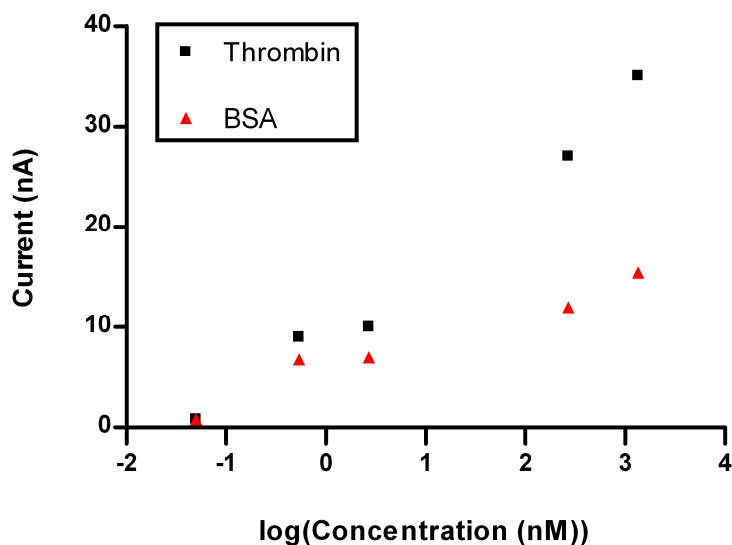


Figure 4. 25. Amperometric aptabeacon based sensor. Response to different concentrations of thrombin and BSA. Thrombin and BSA concentration were plotted logarithmically.

The reproducibility of the chronoamperometric aptabeacon was carried out in five electrodes measured in a home made 20 μL two electrode thin layer cell with a 18 mm^2 square gold sheet as a working electrode opposite to a solid state Pt reference/counter electrode. Standard deviation of the thrombin detection ($18 \mu\text{g mL}^{-1}$), by chronoamperometry is $0.54 + 0.27 \mu\text{A}$.

Real time detection of thrombin–aptabeacon interaction was carried out in the same two-electrode thin layer cell. To achieve this, the mixed self-assembled monolayer was constructed incubating the gold electrode simultaneously in 160 μM MP-11 and 35 nM thiol-aptamer-ferrocene in NaH_2PO_4 . The real time detection of various concentrations of thrombin or BSA, in the case of control, was carried out by chronoamperometry. - 0.1 V was applied in a solution of 1 mM H_2O_2 in 50 mM citrate buffer pH 5, 100 mM NaCl, after 100 seconds the target was injected into the electrochemical cell and left to react, meanwhile the change on the electrode surface due to thrombin interaction were recorded on the chronoamperograph. Afterwards a CV (scan rate of 0.01 V s^{-1} , scan between -0.3 V and 0.4 V) was recorded (Figure 4.26).

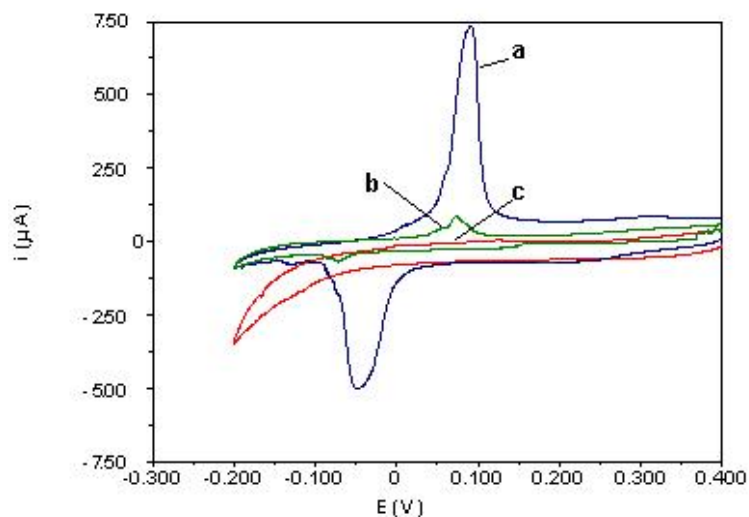


Figure 4. 26. CV of MP-11 and thiol-aptamer-ferrocene mixed monolayer modified electrodes in 50 mM citrate buffer pH 5, 100 mM NaCl, at 0.01 V s^{-1} using a 18 mm^2 Au electrode. (a) Thrombin interaction with aptamer-ferrocene, (b) control with BSA and (c) initial CV after thiolated redox-aptamer immobilisation and before exposure to thrombin or BSA.

It is also interesting to note that the response was developed in about one minute after injection of thrombin.

As shows figure 4.27, the response was quite reproducible and proportional to the amount of thrombin added. The reagentless nature of this method of detection could be retained if a H_2O_2 -producing enzyme is added to the architecture as described elsewhere (Campbell et al., 1999).

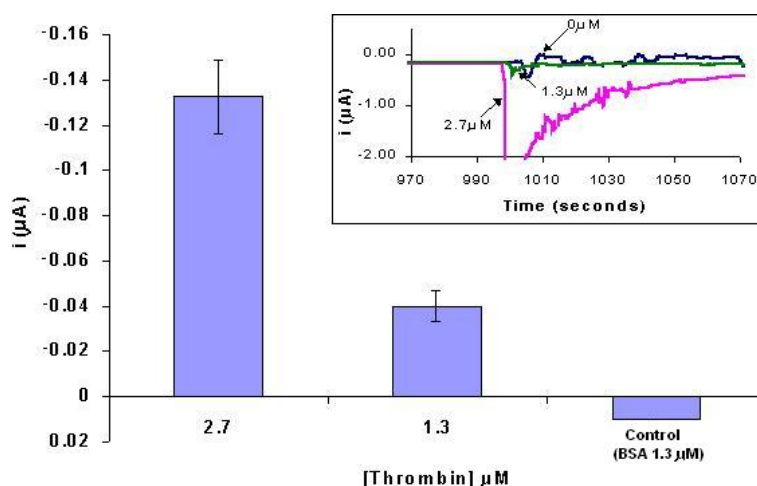


Figure 4. 27. Amperometric aptasensor in real time. Response obtained from different concentrations of thrombin and BSA (control). Applied potential -0.1 V vs. Ag/AgCl in presence of $1 \text{ mM H}_2\text{O}_2$, after 100 seconds different concentrations of thrombin was added. In the inset the amperometry is shown.

Using equation 4.2 cyclic voltamperometry peaks were integrated to obtain the charge passed, which showed apparent surface coverage of $1.7 \times 10^{-13} \text{ mol mm}^{-2}$.

$$Q = nFA\Gamma \quad (\text{Equation 4.2})$$

The theoretical surface coverage for DNA strands is equal to $3.7 \times 10^{-13} \text{ mol mm}^{-2}$ (Li et al., 2005), which is very close to the experimental value obtained.

Once the surface coverage is known, the order of magnitude of the expected current can be calculated following by;

$$i = n\Gamma EAFA \quad (\text{Equation 4.3})$$

Taking into account that enzymatic activity (EA) of MP-11 is equal to $5.5 \times 10^6 \text{ U mol}^{-1}$ (Lotzbever et al., 1995) and U is equivalent to the $\mu\text{mols per minute}$, the values used in the previous equation and the experimental surface coverage reached, the theoretical current that should be achieved is equal to $0.15 \mu\text{A}$, which is quite similar to the current obtained experimentally ($0.13 \mu\text{A}$), as shows figure 4.27.

4.4 Conclusions

It was demonstrated that several configurations can be formulated from electrochemical aptasensor. The five electrochemical aptasensors developed only the aptabeacon strategy is generic, and even in the case, only if the aptamer suffers an important 3-D change upon recognition. This configuration was developed into a novel molecular architecture that yielded the first amperometric molecular switch reported in the literature. However this switch suffers from non-specific adsorption phenomena and low catalytic efficiency. Stills although amperometric recycling was not very efficient,

the electron transfer facility could be very efficiently probed yielding 30 fM detection limit and real time detection.

The results presented with these aptasensors were performed in a matrix far less complex than the anticipated clinical samples. While specifically recognising thrombin, the electrodes may be impacted by interference from other blood chemicals, which could ultimately increase the detection limit of the system.

4.5 References

- Bock L.C., Griffin L.C., Lathan J.A., Vermaas E.H., Toole J.J., *Nature*, 1992, 355, 564-568.
- Brazill S.A., Kuhr W.G., *Analytical Chemistry*, 2002, 74, 3421-3428.
- Campbell C. N., de Lumley-Woodyear T., Heller A., *Fresenius Journal of Analytical Chemistry*, 1999, 364, 165-181.
- Fan C., Plaxco K. W., Heeger A. J., *Proceedings of the National Academy of Sciences*, 2003, 100, 9134-9137
- Gregg B.A., Heller A., *Journal of Physical Chemistry*, 1991. 95, 5970-5975.
- Hamaguchi N., Ellington A. D., Stanton M., *Analytical Biochemistry*, 2001, 294, 126-131
- Heiduschka P., Dittrich J., *Bioelectrochemistry and Bioenergetics*, 1990, 24, 231-239.
- Rydel T.J., Ravichandran K.G., Tulinsky A., Bode W., Huber R., Roitsch C., Fenton J.W., *Science*, 1990, 249, 277-280.
- Katakis I., Heller A., *Analytical Chemistry*, 1992, 64, 1008-1013.
- Levichy R., Herne T.M., Tarlov M.J., Satija S.K., *Journal of American Chemical Society*, 1998, 120, 9787-9792.
- Li J., Chu X., Liu Y., Jiang J., He Z., Zhang Z., Shen G., Yu R., *Nucleic Acids Research*, 2005, 33, 19, 168-177.
- Lide D.R., *CRC Handbook of chemistry and physics*, 86th edition, CRC press, 2005.

- Lin Y., Nieuwlandt D., Magallanez A., Feistner B., Jayasena S.D., *Nucleic Acids Research*, 1996, 24, 3407–3414.
- Liss M., Petersen B., Wolf H., Prohaska E., *Analytical Chemistry*, 2002, 74, 4488-4495.
- Liu J., Werner P.S., Steiner M., *Thrombosis Research*, 2002, 107, 281-282.
- Lotzbever T., Schuhmann W., Schmidt H.L., *The 8th International Conference on Solid-state Sensors and Actuators, and Eurosensors IX*. Stockholm, Sweden, 1995.
- Minunni M., Tombelli S., Gullotto A., Luzzi E., Mascini M., *Biosensors and Bioelectronics*, 2004, 20, 1149–1156.
- Nakayama M., Ihara T., Nakano K., Maeda M., *Talanta*. 2002, 56, 857–866
- Padmanabhan K., Padmanabhan K.P., Ferrara J.D., Sadler J.E., Tulinsky A., *Journal of Biological Chemistry*, 1993, 268, 24, 17651-17654.
- Radi A. E., Acero J. L., Baldrich E., O’Sullivan C. K., *Journal of American Chemical Society*, 2006, 128, 117-124.
- User Manual for Autolab SPIRIT, EcoChemie, 2003
- Vorotyntsev M.A., Daikhin L.I., Levi M.D., *J. Electroanalytical Chemistry* 1994, 364, 37-49.
- Vreeke M.S., Rocca P., Heller A., *Analytical Chemistry*., 1995, 67, 303-306.
- Vreeke M.S., Maidan R., Heller A., *Analytical Chemistry*, 1992, 64, 3084-3090.

Chapter 5. Conclusions and future work

This thesis examined strategies to develop oligonucleotide based-sensors for label-free protein and oligonucleotide electrochemical detection.

Direct DNA electrochemical detection of labelled ssDNA were first optimised to establish a protocol of DNA immobilisation, hybridisation and detection colourimetrically and electrochemically.

A sub-optimum displacement assay to develop a label-free detection of DNA hybridisation was demonstrated. The assay was performed colourimetrically and electrochemically using a sub-optimum HRP labelled, as well as electrochemically through a sub-optimum ferrocene labelled that converts this system in a reagentless device.

Furthermore, different strategies for a label-free oligonucleotide based-sensor to electrochemically detect thrombin were investigated.

- Detection of direct DNA hybridisation

Different electron transfer mediating systems were applied and compared for DNA hybridisation detection.

A 19-mer HRP labelled oligonucleotide has been detected with a diffusional mediator as well as a redox polymer attached to the electrode surface. Non-diffusional transduction with the redox polymer resulted in the doubling of current compared to diffusional transduction. It also offered reduced response time, possibility of use lower sample volumes and provided an easy to use and a quasi-reagentless system.

This system could be used to detect a 255-mer oligonucleotide amplified by PCR, selective for the *Micobacterium tuberculosis* rpoB gene region

The detection of the longer oligonucleotide (255-mer) hybridisation resulted in lower currents due to the insulating character of the 255-mer.

This diffusionless system allowed the elimination of crosstalk in closely spaced electrodes and thus biocompatible photolithography could be used for the selective

immobilisation of biomolecules on an electrochemical microarray. A 22-mer oligonucleotide specific for breast cancer was electrochemically detected on the microarray. A clear differentiation between sample and control and no crosstalk was detected between two interdigitated arrays electrodes separated only by 20 μm .

- Detection of indirect DNA hybridisation by displacement

Sub-optimum displacement assays to detect a label-free oligonucleotide target were carried out. A pre-hybridisation of a labelled mutated oligonucleotide with an immobilised capture probe was performed and due to the higher affinity of the target that is fully complementary to the capture probe, the pre-hybridised labelled mutated oligonucleotide was displaced when the complementary target was introduced in the system. The decrease of the signal verified the presence of the target, which was proportional to the target concentration.

The sub-optimum displacement system was demonstrated colourimetrically and electrochemically using a HRP labelled mutated oligonucleotide as well as electrochemically with a ferrocene labelled oligonucleotide.

Colourimetric detection of sub-optimum displacement with HRP label showed a specific displacement of 38.3 % at 60 °C. The response of the displacement system was proportional to the target concentration. A useful target concentration was in range of μM . The displacement method evaluated colourimetrically achieved the objective of decreasing the response time from 1 hour in direct hybridisation of 19-mer oligonucleotides to 5 minutes in the case of displacement detection.

Electrochemical detection of sub-optimum displacement with HRP label showed a specific displacement of 22.5 %. However, the design of the electrochemical cell did not allow the application of temperature, so although optimisations in ELONA demonstrated better displacement at 60 °C, electrochemical detection was done at 25 °C, which reduced the percentage of displacement obtained.

Ferrocene labelled sub-optimum hybridisation displacement for detection of the cystic fibrosis gene region was demonstrated by seven methods, SPR, CV in buffer, DPV in buffer, impedance in buffer, CV in ferrocyanide/ferricyanide, DPV in ferrocyanide/ferricyanide and impedance in ferrocyanide/ferricyanide. Compared with the previous electrochemical system using HRP labelled for the displacement detection,

lower percentage of displacement was obtained with ferrocene labelled, 14 % versus 22 % of HRP displacement. A similar range of detection limit was demonstrated with both systems. However in this case a completely reagentless system was achieved and a lower relative standard deviation was obtained ($6.2 \pm 0.3 \mu\text{A}$ versus $0.12 \pm 0.03 \mu\text{A}$ with HRP system). Furthermore this system demonstrated the benefit in sensitivity when ferrocyanide was inserted in the system. However, this approach leads to a sensor that is no longer reagentless.

- Electrochemical detection of protein-DNA interaction

Five configurations of an aptamer based sensor for thrombin detection based on electrochemical transduction were investigated. The first strategy employed a thrombin specific aptamer immobilised on an electrode surface. Aptamer bound thrombin was detected by quantifying the p-nitroaniline reaction product produced by the thrombin catalysed hydrolysis of β -Ala-Gly-Arg-p-nitroaniline. The electrochemical detection of p-nitroaniline was 60 fold faster than the optical reference method. The second approach detected the thrombin using two aptamers in a sandwich configuration achieving a limit of detection of 35 nM, higher than the obtained in the third system employing thrombin immobilised on a modified gold electrode and detection with HRP labelled aptamer, where was achieved 2.75 nM of detection limit. The fourth strategy demonstrates a switch on approach completely reagentless based on a beacon system. However more reproducible and sensitive response was obtained in the fifth design where the aptabeacon was improved with an enzyme layer co-immobilised to catalyse the response. This last strategy was demonstrated with SPR, chronoamperometry and impedance spectroscopy. The lowest limit of detection was achieved with impedance detection and it was, 30 fM. Furthermore a real time detection of thrombin-aptamer-ferrocene interaction was demonstrated chronoamperometrically with the co-immobilised aptabeacon- MP-11 system.

As every experimental work, this are also probably created were questions than it answered. Some of the most important considerations are the following:

- The present non-specific adsorption in direct DNA sensors and aptamer-based sensors needs to be reduced. To avoid non-specific immobilisation of succeeding reactants, blocking agents were used to prevent possible excess to the solid surface after coating with oligonucleotide capture probe. Different kinds of blocking agents were tested in this thesis. However, a deeper study should be done to reduce the still high non-specific adsorption and improve the sensitivity of the system.

- PCR to amplify and label DNA samples is a general procedure employed before analysis of the sample in a DNA sensor. The PCR step increases the cost of the DNA sensor and requires skilled personnel and costly laboratory instruments. This is not feasible in the point of care or in home-diagnostic environment. The use of the sub-optimum displacement assay demonstrates that the labelling step could be eliminated. However, to avoid completely the use of PCR lower limit of detection in displacement assay is required. Different methods of signal amplification are reported in the literature and can be adapted to the sub-optimum displacement assay to eliminate the use of PCR prior to DNA sensor detection. Gold, silver or CdS nanoparticles are widely used for signal amplification in DNA sensors (Yao et al., 2006; Wang et al., 2006; Travas-Sejdiv et al., 2006). Different enzymatic cascades were used for electrochemical amplification (Tang and Johansson, 1995). Kumada et al., 2006, reported the use of liposomes to encapsulate some molecules of HRP and then use the liposomes as an amplifier reporter biomolecule. Coating of the electrode surface with a branched molecule such as dendrimers to increase the surface and then increase signal has been broadly used (Patolsky et al., 2000; Zhao et al., 2001).

- Different kinds of sequences for the displacement assay should be examined. They should take into account different numbers of mutations, different positions of mutations and different kinds of base-mismatches. The sequences should be synthesised and tested using SPR to obtain the association constant and the dissociation constant.

- Modelling of displacement method with the different sequences tested by SPR should be carried out. An algorithm should be developed to predict the most suitable mismatched sequence for each target of interest.
- The displacement assay should be optimised to be performed at room temperature for a future low cost device.
- The displacement assay and aptamer-based sensors should be tested in an array with different targets. The generic nature of aptasensors needs to be demonstrated if these molecules are to fulfil the expectations that have created the proteomics.
- The mismatch discrimination capacity of the displacement assay should be carried out and compared with the discrimination capacity of direct hybridisation. Probably, mismatched strands might have more difficulties to hybridise in displacement assay than in direct hybridisation, because before the hybridisation in displacement assay the complementary strands need first to displace the sub-optimum strand.
- In the case that any of the developed strategies of oligonucleotide-based sensors for DNA or protein detection were to be commercialised. The sensor will have to be stable in storage and dependable in use. Long term studies must be undertaken to test their stability and reliability. Moreover sensors should be tested with real clinical samples in a complex matrix.

5.1 References

Kumada Y., Maehara M., Minami N., Nogami M., Katoh S., *Biochemical Engineering Journal*, 2006, 29, 1-2, 98-102.

Patolsky F. ranjit K.T., Lichtenstein A., Wilner I., Chemical Communications, 2000, 12, 1025-1027.

Tang X., Johansson G., Analytical Letters, 1995, 28, 2595-2599.

Travas-Sejdic J., Peng H., Cooney R.P., Bowmaker G.A., Cannell M.B., Soeller C. Current Applied Physics, 2006, 6,3 , 562-566.

Wang Y., Yin X., Shi M., Li W., Zhang L., Kong J., Talanta, 2006, 69, 5, 1240-1245.

Yao X., Li X., Toledo F., Zurita-Lopez C., Gutova M., Momand J., Zhou F. Analytical Biochemistry , 2006, 354, 2, 220-228.

Zhao H.Q., Lin L., Li J.R., Tang J.A., Duan M.X., Jiang L., Nanoparticles. Research, 2001, 3, 321-325.